

**INTERACTIONS BETWEEN SOLUTES IN DISPLACEMENT SOLUTIONS
AND OIL BEARING ROCKS**

by

David William Martin, B. Sc.

1995

**This thesis is submitted in partial fulfilment of the requirements for the
degree of Doctor of Philosophy of Liverpool John Moores University.**

Sponsoring Establishment

Department of Trade and Industry through PEDSU, AEA, Winfrith.

Table of Contents

	Page
ACKNOWLEDGEMENTS	v
ABSTRACT	vi
CHAPTER 1 - INTRODUCTION	1
1.1 Petroleum and the Petroleum Reservoir	2
1.2 Oil Recovery Processes	3
1.3 Properties of Surfactants	10
1.4 Emulsion Formation and Oil Recovery	26
1.5 Clay Mineral Structure and Charge Distribution	30
1.6 The Electrical Double Layer	36
CHAPTER 2 - EXPERIMENTAL	46
2.1 Minerals	47
2.2 Chemicals	47
2.3 Preparation of Isomerically Pure 4- ϕ -C ₁₂ ABS	49
2.4 Preparation of Kaolin and Ion-Washed Kaolins	54
2.5 Experimental Techniques	56
2.6 Surface Tension Measurements	85
2.7 Adsorption Studies	87

2.8	Electrophoresis Measurements	89
2.9	Atomic Absorption Spectrophotometry	94
CHAPTER 3 - RESULTS		100
3.1	Characterisation of Kaolin and Ion-Washed Kaolins	101
3.2	Characterisation of North Sea Reservoir Rock	114
3.3	Adsorption of 4- ϕ -C ₁₂ ABS at the Air-Solution Interface	123
3.4	Adsorption at the Kaolin-Aqueous Solution Interface	130
3.5	Effect of Ion-Washed Kaolin on the Adsorption at the Kaolin-Aqueous Interface	146
3.6	Adsorption of 4- ϕ -C ₁₂ ABS onto North Sea Reservoir Rock Samples	149
3.7	Effect of Formation Water on 4- ϕ -C ₁₂ ABS Adsorption at the Kaolin-Aqueous Interface	153
3.8	Adsorption of 4- ϕ -C ₁₂ ABS at the Kaolin-Aqueous Interface in the presence of nonionic surfactant Synperonic N	167
3.9	Adsorption of other anionic surfactants at the solution-air and Kaolin-Aqueous interface	167
3.10	Determination of calcium ions in solution using an Ion-Selective Electrode	193

CHAPTER 4 - DISCUSSION	197
4.1 Characterisation of Kaolin and its Ion Exchanged forms	198
4.2 Adsorption of surfactants at the air-aqueous interface	202
4.3 Surfactant adsorption at the Kaolin-Aqueous interface	208
4.4 Surfactant adsorption at the core sample - aqueous interface	217
4.5 Mixed and other surfactant systems	218
4.6 Determination of counter-ion concentration	220
CONCLUSIONS	226
REFERENCES	232
APPENDICES	249
GLOSSARY	269

Dedication

This thesis is dedicated to my wife, Jenny, for all her hard work, patience and encouragement over the last four years. Also, to my daughter Kathryn and my parents.

Acknowledgements

Acknowledgement is made to the Department of Trade and Industry, and the Winfrith Atomic Energy Establishment, for the financial assistance given to this project, and additional thanks are extended to the PEDSU staff at Winfrith, particularly Dr. Andy Fisher, for the discussions and guidance given during the development of the research.

I would also like to thank the Chemistry Lab Staff, particularly Mike Fitzsimmons and Geoff Henshaw, for their help and allowing the use of any relevant equipment.

Finally, I would like to extend my sincerest thanks to Professor G.G. Jayson and Dr. H Morris for their support and encouragement during this work and their help and guidance in the writing of this thesis.

Abstract

INTERACTIONS BETWEEN SOLUTES IN DISPLACEMENT SOLUTIONS AND OIL BEARING MINERALS.

David William Martin

Studies of adsorption of several surfactants from aqueous solution onto kaolin have been made, such as might be employed in an enhanced oil recovery process. Investigations of the surfactants were carried out with regard to pH, ionic strength, temperature, the addition of short chain aliphatic alcohols, the addition of sacrificial complexing agents and various ion-exchanged forms of kaolin. The various forms of kaolin were synthesised to simulate the effect of clay contact with sea water and/or formation water.

To try and understand the surfactant solution more fully an attempt was made to determine the number of bound Ca^{2+} ions and Al^{3+} ions using an ion-selective electrode and atomic adsorption spectroscopy techniques.

The results of the adsorption experiments show that monolayer coverage of the kaolin takes place, and the minimum adsorption is favoured by the following conditions : high pH, low ionic strength and elevated temperatures. The presence of butan-1-ol and sodium citrate are also beneficial. In the presence of high ionic strength solutions, the anionic surfactant may also be lost due to salt formation with the metal ion present and hence be precipitated from solution.

In the absence of the short chain alcohols the adsorption isotherms of the anionic surfactants can be said, at low concentrations ($< 10^{-3} \text{ mol dm}^{-3}$), to be due to electrostatic interactions between the edge of the clay particles and the charged surfactant. At higher concentrations the adsorption becomes limited due to the formation of micelles. At concentrations $> 10^{-2} \text{ mol dm}^{-3}$ the surfactants appear to desorb into solution. This is due to the resolubilisation of the adsorbed surfactant-metal ion species by the excess micelles which exist at these surfactant concentrations.

The determination of bound counter ions has been investigated and found to give acceptable results comparable to those that would be expected. However, slight reservations are made as to the total accuracy of the test method.

This study has been able to define the conditions which will allow various anionic surfactants to be used in conjunction with other chemical species in enhanced oil recovery processes for both land or sea based wells.

Chapter 1

Introduction

1 Introduction

1.1 Petroleum and the Petroleum Reservoir

Petroleum is a naturally occurring mixture of hydrocarbons which may exist in all states i.e. solid, liquid or gaseous with virtually all produced petroleum being made up of the latter two. These are referred to as *Crude Oil* and *Natural Gas* respectively and are found in a petroleum reservoir which consists of porous and permeable rock which is typically made up of carbonates, silicates and clays through which fluids such as oil, water and gas may flow towards recovery openings (Wells) either by utilising the pressures that exist within the system (*Primary Recovery*, Section 1.2.1) or under pressures applied to the system (*Secondary Recovery*, Section 1.2.2).

All connecting pore space within the productive formation is properly a part of the rock, and therefore this may include several individual rock strata. The size of a reservoir is only dependent upon the continuation of the pore space and the ability of fluids to move through the rock under the pressures available. An oil-field can therefore be viewed as being an aggregate of well bores which access one or more of these petroleum reservoirs.

1.2 Oil Recovery Processes

1.2.1 Primary Oil Recovery

Wells bored into reservoir rock formations serve as pressure sinks that allow oil to be recovered. Normal depletion, called *Primary Recovery*, is reliant upon the natural energy of the reservoir to force the petroleum to the well bore and hence to be recovered. This driving pressure arises from the expansion of the hydrocarbon fluids as the confining pressure is released. In addition the driving pressure may be supplemented by the release and expansion of natural gases dissolved in the liquid petroleum fraction thereby sustaining the pressure and increasing the amount of oil recovered.

Water trapped in rock formations (*Aquifers*) may also provide further energy for oil recovery. This water, known as *Connate Water* is also trapped at elevated pressures and withdrawal of the petroleum fluids from the reservoir causes the structure itself to act as a pressure sink allowing the water to expand into the pore space and therefore displace more oil toward the well bore ultimately to be recovered.

These natural pressure drives may occur in a reservoir either simultaneously or at various times throughout the life of the well. However, no matter when these processes occur it is found that much of the oil-in-place remains unrecovered as the natural pressure is depleted. In order to improve recovery a secondary pressure drive

is employed in the form of fluid injections. These injections may be used during the primary recovery process in order to maintain the pressure or into a depleted reservoir in a process known as *Secondary Oil Recovery* (Section 1.2.2).

1.2.2 Secondary Oil Recovery

Following primary recovery or supplementing the process, fluid in the form of water or miscible gas (usually CO₂) is injected into the reservoir to provide a secondary pressure drive. This injected fluid displaces much of the resident brine and part of the oil-in-place thus increasing production of the well.

In addition to increasing the reservoir energy the injected fluid must displace the oil and drive it to the surface. The success of this depends upon the efficiency of the fluid to displace the oil (*Displacement Efficiency*), and the volume of reservoir the fluid enters (*Conformance* or *Sweep Efficiency*). In most cases gas will do neither of these as efficiently as water, although gas does have some advantages in that it is readily available and it is easier to inject (B1, H1). If a well is continually injected then eventually the recovered product will become solely the injected fluid leaving any unrecovered oil as *Residual Oil*. This oil represents an enormously valuable resource of known location, and as such has prompted large investment from industry to develop methods of recovering this oil, but only to the extent that its recovery is economically viable. Known as *Enhanced* or *Tertiary Oil Recovery*, these processes try to improve oil recovery by modifying the oil-water interfacial tension.

1.2.3 Residual Oil and Tertiary Oil Recovery

Oil remains trapped as small droplets in a reservoir through the action of strong capillary forces. These forces hold the droplets (*Oil Ganglions*) in narrow pore spaces in the structure and must be reduced to recover the oil. The simplest model of a trapped oil ganglion is shown in Figure 1. Water flowing through connecting pore spaces establishes a pressure gradient across the droplet. The drop moves in the direction closest to the gradient direction until the droplet can continue no further through the pore. Essentially the droplet becomes "stuck". The pressure gradient required to displace this droplet is given by Laplace's equation (T1);

$$\Delta P = P_{w2} - P_{w1} - 2\gamma (1/r_1 - 1/r_2) \quad (1.1)$$

in which P = the pressure gradient in dynes cm^{-2} ,

r = the pore radius in cm,

γ = the oil-water interfacial tension dynes cm^{-1} .

A typical value for ΔP is approx. 3.4×10^7 dyne cm^{-2} (T1) to displace this oil whereas a practical limit of pressure attainable in real field situations is between 2.3 and 4.6×10^5 dyne cm^{-2} m^{-1} (H2,P1). Therefore in order to displace the oil a reduction of interfacial tension is required. This reduction must be of the order of 10^2 dyne cm^{-1} (M1,W1).

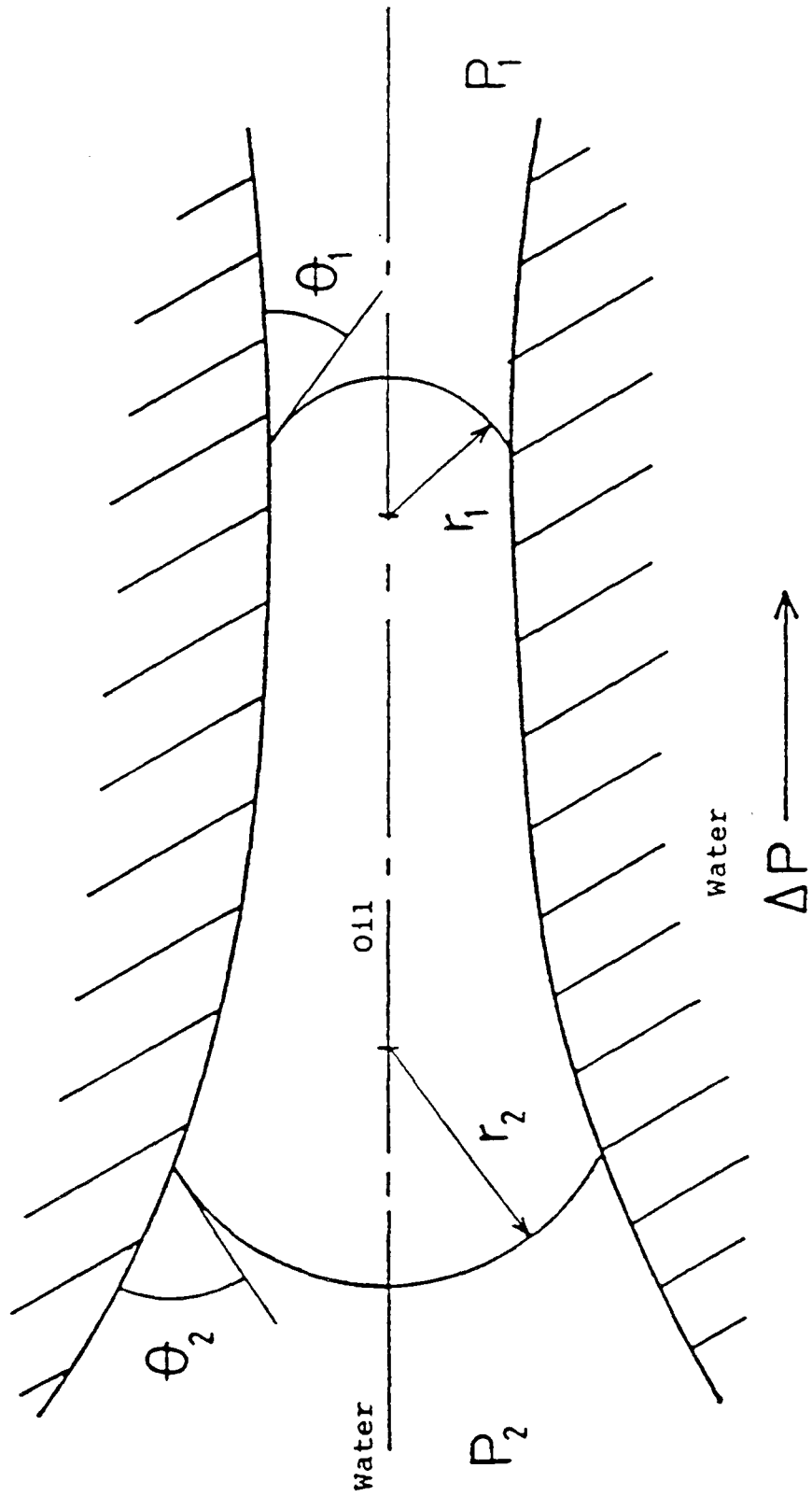


Figure 1. Model of an Oil ganglion trapped by capillarity and a pore Constriction

The relationship between the capillary and viscous forces acting on the droplet is expressed by the dimensionless capillary number, N_c (T1,M1):

$$N_c = (\text{velocity} \times \text{viscosity}) / \gamma \quad (1.2)$$

in which the velocity in ft per day and the viscosity in centipoise refer to the injected fluid and γ , in mN m⁻¹, is measured between the oil and the injected fluid.

This capillary number has been defined by several workers (T1,L1,T2) who conclude that to achieve low residual oil saturations a high capillary number is required. In order to recover significant amounts of residual oil the capillary number must have a value of about 10^2 (S1,G1). This is attainable but only with a reduction of interfacial tension to an ultralow value ca. 10^{-3} mN⁻¹. Hence, methods designed towards applications in tertiary oil recovery utilise the need to reduce interfacial tension to ultralow values thereby displacing the oil by a miscible process.

1.2.3.1 Miscible Gas Drives

In this process, residual oil can be mobilised by an injected gas (usually CO₂) which is miscible with the oil. Displacement of the oil can be controlled by either a *First Contact* or a *Multi-contact* mechanism. In the former, solvents which are miscible with the reservoir oil are injected. Typically, these are liquified petroleum gas fractions (LPG's) which are usually the smaller carbon chain alkanes i.e. ethane to hexane (C₂ - C₆). The LPG's mix with the oil in all proportions and no phase separation occurs. An enriched gas process can also be used where the solvent is

supported by a miscible gas drive. The only difference between the two systems is in the LPG process the small chain alkanes move from the oil to the gas while for the enriched gas process these components move from the gas to the oil.

Multiple contact miscible agents include methane, carbon dioxide, and nitrogen. These will not mix in all proportions and hence this may lead to phase separation.

In either of the above processes, residual oil is mobilised as a single phase mixture with the reduced viscosity and removal of the interface making recovery possible.

1.2.3.2 Thermal Processes

Generally applied to heavy oils, this process uses heat generated either above ground or in situ, to reduce the viscosity of the trapped oil and hence make it able to be recovered. The simplest method involves steam injection. Steam is used as a driving fluid to displace the oil from an injector to a producer well, or in a cyclic injection-production sequence. The latter allows the same well to be used as both injector and producer, with a soak period to heat the well. This is known as the "steam soak" process (P2).

Underground, or in situ, combustion processes use injected air or oxygen and hydrocarbons within the reservoir as fuel.

1.2.3.3 Surfactant Flooding

In this tertiary oil recovery process, an aqueous solution of a surfactant (see Section 1.3) is injected to the reservoir to displace residual oil. The concentration of the surfactant solution must be sufficiently great so that the molecules aggregate and form micelles (see Section 1.3.3). The mechanism by which this method recovers the oil is to reduce the interfacial tension between the oil and the displacing phase to an ultralow value (see Section 1.2.3). The aim of a surfactant injection is to solubilise the residual oil in the micellar solution thereby creating a microemulsion phase (R1) which will result in the displacement of trapped oil ganglia.

The process of surfactant flooding is potentially applicable to a wider range of oil-fields than any other enhanced oil recovery technique, however, one major drawback using this method is the loss of surfactant from the surfactant slug by adsorption onto the surfaces of materials in the reservoir (particularly clays). This loss of surfactant affects the ability to maintain the microemulsion thereby affecting the displacement of the trapped oil.

1.3 Properties of Surfactants

In order to understand how to use surfactants in enhanced oil recovery, such that maximum efficiency is attained, the properties of these surfactants and the dependence of these properties on surfactant structure must be understood. The property of major importance to the recovery of oil is the ability to lower the surface tension between oil and water as this is essential to raise the capillary number (Section 1.2.2.3). Surfactants are substances which have a characteristic molecular structure which consists of two structural groups; one which has an affinity for the solvent, lyophilic, and the other which has little or no affinity for the solvent, lyophobic group. The presence of these two groups in one molecule gives the *amphipathic* nature observed in all surfactants.

Surfactants are classified according to the ionic nature, as anionic, cationic, zwitterionic and nonionic. These surfactants can be oil soluble, but not water soluble, or vice versa. Some surfactants occur naturally in biological systems such as monoglycerides and lecithin.

As a result of this amphipathic structure surfactants have some highly characteristic properties:

- (i) Surface Activity
- (ii) Orientation of Adsorbed molecules at interfaces
- (iii) Micelle Formation
- (iv) Solubilisation and Emulsification

Due to these properties, surfactants can be effective in such processes as wetting , dispersion, suspension of small solids in liquids (particularly useful in the paint industry), and stabilisation of emulsions.

1.3.1 Surface Activity

Dissolution of a surfactant in a solvent causes a distortion of the liquid structure, and a subsequent increase in free energy of the system, due to the presence of the lyophobic group. As the free energy is increased then less work needs to be done to remove the surfactant molecules to the interface than that needed for the solvent molecules. Resulting in the surfactant molecules concentrating at the interface.

At an interface the amphipathic structure gives rise to orientation of the molecules, such that the lyophobic group is excluded from the solvent whilst the lyophilic group remains in contact with the solution. This situation thermodynamically satisfies the dual nature of the surfactant molecules. The accumulation, or adsorption, of surfactant molecules at an interface in the form of orientated molecules is termed *Surface Activity*. This is a dynamic phenomenon, the final state of the surface, or interface, representing a balance between adsorption and mixing, the latter arising from natural thermal motion.

At a fluid-fluid interface, the adsorption of surfactant molecules favours an expansion of the interface, and this must be balanced against the tendency for this area to contract under normal surface tension forces. This "expanding pressure" (or

Surface Pressure) of an adsorbed layer of surfactant is denoted by π and is related to the surface (or interfacial) tension by the expression (G2):

$$\gamma = \gamma_0 - \pi$$

Where γ_0 = Surface tension of the pure solvent in mN m^{-1}

γ = Surface tension of the surfactant solution in mN m^{-1}

The size of π depends upon the nature of the lyophobic part of the surfactant molecules. As the group becomes more lyophobic so does the value of π increase. A rough generalisation known as Traube's rule, is that for a given homologous series, the concentration of surfactant required for an equal lowering of surface tension, in dilute solution, decreases by a factor of approximately 3 for each additional CH_2 group in the chain (S2).

If upon addition of the surfactant, the interfacial tension between the two liquids is reduced sufficiently, then emulsification will take place (Section 1.4). This occurs because only a relatively small increase in surface free energy is involved. If $\pi > \gamma_0$ either the liquids will become miscible or spontaneous emulsification may occur.

1.3.2 Thermodynamics of Adsorption ; Gibbs Adsorption Equation

From section 1.3.1 it is evident that there is an excess of surfactant molecules present in the interfacial/surface region compared to that in an equivalent portion of

the bulk phase. This is known as the surface excess concentration (Γ) of the surfactant. The extent of adsorption is dependant on the concentration of surfactant present in the bulk phase; for a particular surfactant under specified conditions. However, this may not be the case for adsorption onto solids as the surfaces can be very large and non-electrostatic forces may be involved.

The extent of adsorption of a surfactant at a fluid-fluid interface is usually determined indirectly from values of surface tension or interfacial tension, γ . Changes in γ are related to the amount of component, i (Γ_i) and the change in chemical potential of i (μ_i) by the Gibbs equation (B2):

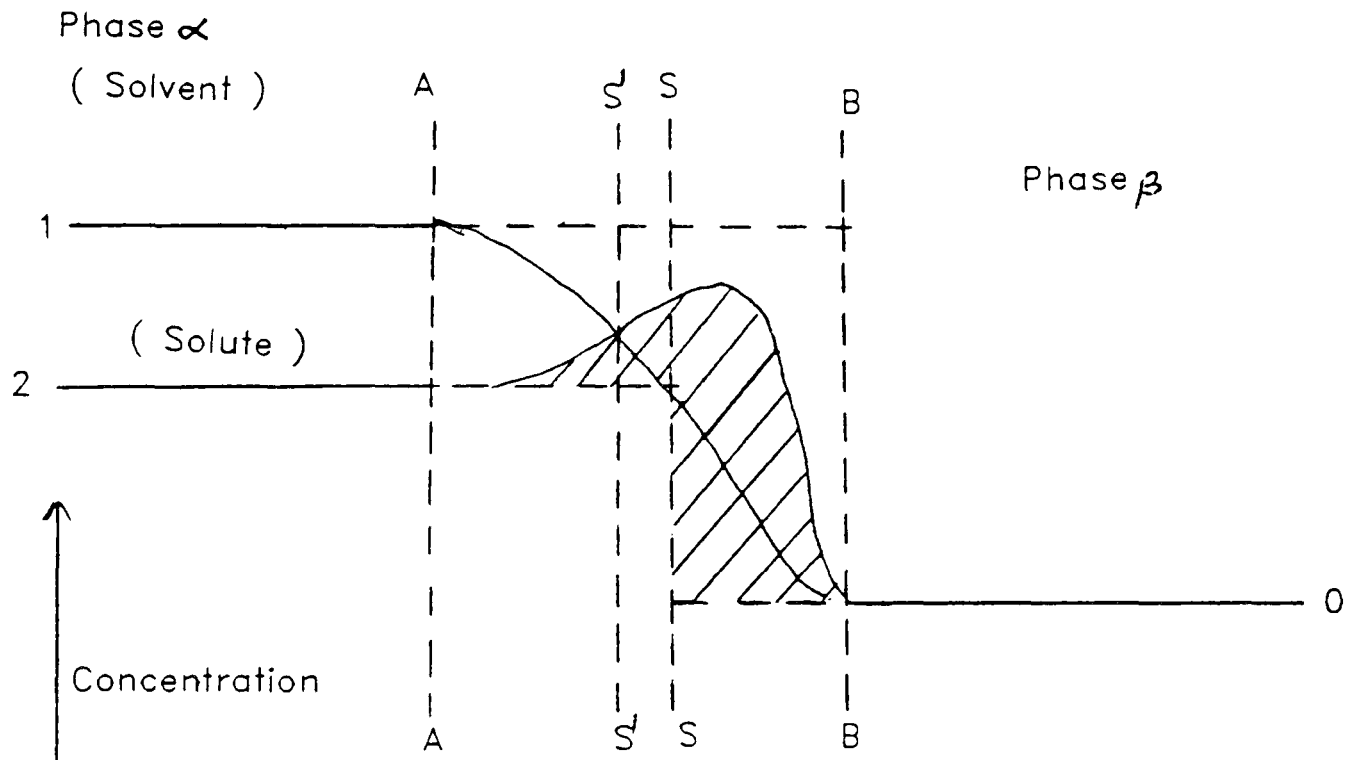
$$-d\gamma = \sum_i \Gamma_i d\mu_i \quad (1.4)$$

The simplest case of this isotherm is a two component system in which the solute (2) is surface active i.e. it is adsorbed at the surface of the solvent (Fig 2). For such a case equation 1.4 may be written :

$$-d\gamma = \Gamma_1 d\mu_1 + \Gamma_2 d\mu_2 \quad (1.5)$$

If the *Gibbs Dividing Surface* is used (the plane at which the solvent concentration is zero) (Fig 2), $\Gamma_1 = 0$ and equation 1.5 becomes

$$-d\gamma = \Gamma_2^{(1)} \cdot d\mu_2 \quad (1.6)$$



- (I) Region Between A and B is regarded as a Surface Phase Having Finite Thickness.
- (II) Gibb's Model Proposes the Two Phases Meet at an Arbitrary Surface (S - S) and the Amount of Adsorption of a Component here is Defined as the Surface Excess of that component.

The Plane S' - S', For which one Component (usually the solvent) is Ten, is the Gibb's Dividing Surface.

Figure 2. Model of adsorption in the surface phase.

Where $\Gamma_2^{(1)}$ is the *relative adsorption* of (2) with respect to (1).

In the bulk solution, at equilibrium with the surface, the chemical potential of the solute, μ_2 , is related to its activity, a_2 , by

$$\mu_2 = \mu_2^\circ + RT \ln a_2 \quad (1.7)$$

in which the standard chemical potential of (2), μ_2° , refers to a solution of ideal activity with either $a_2 = c_2 f_2$, or $a_2 = x_2 f_2$, where c_2 is the bulk concentration of (2), x_2 its mole fraction and f_2 is the appropriate activity coefficient.

Differentiating equation 1.7 gives

$$d\mu_2 = RT d(\ln a_2) \quad (1.8)$$

and substituting for $d\mu_2$ from 1.8 into equation 1.6 gives

$$\Gamma_2^{(1)} = -\frac{1}{RT} \cdot \frac{d\gamma}{d \ln a} \quad (1.9)$$

For dilute solutions a_2 approximates to c_2 giving

$$\Gamma_2^{(1)} = -\frac{1}{RT} \cdot \frac{d\gamma}{d \ln c_2} \quad (1.10)$$

which is the usual form of the Gibbs equation.

For a solution of an ionic surfactant, in the absence of any other electrolyte, Aveyard, Haydon and co-workers (A1,H3) have argued that equations 1.9 and 1.10 should be modified to allow for the fact that both the surfactant molecules and their counter-ions will adsorb at the interface in order to maintain local electrical neutrality. For a solution of a 1:1 ionic surfactant, a factor of 2 is required to allow for this simultaneous adsorption, and a more general form of the Gibbs equation is thus

$$\Gamma_2^1 = -\frac{c_2}{nRT} \cdot \frac{d\gamma}{dc_2} \quad (1.11)$$

in which,

$n = 2$ for ionic surfactants in the absence of inert electrolyte, and

$n = 1$ for nonionic surfactants, and ionic surfactants in the presence of excess inert electrolyte.

That this factor should be used is supported by evidence from direct measurements of surfactant molecules adsorbed at the air-water interface using radio-labelled materials (C1).

1.3.3 Micelle Formation

In addition to adsorption at the interface, surfactant molecules can form aggregates called *Micelles*. These form through the interactions of the lyophobic part of the molecule, usually a long hydrocarbon chain, when the concentration of surfactant in solution reaches a specific critical value. A lowering in free energy occurs on

formation of these aggregates. A schematic representation of a micelle for an ionic surfactant in aqueous solution is shown in Fig 3. It has been observed (J1,P3,M2) that physical properties of surfactant solutions, which normally depend upon the number of solute molecules per unit volume of solution, often show a discontinuity at a particular concentration, called the *Critical Micelle Concentration (CMC)* above which the rate of change of the physical properties change very slowly with respect to the surfactant concentration (Fig 4).

The energetics of micellisation can be explained in terms of the lyophobic portion of the surfactant molecule, assuming the following is taken into account :

- (i) The intermolecular attractions between the hydrocarbon chains in the interior of the micelle represent an energetically favourable situation; however, in the case of single dissolved surfactant molecules, it is not one which is significantly more favourable than that which results from the alternative hydrocarbon-water interaction.
- (ii) Micellisation permits, in aqueous solution, strong water-water interaction (hydrogen bonding) which would be otherwise prevented if the solute were to be in solution as individual molecules sandwiched between the solvent water molecules. This is a very important factor, both in micelle formation and any adsorption process at an aqueous interface. This is known as the *Hydrophobic Effect (T3)*.

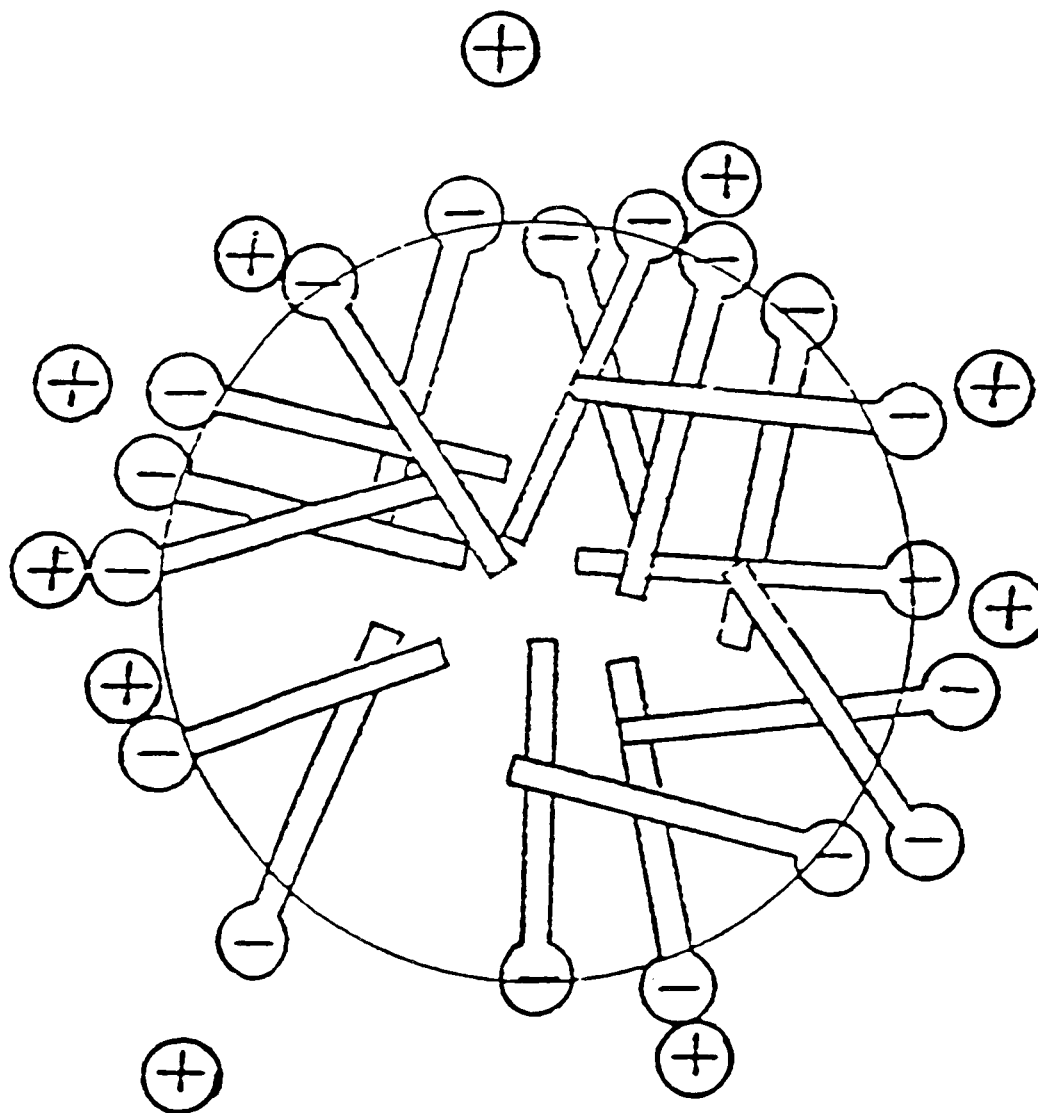


Figure 3. A schematic representation of an ionic micelle.

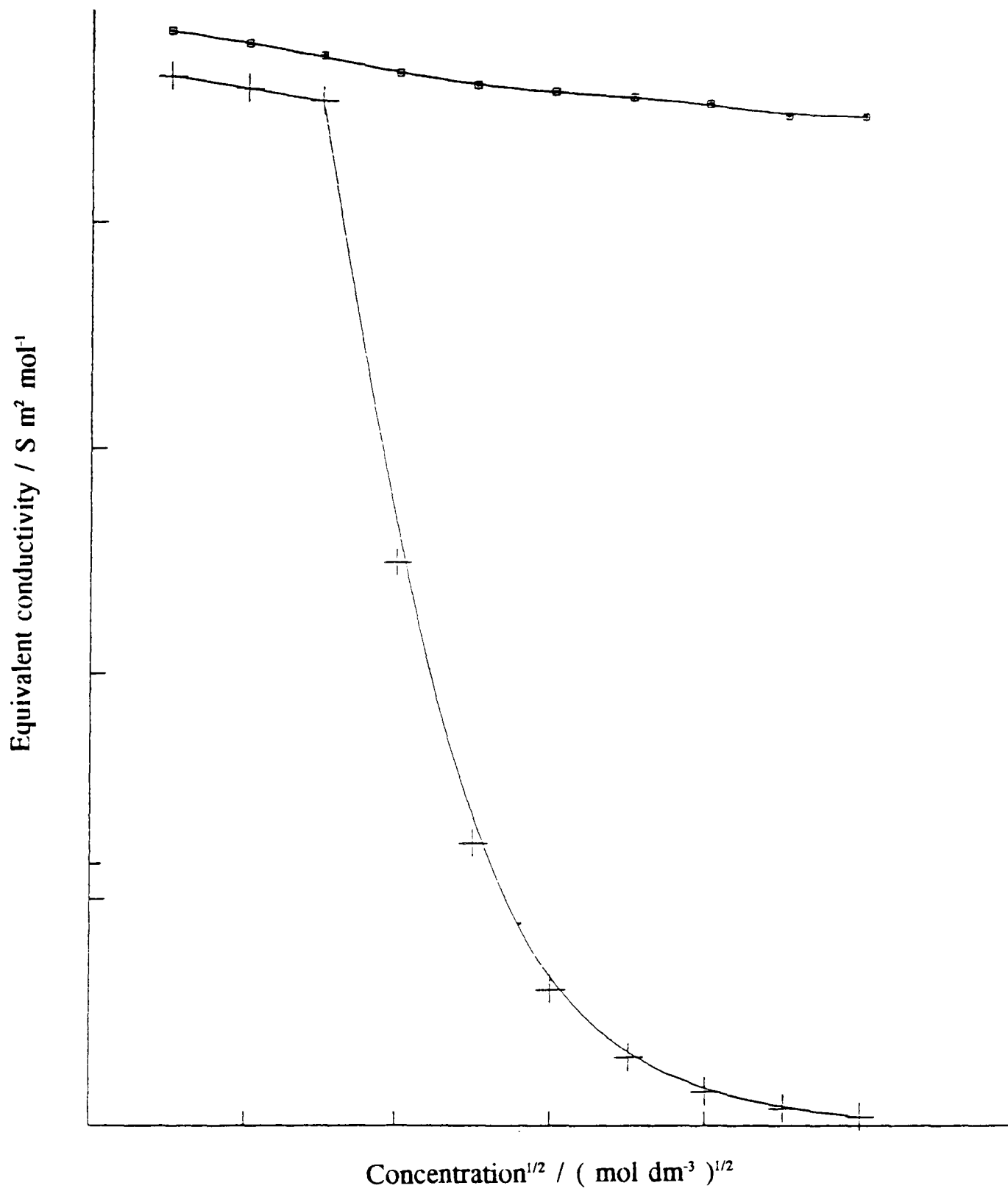


Figure 4. Variation of equivalent conductivity with the square root of the concentration for aqueous solutions of a surfactant and non-surfactant electrolyte (taken from ref R2).

1.3.3.1 The Phase Separation Model

This model gives the clearest definition of the CMC and may be formulated by assuming that the chemical potential of the surfactant in the micellar state is constant at a given temperature and may be adopted as the standard chemical potential, analogous to the standard chemical potential of a pure liquid or solid (S3).

Micelles are considered to be a separate phase with phase separation occurring at the CMC. Therefore the monomeric surfactant and the micellar surfactant are only in equilibrium at the CMC and the monomer activity should therefore remain constant above the CMC.

Representing the equilibrium by :

$$\mu_m = \mu_1 + RT \ln a_1$$

where,

μ_1 = the standard chemical potential of the surfactant monomer in solution,

μ_m = The standard chemical potential of the surfactant in the micellar state,

a_1 = The activity of the surfactant monomer in solution.

It can be shown that the standard free energy of micellisation,

$$\Delta G_m = RT \ln (\text{CMC}) \quad (1.12)$$

1.3.3.2 Mass Action Model

In its basic form this model postulates a dynamic equilibrium between monomers and a single micellar species (H4,E1). For a nonionic surfactant, if c is the concentration of surfactant in solution, x the fraction of monomer aggregated and m the number of monomer units in a micelle, then

$$mX = (X)_m$$

i.e. $c(1-x) = cx / m$

Applying the law of mass action,

$$K_m = \frac{c x m^{-1}}{[C(1-x)]^m}$$

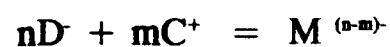
For large values of m (> 50), the standard free energy of micellisation, ΔG_m , can be shown to be :

$$\Delta G_m = RT \ln (CMC) \quad (1.13)$$

which is the same expression as that from the phase separation model for micellisation. This model assumes that the association of monomers into the micelle is a co-operative process and that micelles with small values of m are unstable: a

situation which in more recent times has been questioned as valid (J2). The model permits an extension to be made to ionic surfactant micelle formation, in which the micelles attract a substantial number of counter-ions into an attached layer.

For anionic surfactants, the equilibrium model may be represented as :



where,

D^- are surfactant monomers, and

C^+ are bound counter-ions.

Upon micellisation, only a fraction of the charge is neutralised; thus a micelle is formed which has an effective charge of p units (= $n-m$).

From the law of mass action :

$$K_m = \frac{M^{-p}}{[C^+]^m [D^-]^n}$$

It has been shown (A2,P4) that providing n is large, there is a rapid increase in M^p which occurs over a narrow range of $[D^-]$.

The free energy of micellisation can then be shown to be (S3):

$$\Delta G_m = RT (1+m/n) \ln (CMC) \quad (1.14)$$

and this may be compared to equation 1.13 for nonionics.

Both the phase separation model and the mass action model of micellisation represent a simple picture of micelle formation and make several assumptions (F1).

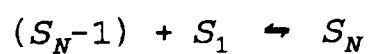
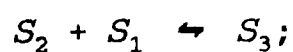
- i) Interactions between monomers and micelles at the CMC are negligible. This would appear to be untrue as a rapid dynamic equilibrium has been shown to exist (G3).
- ii) Counterions are considered to be either bound or unbound, i.e. there are no intermediate states.
- iii) The micelle is assumed not to contain any solvent. Evidence, however, has shown that solvent may penetrate the palisade layer of the micelle (R2).

Despite the above assumptions both models do fit reasonably well with observed data.

1.3.3.3 Multiple Equilibrium Model

There is much evidence that the aggregation number of micelles varies greatly with temperature (Z1), especially for nonionic surfactants (B3), and there is also reason to suppose that aggregation numbers may vary with the total concentration of surfactant available (B4). An extension of the mass action model allows for the

existence of a range of values of N by postulating a multiple equilibrium, characterised by a series of equilibrium constants, K_2, K_3, K_4, \dots



These equilibria may also be represented by a series of association reactions of monomers :



Where $N = 2, 3, 4, \dots$

such that

$$K_N = \frac{[S_N]}{[S_1]^N}$$

and then ,

$$K_N = \sum_{i=2}^N k_i$$

or

$$\ln K_N = \sum_2^N \ln K_i$$

A series of standard free energies can be equated to each of these equilibrium constants. It is more convenient to represent the standard free energy change by use of a standard chemical potential, $\mu_{mic,N}^\circ$, per surfactant molecule (T3). The distribution of surfactant molecules between micelles of different sizes, N, can then be determined by the variation of $\mu_{mic,N}^\circ$ with N. The chemical potential per mol of surfactant in the micelle of aggregation number N, is thus given by

$$\mu_{mic,N} = \mu_{mic,N}^\circ + \frac{RT}{N} \ln \frac{X_N}{N}$$

In which X_N is the mol fraction of surfactant in the micelle of this size.

For an enclosed volume of any shape, the ratio of surface to volume decreases as the volume increases, so that the area of the surface of the micelles per hydrocarbon chain contained decreases. Therefore the Hydrophobic effect (Section 1.3.3) ensures that $\mu_{mic,N}^\circ$ will decrease sharply as N increases, at least until the total volume of the micelle-core attains that of a sphere of radius equal to the extended length of the hydrocarbon chain. This is the *Cooperative effect* which precludes low values of N. It has been suggested (T3) that as the surface area per surfactant molecule decreases,

repulsion forces between head groups cause $\mu_{mic,N}^*$ to increase, and the optimum value, N^* , arises from a balance of these opposing forces.

1.4 Emulsion Formation and Oil Recovery

Emulsions are suspensions of droplets of one liquid in a second immiscible liquid. They are generally quite stable and can be divided into two types; oil-in-water and water-in-oil depending upon the nature of the suspending medium. Pure liquids cannot form emulsions and the addition of an emulsifier or stabiliser is required. These emulsifier or stabilisers are usually surfactants.

During oil-field production the most commonly encountered emulsion is that of water-in-oil. The process of oil recovery causes these emulsions to form and while this is usually an undesirable situation, it is one which is deliberately introduced during tertiary oil recovery. However, these emulsions must be separated into their component parts which can place great economic demand on the process (W2).

1.4.1 Emulsions in Primary and Secondary Oil Recovery

In primary oil recovery large pressure drops occur due to the bore holes acting as pressure sinks and also the expansion of gases within the oil which causes the reservoir fluid to migrate often at considerable velocities through porous rock structures which provide the opportunity for the mixing and formation of small droplets. The emulsions formed are then stabilised by naturally occurring surface

active agents within the crude oil such as long chain fatty acids and esters, and porphyrins.

The formation of emulsions during secondary oil recovery is almost inevitable as both polymers and surfactants may be added to waterfloods which will stabilise any emulsions formed. Therefore as a result of this the correct choice of both polymer and surfactant must be made so that the breaking of the formed emulsion is done as easily as possible so that the process can be performed as economically as possible. In either primary or secondary oil recovery processes, once emulsions have been collected, the emulsions must be broken into their constituent parts. These emulsions are usually oil-in-water and can constitute up to 40% water. Most emulsions are only temporarily stable and can be resolved simply by allowing the fluids to stand until separation occurs. This can be speeded up by heating to reduce the viscosity and lower the effect of the naturally occurring emulsifiers. Another technique of breaking emulsions is by centrifugation (W2).

1.4.2 Emulsions in Tertiary Oil Recovery : Microemulsions

Microemulsions (S4,P5) are apparently homogeneous mixtures of oil and water which form spontaneously. They are thermodynamically stable and contain such small particles that turbidity is low. Spontaneous formation of an emulsion, with the associated decrease in free energy, is only attainable if the remaining liquid-liquid interfacial free energy can be compensated for by the entropy of dispersion of the droplets in the medium. While surfactants do lower interfacial tensions, in most

cases the CMC or solubility limit is reached before the interfacial tension is reduced to a low enough value (ca. 10^{-3} mN m⁻¹) for spontaneous emulsification to occur. The addition of a second surfactant (*Co-surfactant*), usually of completely different chemical nature to the first can help reduce the interfacial tension to an ultralow value.

By considering the Gibbs equation for a two component system the effectiveness that the addition of a co-surfactant can have on the interfacial tension between two liquids can be illustrated. For a two component system, the change in interfacial tension can be related to the interfacial excess concentration, Γ_i , and change in chemical potential through

$$d\gamma = -(\Gamma_1 \cdot d\mu_1 + \Gamma_2 \cdot d\mu_2) \quad (1.16)$$

Equation 1.16 shows that the addition of a co-surfactant, which is positively adsorbed at the interface, will always produce a further lowering of γ . It might be noted that, in some cases, certain single surfactants will lower γ far enough for microemulsion formation to occur, for example the surfactant Aerosol AOT (sodium diethylhexylsulpho-succinate). However it is usual to add a co-surfactant to achieve ultra-low surface tensions.

1.4.3 Microemulsions in Tertiary Oil Recovery (B5)

The technique of surfactant flooding to recover residual oil from a well has been

discussed previously (Section 1.2.3.3). As mentioned, the mechanism by which the oil is recovered using this technique is the reduction of the oil-water interfacial tension to an ultralow value. Reduction of the interfacial tension to such a value causes spontaneous emulsification to occur with the formation of microemulsions. The purpose of forming these microemulsions is to enable the residual oil to be removed from sandstone pores and to allow the recovered oil to be pushed through the capillary structure without being hampered by the pressure drop at the curved oil-water interface with a normal interfacial tension (Section 1.2.3). This process is not simple, however, being complicated by the reservoir temperature, salt concentration and loss of surfactant by adsorption and precipitation in the well. The loss of surfactant by adsorption is thought to take place at a clay-water interface which leads to a loss in the concentration of surfactant in solution and ultimately to the loss of the ultralow interfacial tension.

1.5 Clay Mineral Structure and Charge Distribution

Reservoir structures are comprised typically of silicate (or carbonate) rock which contain clay minerals. The clay component is of major importance when considering tertiary oil recovery mechanisms as this is where most surfactant will be lost due to adsorption. Therefore, an understanding of the structure of clay minerals is important in understanding the mechanisms by which the surfactants are lost.

1.5.1 The Mineral Structure of Clays

The principal building elements of clay minerals are two-dimensional arrays of silicon-oxygen tetrahedra, and aluminium (or magnesium) oxygen-hydroxyl octahedra. Due to the similar symmetry of these structures sharing of oxygen atoms between "sheets" can occur.

This can happen in two ways;

- (i) the oxygen atoms between one silica and one alumina sheet are shared to form a "two-layer" mineral or a 1:1 structure and,
- (ii) the oxygen between two silica and one alumina (this being the central sheet) to form a "three-layer" or 2:1 structure.

These combined sheets constitute a unit layer which when stacked parallel to each other form the clay mineral.

Clays can be classified into two groups :

- (i) an amorphous group which includes such minerals as allophane and evansite, and
- (ii) a crystalline group which includes Kaolins, Illites and Montmorillonites.

The work carried out in this report is concerned mainly with the kaolinite group and a description of structure is given below.

1.5.2 Structure of Kaolin

The Kaolin group is an almost perfect two-layer structure and consists mainly of the minerals Kaolinite, Dickite, Nacrite and Halloysite. These minerals are non-expandable and the main difference between them is due to the stacking of the unit layer.

Kaolinite is the mineral most abundant in this group and samples used consist of up to 98% of this mineral. Electron micrographs of the kaolin samples used in this study show the material to be made up of hexagonal type plates about 1 μm in length (Figure 5).

The lattice structure of Kaolin consists of a tetrahedrally coordinated sheet of silicon (with oxygen) and an octahedrally coordinated sheet of aluminium (with oxygen and hydroxyl groups), giving a 1:1 structure. An additional layer of hydroxyl ions completes the charge requirements of the octahedral sheet (Figure 6).



Figure 5. Scanning Electron Micrograph showing the structure of the kaolin platelets.

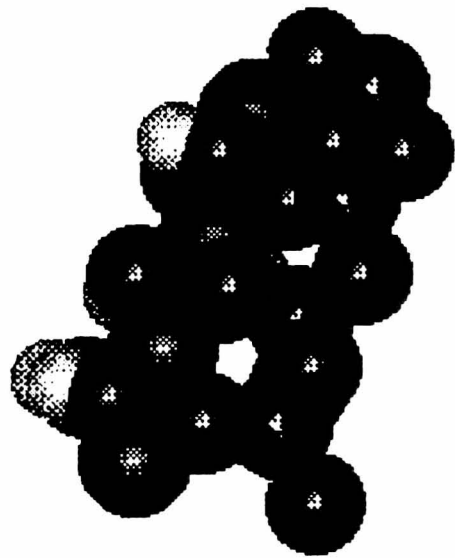


Figure 6. Atom arrangement in the unit cell of a two-layer mineral

1.5.3 The Origins of Charge and Potentials on Clays

Most workers accept the "heteropolar" model for surface charges proposed by Van Olphen in 1951 based upon electron micrograph evidence (O1). This has since been supported by Schofield and Samson using ion adsorption and rheological measurements (S5). The results suggest that the charge distribution through a kaolin particle is unequal, with the face carrying a negative charge which is unaffected by solution conditions whilst the edge charge can vary from positive to negative depending upon solution conditions (W3,F2,R3,T4,S6,O2).

Charges at the face of the Kaolin particles arise due to isomorphous substitutions of Al(III) for Si(IV) at the tetrahedral sites, or either Mg(II) or Fe(II) for Al(III) at the octahedral sites. The resulting negative charge is therefore internal to the structure and is thus fixed by the composition of the clay and will therefore not alter with changing solution condition. As the charge will remain constant there will be no point of zero charge (PZC) associated with the structural charge. The charge is distributed throughout the particle volume and hence interacts mainly through the flat-layer surfaces.

Unlike the face surfaces the edges of the clay mineral sheets terminate in broken, or unsatisfied, Si-O or Al-O bonds. These bonds hydroxylate in water producing SiOH and AlOH sites that are capable of amphoteric dissociation. Therefore, the edges of the clay particles develop a pH-dependent "surface" charge which can be positive or negative and capable of a PZC.

Hence, the net charge on the clay is the combination of the charge internal to the structure plus that from the edge sites. When the edge charge is negative then obviously as the internal charge is negative then the overall charge will be negative. If, however, the edge charge is sufficiently positive then neutralisation of the face charge can occur giving the particle an overall charge of zero. However, at the point where pH gives an overall zero particle charge is not a point of zero charge. The two reasons for this are as follows:

- (i) A PZC is defined in terms of a potential determining ion and the particle charge is not determined exclusively by potential determining ion adsorption.
- (ii) The surface potential should be zero at the PZC. The potentials between the particle faces and the solution, and between the particle edges and solution, are certainly not zero when the particle charge is zero as a net surface charge is required to neutralise the internal permanent structural charge.

The pH at which the net particle charge is zero in the presence of indifferent electrolyte is known as the iso-electric point (IEP). If the maximum edge charge is small relative to the structural charge, it may not be possible to achieve a net zero charge on the particle without first adsorbing a positive species to the particle.

1.6 The Electrical Double Layer

Most substances acquire a surface electric charge when brought into contact with a polar (e.g. aqueous) medium, the possible charging mechanisms being ionisation, uneven ion adsorption and ion dissolution. This surface charge generates an ionic atmosphere, part of which is diffuse, in which ions of opposite charge to that of the particle (the *counter-ions*) are concentrated close to the surface while those of similar charge (the *co-ions*) are repelled. Such a distribution of charge comprises the electric double layer of the particle, a concept first introduced by Helmholtz in 1879 and later modified by Gouy and Chapman (1917-19) and Stern (1924), and which has been described extensively in the literature of colloid chemistry (O1,O3,H5) and electrochemistry (G4,C2,S7).

The net result of this ion distribution is that close to the charged surface there is an excess of counter-ions over co-ions, the difference decreasing with distance until in the bulk solution they are equivalent in order to maintain electroneutrality. The potential, ψ , within the diffuse layer decreases exponentially with distance x from its value ψ_0 at the surface, until it reaches zero in the bulk solution. The mathematical treatment of the double layer is complex and has only been solved satisfactorily for the special cases where the surface is represented as either a sphere or a flat plate. For the latter case the fundamental equation for the double layer may be expressed as (O3):

$$\frac{d^2\psi}{dx^2} = -\frac{2 Z e n_0}{\epsilon} \sinh\left[\frac{Z e \psi}{kT}\right]$$

with the boundary condition that for $x = 0$, $\psi = \psi_0$, and when $x = \infty$, $d\psi/dx = 0$, the solution of which is given by:

$$\psi = \frac{2 kT}{Z e} \ln \left(\frac{1 + \gamma \exp[-\kappa x]}{1 - \gamma \exp[-\kappa x]} \right)$$

where,

$$\gamma = \frac{\exp [Z e \psi_0 / 2 kT] - 1}{\exp [Z e \psi_0 / 2 kT] + 1}$$

and

$$\kappa = \left(\frac{2 e^2 n_0 Z^2}{\epsilon kT} \right)^{1/2}$$

in which, $e =$ the electronic charge / C

$n_0 =$ the bulk concentration of ions / mols m^{-3}

$Z =$ the valency of the ions

$\epsilon =$ the static permittivity of the medium / F m^{-1} .

Equation (1.17) describes the reduction in potential as a function of distance from the surface, and at small surface potential, viz: $\psi_0 \ll 25$ mV such that $(Z e \psi_0 / 2 kT) \ll 1$, the equation reduces to (ref 53):

$$\psi = \psi_0 \exp(-\kappa x) \quad (1.21)$$

showing that the potential decreases exponentially with distance from the surface.

The surface charge, σ_0 , is related to the surface potential, ψ_0 by (H6):

$$\sigma_o = (8n_o \epsilon kT)^{1/2} \sinh\left(\frac{Ze\psi_o}{2kT}\right)$$

which for small surface potentials ($\psi_o \ll 25$ mV) reduces to:

$$\sigma_o = (8n_o \epsilon kT)^{1/2} \cdot (Ze\psi_o) = \epsilon \kappa \psi_o$$

and hence the double layer is theoretically equivalent to a parallel plate condenser with a distance $1/\kappa$ between the plates. This is equivalent to assuming that all the ions in the diffuse part of the double layer are located in a single plane at a distance $1/\kappa$ from the surface. The distance $1/\kappa$ is called the *double layer thickness* and its magnitude varies with electrolyte concentration, viz 1 nm (10 Å) in 0.1 mol dm⁻³ to 100 nm (1000 Å) in 10⁻⁵ mol dm⁻³ monovalent electrolyte solution.

Electrical Double Layer Capacitance

The Gouy-Chapman theory of the electric double layer, based upon the assumption that:

- i) electrolyte ions are point charges, and
- ii) the solvent has no structure and is of constant permittivity,

was modified by Stern to allow for the finite size of hydrated ions. The capacitance, C, of such a model may be defined by the equation (S2):

$$C = \frac{d\sigma_o}{d\psi_o}$$

which, upon differentiation of equation (1.21) is given by:

$$\frac{d\sigma_o}{d\psi_o} = \epsilon \kappa \cosh\left[\frac{Z e \psi_o}{2 kT}\right]$$

$$= 228.5 Z c^{1/2} \cosh(19.46 Z \psi_o) \mu\text{F cm}^{-2}$$

where the electrolyte concentration, c , is expressed in mol dm^{-3} , at 25°C , and ψ_o in volts.

Addition of electrolyte to the system, while reducing the double layer thickness, increases its capacitance, thus increasing the σ_o/ψ_o ratio. The response of the two types of double layer (constant charge and constant potential) to the increase in electrolyte concentration will therefore differ (S2):

ψ_o decreases if σ_o is constant, and

σ_o increases if ψ_o is constant.

Zeta Potential

According to the Stern model of the electric double layer, ions may adsorb at solid surfaces, either specifically or nonspecifically (see earlier), such that they overcome thermal agitation. The double layer is then considered as being made up of two parts, the first a compact layer of thickness δ adjacent to the surface and the second consisting of the diffuse Gouy layer (Fig 7). The potential at the boundary between the Stern and Gouy layers ψ_s , which determines the potential decay within the solution, may have the same or opposite sign to that of the surface, or may be zero. There is no satisfactory method of determining ψ_o and ψ_s for hydrophobic systems, however, from the measurement of the velocity of a charged particle in an electric field a potential called the *zeta potential* (ζ), can be obtained. The zeta potential is defined as the potential at the surface of the shear separating the particle, with any attached solvent and ions which move with the particle, from the electrolyte solution. The technique of microelectrophoresis is the most accurate method for measurement of the electrophoretic velocity of lyophobic systems and provides a number of advantages over other methods of measurement, such as moving boundaries (S8):

- i) the particles are observed in the normal solution environment,
- ii) very dilute solutions can be studied so that flocculation rates, even at high electrolyte concentration or near the point of zero charge, are negligible,

- iii) the high magnification of the ultramicroscope system leads to short observation times and high sensitivity, and
- iv) in a polydisperse solution the particles in a chosen size range can be observed while others are ignored.

The relationship between the electrophoretic velocity, V , and zeta potential, ζ , of a particle depends upon the magnitude of the product $\kappa\alpha$, that is on the relative magnitudes of the particle radius, α , and the double layer thickness.

When $\kappa\alpha \gg 1$, the Smoluchowski approximation (S9), the electrophoretic retardation is communicated to the particle (D1).

Henry (1931) resolved the situation by consideration of the applied field. Smoluchowski had assumed the field to be parallel to the particle surface, while Hückel had disregarded the deformation of the applied field by the presence of the particle. As Figure 8 shows, these assumptions are justifiable in the extreme situations of $\kappa\alpha \gg 1$ and $\kappa\alpha \ll 1$ respectively.

Henry showed that when the external field was superimposed on the local field around the particle the velocity could be written:

$$V = \frac{2}{3} \epsilon \zeta \frac{E}{\eta} \cdot f_1(\kappa\alpha)$$

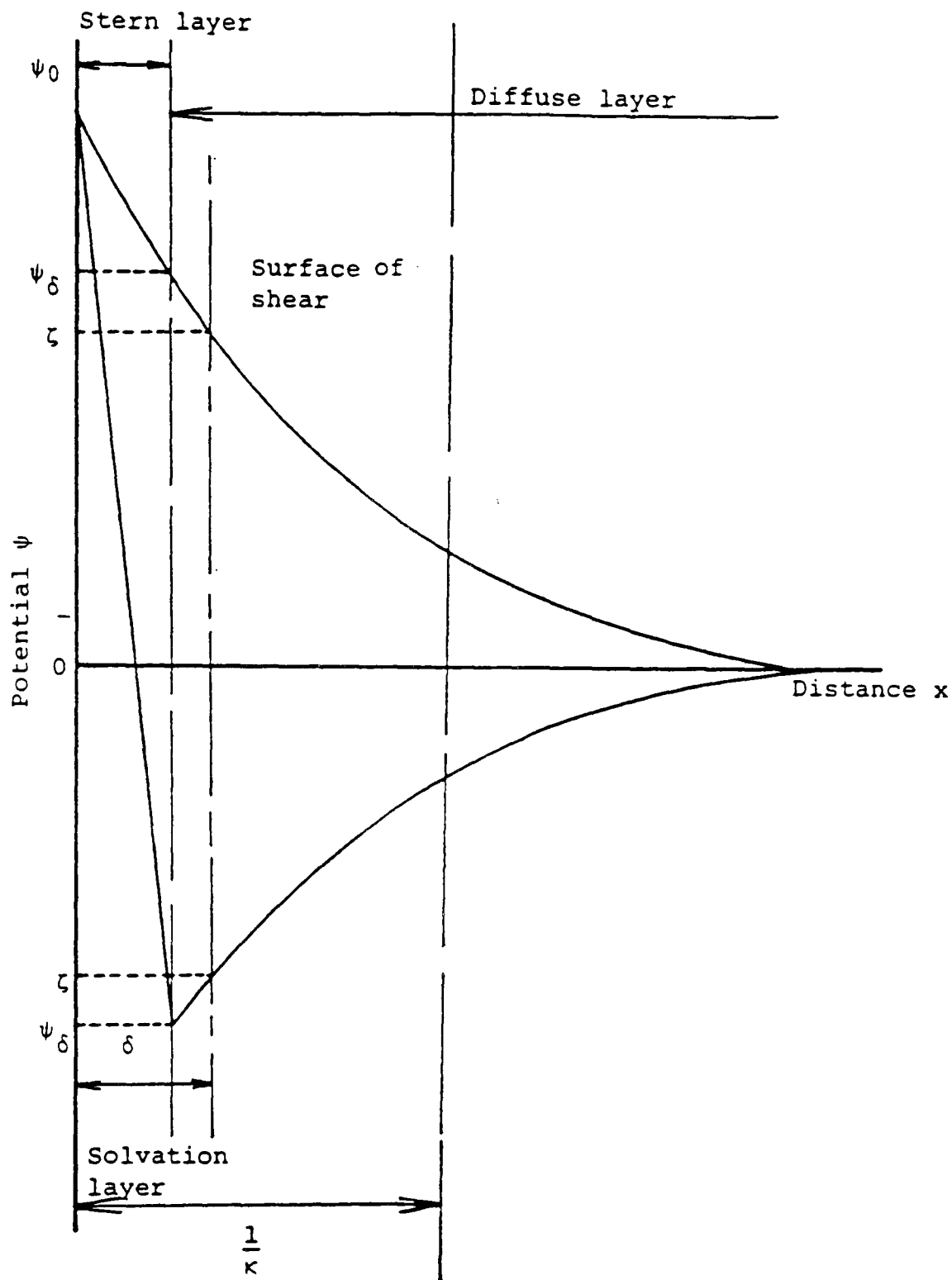


Figure 7. Potential decay curves for an electrical double layer associated with a colloidal particle whose surface potential is ψ_0 . The lower curve results from strong adsorption in the Stern layer.

in which the function $f_1(\kappa\alpha)$ depends on the particle shape. Values of $f_1(\kappa\alpha)$ for a spherical particle are shown in Table 1. Note that $f_1(\kappa\alpha)$ approaches 1 for small $\kappa\alpha$ and 3/2 for large $\kappa\alpha$. The smooth transition from the Hückel to the Smoluchowski equation, as $\kappa\alpha$ increases, is shown in Figure 9 for a non-conducting particle.

Table 1. Values of the Henry correction factor, $f_1(\kappa\alpha)$ to be used in equation (1.28), as a function of $\kappa\alpha$

$\kappa\alpha$	$f_1(\kappa\alpha)^*$	$\kappa\alpha$	$f_1(\kappa\alpha)$
0	1.000	5	1.160
1	1.027	10	1.239
2	1.066	25	1.370
3	1.101	100	1.370
4	1.133	infinity	1.500

* for a sphere, $\kappa\alpha > 1$, where,

$$f_1(\kappa\alpha) = \frac{3}{2} - \frac{9}{2\kappa\alpha} + \frac{75}{2\kappa^2\alpha^2} - \frac{330}{\kappa^3\alpha^3}$$

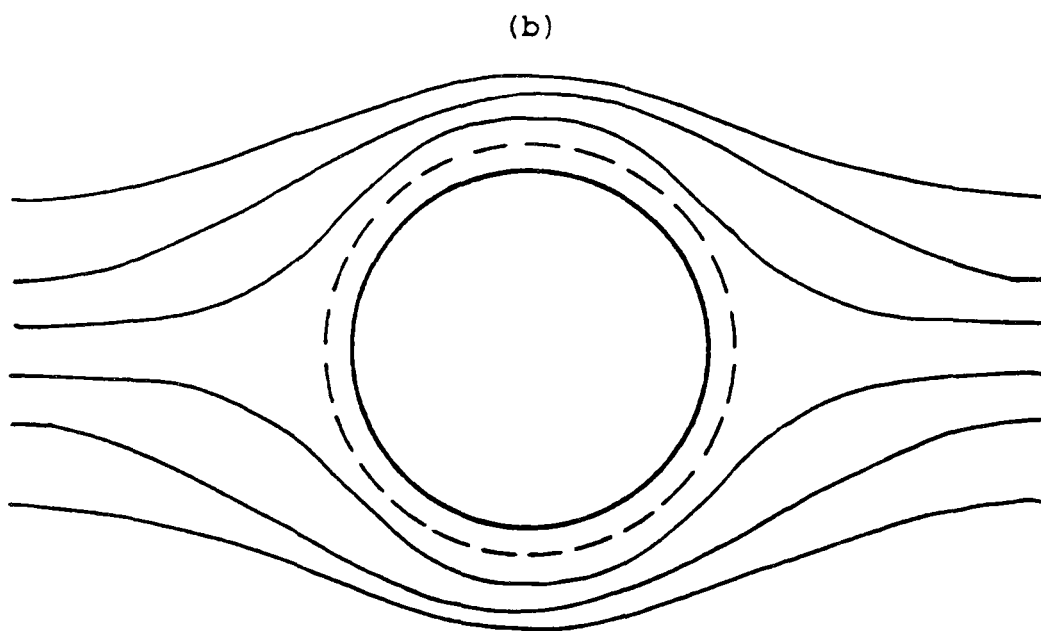
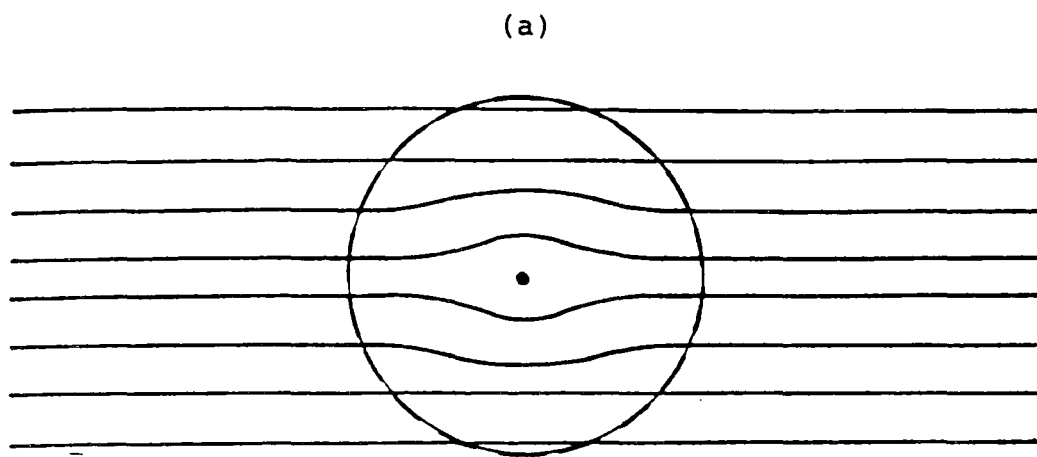


Figure 8. Effect of a non-conducting particle on the applied field
(a) $\kappa\alpha \ll 1$; (b) $\kappa\alpha \gg 1$. The broken line is at a distance $1/\kappa$ from the particle surface.

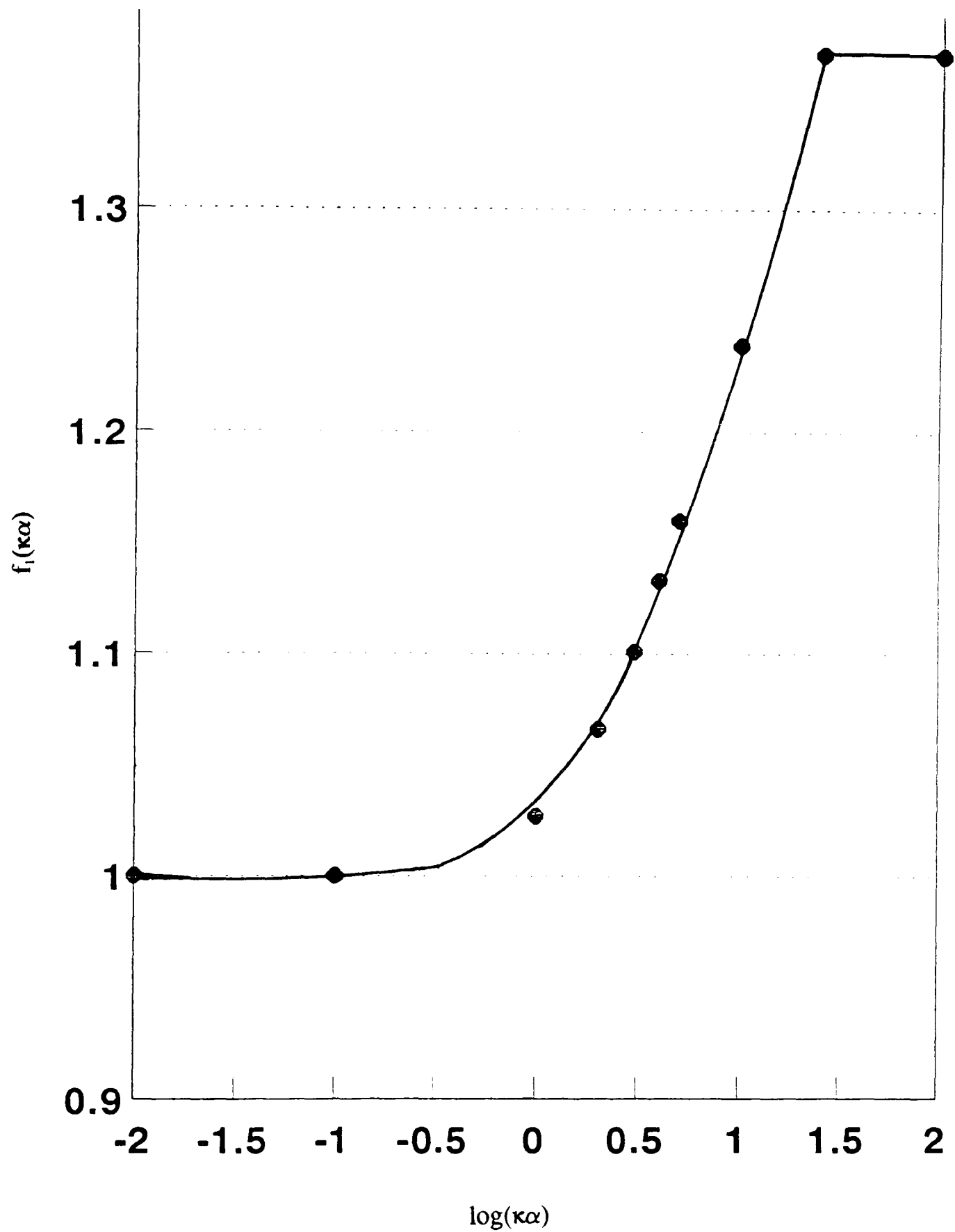


Figure 9. Variation of the Henry function, $f_1(\kappa\alpha)$ with $\log(\kappa\alpha)$, showing the influence of an insulating sphere on an imposed electric field.

Chapter 2

Experimental

2.1 Minerals

Kaolin was purchased from the Aldrich Chemical Company and specified to be approximately 98% kaolinite ($\text{Al}_2\text{Si}_2\text{O}_5(\text{OH})_4$).

North Sea Reservoir Rock samples were obtained from Shell Expro., Aberdeen. These samples were used as obtained.

2.2 Chemicals

2.2.1 General Reagents

Sodium chloride, sodium hydroxide, sodium citrate, sodium pyrophosphate, sodium tripolyphosphate, EDTA, hydrochloric acid, calcium chloride, aluminium nitrate and n-butanol were all purchased as Analar grade reagents.

Potassium dichromate and concentrated sulphuric acid, for use in a chromic acid cleaning solution for the electrophoresis cells, were also purchased as Analar grade materials.

2.2.2 Reagents for the preparation of the isomerically pure surfactant.

All the reagents used in the preparation of the isomerically pure surfactant were

purchased from the Aldrich Chemical Company with the exception of Oleum, which was purchased from BDH.

n-Butyrophenone and n-Bromooctane were found to be within the given specifications by gas chromatography.

Magnesium turnings were purchased as 98% magnesium.

2.2.3 Reagents for the Two-Phase Titration

These were obtained from BDH:

Chloroform was of Analar grade.

Sodium dodecylsulphate (SDS) was purchased as a "specially purified" material and by analysis (see section 2.5.4) was found to be 99% pure.

Hyamine 1622 (Benzethonium chloride) was purchased as both a $0.004 \text{ mol dm}^{-3}$ aqueous solution and as a solid. This solid was used to prepare more concentrated or dilute solutions of the Hyamine for use in titration with the surfactant selective electrode. All solutions, whether purchased or prepared, were standardised against sodium dodecylsulphate.

The mixed indicator used in the two-phase titration (Dimidium bromide - Disulphine

blue VN) was obtained from BDH as a concentrated solution which was diluted and made slightly acidic (see section 2.5.4.1)

2.2.4 Reagents for use in Atomic Adsorption Spectroscopy

Aluminium nitrate was obtained as a 1000 parts per million solution ($37.1 \text{ mmol dm}^{-3}$) from BDH in $0.5 \text{ mol dm}^{-3} \text{ HNO}_3$.

Calcium was also obtained as a 1000 ppm solution.

100 ppm working solutions were prepared for both of the above.

2.3 Preparation of the isomerically pure surfactant - Sodium p-[1-propylnonyl]benzenesulphonate

A pure isomer of sodium dodecylbenzenesulphonate (DBS) was prepared. The isomer sodium p-[1-propylnonyl]benzenesulphonate ($4\text{-}\phi\text{-C}_{12}\text{ABS}$) (**5**) was prepared as outlined in Fig 10 (D2).

The synthesis began with a Grignard reaction between n-butyrophenone (**1**) and octylmagnesium bromide (**2**) which gave the alcohol (**3**). This was then dehydrated over $\text{CuSO}_4/\text{K}_2\text{SO}_4$ to yield a mixture of 4-phenyl-dodec-3-ene and 4-phenyl-dodec-4-ene (see Figs 11 and 12). This was then hydrogenated over a carbon supported palladium catalyst to the hydrocarbon 4-phenyldodecane (**4**) (Fig 13).

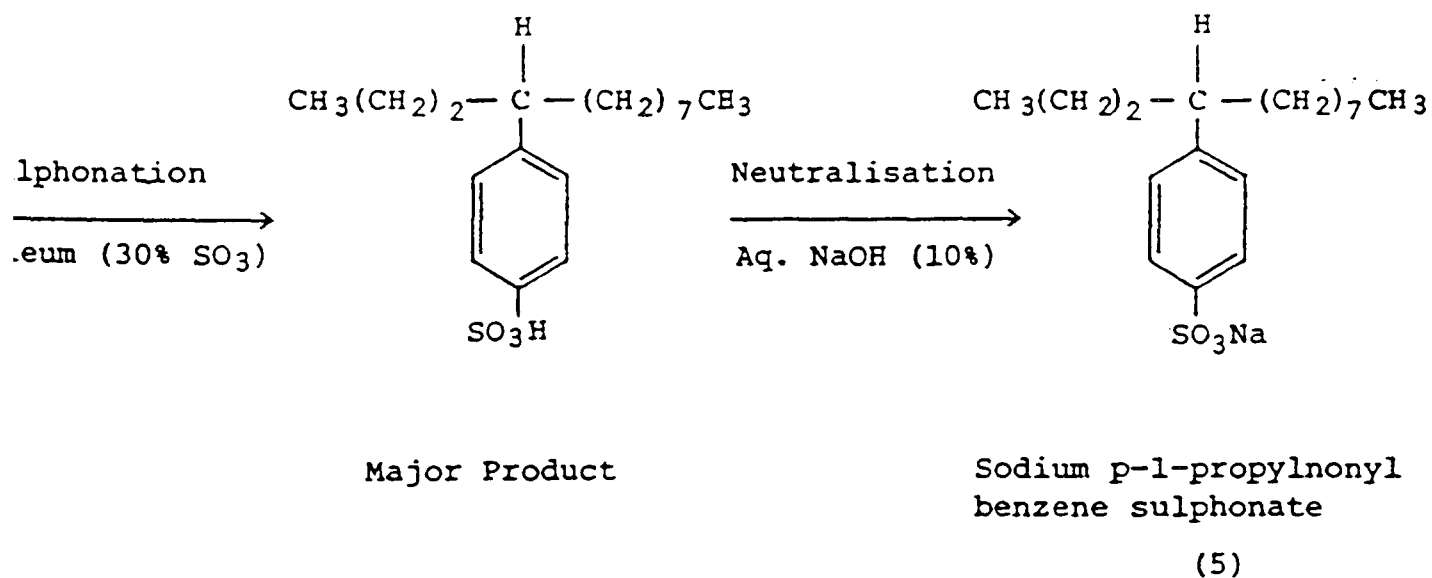
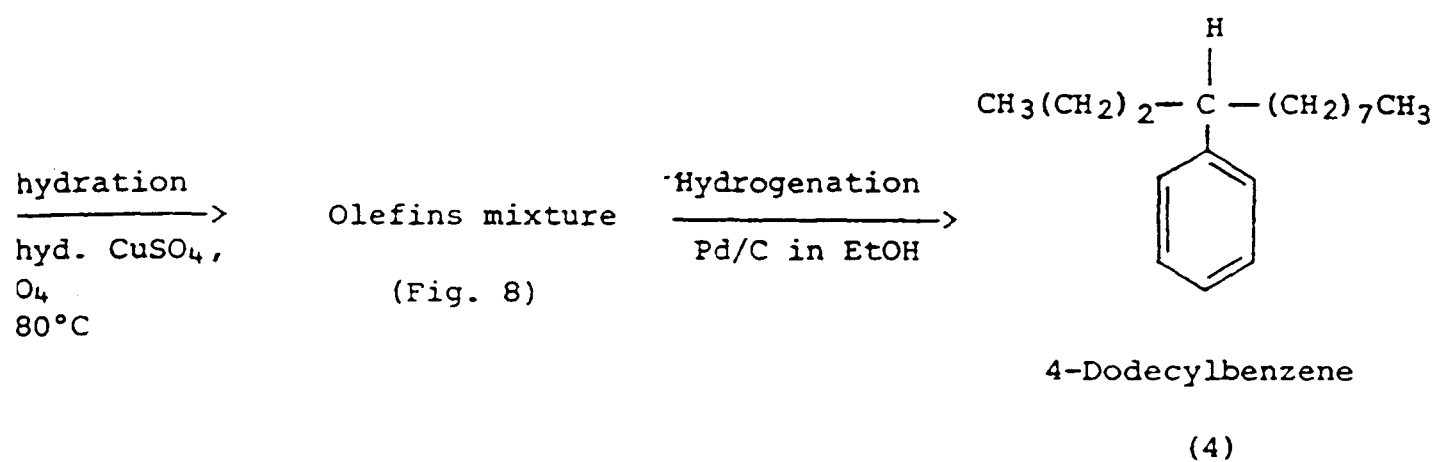
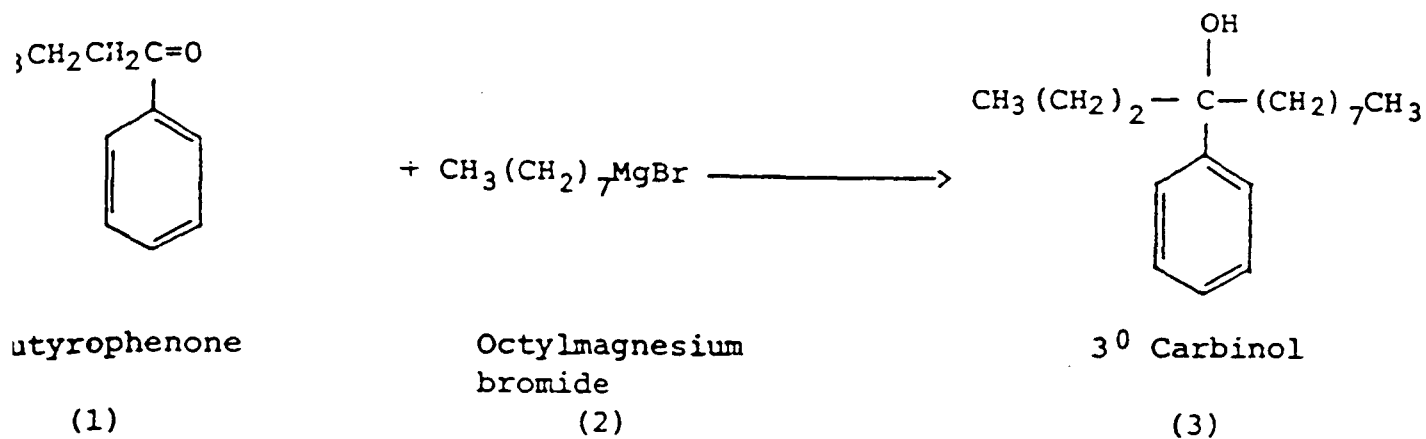


Figure 10. Preparation of isomerically pure surfactant 4- ϕ -C₁₂ABS.

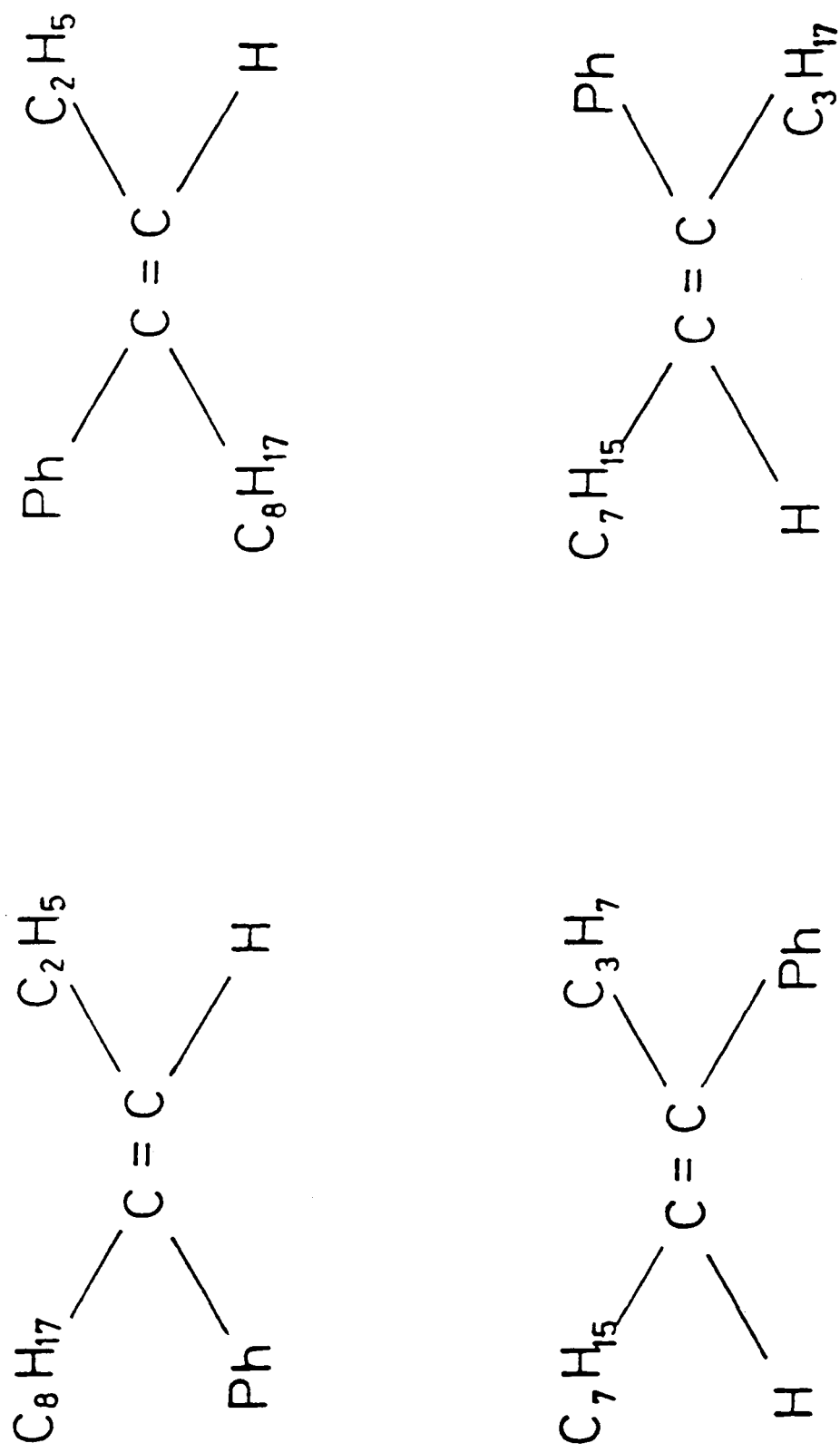


Figure 11. Isomers of 4-phenyldecene

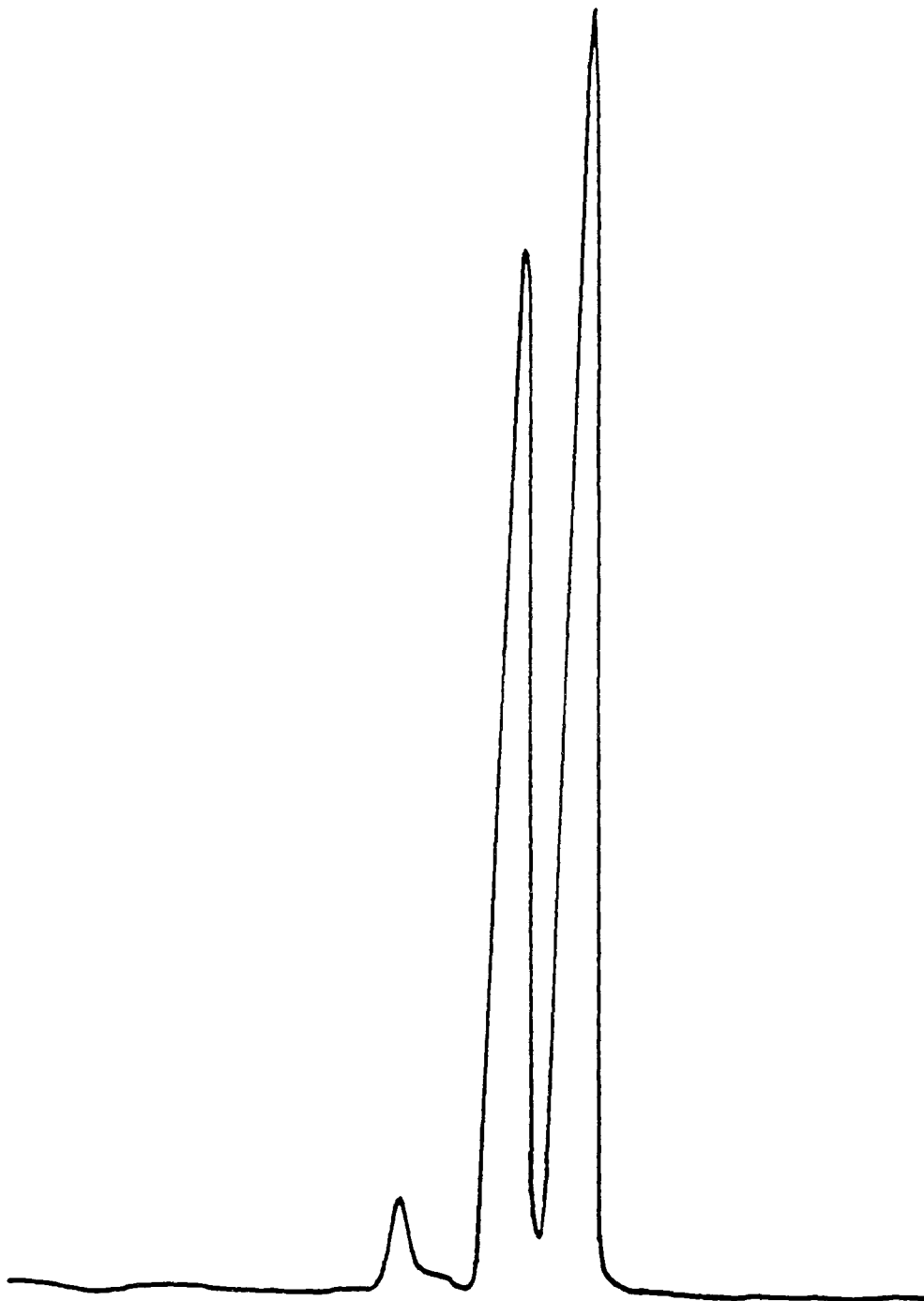


Figure 12. GC analysis of olefins mixture in preparation of 4- ϕ -C₁₂ABS.

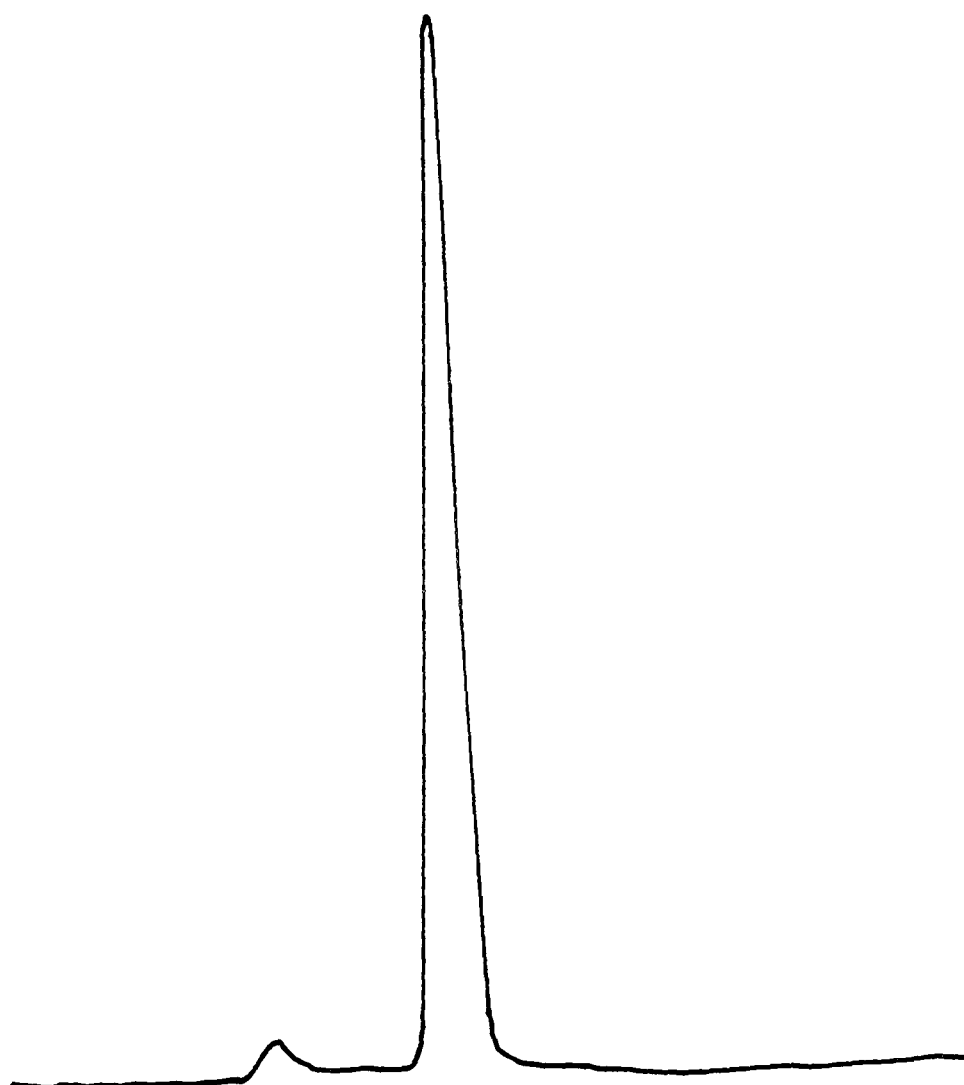


Figure 13. GC analysis of 4-phenyldodecane in the preparation of
4- ϕ -C₁₂ABS

The aromatic hydrocarbon was then sulphonated at 70°C with oleum at a weight ratio of 1:1 for an hour to yield the sulphonic acid (5). Water was then added to the hot acid mixture and the resultant transferred to a separating funnel and allowed to separate into two layers; the upper layer containing the sulphonic acid. The lower aqueous layer, containing any unreacted H₂SO₄, was then run off and the sulphonic acid was neutralised to approximately pH 8 with 10 % sodium hydroxide solution. The final product was then obtained by freeze drying and recrystallisation with acetone to give a waxy yellow solid.

Analysis by two-phase titration with Hyamine 1622 (section 2.5.4) showed the product to be 99.52 % anionic-active detergent.

2.4 Preparation of Kaolin and Ion-Washed Kaolins

Kaolin was prepared by washing with distilled water between 7 and 10 times until the conductivity of the supernatant liquor remained constant. The ion washed kaolins were prepared using the method of Hanna and Somasundaran (H7). The treatment for washed kaolin (a) and then further treatment to sodium washed kaolin (b,c & d) is given below:

- a) The dry clay was treated with distilled water in a high speed mixer at a solid liquid ratio of 1:2 for approximately 10 minutes. The product was then diluted to 2 to 3 % solids and then allowed to settle before decanting the supernatant which initially contained the

finer material. This was repeated between 7 and 10 times until there was no change in the supernatant conductivity.

- b) The washed kaolin was then agitated with 2 M NaCl solution at a high solid to liquid ratio for 15 minutes. The suspension was then diluted and reagitated for a further 2 hours before being centrifuged at 2,500 rpm for 30 minutes. The supernatant was removed and the process repeated between 7 and 10 times until constant conductivity was reached.
- c) The clay produced in (b) was further treated using the same procedure as in (b) but with 1 M NaCl solution at pH 3 to remove any $\text{Al}(\text{OH})_3$ surface contamination. Again the process was repeated 7 to 10 times.
- d) The product obtained in (c) was then further treated as in (b) now using 0.1 M NaCl solution and washed until constant conductivity. The product was then washed several (3-4) times with distilled water to remove any salt that may have precipitated at the surface. The resulting product was then dried in an oven at 50 C for 3-5 days and stored dry.

Three clays were produced; these being the sodium, calcium and aluminium forms of kaolin.

2.4.1 Preparation of North Sea Core Samples.

The core samples were obtained from Shell Expro. These were prepared by grinding the core to a rough powder and then using the core as obtained. The reference numbers of the cores are the equivalent depth in feet from which they were taken.

2.5 Experimental Techniques

2.5.1 Surface Area Determinations

The surface areas of samples of kaolin and north sea reservoir rock samples have been determined by nitrogen adsorption and BET analysis.

Apparatus

A Micrometrics Instrument Corporation (model 2100D Orr) Accusorb physical adsorption analyser was used for the measurements.

A 15 cm³ glass specimen bulb, supplied by Coulter Electronics Ltd. (part number 9961055), was used to hold the sample.

Computations of surface area were made using the BASIC program given in Appendix 1, on a BBC micro computer.

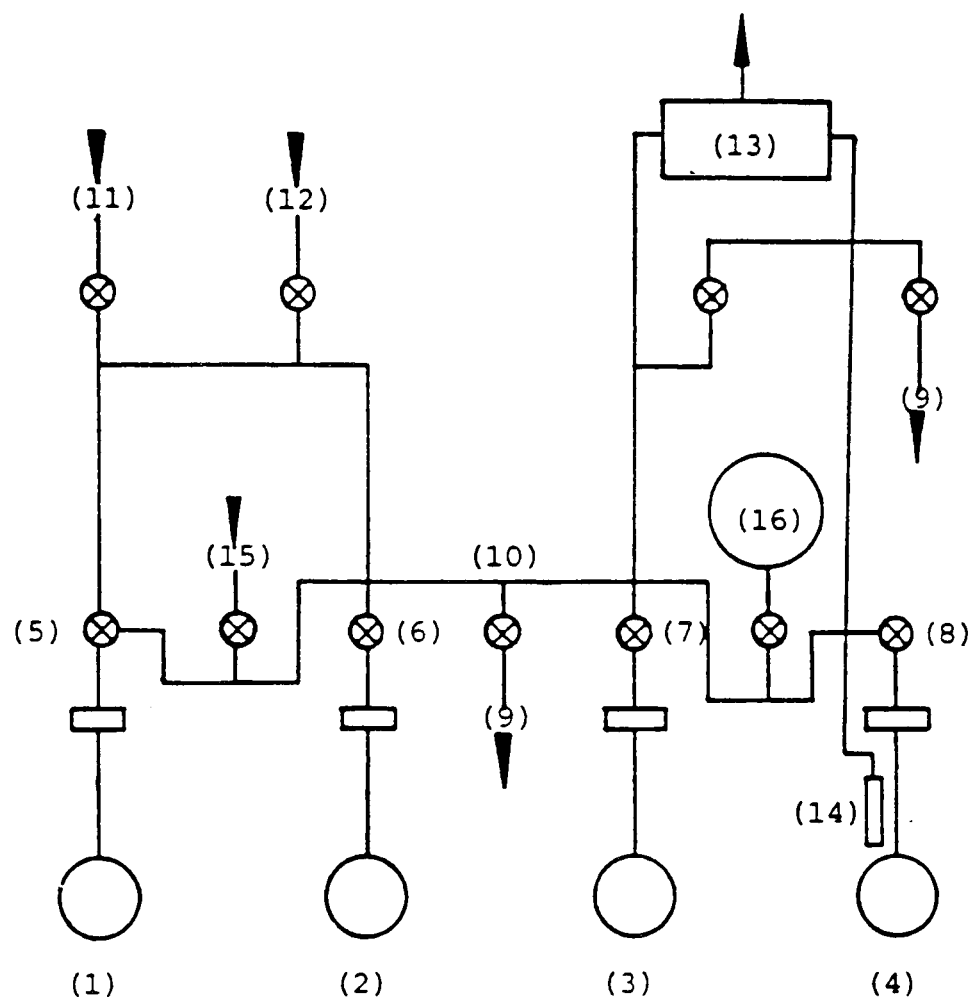
Sample preparation

The gas adsorption apparatus is shown schematically in Figure 14. Approximately 100 mg of sample was accurately weighed (W_s) into one of four sample flasks (1-4), which was then transferred to the apparatus and degassed under a vacuum of 0.07 N m^{-2} at a temperature of approximately 150°C overnight. The sample was then tested for residual gas as follows:

The sample valves 5-8, and valve 9 to the vacuum line were closed (see Figure 14). After approximately 10 minutes the valve linking the sample flask to the manifold (10) was reopened and any increase in the observed pressure was taken as an indication that the sample was not completely degassed. The sample was then degassed until no pressure increase was seen. Once total degassing was achieved the heating mantle surrounding the sample flask was removed and the sample allowed to cool to room temperature.

Determination of the Adsorption Isotherm and Surface Area

The valves 11 and 12, leading to the adsorbate line (N_2), were closed thus isolating the sample. The vacuum was then able to pump on both sides of the pressure transducer (13). After the transducer reading had stabilised, it was adjusted to zero.



- | | | | |
|-----------|-----------------|------|---------------------|
| (1)-(4) | Sample flasks | (13) | Pressure transducer |
| (5)-(8) | Sample valves | (14) | Sorption pump |
| (9) | Vacuum line | (15) | Helium line |
| (10) | Manifold | (16) | Extra volume |
| (11)-(12) | Adsorbate lines | | |

Figure 14. Schematic diagram of the gas adsorption apparatus.

The sample flask and sorption pump (14) were then immersed in liquid nitrogen, the sorption pump acting as a reference by maintaining a constant vacuum to one side of the transducer.

During the determination it is important to know the volume of the sample flask containing the sample accurately. This volume (the volume of the sample flask - the volume of the sample) is known as the "dead space" volume. Helium, which was found not to adsorb on the surface of any of the samples at liquid nitrogen temperatures, was used to determine this dead space as follows (M3):

The helium line was opened (15) to give a pressure in the manifold of approximately 550 mm Hg, the actual pressure (H_1) was accurately recorded on the transducer. Valve 15 was then closed before opening valve 11 so allowing Helium to move from the manifold to the sample flask. After equilibration (indicated by a steady transducer reading) the new combined manifold and sample pressure (H_2) was recorded. Valve 5 was then re-opened in order to pump helium from the apparatus. From these readings the dead space of the sample flask can be determined using a computer program (Appendix 1).

Having removed the helium thus reducing the pressure in the apparatus to zero on the transducer, the surface area determination of the sample could be made as follows :

With valve 1 closed nitrogen was introduced into the manifold, via valve 11, giving a pressure of approximately 200 -250 mm Hg. The actual pressure reading was noted (P_1) before opening valve 1, which allowed the nitrogen gas to enter the sample flask. After equilibration the new pressure reading (P_2) was recorded. Valve 1 was then closed and additional nitrogen gas was introduced into the manifold to give a further pressure (P_3) which was in excess of P_1 , usually this excess was of the order of 50 mm Hg.

Valve 1 was again opened and a new resultant pressure recorded (P_4). This procedure was continued until the pressure in the manifold reached saturation. The saturation vapour pressure of nitrogen for a given temperature was determined from a plot of the vapour pressure of nitrogen versus temperature (Figure 15). This data was obtained from the references J3 and Z2.

Nitrogen Adsorption Isotherms

Nitrogen adsorption isotherms have been determined for all of the washed kaolin samples and the North Sea reservoir rock samples. These can be seen in Figure 16.

From the adsorption data, for partial pressures between 0.05 and 0.35 (i.e. the region of BET analysis (G2)), the specific surface areas of the samples have been evaluated; washed kaolin was found to be $15.08 \text{ m}^2 \text{ g}^{-1}$ with the sodium, calcium and aluminium forms of the clay having the values 8.98, 8.48 and 8.08 respectively. The reservoir rock samples have the values 383.84, 360.51 and 399.30 for the samples 12395, 12417 and 12498.2 respectively.

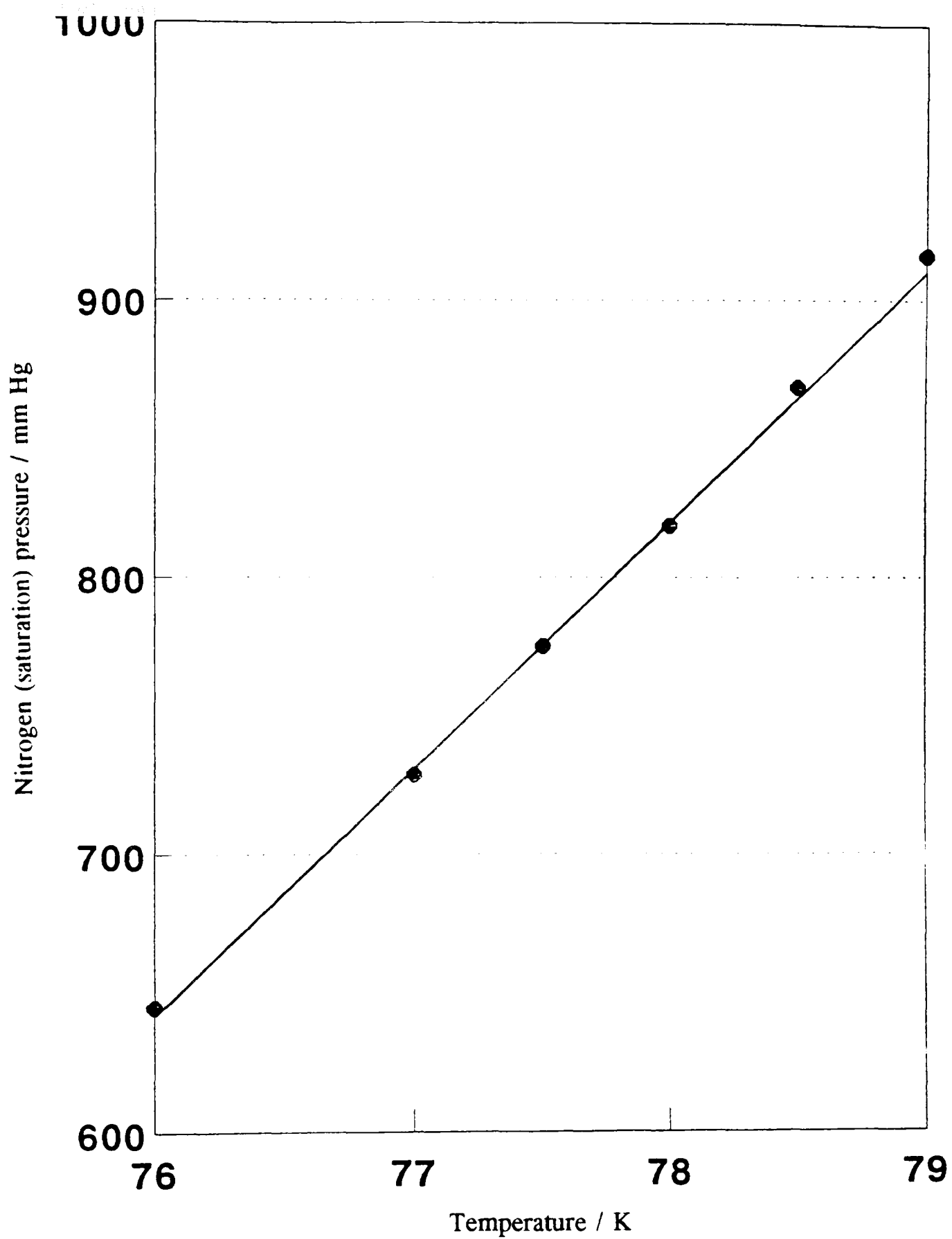


Figure 15. Nitrogen (saturation) vapour pressure as a function of absolute temperature. Plotted from data obtained in references J3 and Z2.

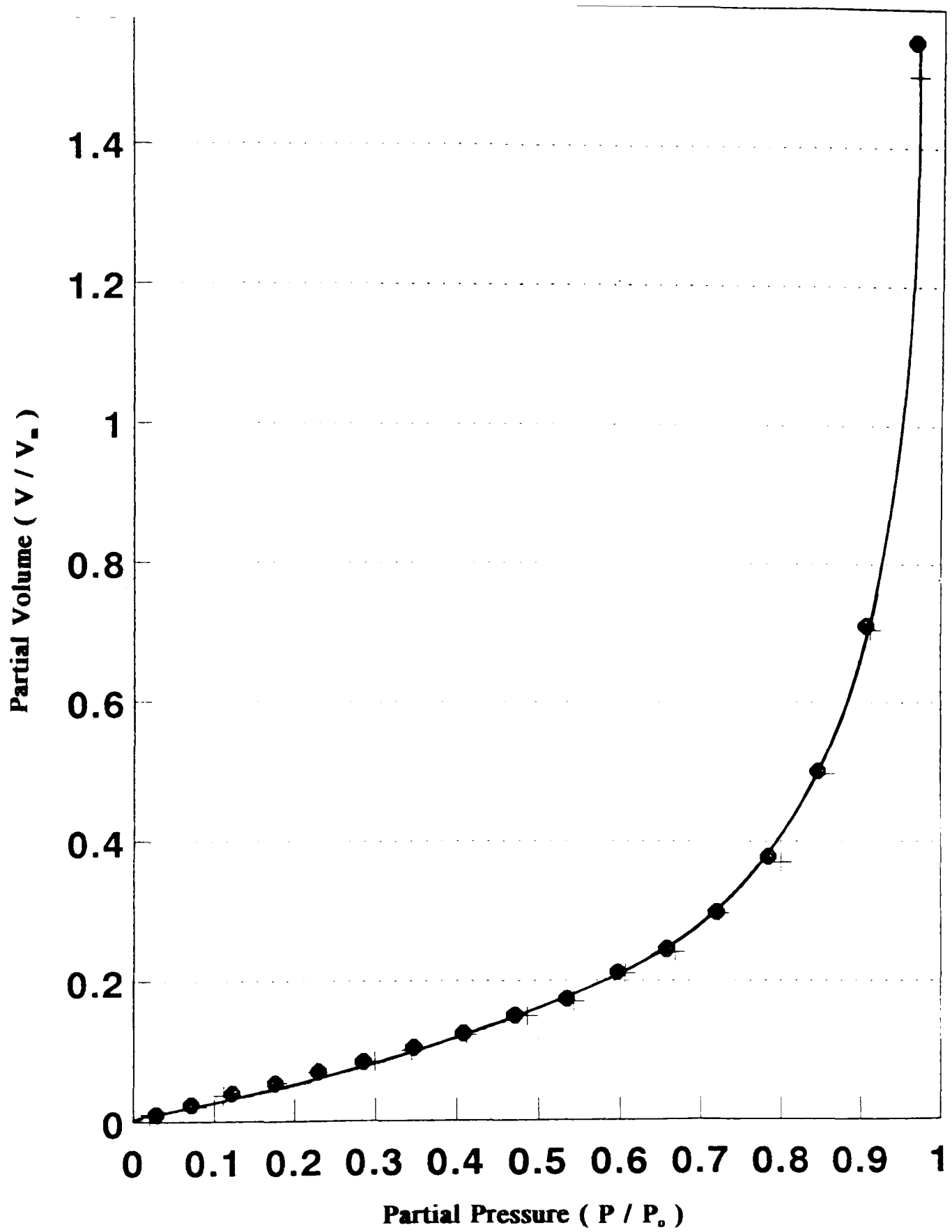


Figure 16 Adsorption / Desorption for N_2 onto Kaolin at 77.7K

2.5.3 Scanning Electron Microscopy

Scanning electron micrographs of the kaolin samples and the reservoir rock samples were determined using a JEM-1200 EX scanning electron microscope. The samples were mounted on brass supports using silver (DAG) glue, and sputter-coated with gold using a Polaron SEM coating unit E5000.

2.5.4 Analysis of the Isomerically pure sodium p-[1-propylnonyl] benzenesulphonate

2.5.4.1 Infra-red Spectroscopy

Infra-red spectra of the sample was determined using a Perkin-Elmer 1600 FT-IR spectrometer.

The solid sample was prepared by grinding the sample with dry KBr. This mixture was then pressed to form a transparent disc which was then used in the apparatus. This is a very widely used form of sample preparation and is detailed in many papers (for example B6).

Spectra

The infra-red spectrum of the pure DBS is shown in Figure 17. Assignment of the adsorption bands is given in Table 2.

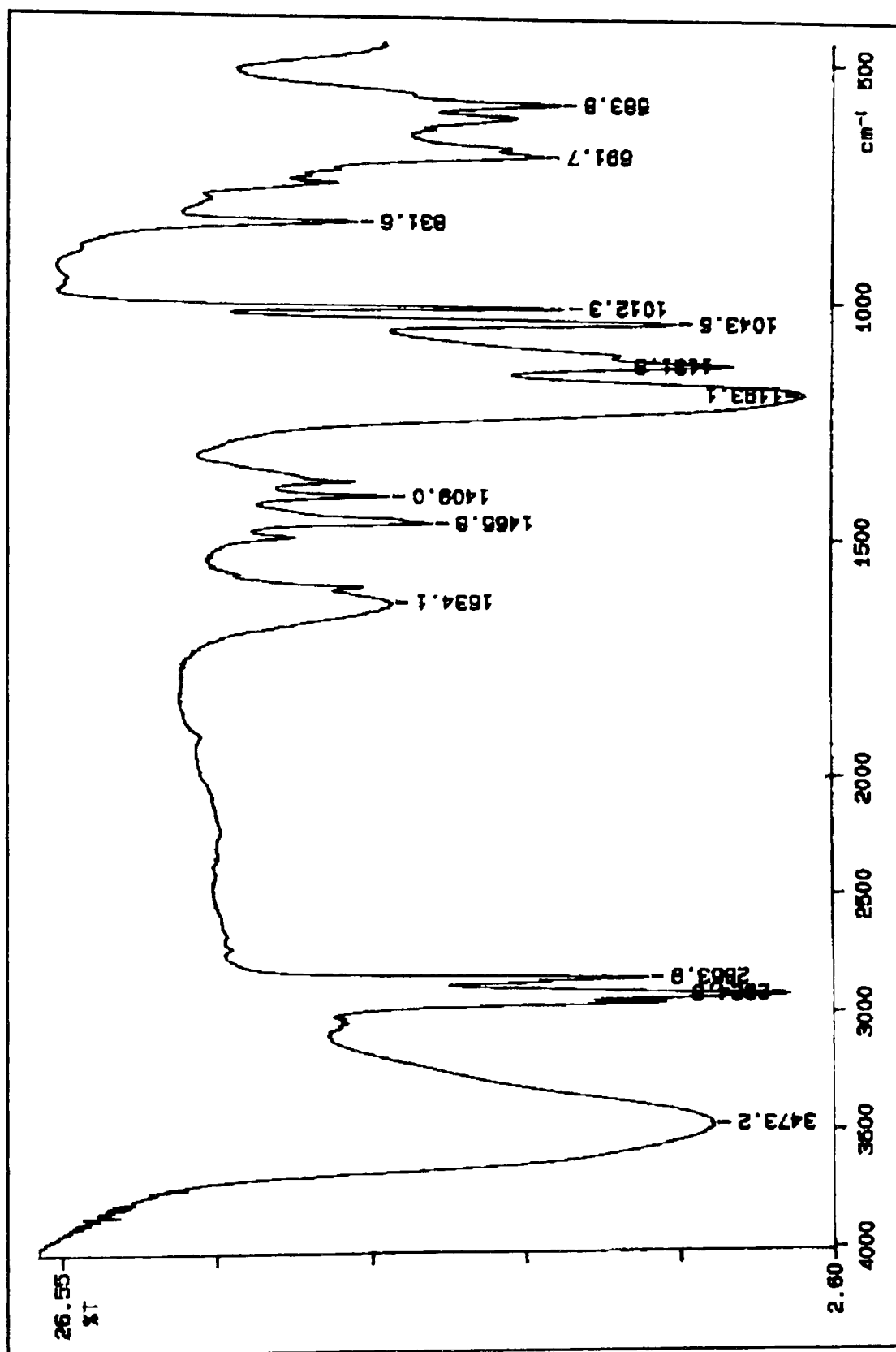


Figure 17. Infrared spectrum of 4-φ-C₁₂ABS

Table 2. The adsorption peaks in the Infra-red Spectra of sodium p-[1-propylonyl] benzenesulphonate.

Wave Number cm^{-1}	Assignment (ref 119)
3700-3100	O-H stretch (damp disc)
3050	C-H aromatic stretch
2990-2740	C-H stretch
1900-1660	Combination bands
1580	C=C aromatic ring stretch
1460	CH_2 bend
1400	CH_3 deformation mode
1370	CH_3 bend
1180	Asymmetric S-O stretch
1115	C-H aromatic bend
1040	symmetric S-O bend
1010	C-H aromatic bend

2.5.4 Determination of Anionic surfactants in Aqueous Solution

Initially anionic surfactant determinations were made using the Epton titration technique (see section 2.5.4.1) involving a two-phase system and indicator to detect the end-point (R4). This method has since been replaced by a Mettler Autotitrator (DL40RC) system incorporating a surfactant selective electrode (Orion) (see section 2.5.5.3).

Below surfactant concentrations of 1×10^{-4} mol dm⁻³ the Ultra-Violet absorbance of the surfactant was used to determine the concentration (see section 2.5.5.2).

2.5.4.1 Two-Phase Titration

Above surfactant concentrations of 1×10^{-4} mol dm⁻³ the two-phase titration technique of Reid, Longman and Heinerth (R4) was employed. A summary of this method is given below.

The anionic surfactant concentration was determined by titration of the sample with a standard cationic surfactant solution (Hyamine 1622). The titration was carried out in a two-phase aqueous/chloroform system with a mixed indicator of a cationic dye (Dimidium Bromide) and an anionic dye (Disulphine Blue VN). The anionic surfactant forms a chloroform soluble salt with the Dimidium Bromide imparting a pink/red colour. The end-point of the titration is reached when the colour from the chloroform layer is removed. This occurs due to the Hyamine cation displacing the

Dimidium cation from the chloroform soluble salt. When added in excess, Hyamine forms a salt with the Disulphine Blue VN in the chloroform layer giving it a blue colouration.

Preparation of Solutions

Hyamine 1622 ($4 \times 10^{-3} \text{ mol dm}^{-3}$) Solution

A prepared solution was purchased from BDH Chemicals. The solution was specified to be $0.004 \text{ mol dm}^{-3}$. This was standardised using a $0.004 \text{ mol dm}^{-3}$ sodium dodecylsulphate solution (R4).

Preparation of Mixed Indicator Solution

A stock solution of the indicator was purchased from BDH Chemicals. The solution was then prepared by diluting 20 cm^3 of this stock solution with 200 cm^3 of distilled water. The solution was then acidified using 20 cm^3 of $2.5 \text{ mol dm}^{-3} \text{ H}_2\text{SO}_4$ solution and the resulting solution was diluted to 500 cm^3 in a volumetric flask with distilled water. A fresh solution was prepared each week and the solution stored out of direct sunlight.

Preparation of Surfactant Solutions

Standard surfactant solutions were prepared by accurately weighing samples of the surfactant into a beaker, transferring the contents to a volumetric flask and making up to the required volume with distilled water.

Titration Procedure

Standardisation of Hyamine 1622 Solution

To 20 cm³ of a standard SDS solution, 10 cm³ of distilled water, 15 cm³ of chloroform and 10 cm³ of acid indicator solution were added in a 200cm³ glass stoppered flask. The solution was then titrated with Hyamine 1622 with vigorous shaking between each addition. The titration was continued until the pink colour was removed from the chloroform layer. This was taken as the end-point. The concentration of the Hyamine solution could then be determined using the equation given below :

$$\text{Concentration of Hyamine} = (L \times 20) / V_H$$

where, L = molarity of the SDS solution, mol dm⁻³

V_H = Volume of Hyamine used to reach the end-point, cm³

This procedure was repeated in triplicate for any samples purchased.

Determination of Sodium Dodecylbenzenesulphonate

A sample of the surfactant was accurately weighed (approximately 0.3g), and then dissolved in distilled water (100 cm³) and then diluted to 250 cm³ in a volumetric flask. A 20 cm³ aliquot of this sample was then used to determine the anionic active matter in the solution by titration with Hyamine 1622 using either the Epton technique or that of the surfactant selective electrode (see sections 2.5.5.1 and 2.5.5.3).

From the results obtained the percentage anionic active matter in the sample could be determined using the equation below :

$$\% \text{ wt. surface active matter} = \frac{T \times f \times 250 \times m}{20 \times 100 \times W_3} \times 100$$

where T = volume of the titrant added (cm³) to reach the end-point for a 20 cm³ aliquot of the sample solution,

m = molecular weight of the anionic matter = 347.47

W₃ = weight of sample taken, g

f = concentration of Hyamine 1622 solution in mol dm⁻³.

from the results, the percentage weight of surface active matter for the surfactants were found to be 79.8 % for the commercial BDH sample and 99.5 for the pure 4-φ-C₁₂ABS surfactant.

Preparation of a Calibration plot for 4- ϕ -C₁₂ABS in Solution

To determine whether the titration of Hyamine 1622 solution against the surfactant was a viable method of determining the concentration of surfactant in solution, a calibration plot was prepared by titrating standard surfactant solutions (of known concentration) against standardised Hyamine 1622 solution. The titration procedure was that given previously and the results are shown in Fig 18.

From the results in Fig 18, it can be seen that the titration of 4- ϕ -C₁₂ABS with Hyamine 1622 solution is linear over the range studied, i.e. from zero to 4×10^{-3} mol dm⁻³ of surfactant. To keep the volume of titrant within the same range, the volume of surfactant solution was varied according to its concentration.

The effect of several variables have been investigated, including pH, sodium chloride concentration and butan-1-ol concentration. The calibration plots for these can also be seen in Fig 23.

2.5.5.2 Determination of 4- ϕ -C₁₂ABS by Ultraviolet Spectroscopy

At concentrations below 1×10^{-4} mol dm⁻³ the concentration of 4- ϕ -C₁₂ABS cannot be measured accurately by titration in aqueous solution. Absorption of UV light, by the aromatic group of the surfactant, is a more sensitive method and can be used for surfactant concentrations between 10^{-6} and 10^{-4} mol dm⁻³. The absorbance maxima are shown in Fig 19 and were found to be at 223.1 and 188.8 nm.

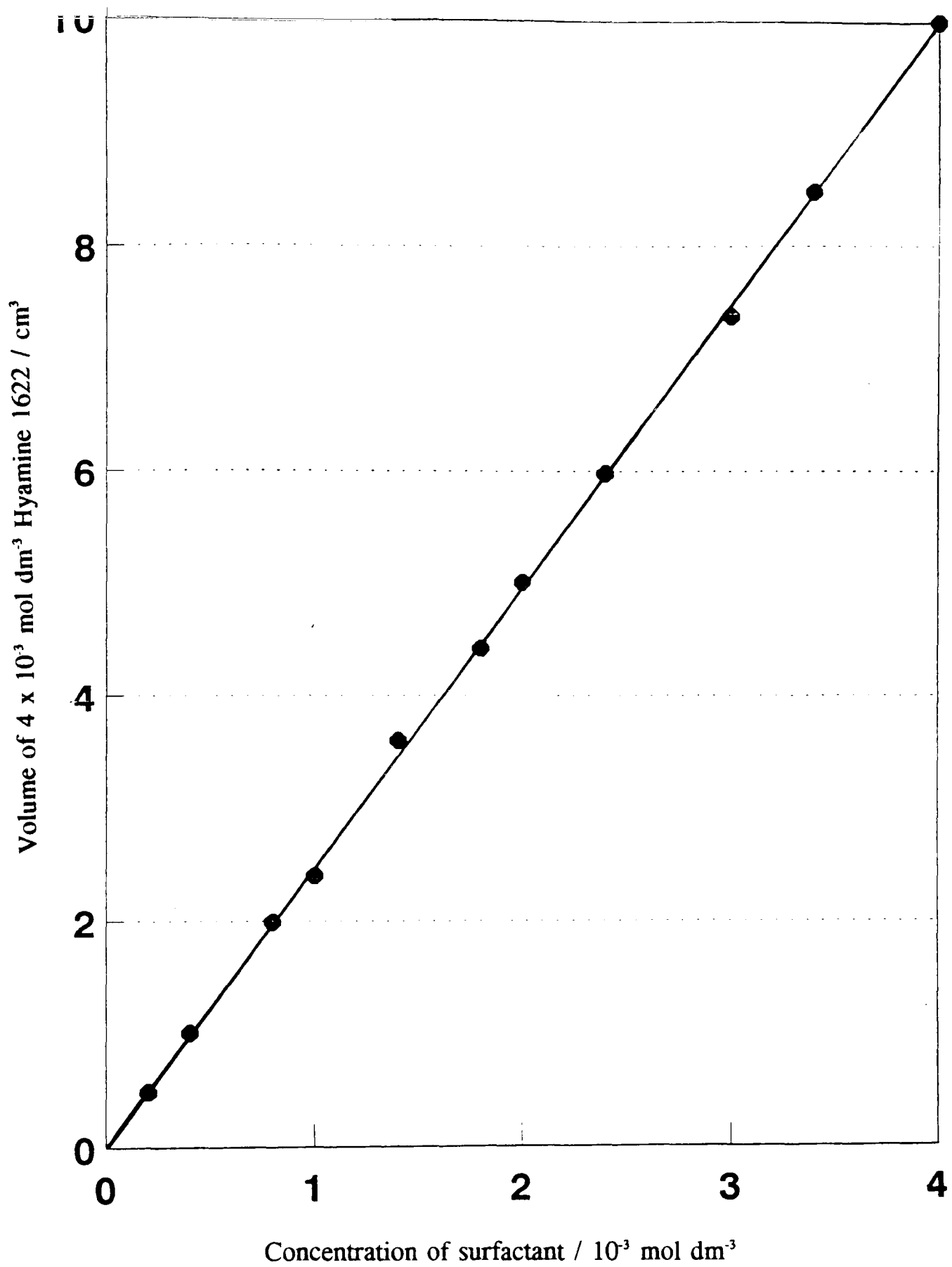


Figure 18. Calibration plot for titration of 10 cm³ 4-φ-C₁₂ABS solution with Hyamine 1622 solution (4 x 10⁻³ mol dm⁻³).

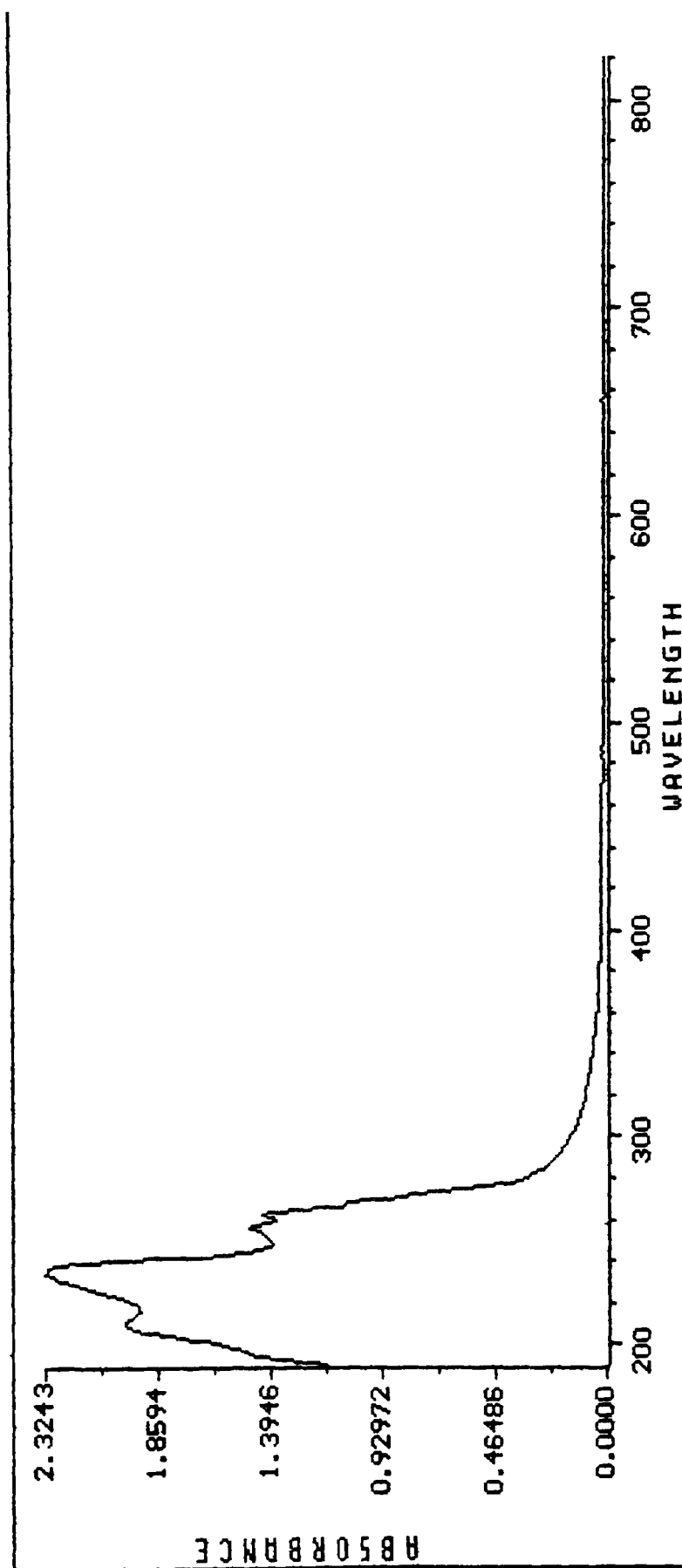


Figure 19. UV absorbance spectra of 4-φ-C₁₂ABS.

Determinations of the surfactant concentration, in aqueous solution, were made using the 223.1 nm absorbance. A linear relationship was found up to the maximum concentration used, i.e. 1×10^{-4} mol dm⁻³, as shown in Fig 20.

Apparatus

All surfactant determinations by UV were made using a Hewlett-Packard HP8452A ultraviolet spectrophotometer, using a 1 cm quartz cell.

Calibration Graphs

The absorbance of a series of surfactant solutions was determined at 223.1 nm. The surfactant solutions ranged in concentration from 1×10^{-6} to 1×10^{-4} mol dm⁻³. The resulting calibration plot can be seen in Fig 20.

The effect of pH and sodium chloride concentration on the absorbance was determined and was found not to interfere with the determination. The effect of butan-1-ol was also determined and was found to lower the absorbance of the solution. However, by incorporating the same amount of butan-1-ol into the "blank" solution the concentration of surfactant could still be determined (Fig 21).

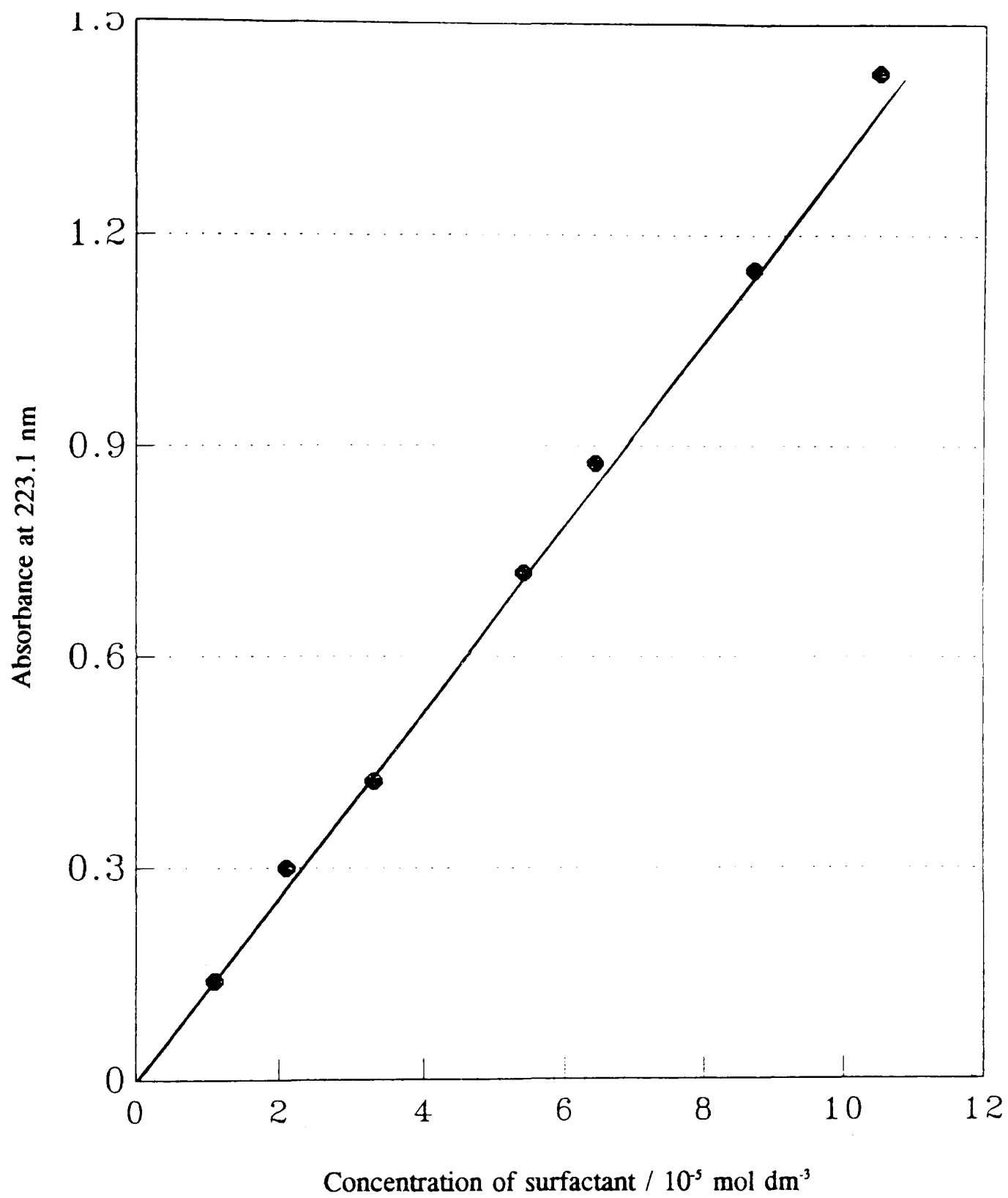


Figure 20. Calibration of 4- ϕ -C₁₂ABS in aqueous solution, measured at 223.1 nm.

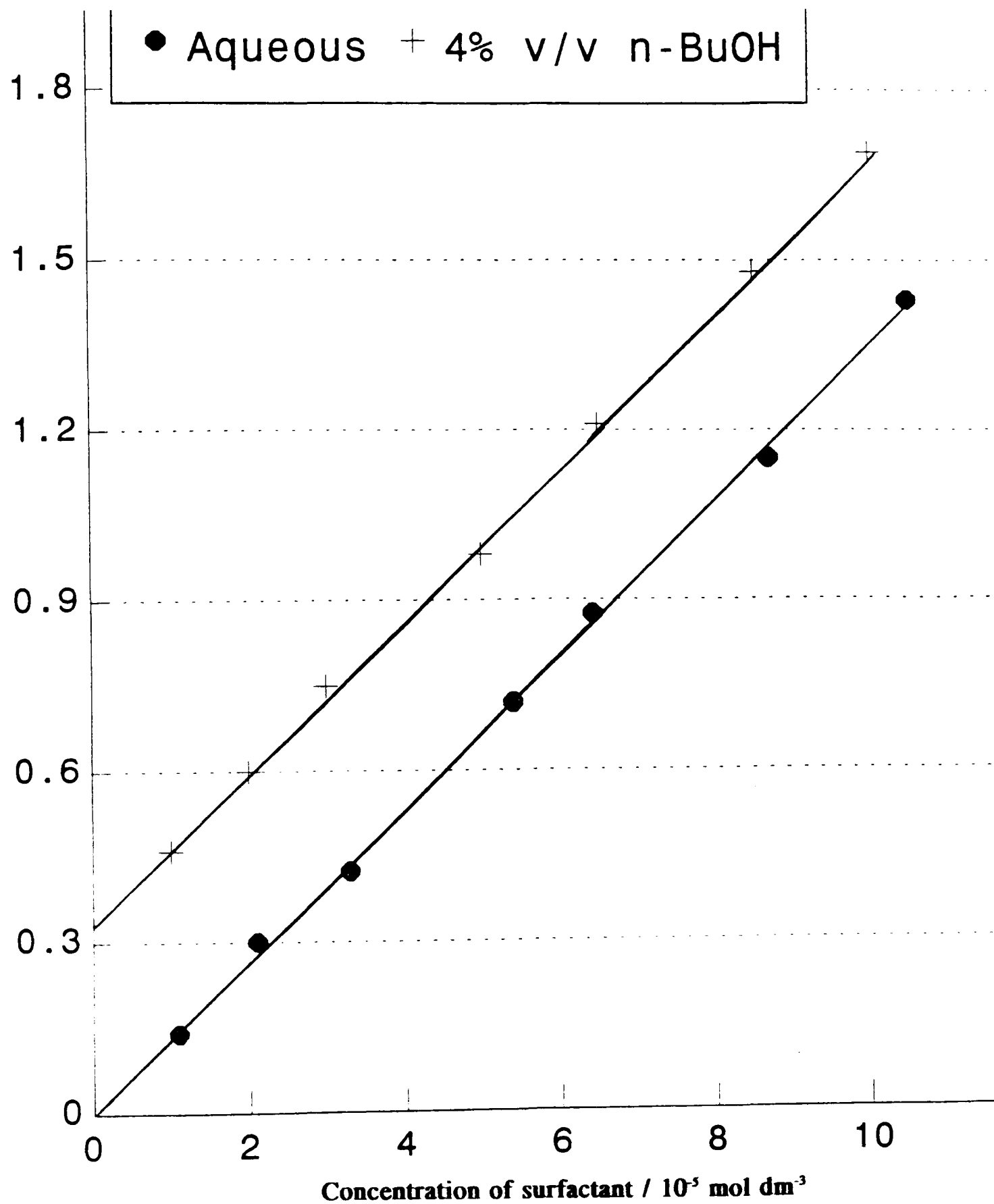


Figure 21. Effect of 4% v/v butan-1-ol solution on the UV absorbance of 4- ϕ -C₁₂ABS.

2.5.5.3 Determination of 4- ϕ -C₁₂ABS using an Automatic Titration system in conjunction with a Surfactant Selective Electrode

The titration technique used in 2.5.5.1 has since been replaced by that of an automatic system using a surfactant selective electrode. Using this technique means that the use of a second phase (chloroform) and an indicator system were no longer necessary.

Apparatus

The surfactant determinations were carried out using a Mettler Autotitrator (DL40RC) with a surfactant selective electrode (Orion). The electrode was dipped into the aqueous solution and balanced against a double junction reference electrode (Orion), during the addition of Hyamine 1622.

Calibration Plots

A series of calibration graphs were determined for the measurement of surfactant by titration with a surfactant electrode. The addition of Hyamine gave rise to a change in potential of the solution. By plotting this change in potential against the volume of Hyamine added the endpoint of the titration could be determined,

Fig 22. The effect of pH, butan-1-ol and sodium chloride concentration on the endpoint determination was also been investigated and is illustrated in Fig 22.

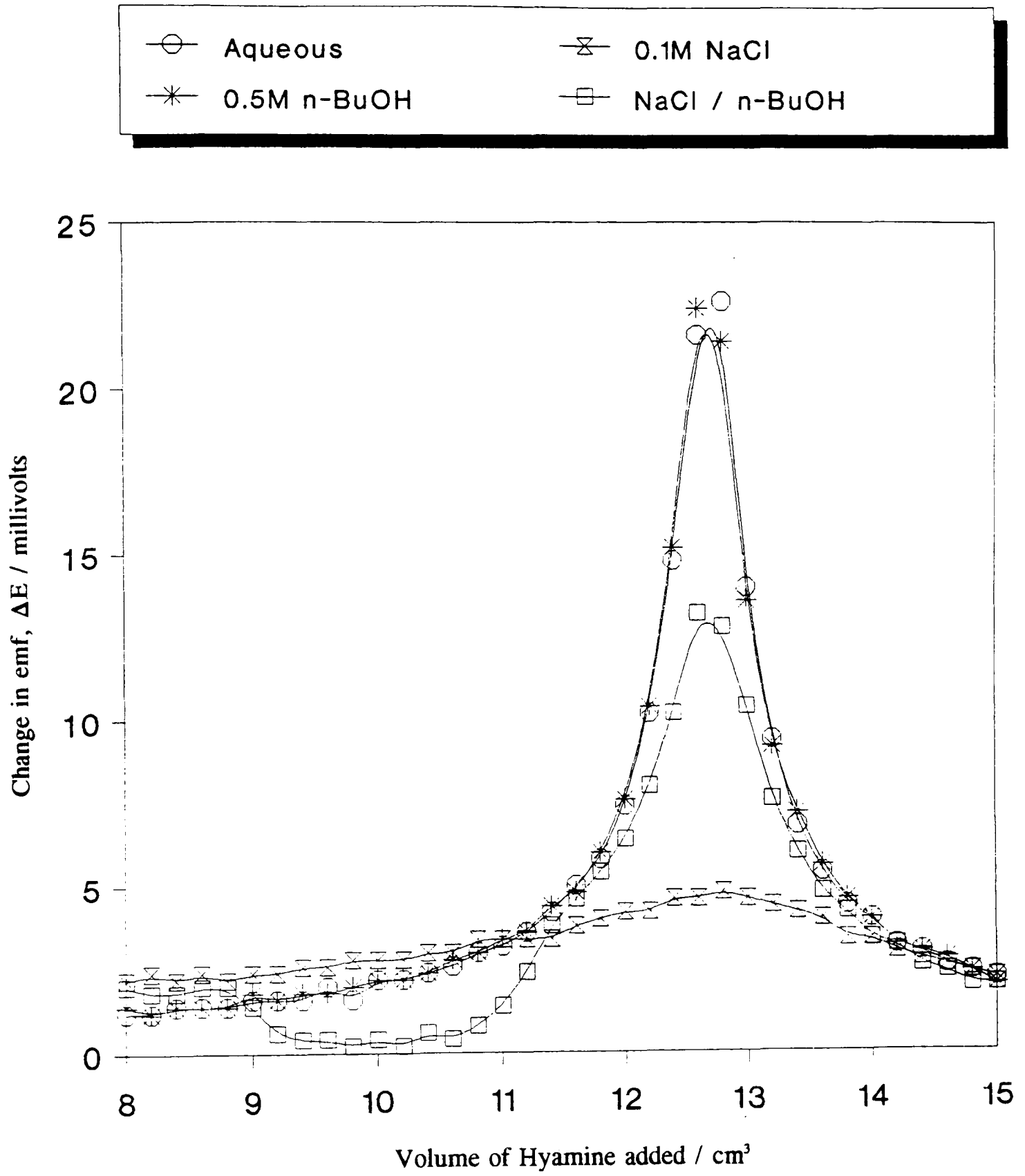


Figure 22. Endpoint determinations using a surfactant selective electrode measuring change in potential with volume of titrant added.

The concentration of a series of standard surfactant solutions was determined and a graph of the actual concentration versus determined concentration plotted for the surfactant in the presence of sodium chloride, butan-1-ol and a combination of sodium chloride and butan-1-ol. This can be seen in Fig 23.

The electrode, in addition to showing the endpoint in an anionic vs cationic titration, is capable of measuring the free monosurfactant concentration in solution directly. By dipping the electrode into solution and allowing it to equilibrate the millivolt value (an electrical potential determined by the electrode) for a particular concentration of surfactant can be found, Fig 24.

It can be seen that after approximately 20 minutes the mV reading becomes constant. Repeating this for a series of surfactant concentrations and then plotting the millivolt value against the concentration of the sample gives a calibration plot, Fig 25.

The discontinuity in this graph (Fig 25), at $-\log(c)$ is approximately equal to 4, can be attributed to the formation of micelles and hence yields the value of the CMC. The values obtained for the CMC agree reasonably well with previous findings (M4). This value can then be used to determine the concentration of the surfactant monomer and the concentration of micelles in solution.

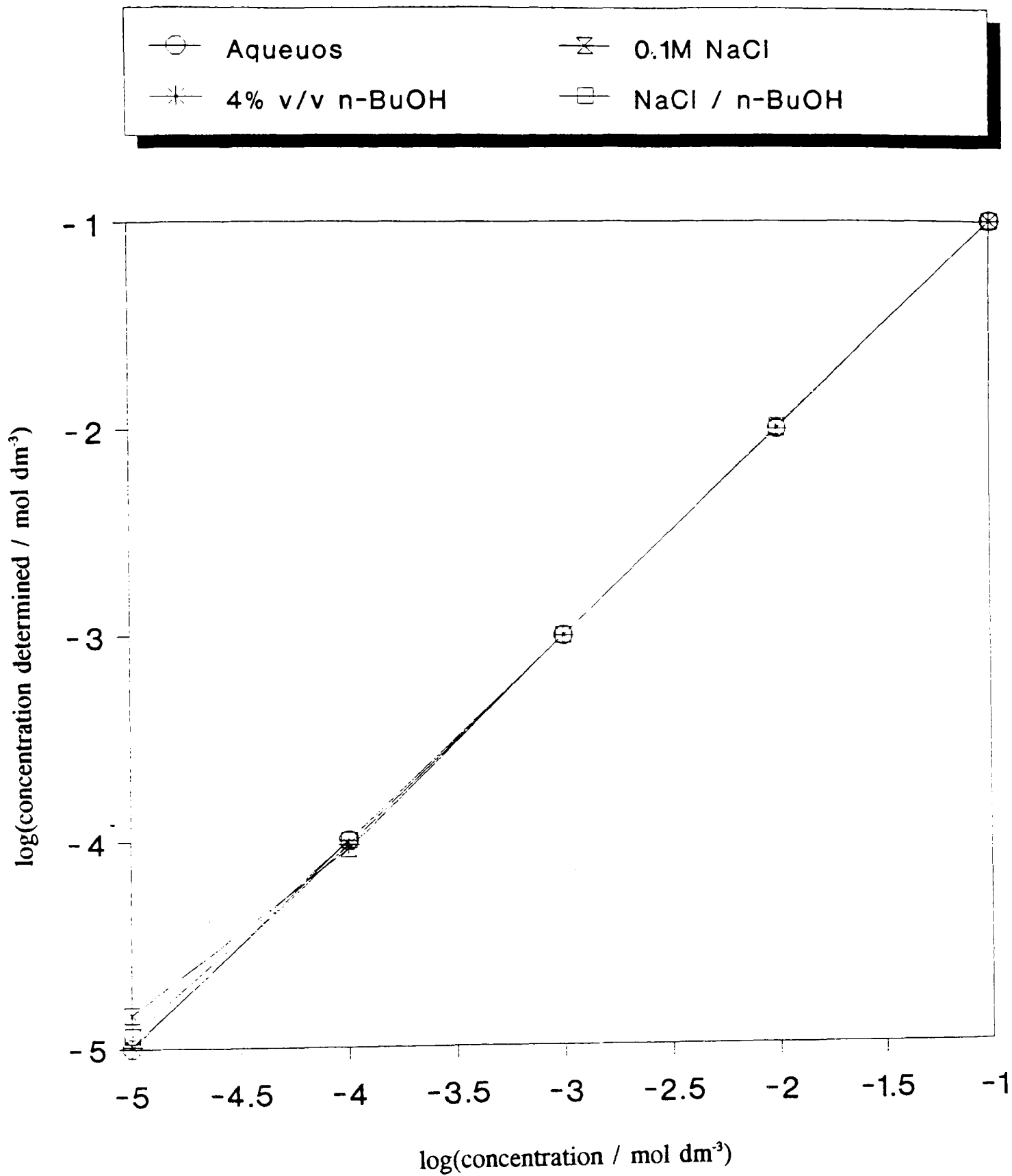


Figure 23. Calibration graph using the Surfactant selective electrode for standard solutions of 4-φ-C₁₂ABS.

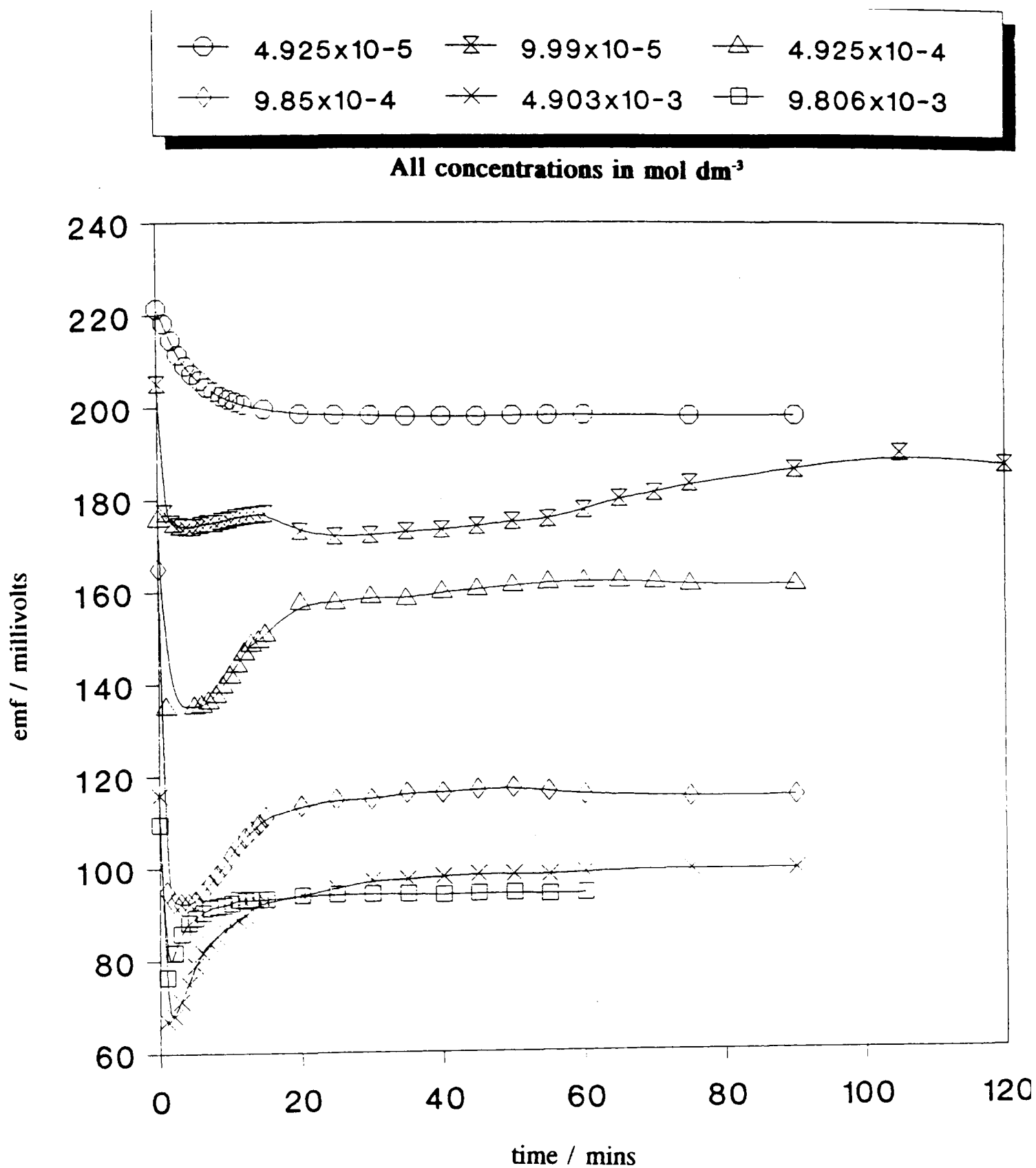


Figure 24. Determination of electrical potential for solutions of the surfactant $4\text{-}\phi\text{-C}_{12}\text{ABS}$ using the surfactant selective electrode.

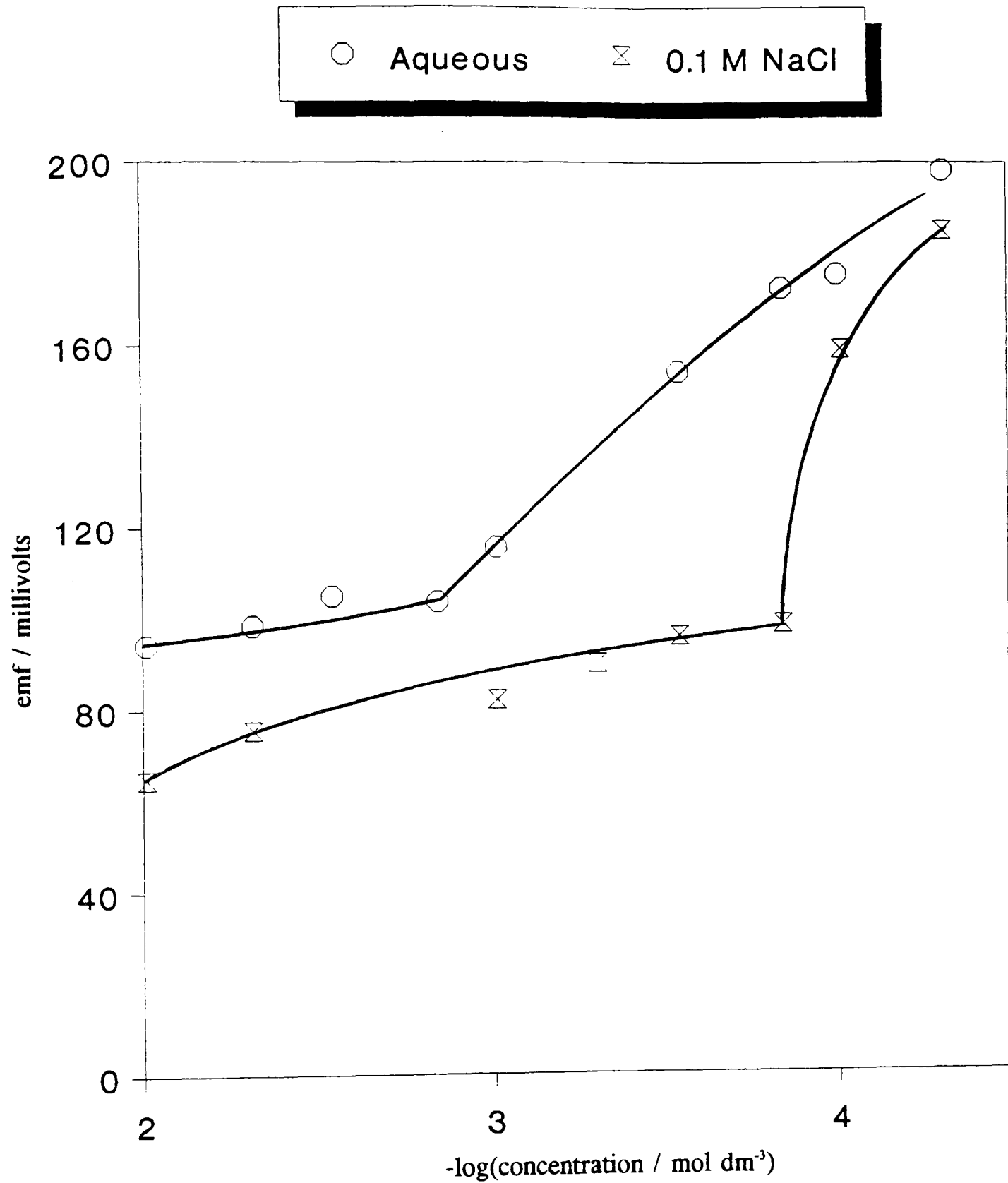


Figure 25. Calibration of determined electrical potential against surfactant concentration for 4- ϕ -C₁₂ABS solutions.

2.5.5.4 Determination of Aerosol OT surfactant solutions

The surfactant Aerosol OT was determined using the method outlined for 4- ϕ -C₁₂ABS in section 2.5.5.3 using the surfactant selective electrode. It was found that as long as the electrode was presoaked in a solution of Aerosol OT prior to use good reproducibility of results were obtained.

2.5.5.5 Determination of Lignin Sulphonates by U.V Spectroscopy

The lignin surfactants could not be determined using the electrode method given in 2.5.5.3 (see above). The use of U.V. spectroscopy was therefore investigated. A U.V. spectra of both samples was determined (Fig 26) and it was found that both samples adsorbed quite strongly at 300nm. A series of calibration standards were prepared and concentrations of lignin solutions were determined in the same manner as 4- ϕ -C₁₂ABS in section 2.5.5.2. Calibration graphs have been determined and are shown in Fig 27.

2.5.6 Determination of complexing agents

In order to determine whether or not the complexing agents were being lost from the system by either adsorption or precipitation then it was necessary to evaluate the concentration of complexing agent in solution.

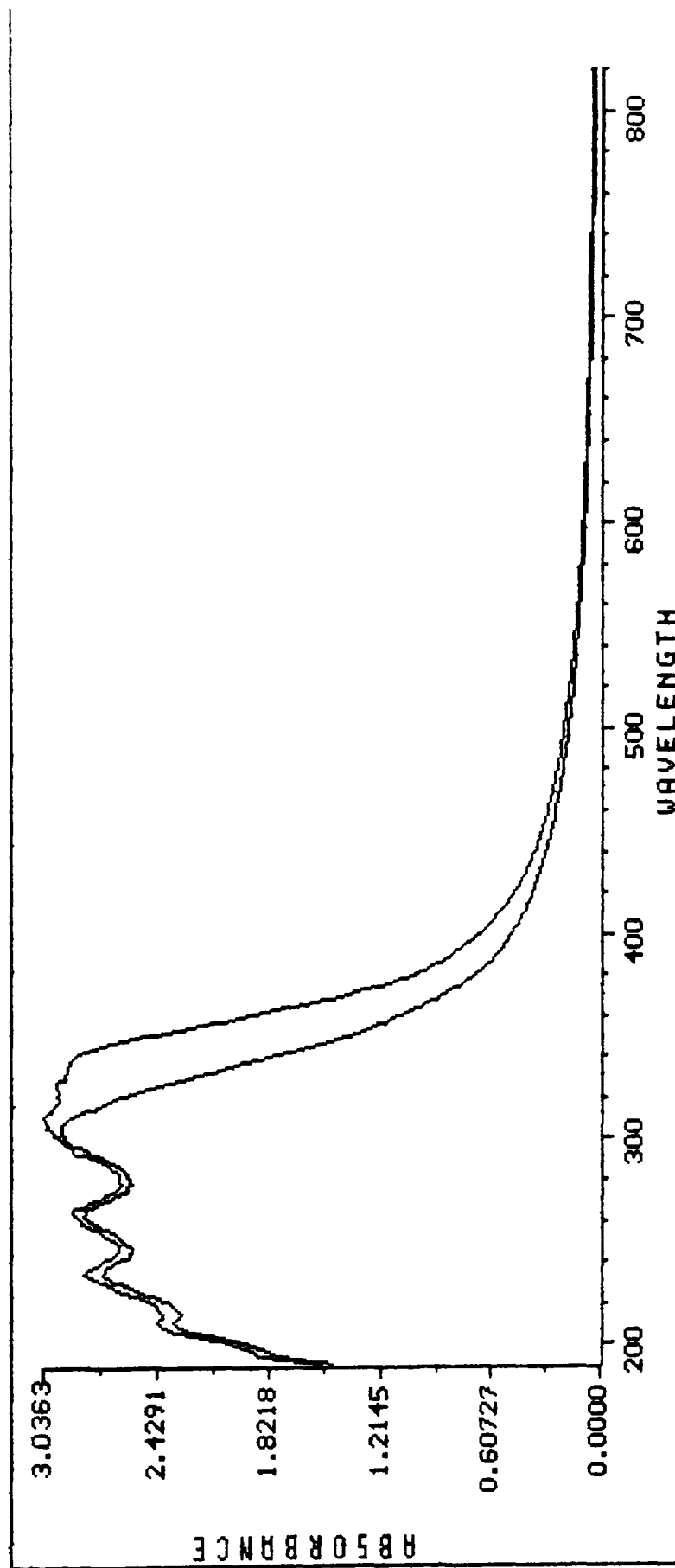


Figure 26. UV spectra of the lignin sulphonate samples

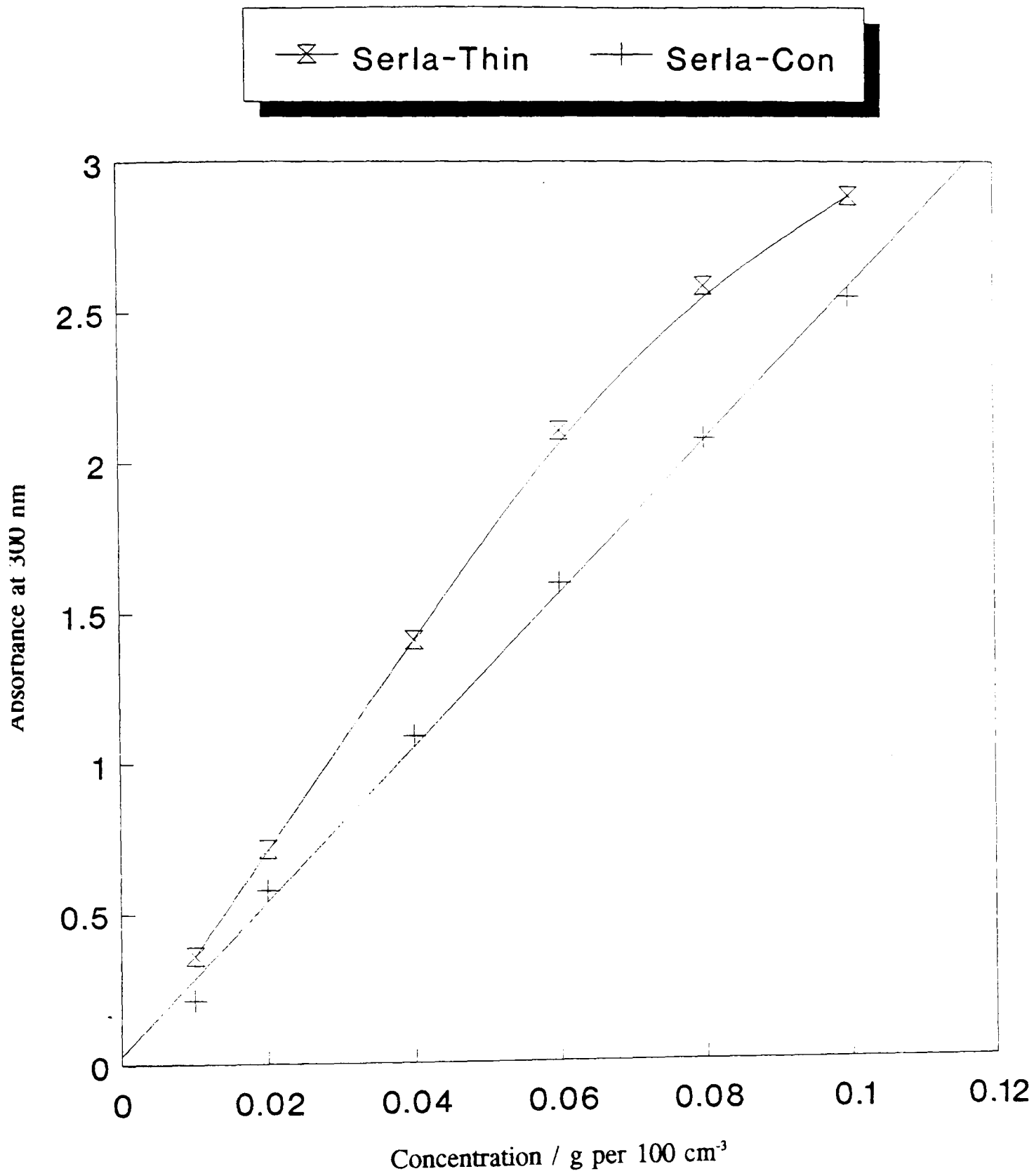


Figure 27. UV calibration graph of lignin sulphonates at 300 nm

2.5.6.1 Determination of tripolyphosphate in solution.

The amount of tripolyphosphate can be determined quite easily by titrating with 0.01 mol dm⁻³ hydrochloric acid and following the potentiometric changes with a combination glass electrode. This is a standard method and is used in many texts e.g.(V1). As there are three phosphate groups present then three end-points would be expected in the titration. These can be seen in fig 28.

2.5.6.2 Determination of sodium citrate in solution.

This was determined using the same method as tripolyphosphate (section 2.5.6.1).

2.6 Surface Tension Measurements

Surface tension measurements have been made using the du Nouy method, the point of detachment of a platinum ring from the surface being used as a measure of the tension.

Apparatus

The apparatus used was a Surface Tension and Interfacial Tension torsion balance, type OS, purchased from the White Electrical Instrument Co. Ltd.

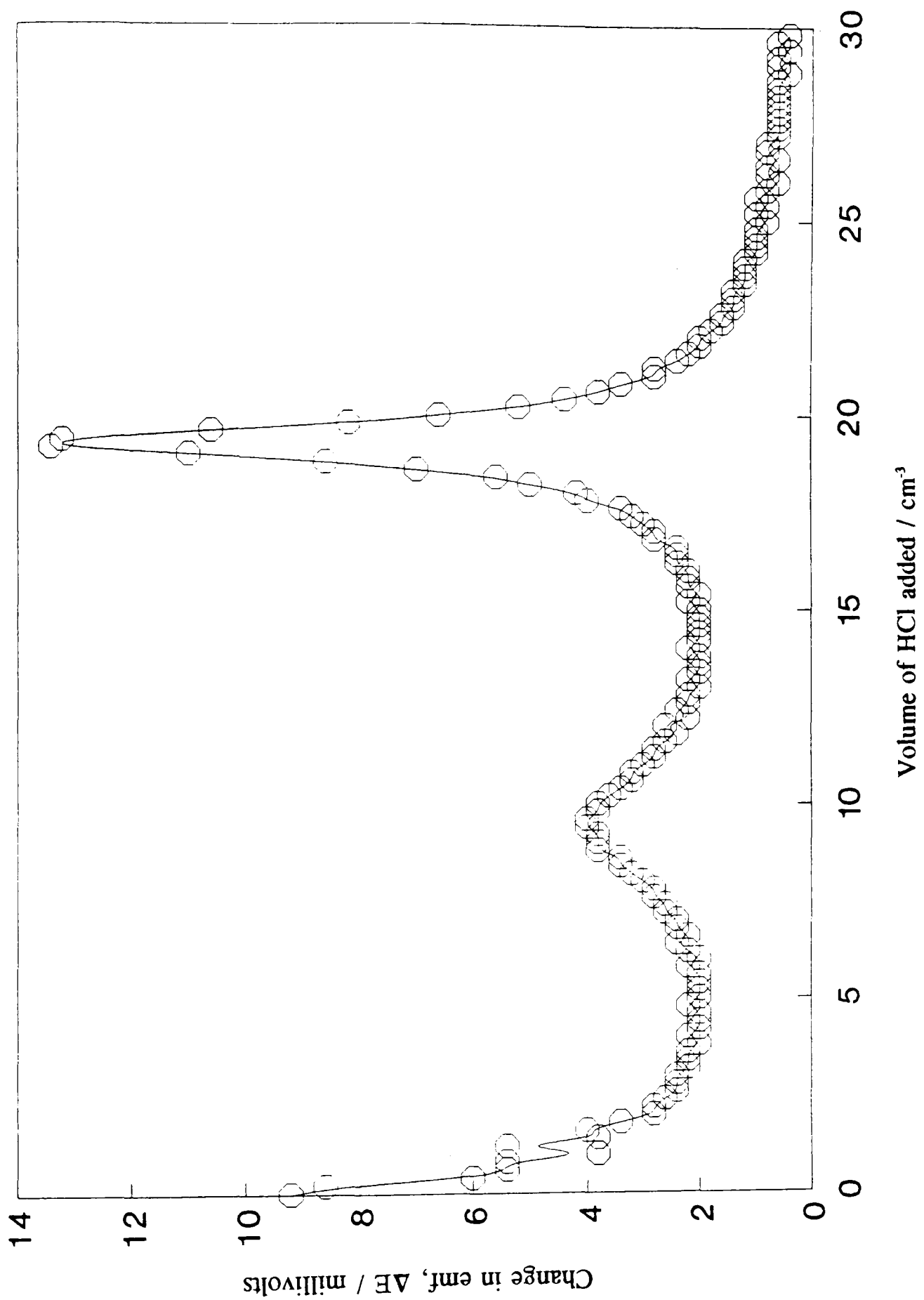


Figure 28. Determination of sodium tripolyphosphate by potentiometric titration.

The platinum ring, also from the White Electrical Co. Ltd., was 1 cm in diameter. This was cleaned by immersion in distilled water and then purging in a bunsen flame.

Surface tension measurements

These were made at the air-water interface by contacting the platinum ring with the surface and measuring the force needed to detach the ring from the surface. The surface tension can then be measured directly from the instrument scale in mN m^{-1} .

2.7 Adsorption Studies

Adsorption tests were conducted in 250 ml ground stoppered Pyrex flasks by pre-equilibrating approximately 5 g of solid with water or salt solution, of fixed pH for 2 hours. This equilibration is needed for steady pH conditions to be reached in the presence of kaolin. Below a 2 hour equilibration time the solution pH is known to drift (M5) from that required towards a neutral pH.

The solution volume, after pre-equilibration, was made up with surfactant solution to give the required solid/solution ratio (usually 10 %). The flasks were sealed and then agitated for 24 hours in a thermostatted bath.

At the end of the test the solution was separated from the solid using a centrifuge at 5000 r.p.m for 30 mins and the solution could be analysed to determine the

amount of surfactant adsorbed on the solid surface.

2.7.1 Loss of Surfactant from Solution

After centrifugation the concentration of surfactant in the supernatant liquor was determined by titration (section 2.5.5.3) or by U.V. absorbance (section 2.5.5.2).

From the difference between the initial and final surfactant concentrations the amount adsorbed onto the solid, in mol g⁻¹, was calculated using the equation:

$$\Gamma = (C_i - C_f) \times \frac{V}{m}$$

where, Γ = amount of surfactant adsorbed, mol g⁻¹

C_i, C_f = initial and final surfactant concentrations respectively, mol dm⁻³

V = volume of test solution, dm³

m = mass of solid sample, g

2.7.2 Loss of complexing agent from solution

The adsorption of complexing agents was determined using the same procedures as for the anionic surfactants with only the method of determining the agent being different (see section 2.5.6).

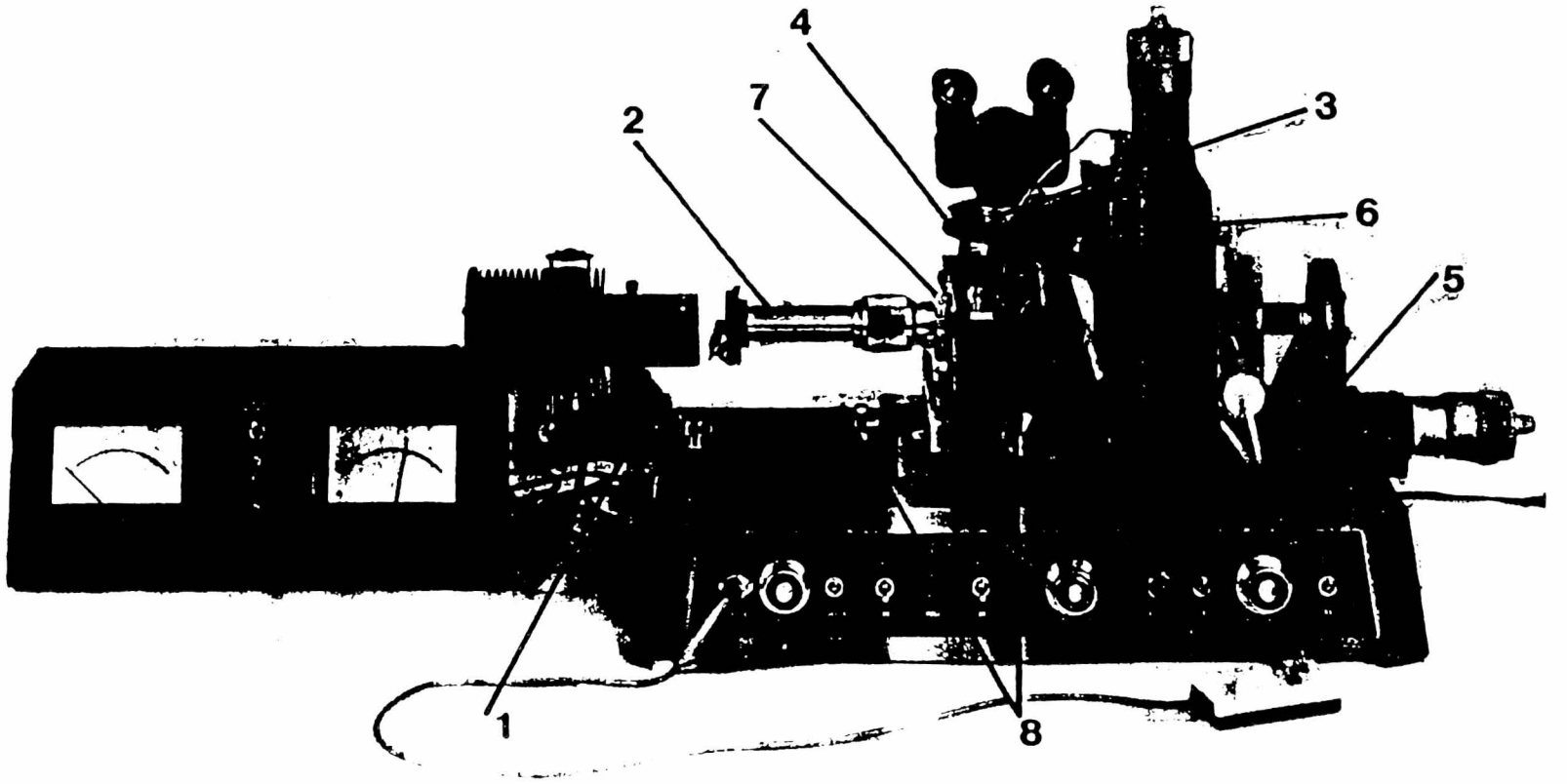
2.8 Electrophoresis Measurements

A single particle microelectrophoresis apparatus (Rank brothers Mk II) (Fig 29) with auxiliary water bath (receiving water from and returning water to, a thermostatted water reservoir) was used for the electrophoresis measurements. The length of one division of the eyepiece graticule was $17.8 \mu\text{m}$.

A thin-walled van Gils cylindrical cell, incorporating platinum electrodes, was used for mobility measurements. The cell had an internal diameter of $1951 \mu\text{m}$ and a wall thickness of $82 \mu\text{m}$. The apparatus was fitted with cylindrical platinum electrodes for use with the cylindrical cell.

Platinisation of the Electrodes

The platinum metal electrodes were cleaned in warm soapy water with a small brush and then rinsed thoroughly using hot distilled water. The electrodes were then placed in a hot chromic acid solution, which was prepared by adding concentrated sulphuric acid to sodium dichromate (5 % w/w) (R5), for thirty minutes and then rinsed with distilled water. The electrodes were then immersed in a platinising solution of Chloroplatinic acid (2% w/w) and lead acetate (0.02% w/w) in an aqueous solution of hydrochloric acid (25 mmol dm^{-3})(R5) and connected to a 12 volt power supply, inducing electrodeposition from the solution onto the anodic electrode. The polarity of the electrodes was reversed every 30 seconds so that an even coating was obtained. Within 30 minutes the electrodes were coated in a thin layer of black



- | | |
|--------------------------------------|---------------------------------|
| 1 Lamp Bracket | 5 Bino Head Mount (Flat Cell) |
| 2 Collimator Tube | 6 Bino Head Mount Locking Screw |
| 3 Binocular Head Locking Screws | 7 Light Beam Height Adjustment |
| 4 Bino Head Mount (Cylindrical Cell) | 8 Positional Adjustment Screws |

Figure 29. Rank Brothers microelectrophoresis apparatus (MK II).

platinum.

Determination of Inter-electrode Distance within the Particle Microelectrophoresis Cell

The interelectrode length of the cell, l_c , was determined by measuring the conductivity when filled with a 0.1 mol dm^{-3} aqueous KCl solution.

A universal conductance bridge was connected to the platinum wires and the conductance, G , of the electrolyte solution was measured. Knowing the conductivity, K , of the KCl solution at 25°C , and the cross-sectional areas, A , of the cell, l_c was determined using the following expression:

$$l_c = \frac{K \cdot A}{G}$$

where $K = 1.28565 \text{ m}^{-1}$ for 0.1 mol dm^{-3} KCl solution at 25°C (L2), and

$$A = \pi d^2 / 4 \text{ m}^2$$

where d = internal diameter of the cell.

For these experiments the determined interelectrode, l_c , distance was found to be 0.0842 m (8.4206 cm).

Position of Stationary Levels within the Cell

Microelectrophoresis measurements are complicated by the simultaneous occurrence of both electrophoretic diffusion and electro-osmosis, which results in a parabolic distribution of liquid speeds with distance from the cell wall (H8). The true electrophoretic velocity is only observable at the so called *stationary levels* in the cell where the electro-osmotic flow and return flow of the liquid cancel. Theoretical considerations show that for a cylindrical cell, the stationary levels are located at a distance of $0.146d$ from the upper and lower walls of the cell, where d is the internal diameter of the cell (S2).

Temperature Control

The temperature coefficient of particle mobilities is about 2% per degree C at room temperature. Efficient thermostating is therefore necessary. The thermostating of the system also helps to avoid convectional disturbances that would otherwise hinder the accurate measurement of the mobilities.

Temperature control was maintained at 25 ± 0.1 °C using a Cal 9000 thermostat and constantly circulating tap water, through the water bath containing the cell, using a BTL CIRCON heater and pump.

Sample Preparation

A series of solutions were prepared spanning the pH range 2-12. All the solutions were of ionic strength 0.1 mol dm^{-3} NaCl. As well as the effect of pH on the electrophoretic mobility of kaolin, the effect was also determined on the ion-washed forms of kaolin. The effect of surfactant addition upon the mobility was also determined.

In order to quickly be able to locate the particles in suspension the solids content of the samples must be sufficiently great to allow ease of particle location yet be low enough to avoid problems associated with sedimentation and interparticle interaction. Street and Buchanan (S6) state that there is no variation in measured mobility if the solid concentration lies between 2×10^{-5} and 2×10^{-4} (w/v). This was achieved by preparing a stock solution so that addition of 1 cm^3 to make up the 50 cm^3 sample gave a solids content in the range stated. The solution pH was adjusted by adding dropwise 0.1 mol dm^{-3} of either HCl or NaOH solutions such that the ionic strength of the solution was unaffected. The flasks were stoppered and shaken and then allowed to stand for approximately 1 hour to allow for any sedimentation of particle aggregates.

Mobility Determinations

With the microscope focused on one of the stationary levels, the platinum electrodes were inserted into the cell and a digital voltmeter was connected across the

electrodes. The particles were illuminated using a quartz-iodine light source and the voltage was adjusted such that the time taken for the particle to move two divisions on the eye-piece graticule was about 10 - 20 seconds.

The voltage polarity was then reversed and the time taken for the particle to move the chosen distance in the reverse direction was recorded. This procedure was repeated for at least 20 particles moving in both directions. The mean of the reciprocal times recorded was used to calculate the average particle electrophoretic mobility.

2.9 Atomic Absorption Spectrophotometry (AAS)

Aluminium and calcium determinations from solution were determined using AAS. These determinations were made so that the interactions of the ions and the surfactant 4- ϕ -C₁₂ABS and also the dissolution of ions from both kaolin and North Sea reservoir rock samples.

Apparatus

The apparatus used was a Pye-Unicam SP9 atomic absorption spectrophotometer fitted with an SP9 computer to process the results, these being printed directly in parts per million (ppm) of the ion being investigated.

A Pye-Unicam aluminium hollow cathode lamp was used as a light source.

Calibration of the Instrument

Standard solutions were prepared by diluting a 1000 ppm standard solution (BDH) for both aluminium and calcium.

A plot of absorbance against metal ion concentration was plotted and can be seen in Figs 30 and 31. The effect of 0.1 mol dm^{-3} NaCl solution on the determination of the metal ion species in solution can also be seen in Figs 30 and 31.

2.9.2 Determination of Calcium ions in solution by Ion-Selective Electrode

Preparation of the Electrode

Before use the electrode (Orion) was soaked in distilled water for 15 minutes and then soaked in a standard solution of calcium ions for at least one hour. This procedure was repeated daily.

Calibration of the Electrode

A series of standard calcium solutions were prepared by diluting a stock solution of $1 \times 10^{-3} \text{ mol dm}^{-3}$ calcium chloride. The electrode was placed in the solution with a double junction reference electrode (Orion) and the millivolt value given on the Autotitrator was followed until a steady reading was obtained. This value was noted and the process repeated for the rest of the standard solutions. A calibration graph

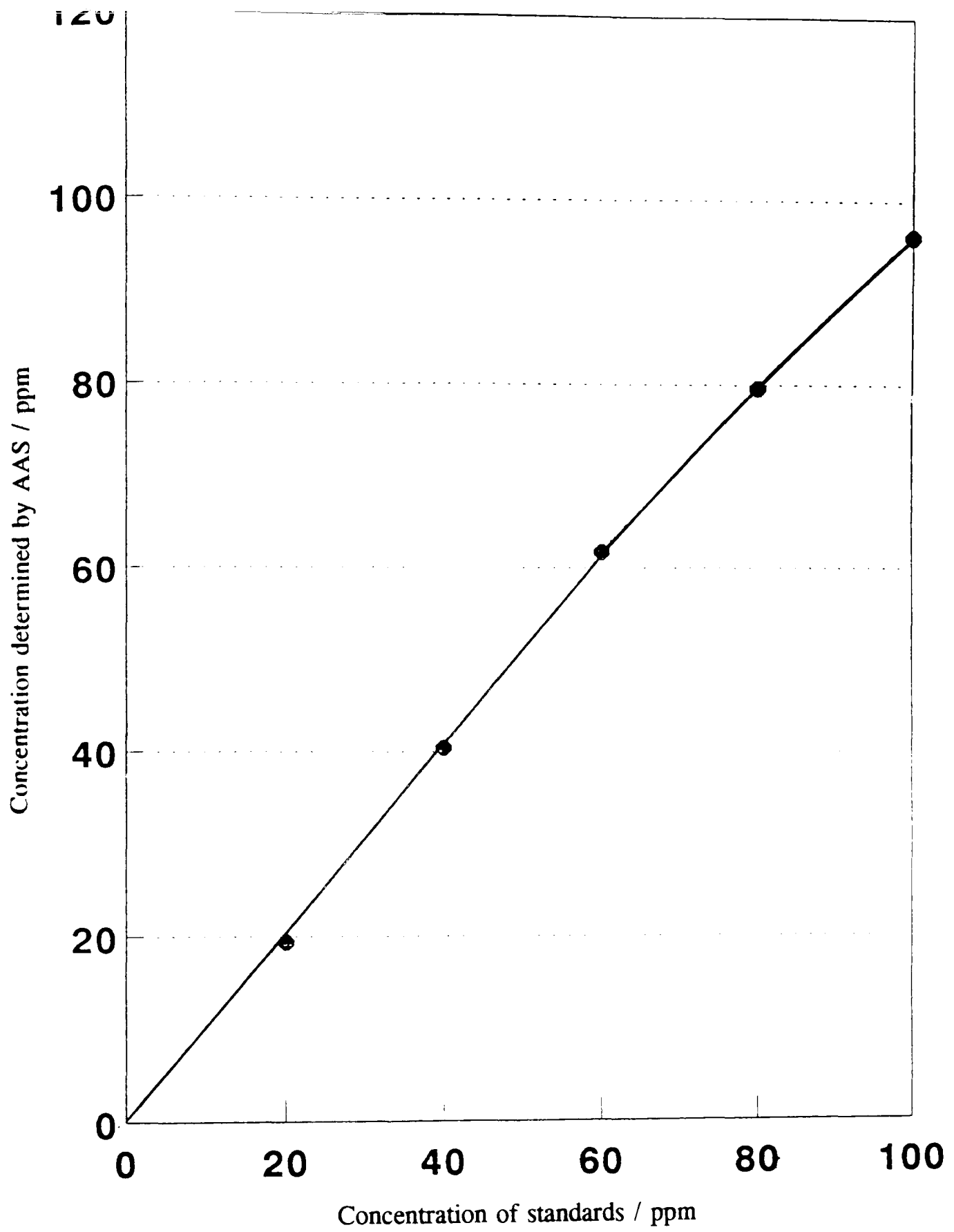


Figure 30. Calibration of Aluminium determination by AAS.

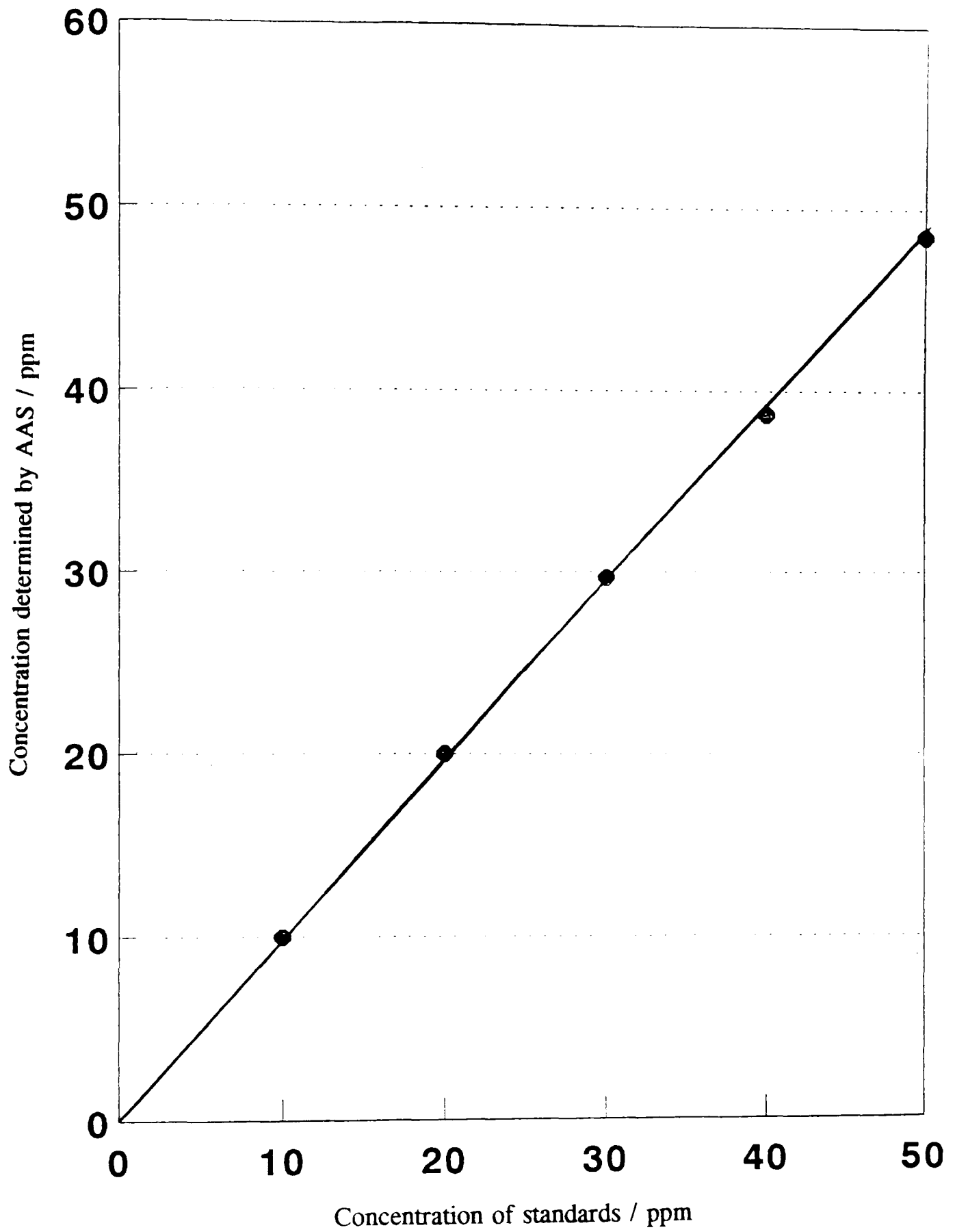


Figure 31. Calibration of calcium determinations by AAS.

was plotted and can be seen in Fig 32. This calibration procedure was performed daily and the slope of the graph calculated. If the slope of the graph had become less than 25 (the ideal value being 27.5) then the electrode was deemed to be contaminated. Therefore, the preparation procedure was carried out again or the sensing module of the electrode was replaced.

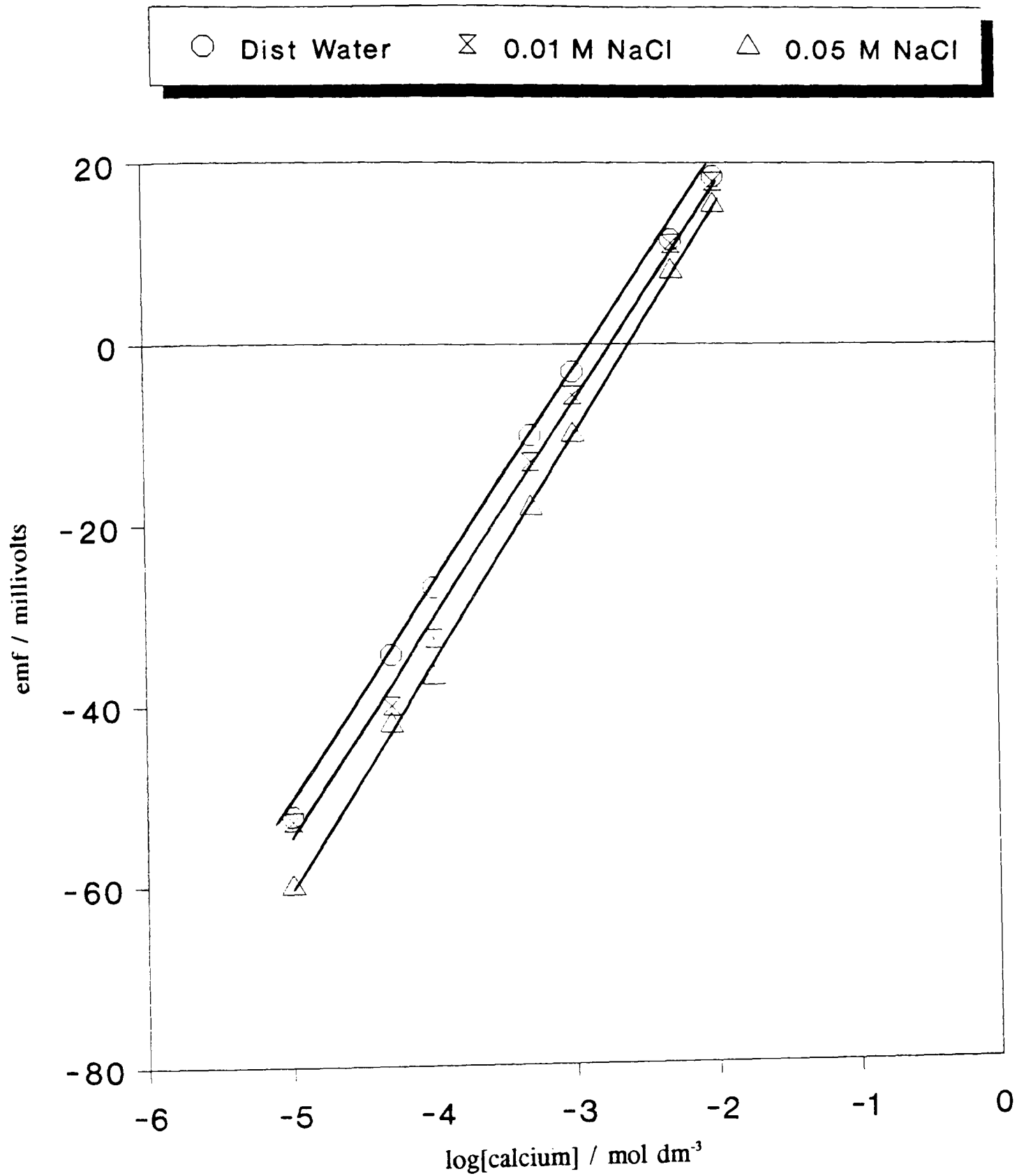


Figure 32. Calibration graph of calcium in solution using the Calcium selective electrode.

Chapter 3.

Results

3 Results

3.1 Characterisation of Kaolin and Ion-washed Kaolin

The characterisation of the washed kaolins was based upon the following techniques:- X-Ray Diffraction (XRD), X-Ray Fluorescence (XRF), Nitrogen adsorption (BET Surface Area Analysis), Scanning Electron Microscopy (SEM) and Electrophoresis.

3.1.1 X-Ray Diffraction

XRD was used to determine the effect of ion washing upon the internal structure of the clay lattice. Comparing the spectra (Fig 33) and its data with that from the JCPDS literature values (see Table 3), excellent agreement is observed indicating that the samples are indeed kaolin and that they have been little changed by the washing process. Although the appearance of a new peak (at approximately 9°) indicates that ion-exchange of the surface ions is occurring for the metal ions from solution.

3.1.2 X-ray Fluorescence

XRF was used to determine whether the surface layers and lattice cells had been affected by the washing process. The spectra of the samples are given in Figs 34-37. It can be seen that the difference in the spectra is only very slight. However, by

converting the signal intensity to a relative concentration the concentration of the elements in the surface could be determined. These are given in Table 4.

Table 3. JCPDS d-values of kaolin compared to those obtained for the ion washed kaolins.

JCPDS d-values for Kaolin	Washed Kaolin	Sodium Kaolin	Calcium Kaolin	Aluminium Kaolin
		9.939	9.990	9.780
7.150	7.138	7.147	7.155	7.067
4.460	4.476	4.460	4.470	4.436
4.340	4.352	4.350	4.360	4.327
4.160	4.181	4.173	4.180	4.146
3.830	3.842	3.837	3.839	3.811
3.720	3.736	3.729	3.741	3.721
3.560	3.756	3.569	3.577	3.551
3.370	3.338	3.380	3.342	3.315
3.140	3.110	3.110	3.106	3.065

Table 4 - Relative concentration of elements in ion-washed kaolins as measured by XRF.

Relative concentration in the surface	Aluminium Kaolinite	Calcium Kaolinite	Sodium Kaolinite	Washed Kaolinite
Aluminium	27.8	27.3	33.1	28.0
Silicon	46.7	46.5	46.6	46.9
Calcium	8.6	8.8	6.2	7.7
Potassium	10.5	10.4	9.2	10.6
Iron	6.4	6.9	4.9	7.0

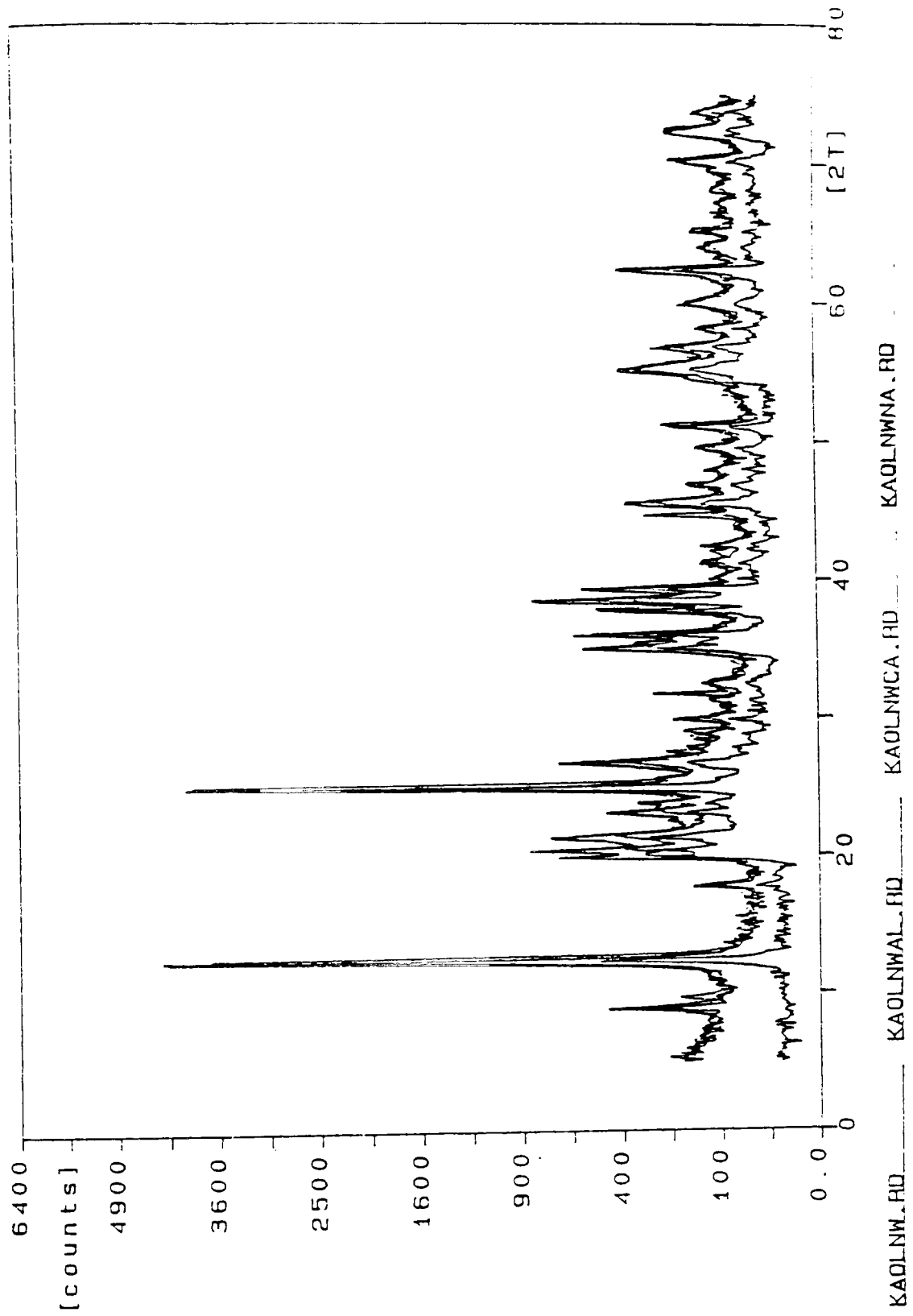


Figure 33. XRD spectra of ion washed kaolins.

RATE = 93 CPS 11:49:16 EDS READY 50 LSEC
 P S = 1448 CNT TIME = PRST = 50 LSEC
 A = WASHED KAOLIN

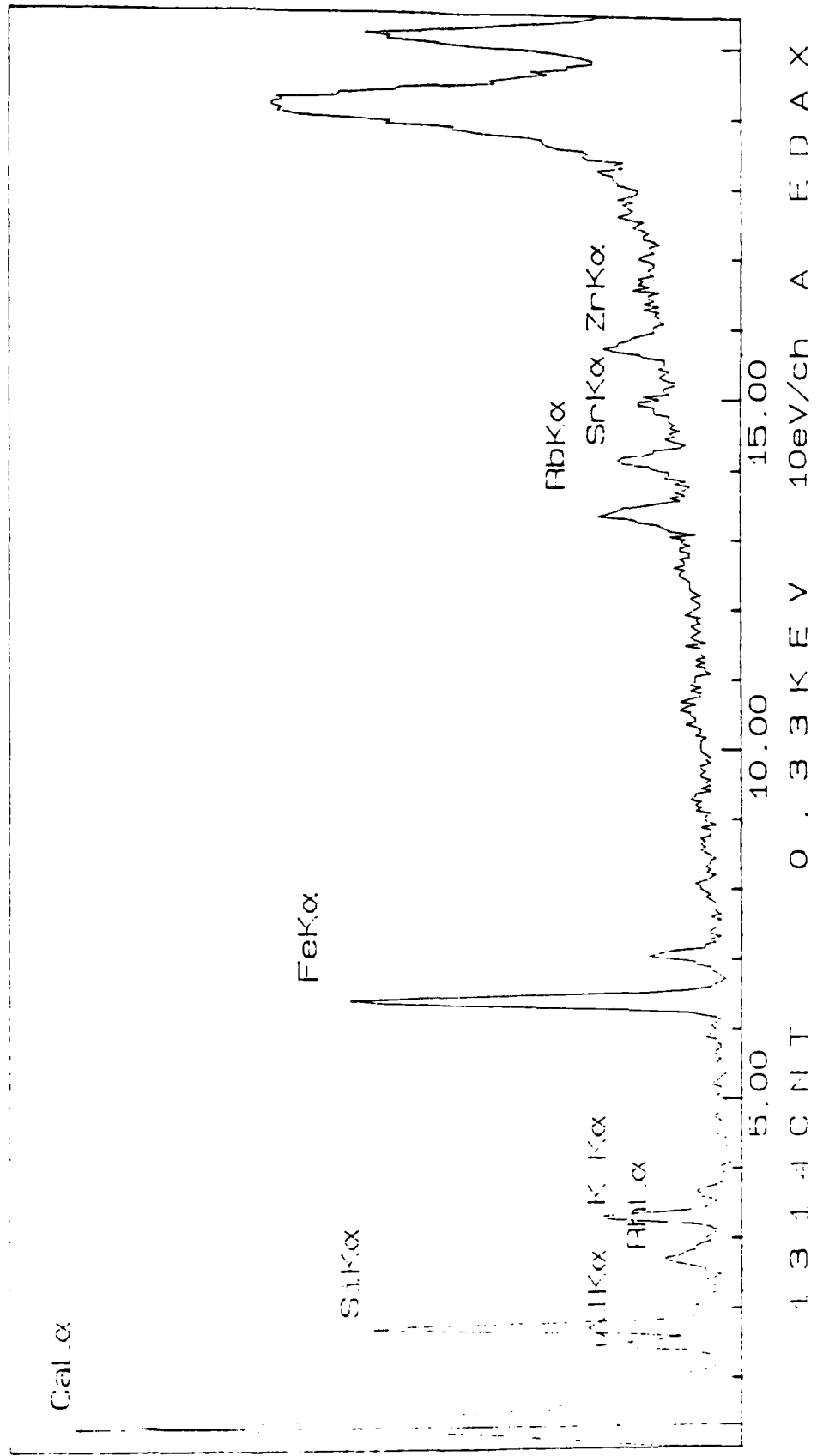


Figure 34. XRF spectra of a washed kaolin sample.

11:57:20 EDS READY
RATE = 47739 CPS TIME = 50 L SEC
FS = 1391 CNT PRST = 50 L SEC
A = SODIUM WASHED KAOLIN

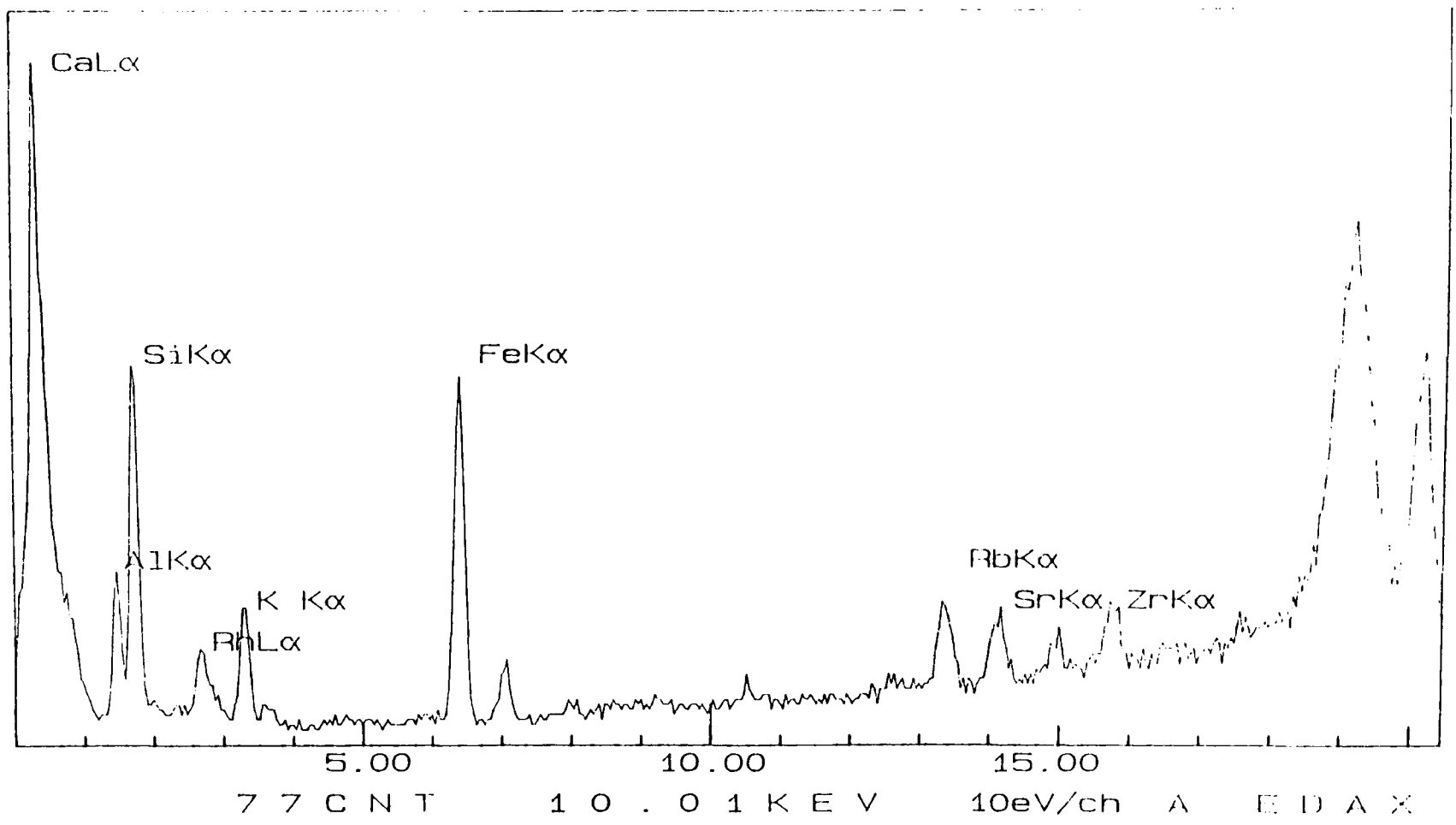


Figure 35. XRF spectra of sodium washed kaolin.

12:05:59 EDS READY
RATE = 47790 CPS TIME = 50 LSEC
FS = 1353 CNT PRST = 50 LSEC
A = CALCIUM WASHED KAOLIN

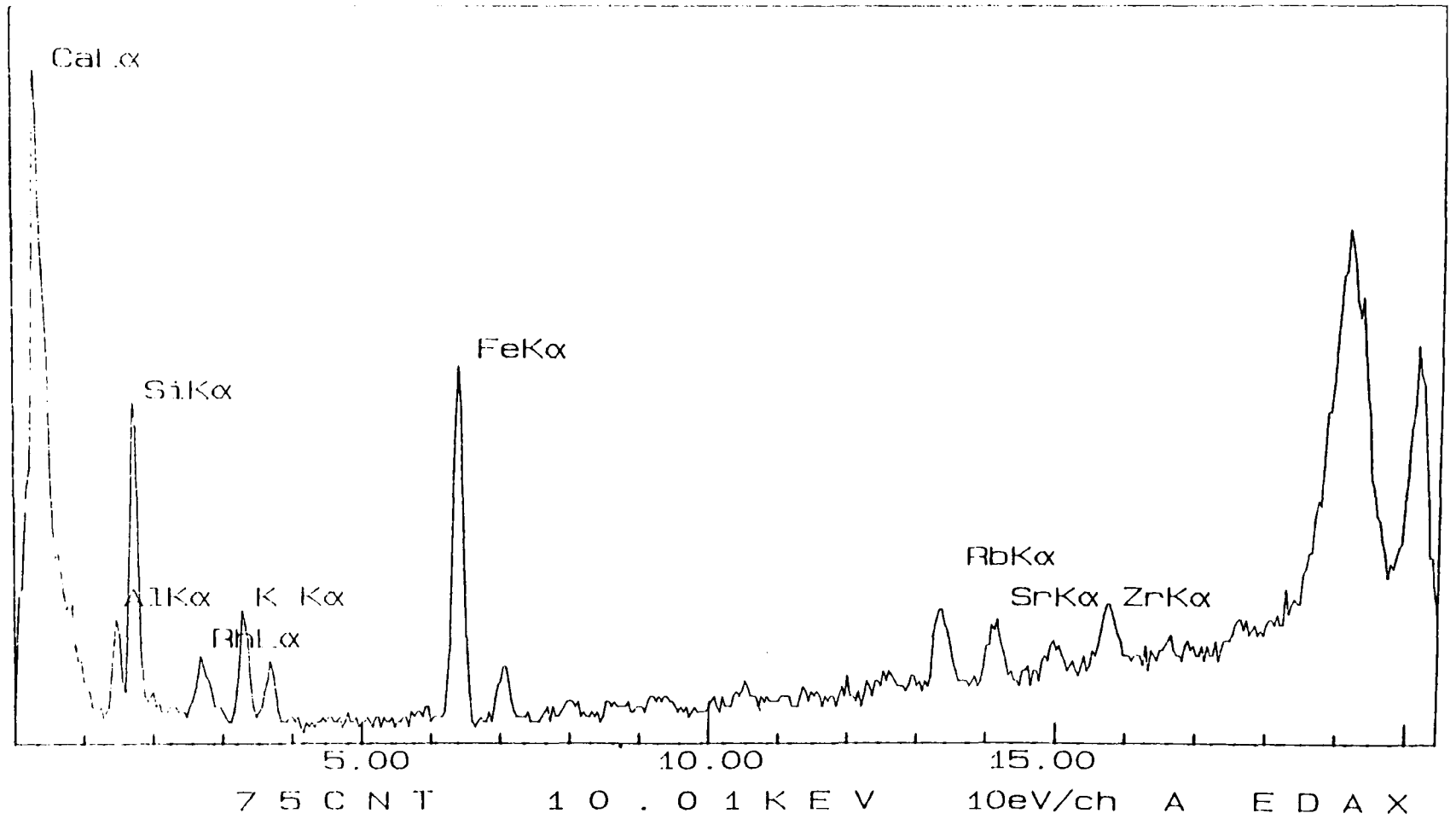


Figure 36. XRF spectra of calcium washed kaolin.

12:14:50 EDS READY
 RATE = 44957 CPS TIME = 50 LSEC
 FS = 1376 CNT PRST = 50 LSEC
 A = ALUMINIUM WASHED KAOLIN

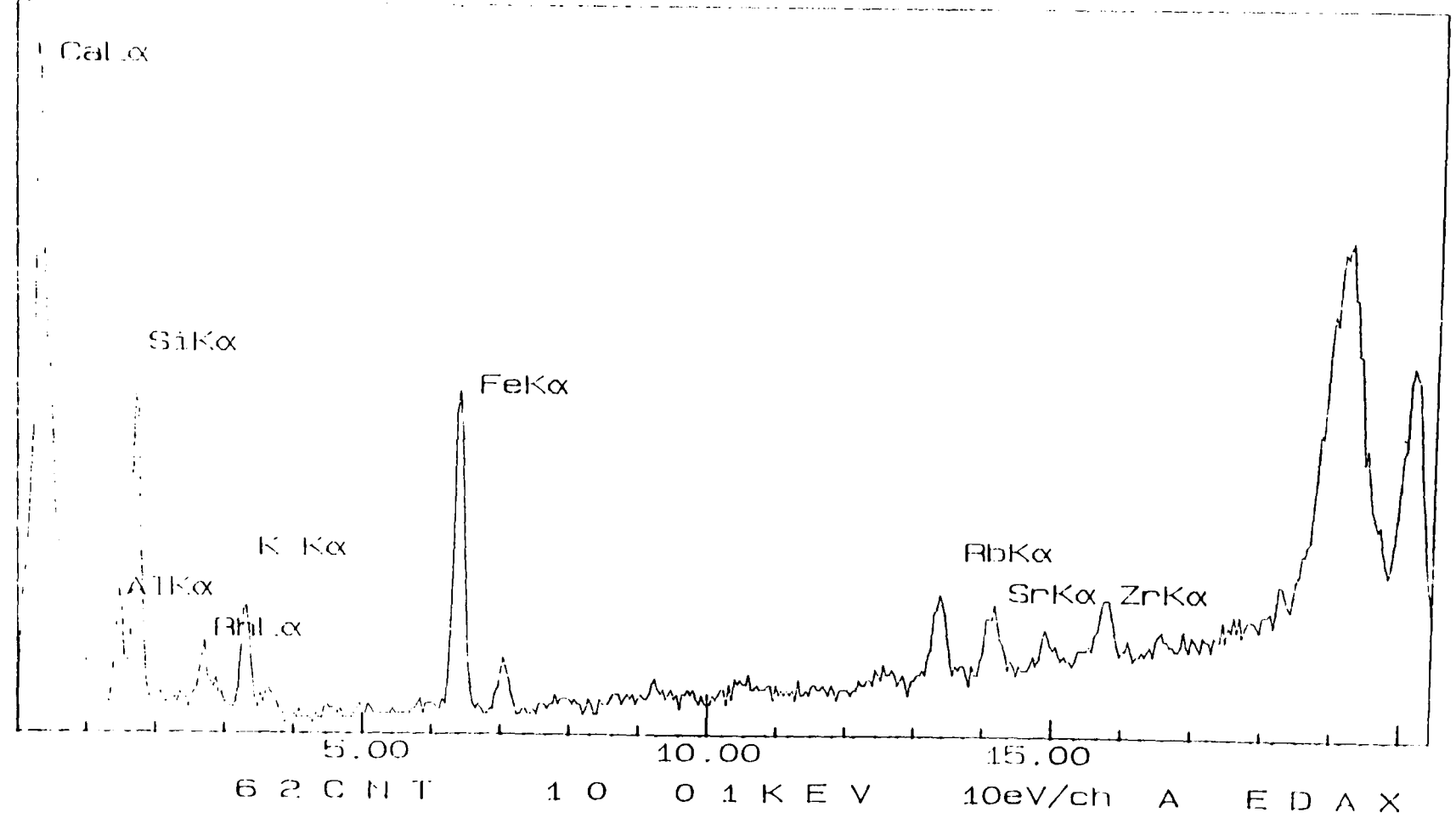


Figure 37. XRF spectra of aluminium washed kaolin.

3.1.3 Surface Area Determinations

From BET, nitrogen adsorption measurements, the surface areas of kaolin and the ion-washed kaolins was determined. It was found that the specific surface area of the washed kaolin was $14.95 \text{ m}^2 \text{ g}^{-1}$ (this shows a similar value to that of Bazin, B7). The sodium calcium and aluminium forms of the clay having the areas 8.98, 8.48 and $8.08 \text{ m}^2 \text{ g}^{-1}$ respectively. On repeating the surface areas the values were found to be $15.08 \text{ m}^2 \text{ g}^{-1}$ for the washed kaolin and 10.73, 7.92, $12.74 \text{ m}^2 \text{ g}^{-1}$ for the sodium, calcium and aluminium forms of the clay respectively. It can be seen that there is quite a discrepancy in the results obtained for the ion-washed forms of the kaolin. The possible reasons for this are considered in the Discussion section.

3.1.4 Scanning Electron Microscopy

The SEM micrographs of the washed kaolins are shown in Fig 38. It can be seen that the size of the kaolin platelets appears to have increased with the valency of the wash ion. Further micrographs have shown a non-uniformity of platelet size within the clays after washing.

3.1.5 Electrophoresis

Electrophoresis of the washed clays was studied so that the effect on zeta potential of the wash ions could be seen. This would give some indication as to how the surface charge would be affected. The mobilities were calculated using the following

equation:

$$m = \frac{d}{t V}$$

where d is the distance travelled by the particle, t is time in seconds and V is the applied voltage.

Using these calculated mobilities the zeta potential of the clays could be determined thus:

$$\zeta = \frac{m\mu}{\epsilon_r}$$

where

ζ = the zeta potential

m = mobility of the particles

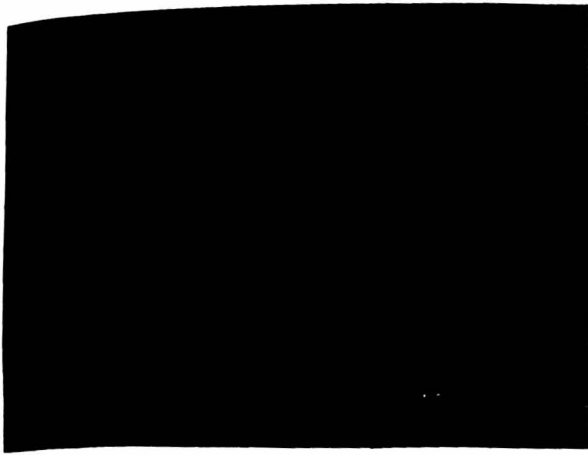
μ = coefficient of viscosity = $8.4 \times 10^{-4} \text{ Kg m}^{-1} \text{ s}^{-1}$

ϵ_r = the relative permittivity of the solution.

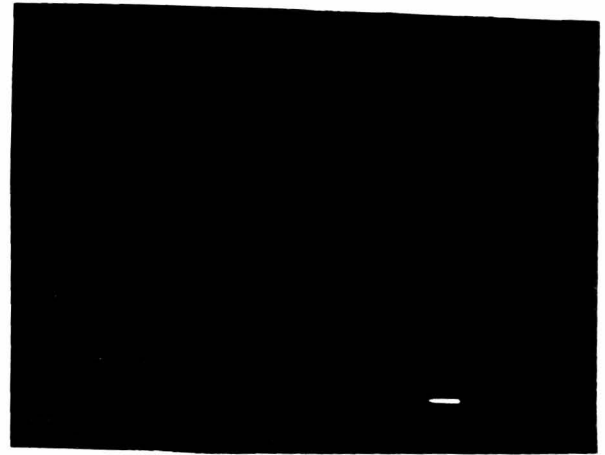
A table of calculated zeta potential is given below and the results are given in Fig 39.

Table 4a - Calculated Zeta potential for the prepared clays.

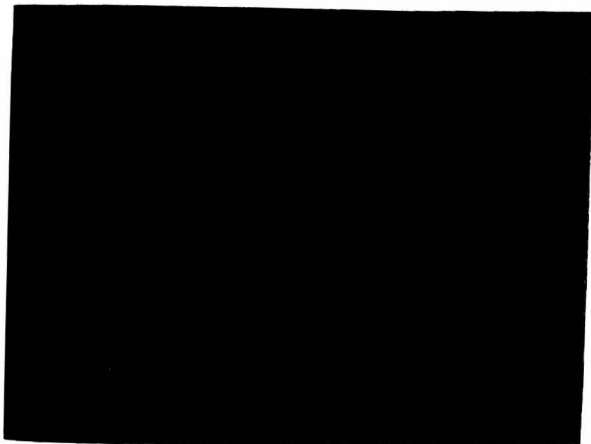
pH	Zeta potential of washed kaolin / mV	Zeta potential of sodium kaolin / mV	Zeta potential of calcium kaolin / mV	Zeta potl of aluminium kaolin /mV
2.00	-1.995	-	-	-
2.30	-	-1.722	-	-1.078
2.80	-	-	-2.398	-2.263
3.00	-	-	-2.079	-
3.30	-	-3.042	-	-
3.80	-2.206	-	-	-
4.50	-	-	-3.294	-
6.20	-	-	-	-4.606
6.80	-	-6.082	-	-
7.70	-	-	-5.058	-
8.50	-4.002	-	-	-
10.2	-3.863	-7.606	-	-4.111
11.35	-	-6.315	-	-
11.80	-3.034	-	-	-
12.00	-	-	-	-1.862



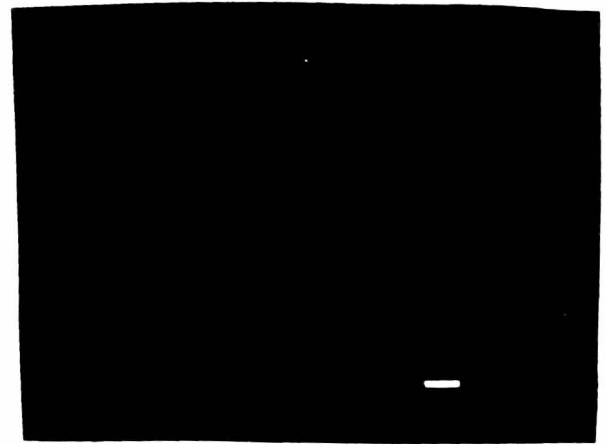
Washed kaolin



sodium kaolin



calcium kaolin



aluminium kaolin

Figure 38. Scanning Electron Micrograph of the various washed kaolins.

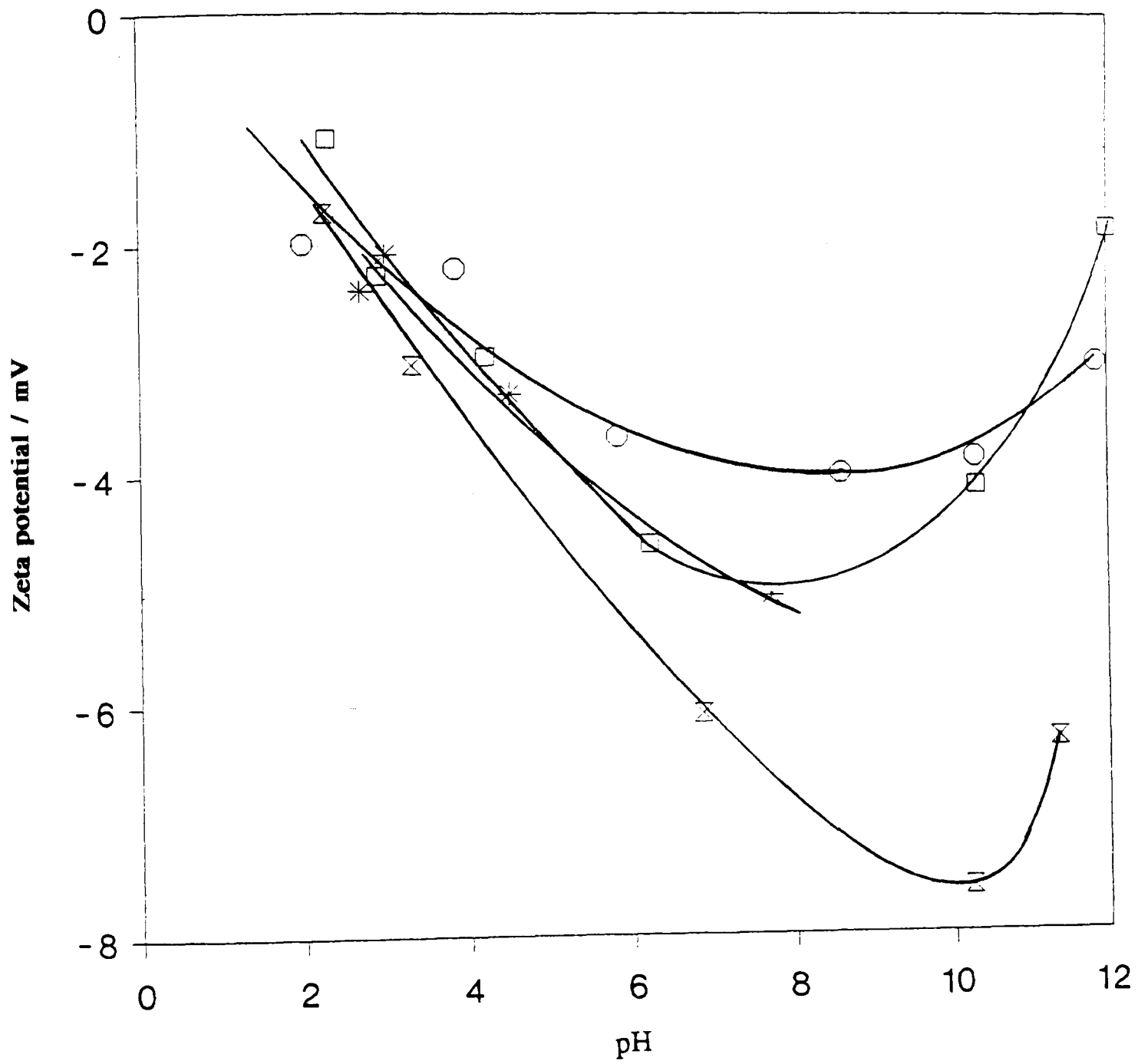
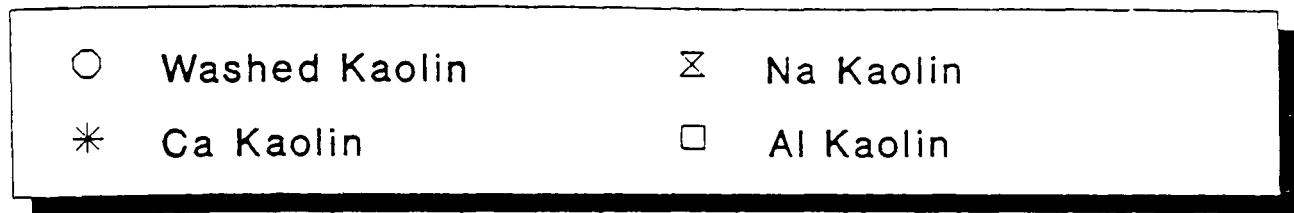


Figure 39. Zeta potential determinations of the various washed kaolins in $0.1 \text{ mol dm}^{-3} \text{ NaCl}$.

3.2 Characterisation of North Sea Reservoir Rock

The core samples have been characterised using the same techniques as for the kaolin samples.

3.2.1 X-Ray Diffraction

XRD was used in this instance not to identify the compound but to determine the amount of kaolin clay held in the structure of the rock sample (the kaolin is usually found in the rock pores). This was achieved by considering the intensity of an XRD peak (known to be present due to kaolin) and incorporating an additional, known, amount of kaolin clay and determining the effect of this addition upon the intensity of the peak. This was repeated until the samples were pure kaolin. Graphs were plotted of intensity against amount of kaolin added (Figs 40-42) and from the amount from these the initial amount of kaolin in the sample was determined by extrapolation to zero. The amounts of clay present in the samples 12395, 12417 and 12498.2 were found to be 2.65, 5.05 and 2.40 percent respectively.

Other forms of clay may also have been present in these samples (i.e. Montmorillonites and illites) which could have increased the total amount of clay in the core samples. As illite has a very similar XRD spectra to kaolin it is thought that this method will actually determine the amount of kaolin plus illite in the sample and not just kaolin alone.

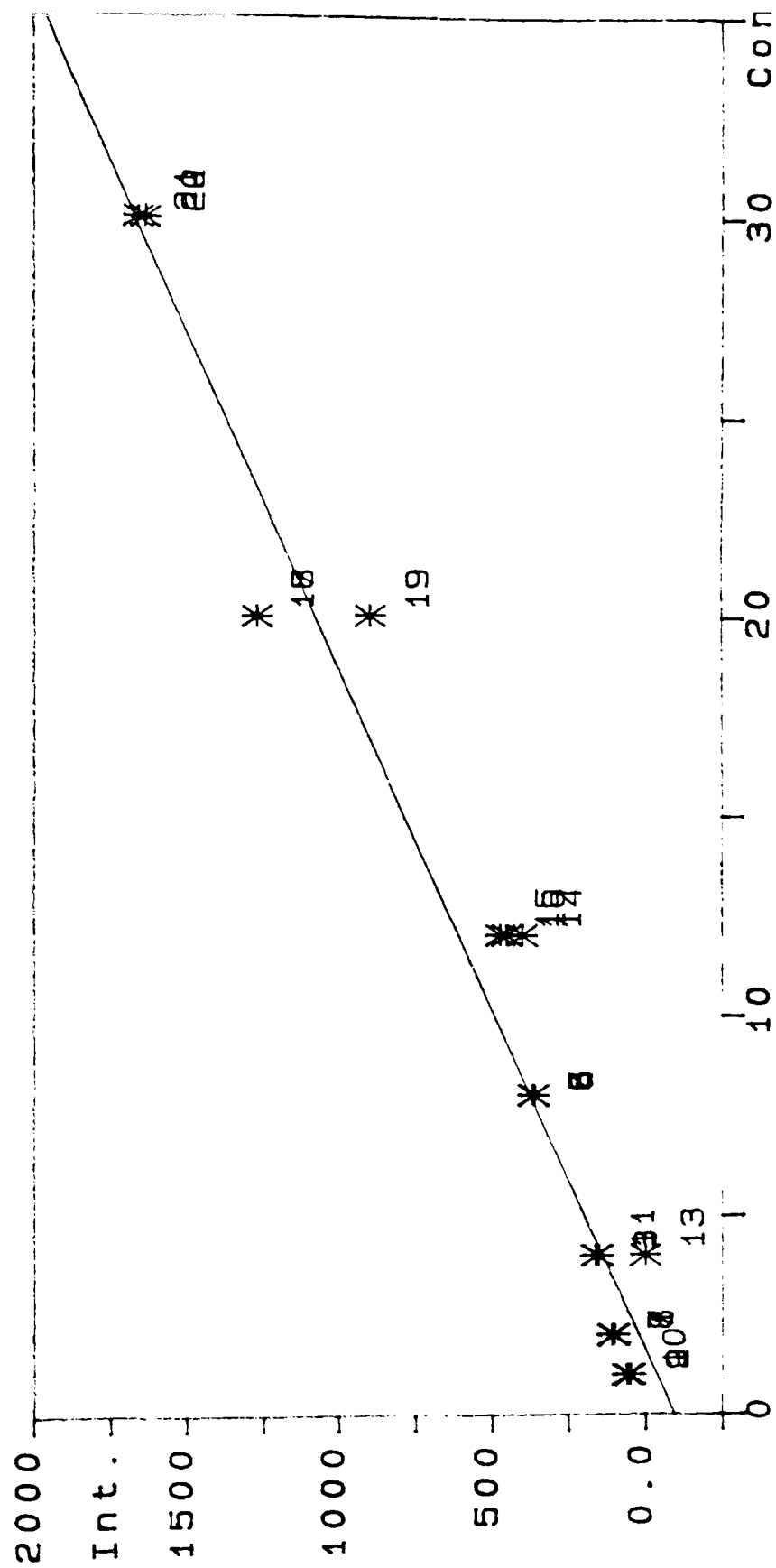


Figure 40. Determination of clay content in core sample 12395 by X-Ray Diffraction.

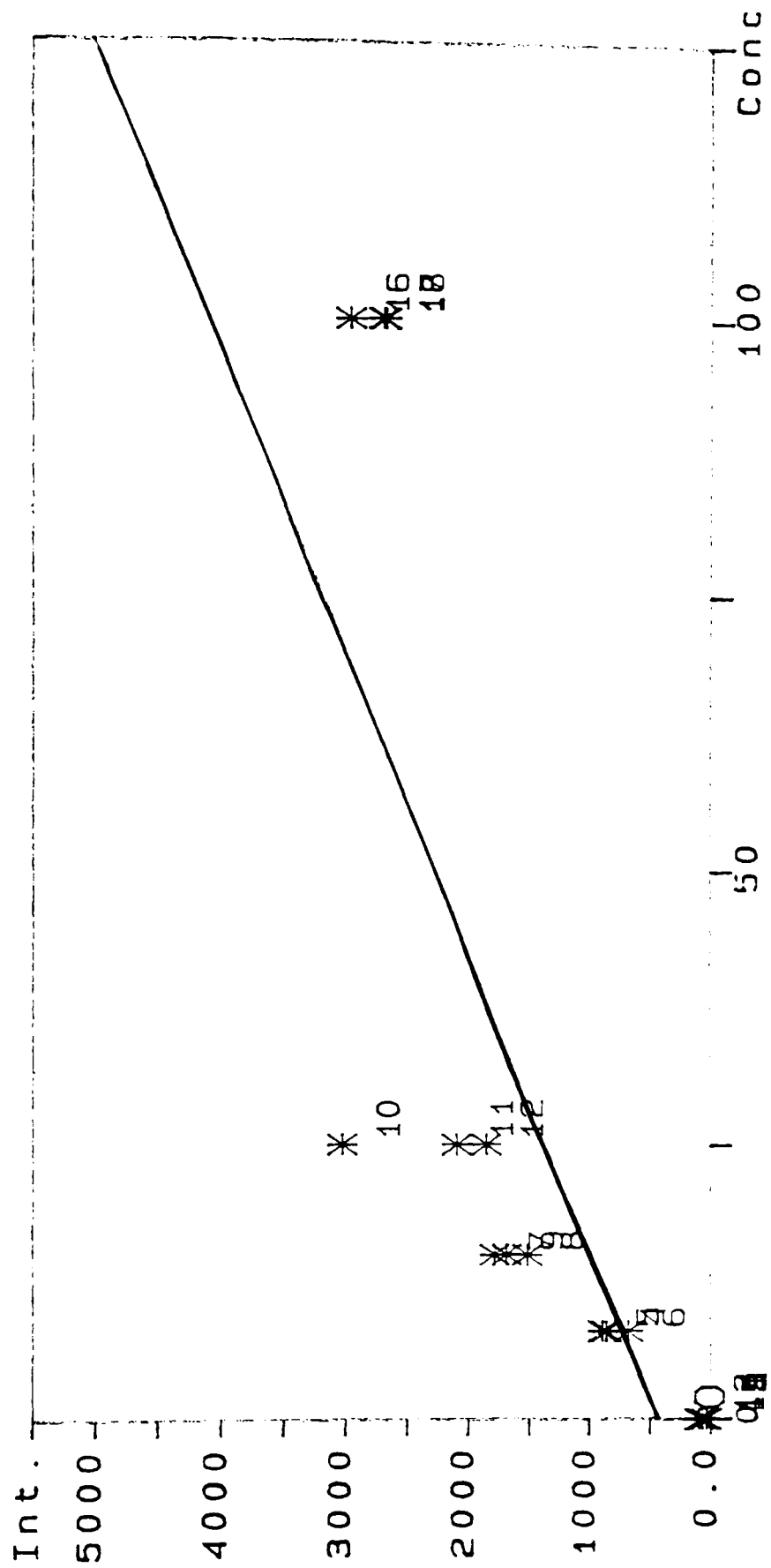


Figure 41. Determination of clay content in core sample 12417 by X-Ray Diffraction.

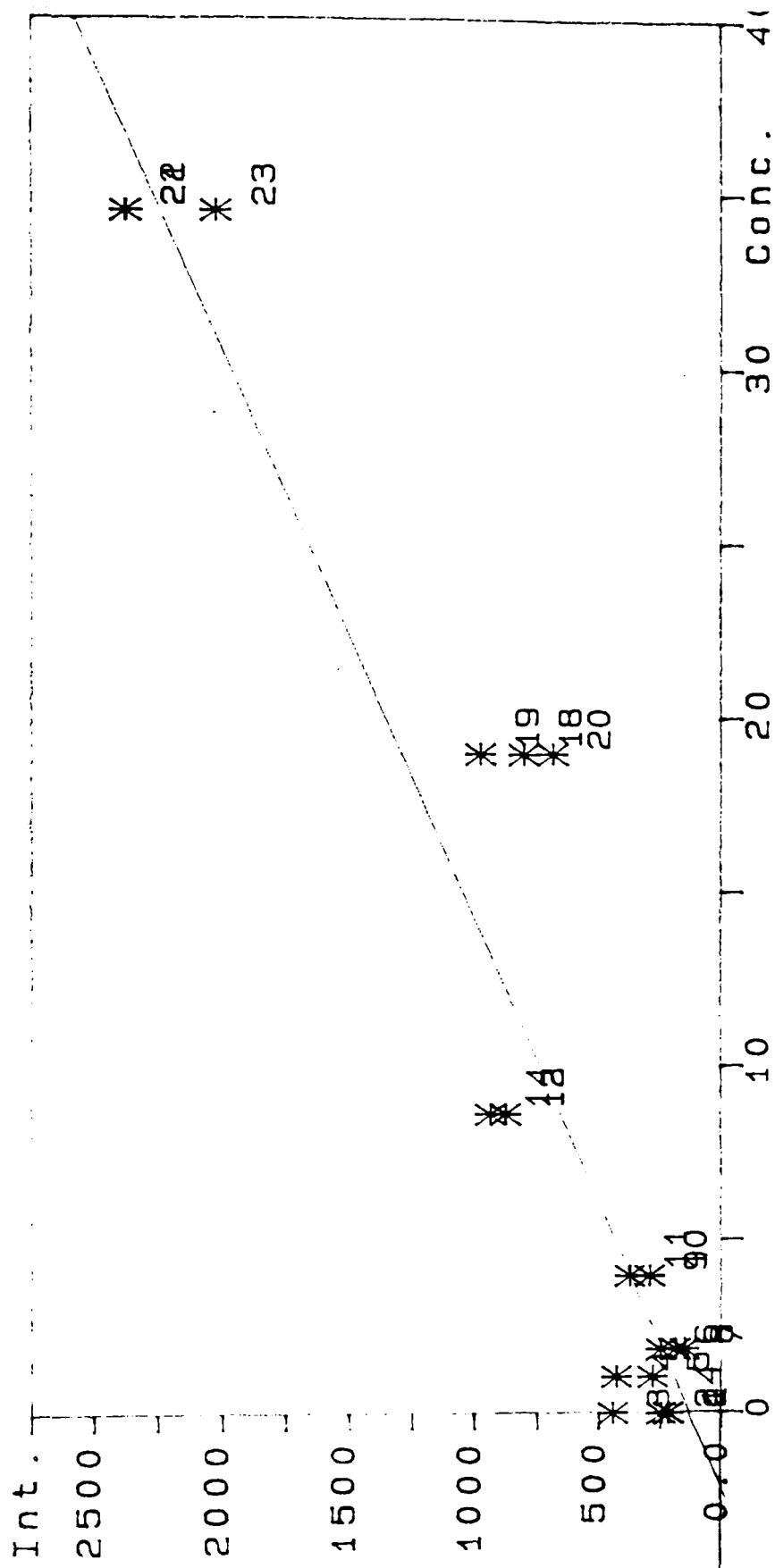


Figure 42. Clay content determination of core sample 12498.2 by X-Ray Diffraction.

3.2.2 X-Ray Fluorescence

XRF spectra of the core samples 12395, 12417 and 12498.2 have been determined. These can be seen in Figs 43-45. It can be seen that the spectra vary slightly, which would be expected due to the different depths from which the samples were taken.

3.2.3 Scanning Electron Microscopy

SEM micrographs were taken of the samples and these confirm that the samples are made up of regions of sandstone interspersed with regions of clay (Fig 46).

3.2.4 Electrophoresis

No determination of zeta potential was possible with these samples as non-uniform particle size prevented a uniform suspension of the core in the electrolyte medium. This caused blockage in the capillary tube making determinations impossible.

RATE= 128CPS
FS= 2222CNT
A =CORE 12395

TIME= 50LSEC
PRST= 50LSEC

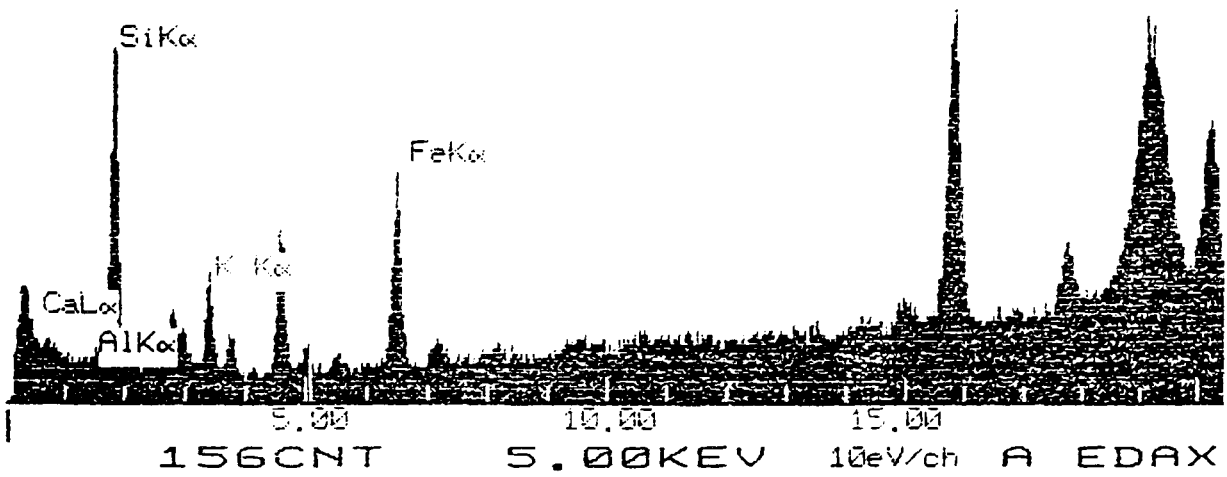


Figure 43. XRF spectra of core sample 12395.

RATE= 319CPS
FS= 2920CNT
A =CORE12417

TIME= 50LSEC
PRST= 50LSEC

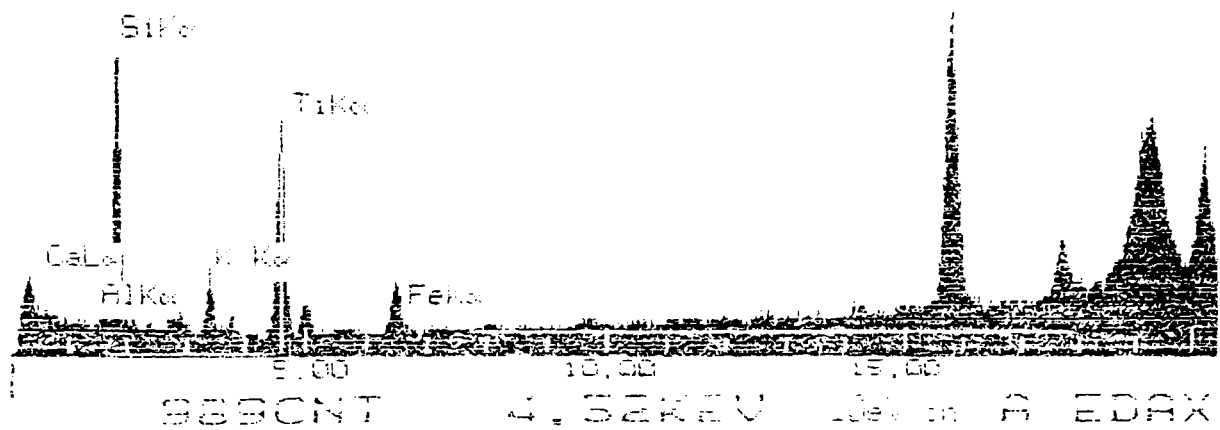


Figure 44. XRF spectra of core sample 12417.

RATE = 135CPS
FS = 3374CNT
A = CORE 12498.2

TIME = 50LSEC
PRST = 50LSEC

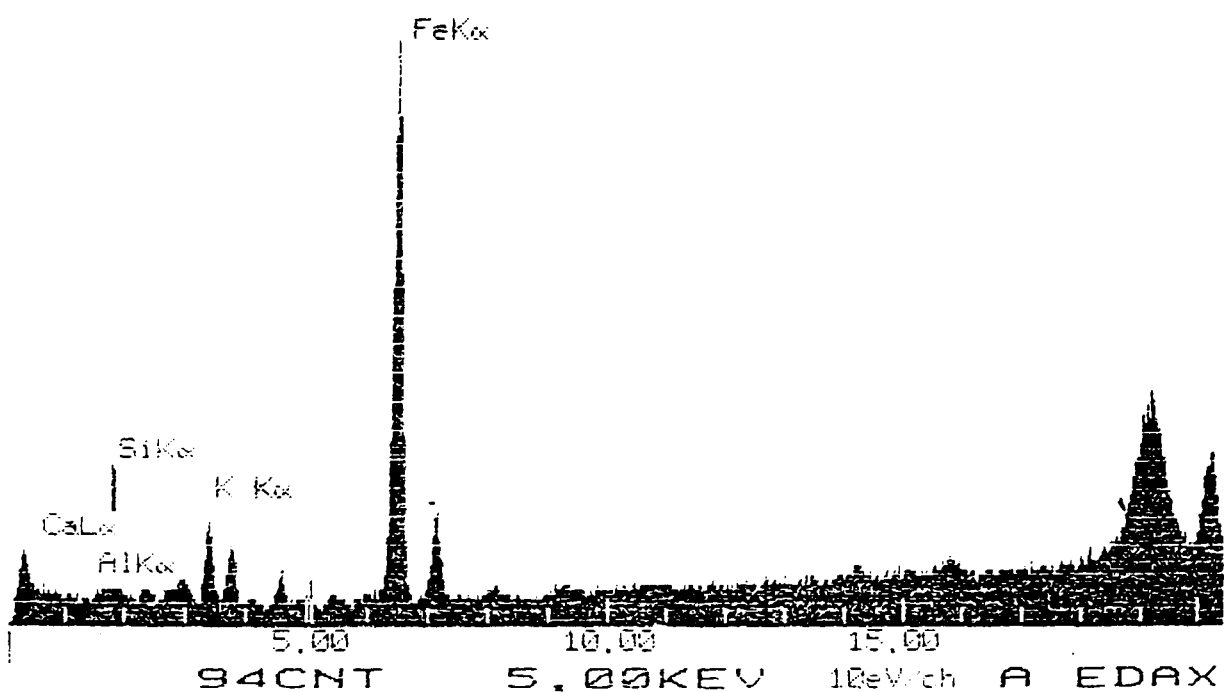
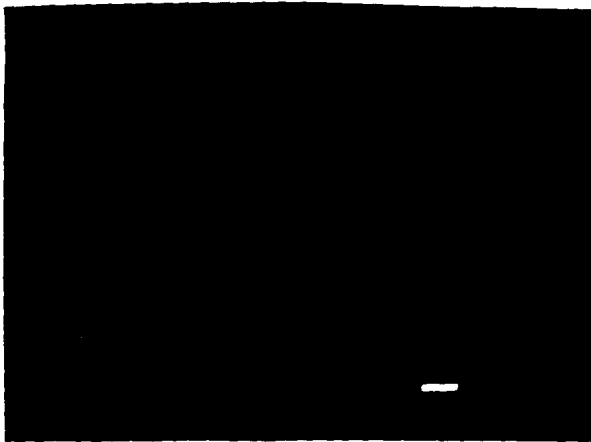


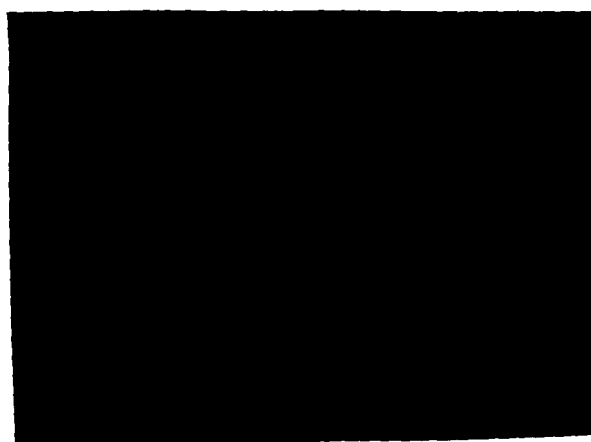
Figure 45. XRF spectra of core sample 12498.2



Core 12395



Core 12417



Core 12498.2

Figure 46. Scanning Electron Micrograph of the core samples.

3.3 Adsorption of 4- ϕ -C₁₂ABS at the Air-Solution Interface

The change in surface tension, γ , at 25°C, of aqueous solutions containing 4- ϕ -C₁₂ABS with concentration, m_D , between 1×10^{-5} and 0.1 mol dm^{-3} are shown in Fig 47. From the obtained data the critical micelle concentration (CMC), the surface excess concentration (Γ) and the area occupied per surfactant molecule at the interface (A_s) can be determined. These are given in Table 5.

3.3.1 The effect of sodium chloride on the adsorption of 4- ϕ -C₁₂ABS at the air-solution interface.

Surface tensions, γ , were measured as a function of 4- ϕ -C₁₂ABS concentration, m_D , at a salt concentrations, m_s , of 0.1 mol dm^{-3} sodium chloride. This is also shown in Fig 47. Again, the CMC, the surface excess concentration and the area per molecule at the interface have been calculated and are given in Table 5.

3.3.2 The effect of short-chained aliphatic alcohols on the adsorption of 4- ϕ -C₁₂ABS at the air-solution interface.

The reduction in aqueous (0.1 mol dm^{-3} NaCl) surface tensions with concentrations of 4- ϕ -C₁₂ABS, at 25°C, with varying short chain alcohols are shown in Fig 48. Due to the solubility restrictions of pentan-1-ol the surface tensions were determined in the presence of 2% v/v of the alcohol. With both propan-1-ol and butan-1-ol surface tensions were determined at both 2% v/v (Fig 48) and 4% v/v alcohol (Fig 49). The

values for CMC, area per molecule at the interface and surface excess concentration have again been determined and are given in Table 5.

3.3.3 The effect of complexing agents on the adsorption of 4- ϕ -C₁₂ABS at the air-solution interface.

Surface tensions have been determined for 4- ϕ -C₁₂ABS, at 25°C, in the presence of the complexing agents sodium tripolyphosphate and sodium citrate and are shown in figure 50.

Table 5. Calculated adsorption parameters for adsorption at the aqueous-air interface for 4- ϕ -C₁₂ABS.

$M_1 / \text{mol dm}^{-3}$	n_{BuOH} / % v/v	n_{PrOH} / % v/v	n_{PeOH} / % v/v	$\Gamma_D / 10^{-6}$ mol g ⁻¹	$A_1 /$ nm ²	CMC / 10 ⁻³ mol dm ⁻³
0.00	-	-	-	2.63	0.63	1.00
0.10	-	-	-	5.01	0.33	0.11
0.10	2	-	-	2.10	1.36	0.18
0.10	4	-	-	1.22	0.79	0.10
0.10	-	2	-	2.16	0.77	0.11
0.10	-	4	-	0.78	2.12	0.10
0.10	-	-	2	0.14	11.8	0.18
0.10	-	-	4	-	-	-

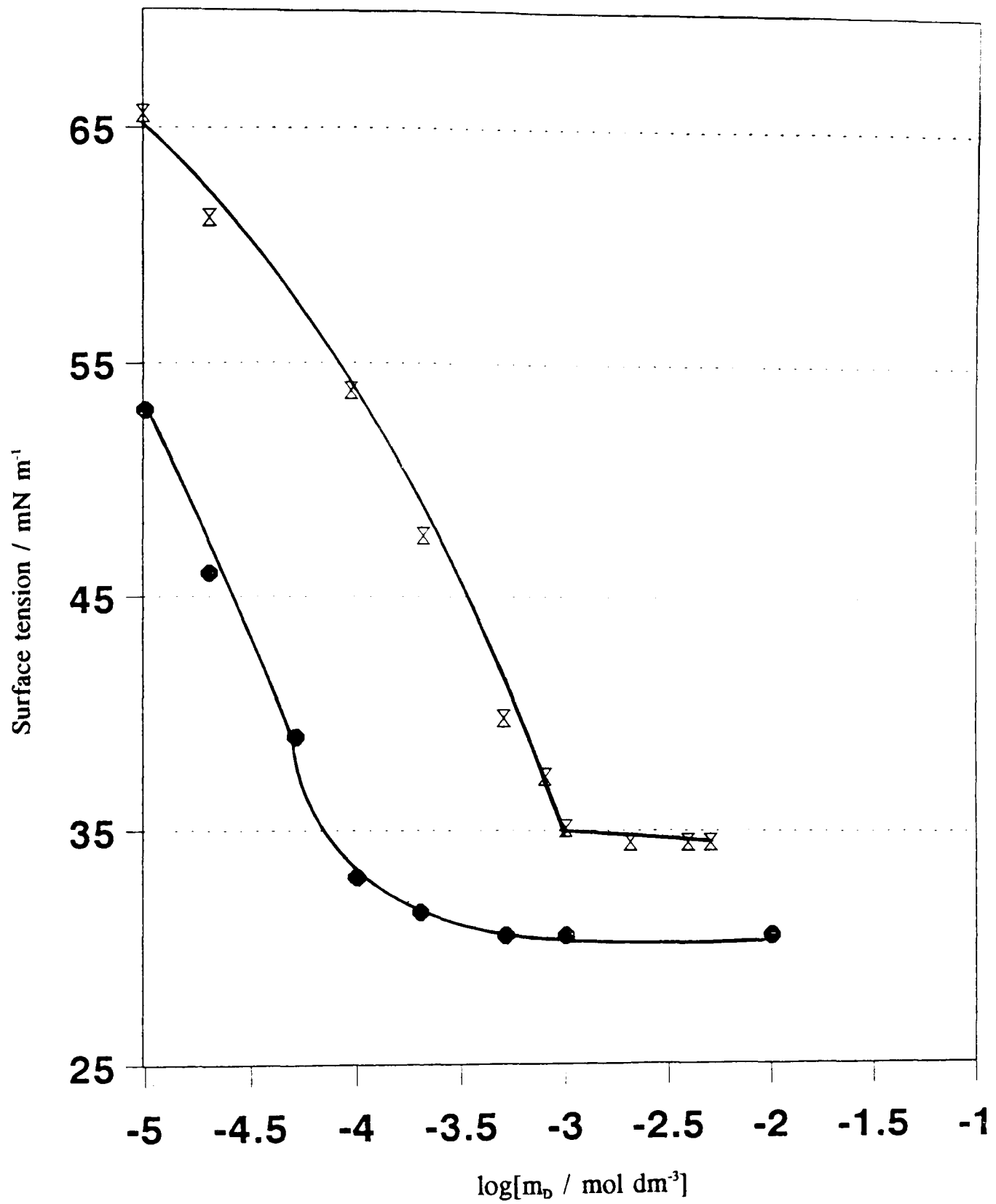


Figure 47. Surface tensions for the air-aqueous NaCl interface at 25°C as a function of 4-φ-C₁₂ABS concentration.

NaCl concentrations of 0.00 (⊗), and 0.10 (●) mol dm⁻³

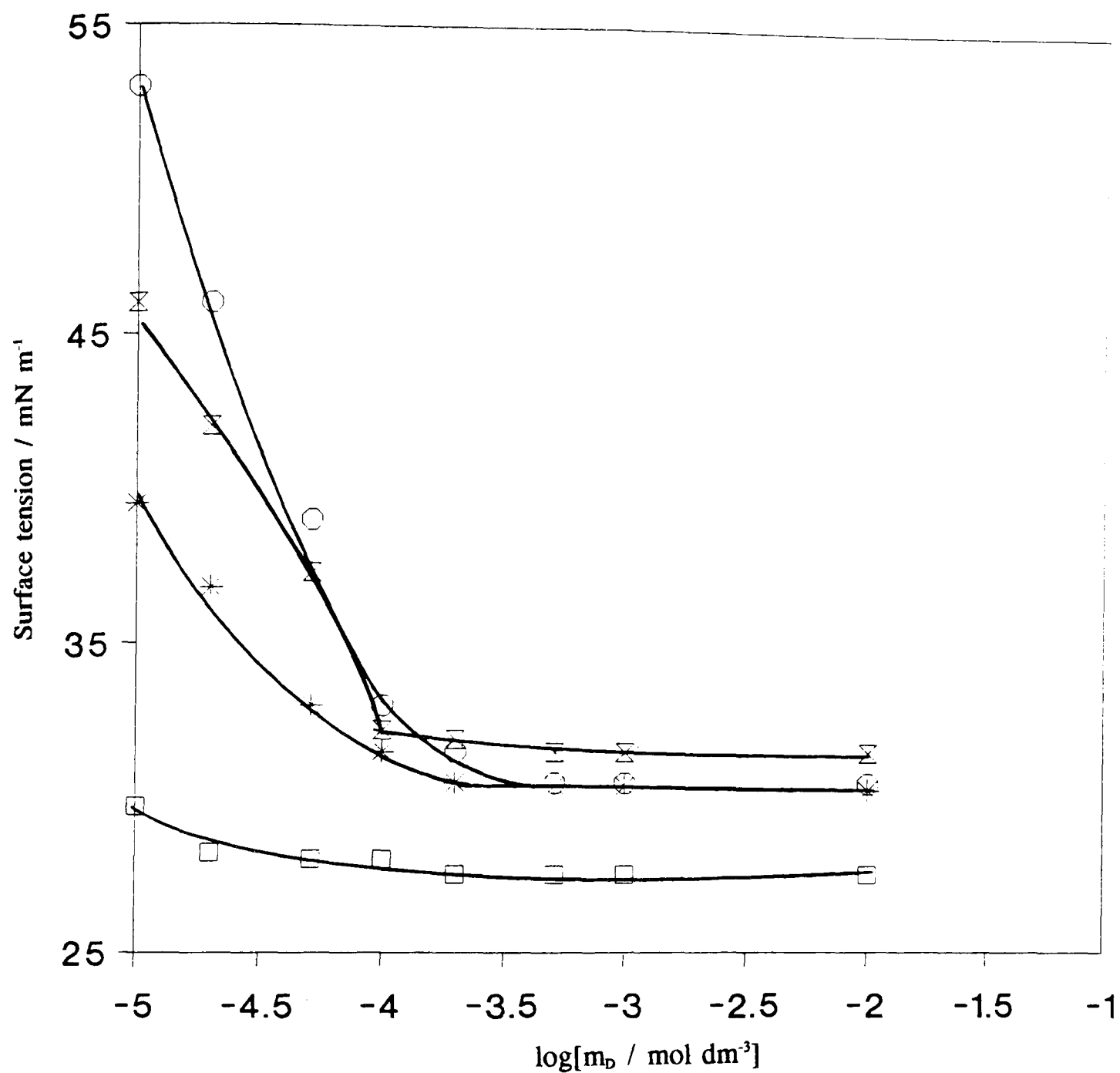


Figure 48. Effect of added short chain aliphatic alcohols (2% v/v) on the surface tension, at 25°C, of 4-φ-C₁₂ABS aqueous NaCl (0.10 mol dm⁻³) solutions.

Propan-1-ol (⊗), Butan-1-ol (⊛) and Pentan-1-ol (◻).

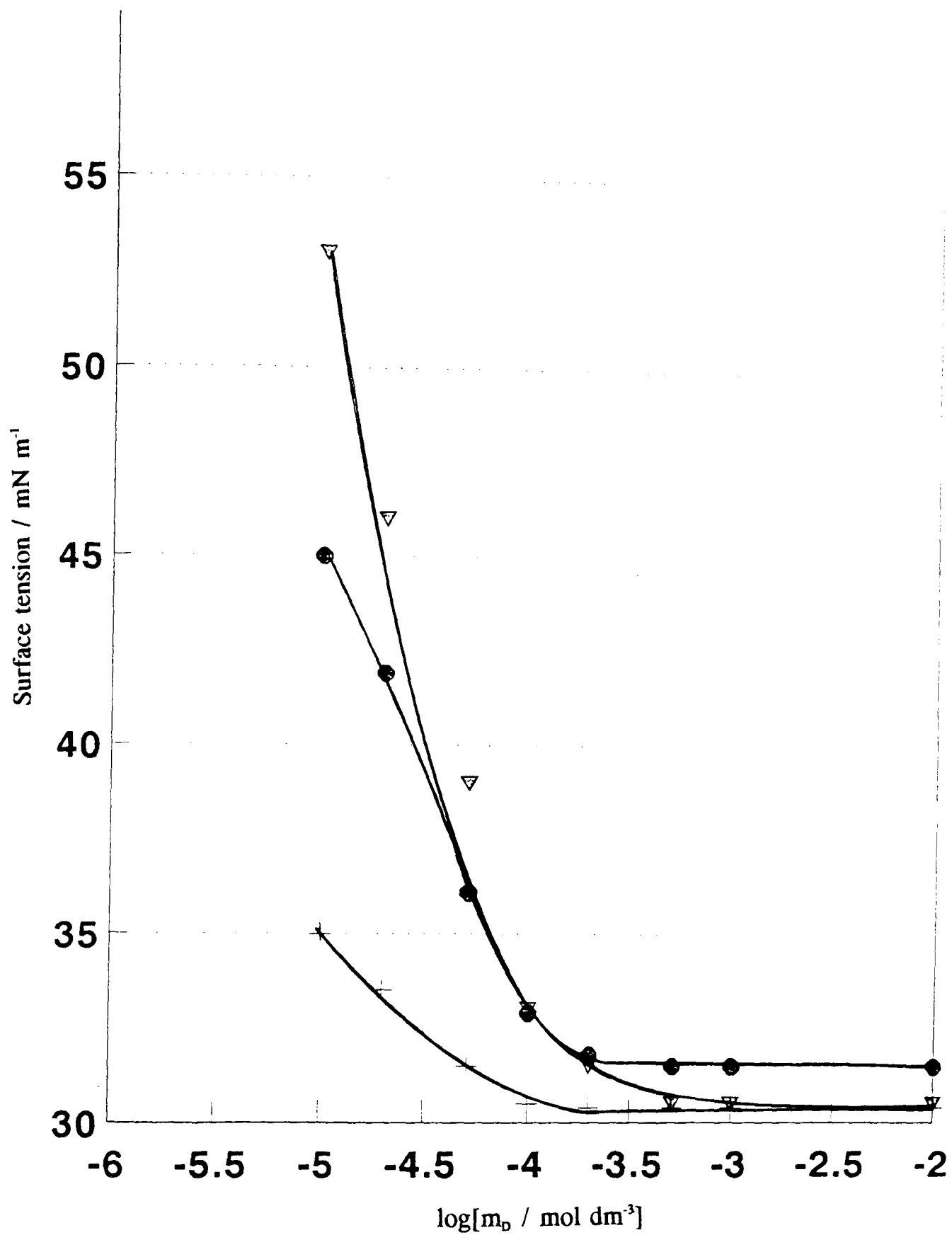


Figure 49. Effect of added short chain aliphatic alcohols (4% v/v) on the surface tension, at 25°C, of 4- ϕ -C₁₂ABS aqueous NaCl (0.10 mol dm⁻³) solutions.

Propan-1-ol (●), and Butan-1-ol (⊕).

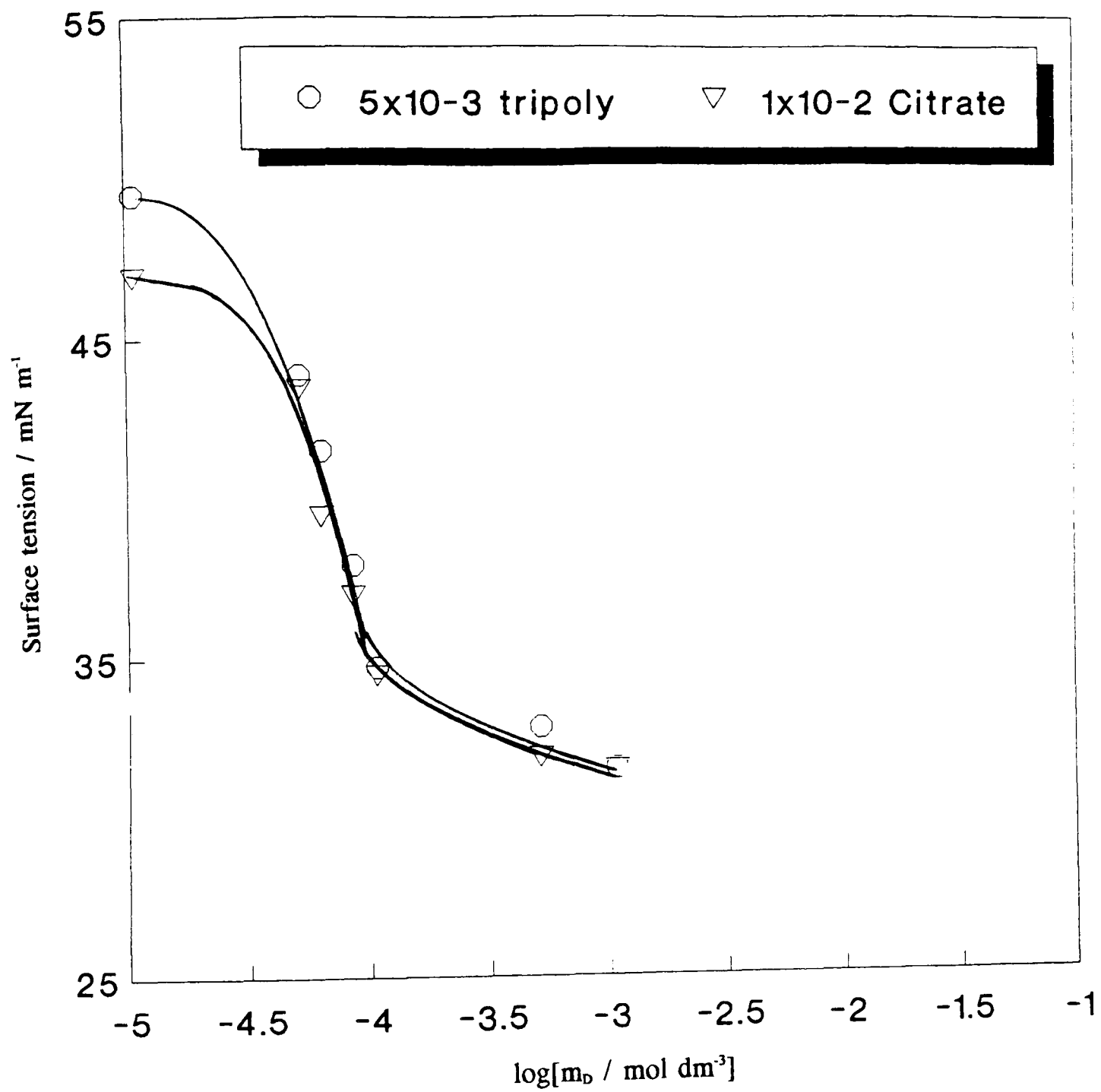


Figure 50. Effect of complexing agents on the adsorption of 4-φ-C₁₂ABS at the air-solution interface.

3.4 Adsorption at the Kaolin-Aqueous Solution Interface

The aim of adding surfactants to aqueous solutions in enhanced oil recovery is to lower the surface tension of the oil-kaolin interface. This will be rendered ineffective if the surfactant is adsorbed onto the kaolin. Therefore, a series of experiments were conducted in order to ascertain the degree of adsorption of 4- ϕ -C₁₂ABS onto kaolin and the primary factors which may affect this adsorption.

3.4.1 Adsorption of 4- ϕ -C₁₂ABS

The adsorption of 4- ϕ -C₁₂ABS, at 25°C, was determined using the method of Somasundaran (S10) discussed in section 2.7. The amount of 4- ϕ -C₁₂ABS adsorbed from a solid/liquid ratio of 10 %, at pH 6.3, after 24 hours, for initial surfactant concentrations between 1×10^{-5} and 1×10^{-2} mol dm³ is shown in Fig 51.

3.4.2 Effect of Sodium Chloride on the 4- ϕ -C₁₂ABS adsorption at the Kaolin-Aqueous Interface.

The adsorption of 4- ϕ -C₁₂ABS has been determined, at 25°C, with salt concentration, m_s , (Fig 51). Values of maximum surface excess (Γ_{\max}), area per molecule adsorbed at the interface (A_s) and percentage coverage (θ), are given in Table 6. The isotherms show the shape expected with the exception that they show a decrease at high concentrations of surfactant. It can be seen that the incorporation of NaCl leads to an increase in surfactant adsorption.

3.4.3 Effect of short-chain aliphatic alcohols on 4- ϕ -C₁₂ABS adsorption at the Kaolin-Aqueous interface.

The effect of 2% v/v alcohol on the adsorption of 4- ϕ -C₁₂ABS at 25°C from 0.1 mol dm⁻³ NaCl solution onto kaolin is shown as a function of surfactant concentration, m_b , in Fig 52. Similarly, the effect of 4% v/v alcohol is shown in Fig 53. It can be seen that the use of 4% butan-1-ol lowers the adsorption most effectively. Also, the shape of the isotherm can be seen to be affected. The effect on the adsorption parameters is shown in Table 6.

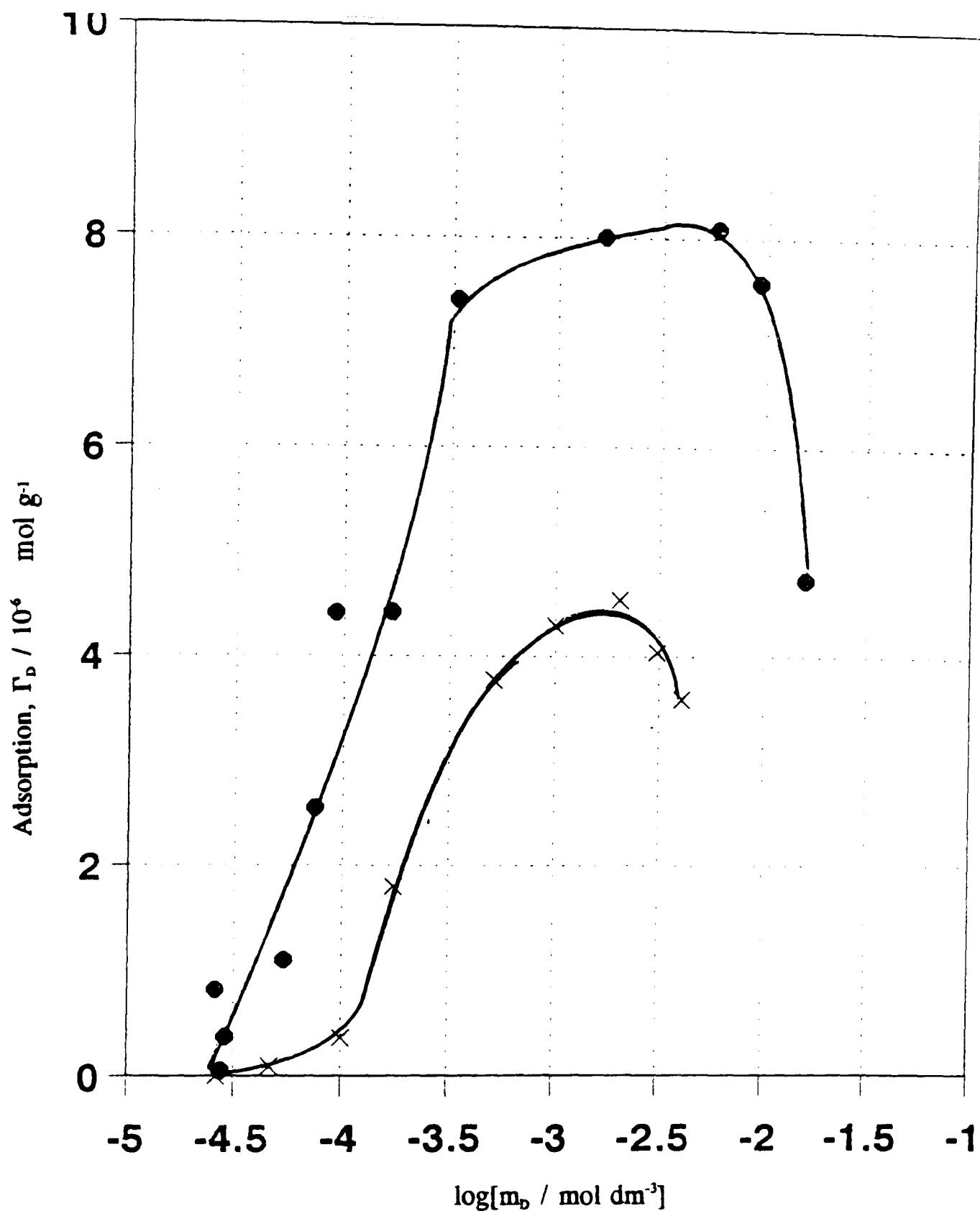


Figure 51. Adsorption of 4- ϕ -C₁₂ABS at the kaolin-aqueous solution interface, at 25°C, as a function of surfactant concentration.

NaCl concentrations = 0.00 (×) and 0.10 (●).

pH = 6.3, % solids = 10 and time = 24 hours.

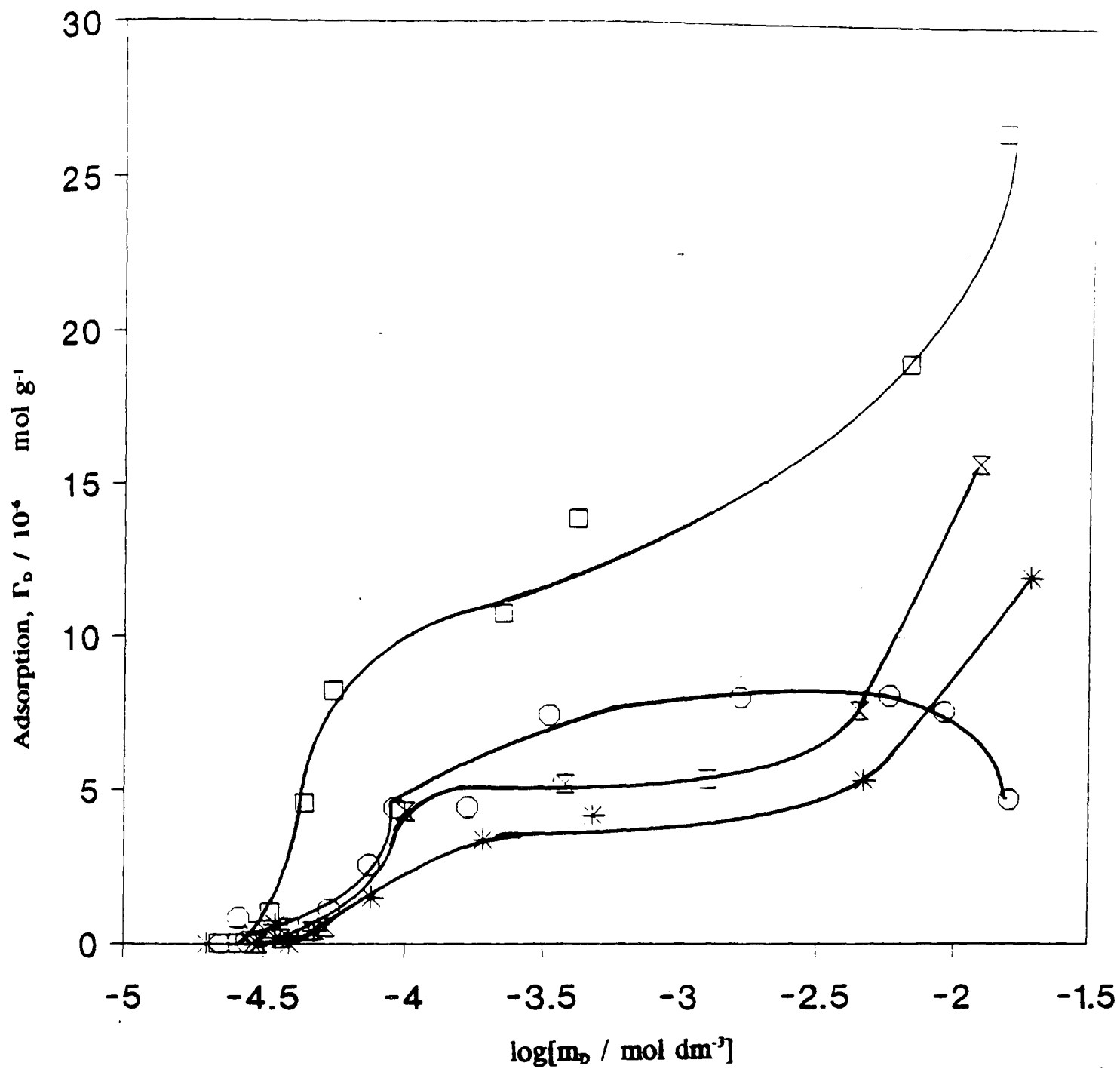


Figure 52. Effect of 2% v/v short chain aliphatic alcohol on 4- ϕ -C₁₂ABS adsorption onto kaolin from 0.1 mol dm⁻³ NaCl solution at pH = 6.3, 25°C, % solids = 10, and time = 24 hours.

Propan-1-ol (⊗), Butan-1-ol (⊗), and Pentan-1-ol (□)

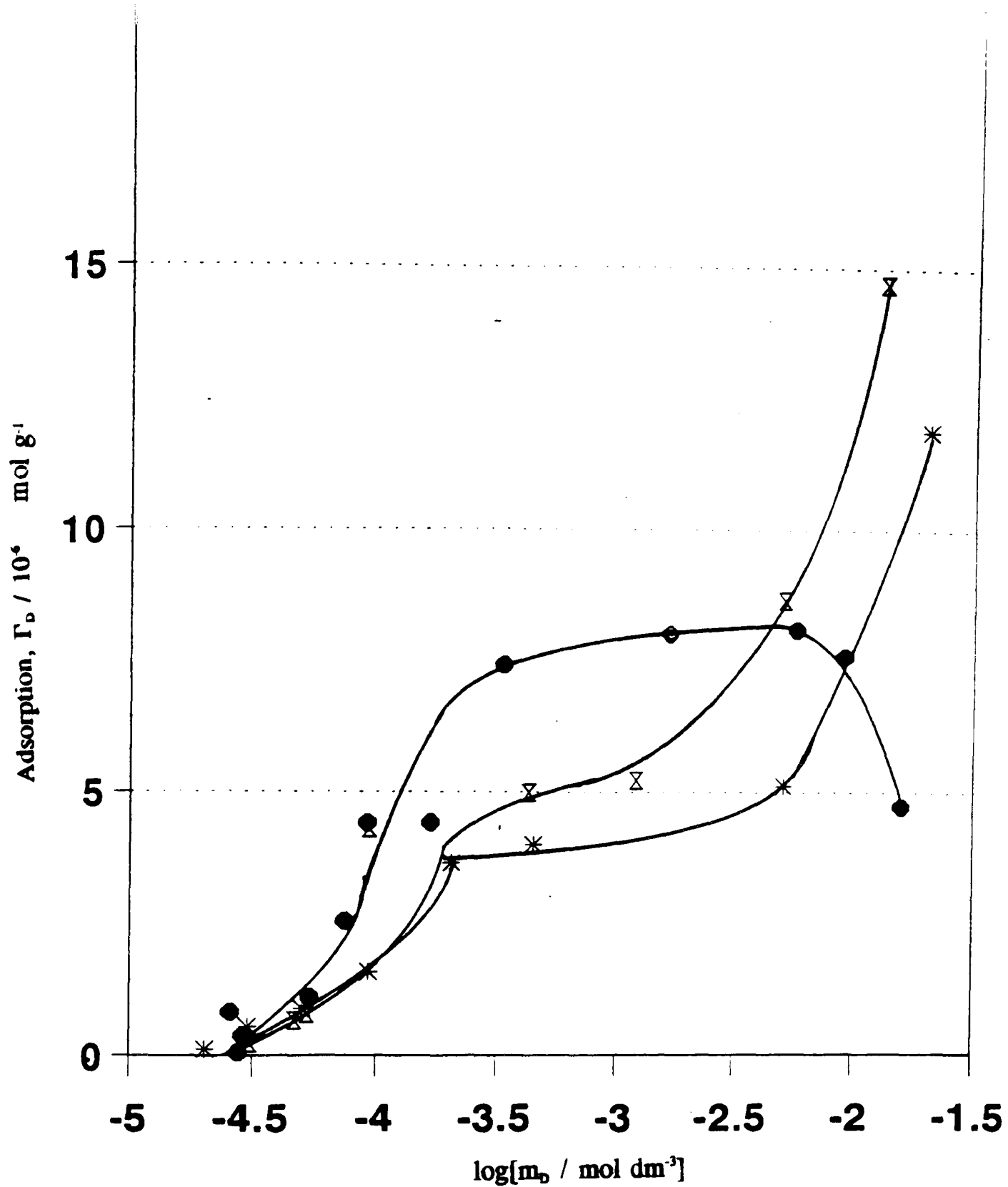


Figure 53. Effect of 4% v/v short chain aliphatic alcohol on 4- ϕ -C₁₂ABS adsorption onto kaolin from 0.1 mol dm⁻³ NaCl solution at pH = 6.3, 25°C, % solids = 10, and time = 24 hours.

Propan-1-ol (⊗), and Butan-1-ol (⊗).

3.4.4 Effect of Temperature on the adsorption of 4- ϕ -C₁₂ABS at the Kaolin-Aqueous interface.

As temperature fluctuations occur in oil reservoirs and the temperature is higher than that found above ground it was necessary to investigate what effect an increase in temperature would have on the adsorption of 4- ϕ -C₁₂ABS from 0.1 mol dm⁻³ NaCl solutions. The isotherms for temperatures of 25°C and 60°C are shown in Figure 54.

3.4.5 Effect of addition of metal complexing agents on 4- ϕ -C₁₂ABS adsorption at the Kaolin-Aqueous interface.

As discussed in Chapter 4, one possible mechanism for the loss of surfactant from solution is leaching of metal ions from the surface of the clay particles. Therefore, a possible method of counteracting this problem is to include a sacrificial complexing agent with the surfactant in the oil well flood. The effectiveness of these agents will depend upon concentration and pH.

Initially three complexing agents were investigated, ethylenediamine tetracetic acid (EDTA), sodium pyrophosphate and sodium tripolyphosphate. EDTA was found not to effect DBS loss at any concentration or pH. Sodium pyrophosphate and sodium tripolyphosphate were found to be most effective at pH 10 with a concentration of 5 x 10⁻³ mol dm⁻³. Sodium Citrate, however, was found to be most effective at a concentration of approximately 1 x 10⁻² mol dm⁻³ and pH 7. This was determined by investigating the effect of increasing complexing agent concentration upon the

adsorption of a $2 \times 10^{-4} \text{ mol dm}^{-3}$ 4- ϕ -C₁₂ABS solution (Figures 55a and 55b). The concentration at which the adsorption of 4- ϕ -C₁₂ABS is at a minimum is taken as the optimum concentration. An isotherm was determined for 0.1 mol dm^{-3} NaCl solutions with the complexing agents under the optimum conditions and concentrations. This can be seen in Fig 56. A further complexing agent was then tested; Pyrocatechol Violet. This compound was used by Anton (A3) at $1 \times 10^{-4} \text{ mol dm}^{-3}$ in the spectrophotometric determination of aluminium. Again an isotherm was determined for 4- ϕ -C₁₂ABS from 0.1 mol dm^{-3} and is given in Fig 57. Table 7 shows the calculated adsorption parameters.

Table 6. Effect of butan-1-ol on the calculated adsorption parameters at the Kaolin-aqueous interface.

NaCl / mol dm^{-3}	n _{BuOH} / % v/v	Γ_{max} / $10^{-6} \text{ mol g}^{-1}$	A _s / nm^{-2}	θ / %
0.00	-	4.54	0.37	52.15
0.10	-	8.08	0.21	92.82
0.10	2	12.03	0.14	138.1
0.10	4	12.07	0.14	138.6

Table 7. Effect of complexing agents on the calculated adsorption parameters at the kaolin-aqueous interface.

Complexing agent	$\Gamma_{\max} / 10^{-6} \text{ mol}^{-1}$	A_s / nm^2	$\theta / \%$
Sodium pyrophosphate	4.81	0.35	55.25
Sodium Tripolyphosphate	4.03	0.41	46.29
Catechol Violet	7.18	0.23	82.48
Sodium Citrate	2.97	0.56	34.12

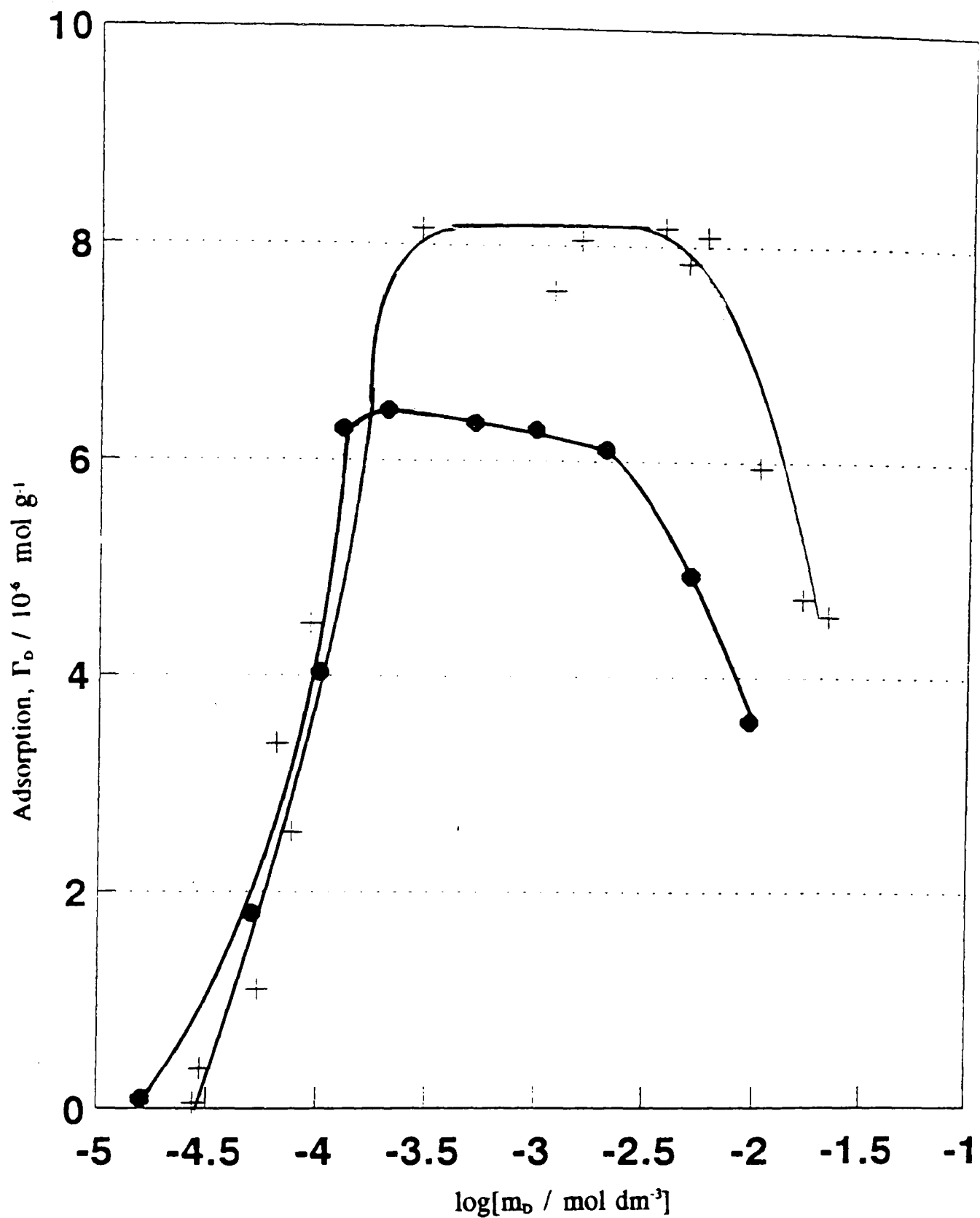


Figure 54. Effect of Temperature on 4- ϕ -C₁₂ABS adsorption from 0.10 mol dm⁻³ NaCl solution onto kaolin. pH = 6.3, % solids = 10 and time = 24 hours. Temperature = 25 (+) and 60 (●) °C.

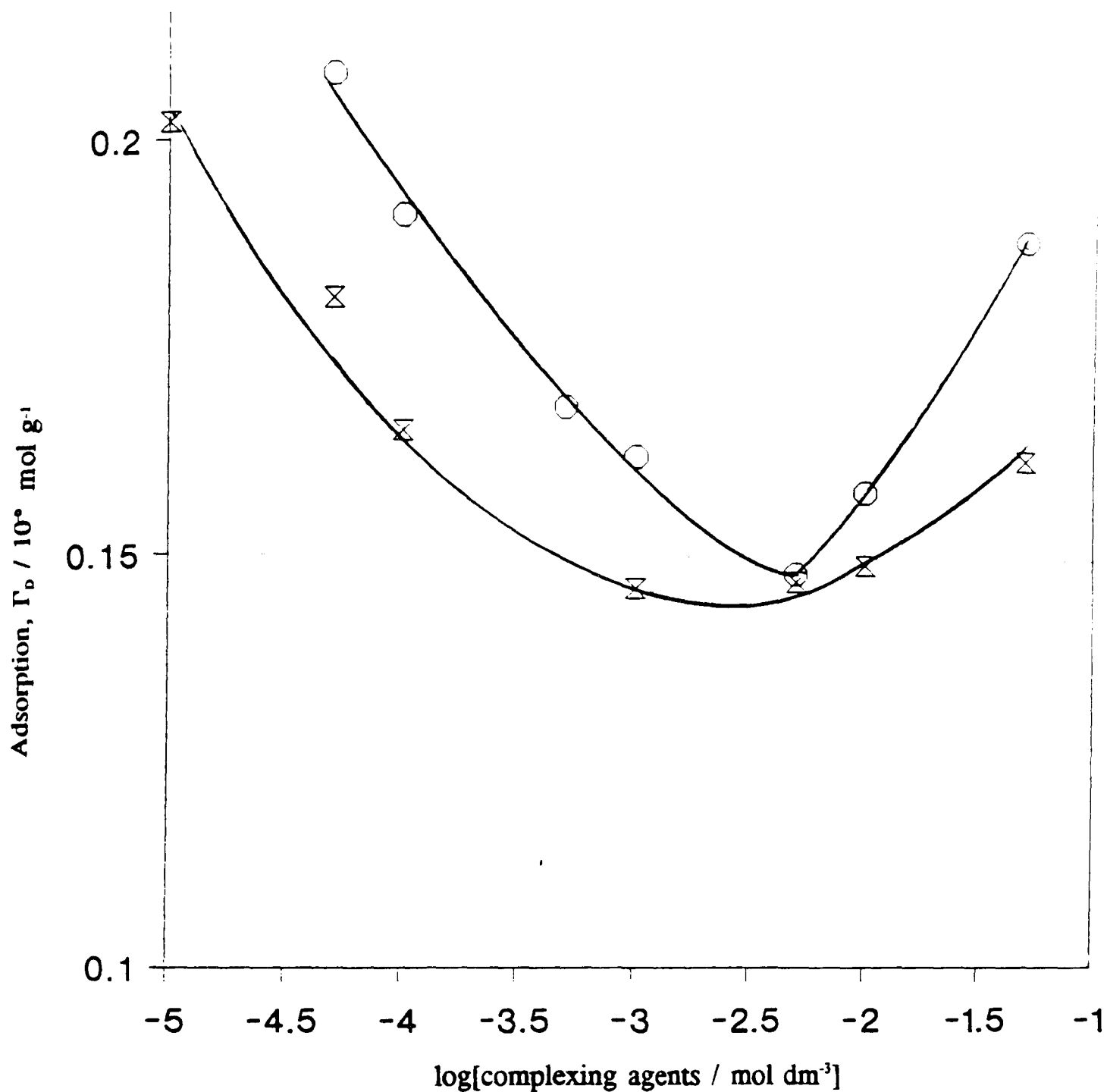


Figure 55a. Determination of the most effective concentration of complexing agent to reduce adsorption of $4\text{-}\phi\text{-C}_{12}\text{ABS}$ from an $8.9 \times 10^{-4} \text{ mol dm}^{-3}$ solution. $\text{NaCl} = 0.1 \text{ mol dm}^{-3}$ at 25°C , $\text{pH} = 10$ and time = 24 hours. Sodium Pyrophosphate (\circ), Sodium Tripolyphosphate (\triangle)

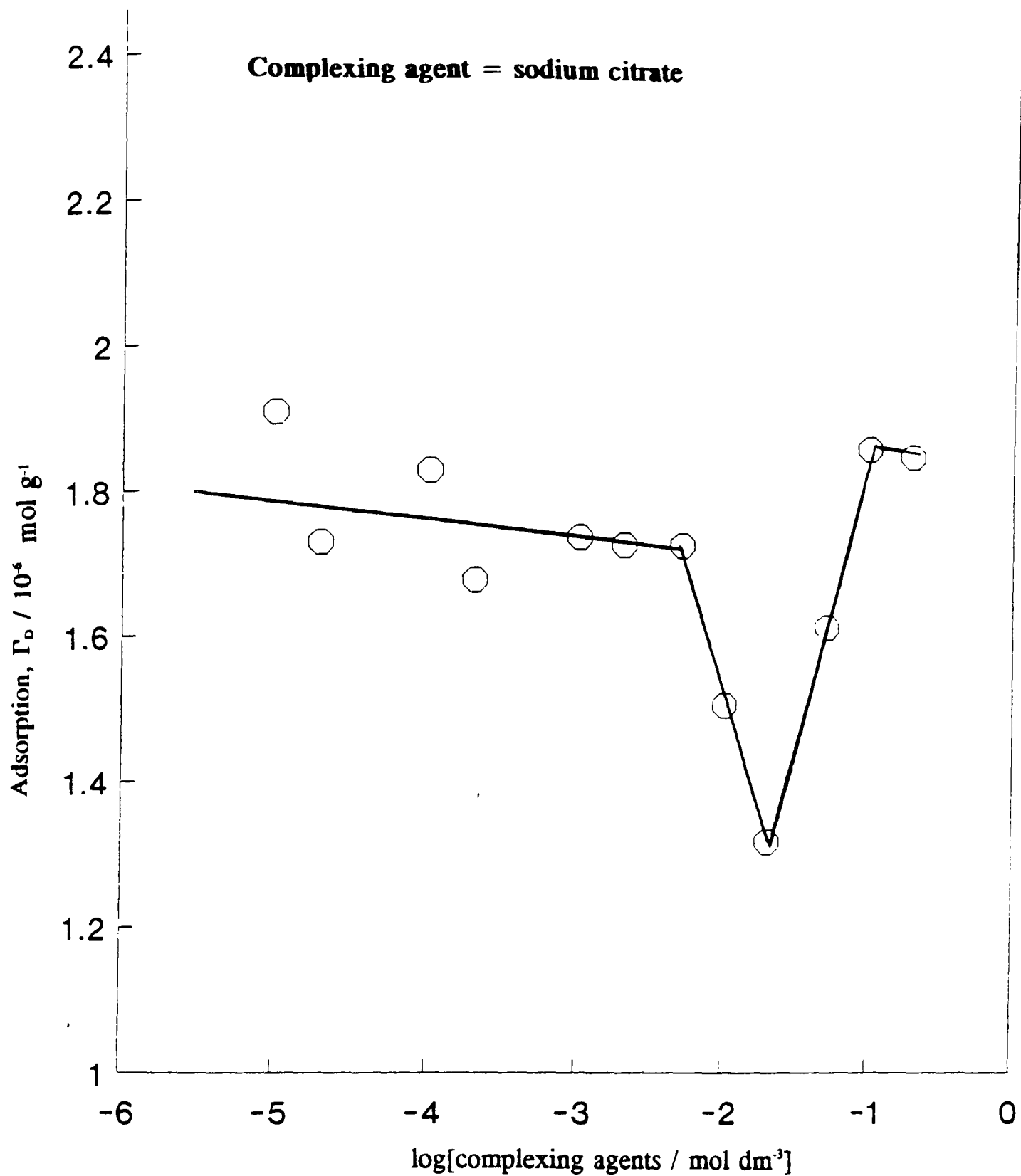


Figure 55b. Determination of the most effective concentration of complexing agent to reduce adsorption of 4- ϕ -C₁₂ABS from an $8.9 \times 10^{-4} \text{ mol dm}^{-3}$ solution. NaCl = 0.1 mol dm⁻³ at 25°C, pH = 10 and time = 24 hours.

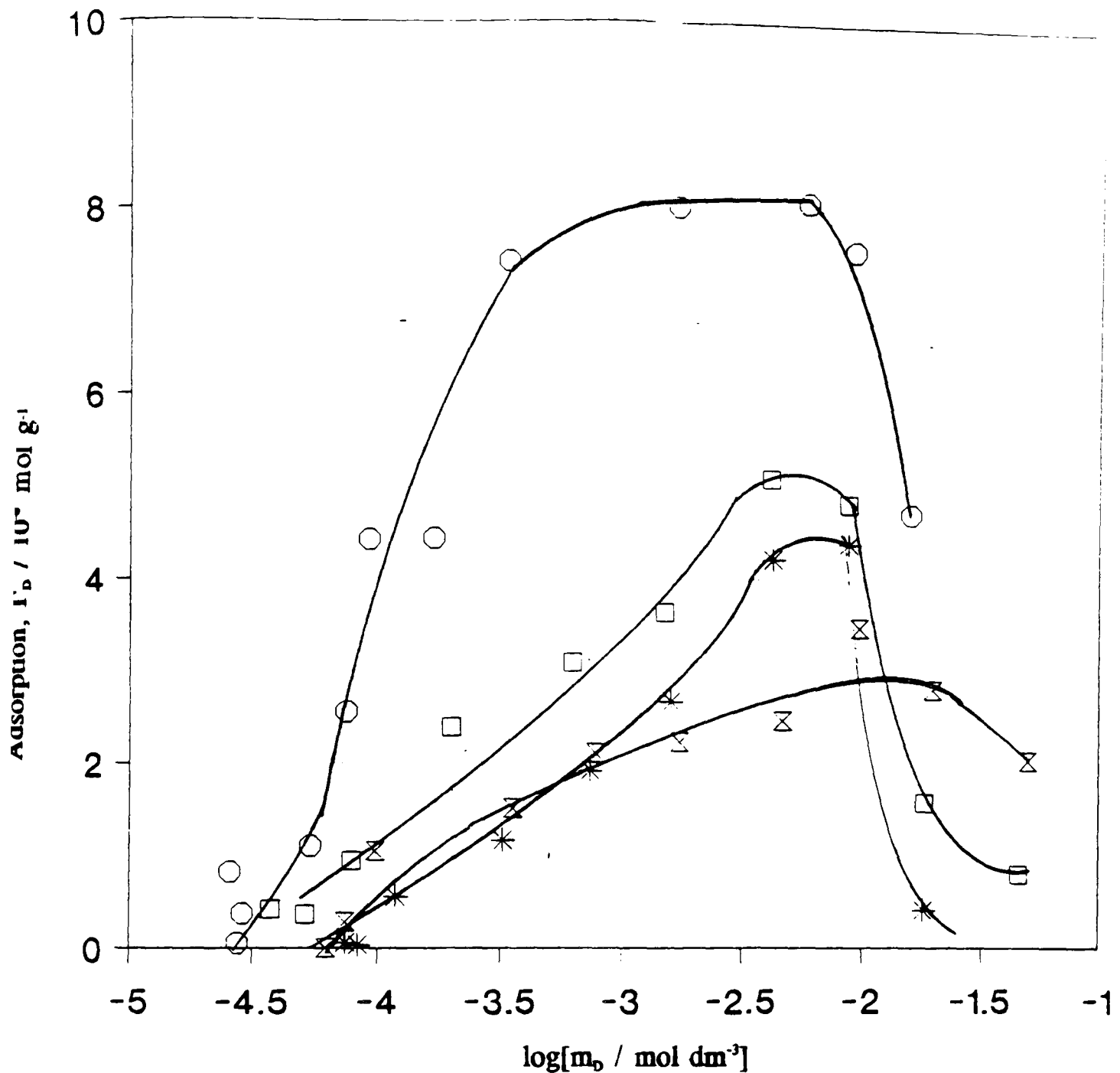


Figure 56. Effect of $5 \times 10^{-3} \text{ mol dm}^{-3}$ sodium pyrophosphate and sodium tripolyphosphate on the adsorption of $4\text{-}\phi\text{-C}_{12}\text{ABS}$ from $0.1 \text{ mol dm}^{-3} \text{ NaCl}$ at 25°C , $\text{pH} = 10$, % solids = 10 and time = 24 hours.

Complexing agent concentrations = 0.00 (□), 0.00 @ pH 6.3 (○)
 5×10^{-3} Pyrophosphate (⊗), and 5×10^{-3} Tripolyphosphate. ⊗

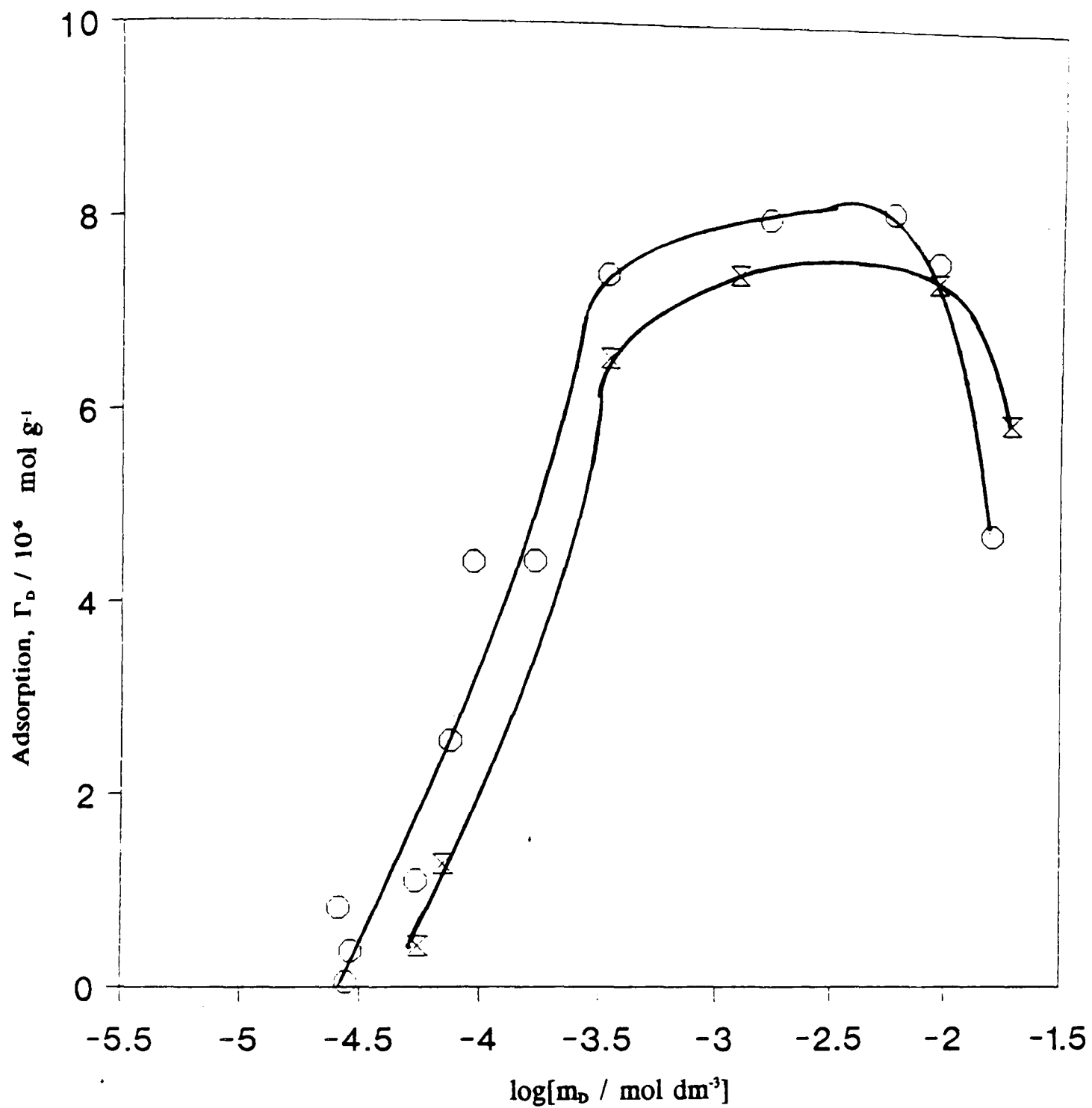


Figure 57. Effect of Catechol violet upon the adsorption of 4- ϕ -C₁₂ABS from 0.1 mol dm⁻³ NaCl solution at 25°C, pH = 6.3, % solids = 10 and time = 24 hours. Catechol violet concentration = 0.00 (○) and 1 x 10⁻⁴ (⊗)

3.4.6 Effect of Sodium citrate on 4- ϕ -C₁₂ABS adsorption at the Kaolin-Aqueous interface.

The optimum concentration of sodium citrate was used to examine the effect of adsorption of 4- ϕ -C₁₂ABS from 0.1 mol dm⁻³ sodium chloride solution (Fig 58) Again the adsorption parameters are shown in Table 7.

3.4.7 Adsorption of sodium tripolyphosphate at the Kaolin-Aqueous interface.

The adsorption of sodium tripolyphosphate was determined onto kaolin at pH 10 from 0.1 mol dm⁻³ NaCl solution and is shown in Fig 59.

3.4.8 Adsorption of sodium citrate at the Kaolin-Aqueous interface.

Adsorption of sodium citrate onto kaolin from 0.1 mol dm⁻³ NaCl solution was determined at pH 7. This is shown in Fig 59.

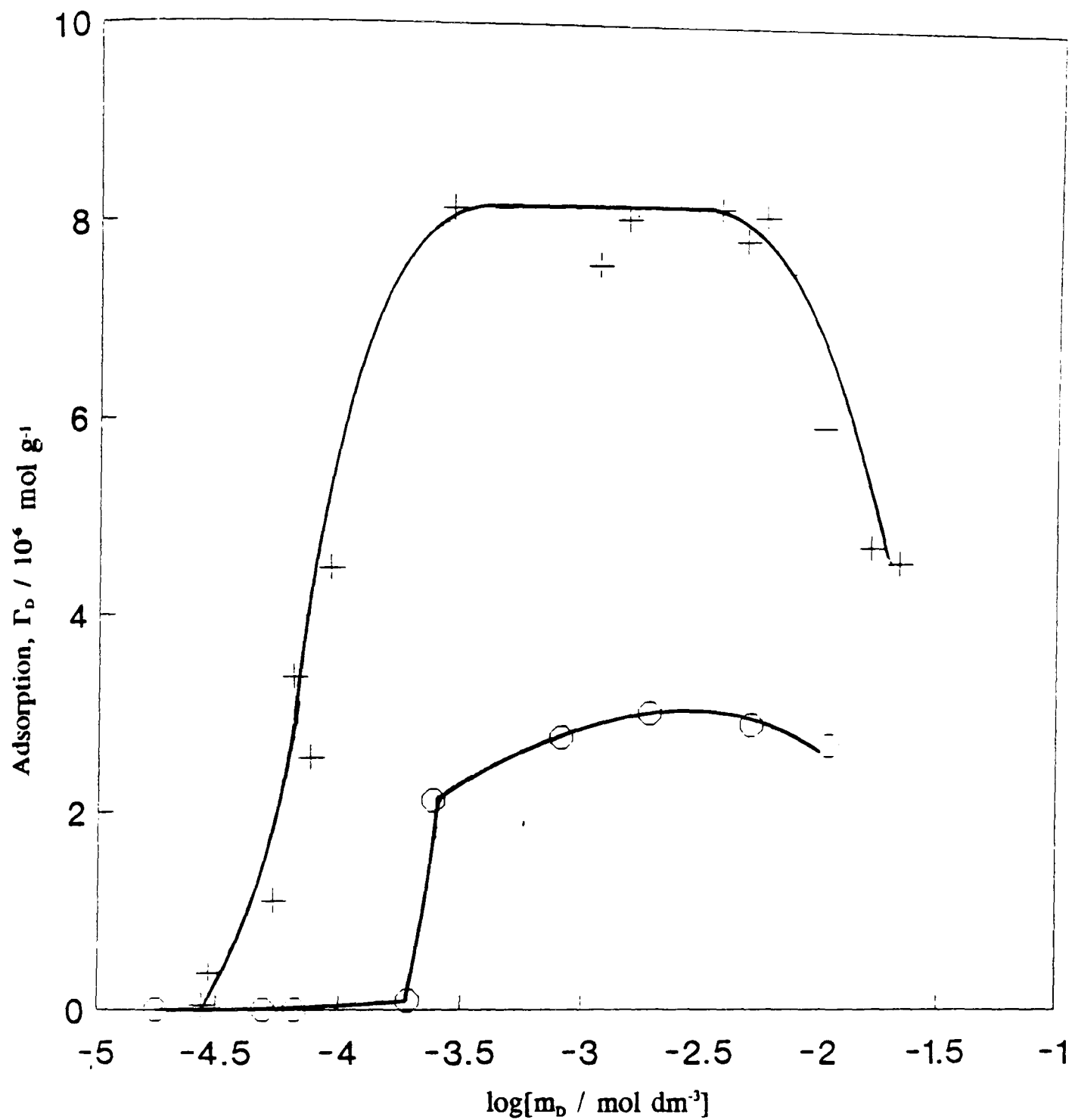


Figure 58. Effect of sodium citrate upon the adsorption of 4- ϕ -C₁₂ABS from 0.1 mol dm⁻³ NaCl solution at 25°C, pH = 6.3, % solids = 10 and time = 24 hours. Sodium citrate = 0.00 (+), and 1 x 10⁻² (o) mol dm⁻³.

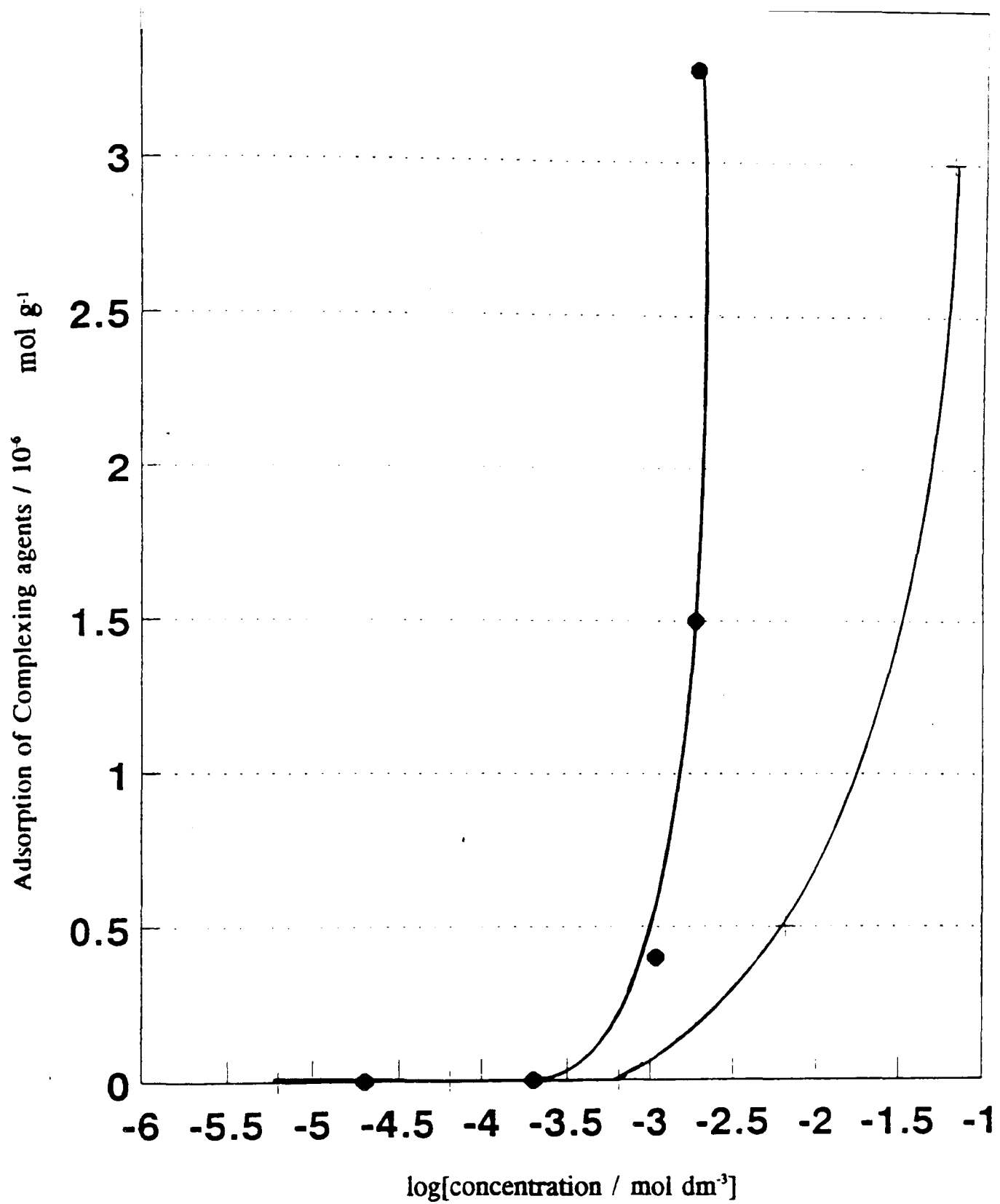


Figure 59. Adsorption of complexing agents at the kaolin - aqueous solution interface at 25°C from 0.1 mol dm⁻³ NaCl solution, % solids = 10, and time = 24 hours. Tripolyphosphate, pH = 10 (†), sodium citrate, pH = 7 (●)

3.5 Effect of ion-washed Kaolin on the 4- ϕ -C₁₂ABS adsorption at the Kaolin-Aqueous interface.

In a North Sea oil reservoir the clay embedded in the rock will be in intimate contact with saline solution containing relatively high concentrations of metal anions Ca²⁺, Al³⁺, in addition to Na⁺. In order to evaluate such a system a series of ion washed clays, in which the clays were washed to constant conductivity, were prepared using Na⁺, Ca²⁺ and Al³⁺.

Fig 60 shows the adsorption profiles for the three prepared clays (see section 2.4) and the washed kaolin. It can be seen that no adsorption parameters can be calculated as no maximum adsorption is observed. This will be discussed further in the Discussion Section.

3.5.1 Effect of butan-1-ol on 4- ϕ -C₁₂ABS adsorption at the Aluminium kaolin-Aqueous interface.

As the adsorption of surfactant is very large on aluminium kaolin (Fig 60) it was felt that this was due to precipitation (see Discussion) via leaching of metal from the kaolin surface. As butan-1-ol is known to have a high salt solubility (S11) it was thought that incorporation of butan-1-ol may prevent some of this precipitation. However, as can be seen from Fig 61 this was found not to be the case.

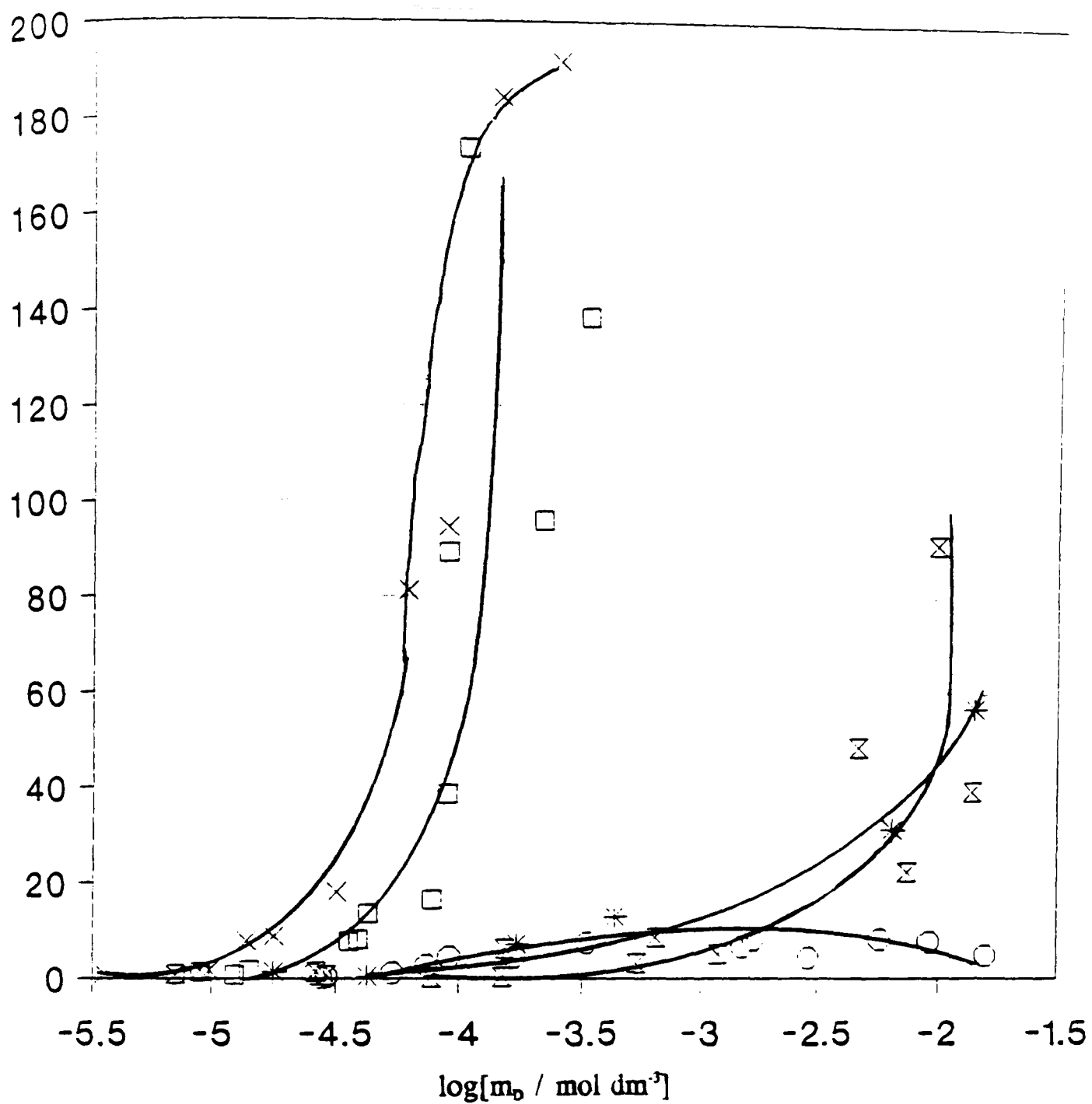


Figure 60. Effect of ion washing of kaolin upon the adsorption of 4-φ-C₁₂ABS at the kaolin - aqueous interface from 0.1 mol dm⁻³ NaCl at pH = 6.3, % solids = 10, T = 25°C and time = 24 hours.

Washed kaolin (○), sodium kaolin (⊛), calcium kaolin (⊞) and aluminium kaolin (⊗) sodium kaolin + butan-1-ol (⊗)

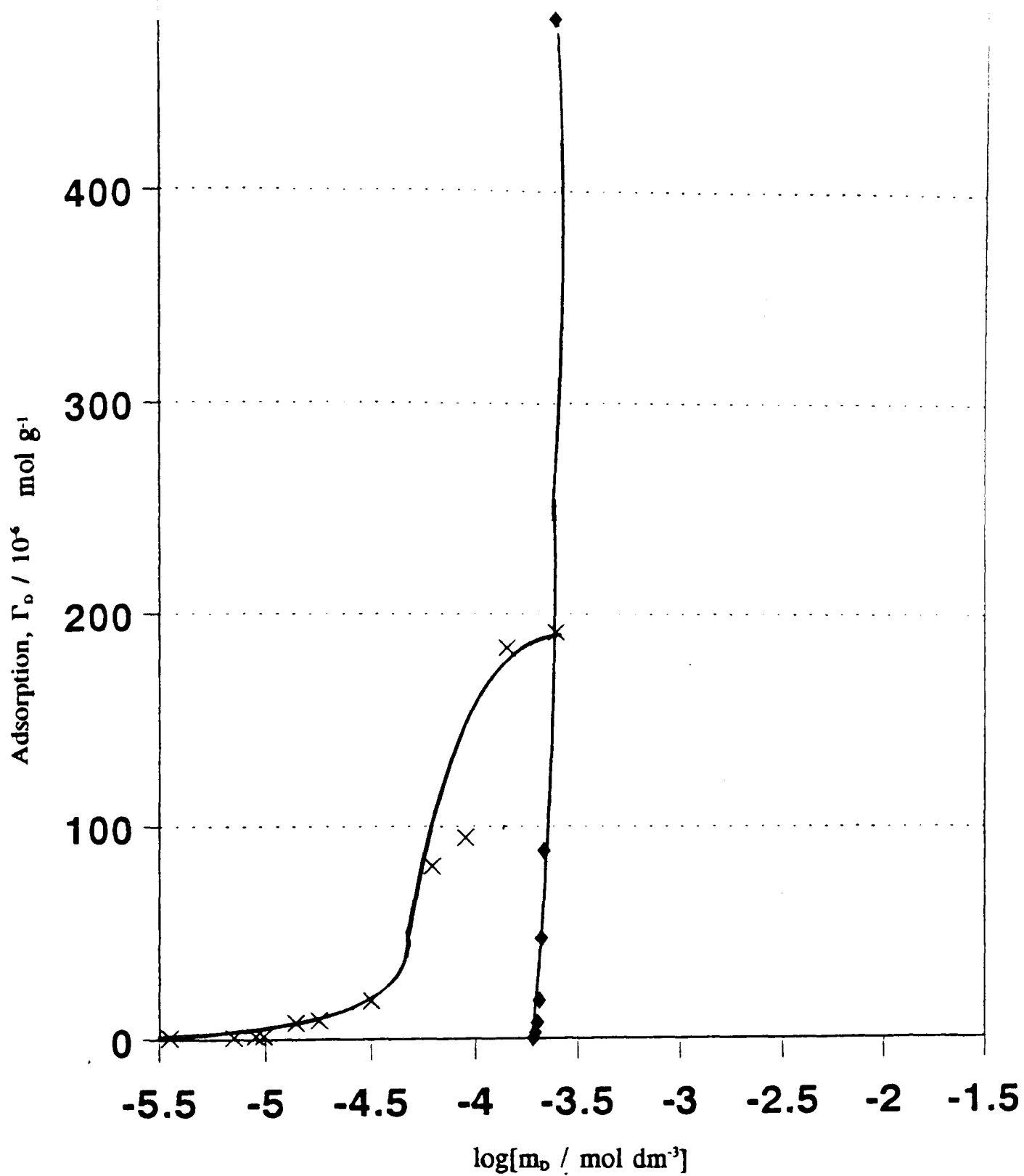


Figure 61. Effect of added butan-1-ol (4% v/v) upon the adsorption of 4-φ-C₁₂ABS at the aluminium kaolin - aqueous interface from 0.1 mol dm⁻³ NaCl at pH = 6.3, % solids = 10, T = 25°C and time = 24 hours.

3.5.2 Effect of complexing agents on 4- ϕ -C₁₂ABS adsorption at the Aluminium Kaolin-Aqueous interface.

Another method to overcome the leaching of metal ions was to complex them out of solution. This was undertaken using the complexing agents sodium tripolyphosphate and sodium citrate under their optimum conditions (see section 3.4.5). The resulting profiles can be seen in Fig 62.

3.6 Adsorption of 4- ϕ -C₁₂ABS onto North Sea Reservoir Rock samples.

In order to determine whether the prepared kaolin samples gave an accurate account of adsorption behaviour in the reservoir it was necessary to determine the adsorption of 4- ϕ -C₁₂ABS onto core samples obtained from the North Sea. These consisted mainly of sandstone interspersed with clay.

The adsorption profiles for 4- ϕ -C₁₂ABS from 0.1 mol dm⁻³ NaCl solution onto three different core samples are shown in Fig 63. The adsorption parameters have been calculated for core sample 12417 and are given in Table 8.

3.6.1 Effect of butan-1-ol addition on 4- ϕ -C₁₂ABS adsorption onto North Sea Reservoir Rock.

Fig 64 shows the effect of butan-1-ol addition on the adsorption of 4- ϕ -C₁₂ABS from 0.1 mol dm⁻³ NaCl solution onto core sample 12417.

The adsorption parameters have been calculated and are shown in Table 8.

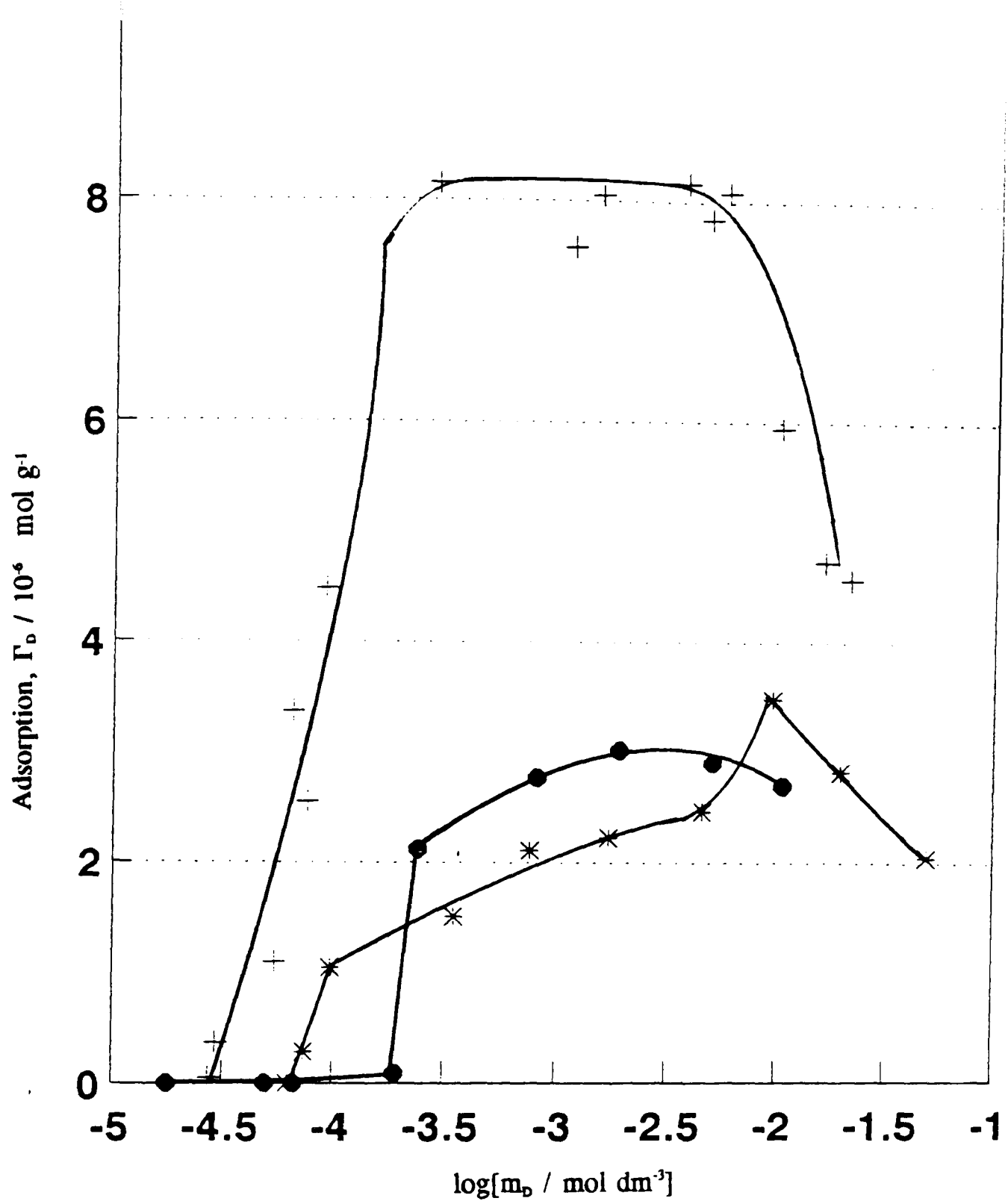


Figure 62. Effect of added complexing agents at their optimum concentrations upon the adsorption of 4- ϕ -C₁₂ABS from 0.1 mol dm⁻³ NaCl solution at 25°C, % solids = 10 and time = 24 hours.

Tripolyphosphate, pH 10 (⊕), Sodium Citrate, pH 7 (●).

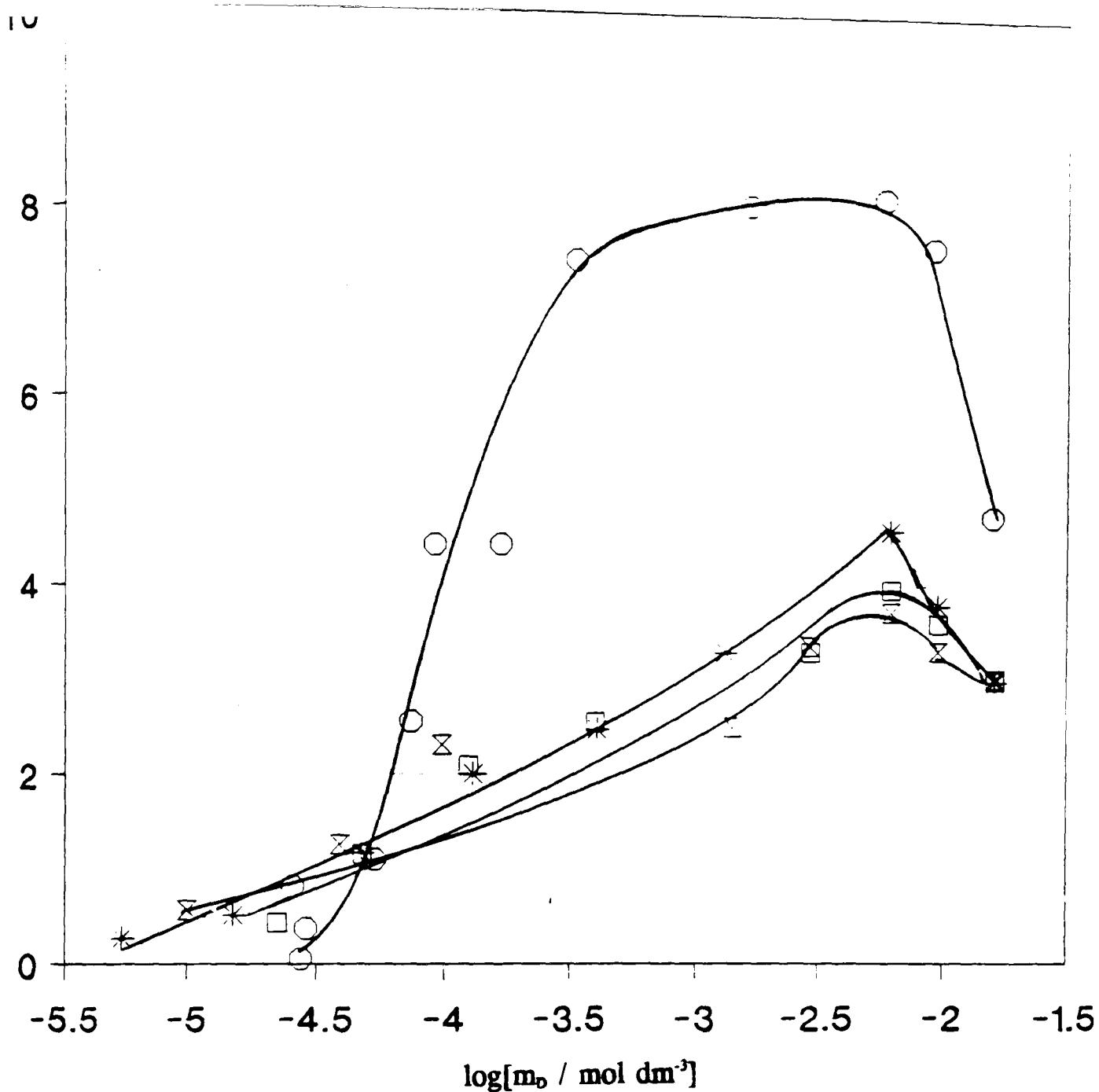


Figure 63. Adsorption of 4- ϕ -C₁₂ABS from 0.1 mol dm⁻³ NaCl solution at the reservoir rock - aqueous solution interface.

T = 25°C, pH = 6.3, % solids = 10 and time = 24 hours.

Core 12395 (⊗), Core 12417 (⊠), Core 12498.2 (⊞) and Washed kaolin (○).

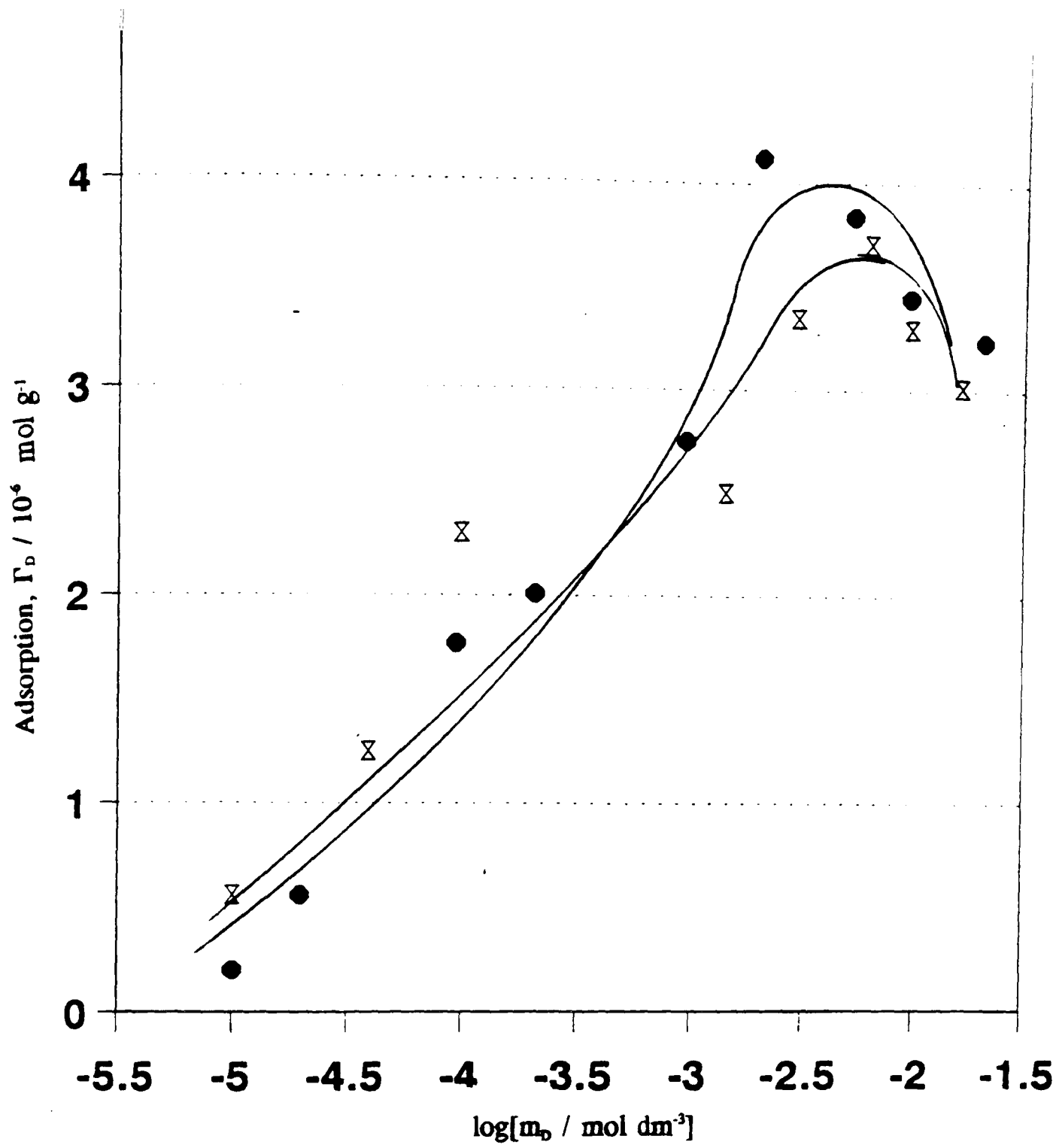


Figure 64. Effect of added butan-1-ol on adsorption of 4- ϕ -C₁₂ABS from 0.1 mol dm⁻³ NaCl solution at the reservoir rock - aqueous solution interface.

T = 25°C, pH = 6.3, % solids = 10 and time = 24 hours.

Core sample = 12395.

Butan-1-ol concentrations = 0.00 (⊗) and 4 % v/v (●).

Table 8. Effect of butan-1-ol on the calculated adsorption parameters at the reservoir rock - solution interface.

NaCl / mol dm ⁻³	n _{BuOH} / % v/v	Γ _{max} / 10 ⁻⁶ mol g ⁻¹	A ₁ / nm ⁻²	θ / %
0.10	-	4.05	0.41	184.2
0.10	4	4.17	0.40	189.7

3.6.2 Effect of complexing agent addition on 4-φ-C₁₂ABS adsorption onto North Sea Reservoir Rock.

The effects of sodium citrate and sodium tripolyphosphate addition on surfactant adsorption from 0.1 mol dm⁻³ NaCl solution were determined on core sample 12395. The resulting profiles are shown in Fig 65.

3.7 Effect of Formation Water on 4-φ-C₁₂ABS adsorption at the Kaolin-Aqueous interface.

As the primary contact of the DBS surfactant solutions in the reservoir may be with residual aqueous solutions in equilibria with core rock, it is of importance that the effect of such *Formation* type water on the adsorption of the 4-φ-C₁₂ABS should be investigated. The recipes for the formation waters are given below in Table 9. The recipe for formation water A was given by Oil Plus (R6) whilst recipes B and C

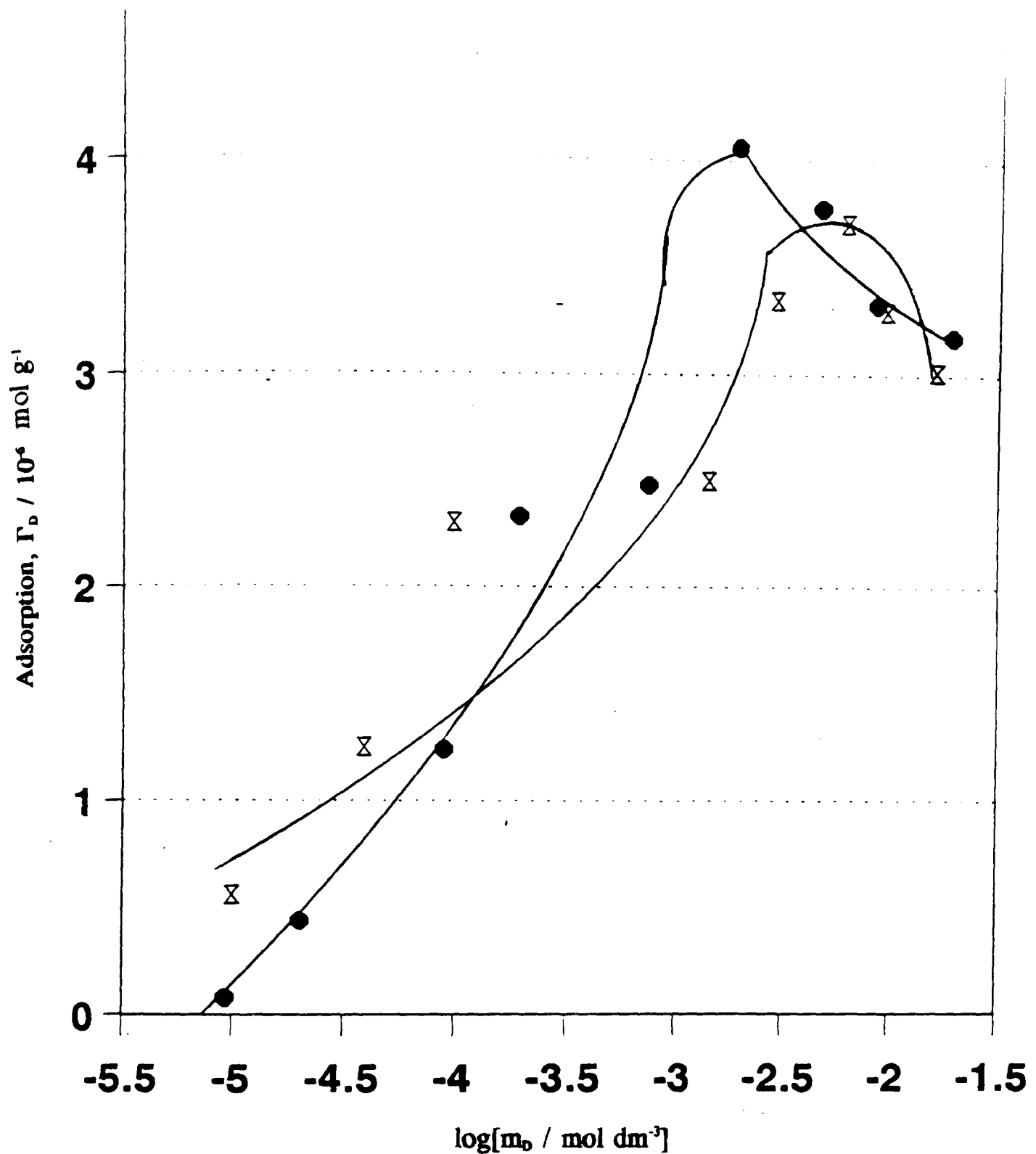


Figure 65. Effect of added complexing agent upon the adsorption of 4- ϕ -C₁₂ABS from 0.1 mol dm⁻³ NaCl solution at the reservoir rock - aqueous solution interface.

T = 25°C, pH = 6.3, % solids = 10,

and time = 24 hours.

Sodium Citrate conc = 0.00 (⊗), and 1×10^{-2} (●) mol dm⁻³.

Table 9 - Formation water recipes in grammes per litre.

Chemical compound	A	B	C
Sodium chloride	81.70	76.66	36.59
Potassium chloride	1.34	0.72	0.61
Calcium Chloride	29.52	8.66	2.91
Magnesium Chloride	1.81	2.38	1.53
Barium Chloride	2.50	0.45	0.08
Iron Sulphate	0.15	-	-
Barium Sulphate	0.23	-	-

were given in the paper by Gilje (G5).

As actual formation water in oil bearing reservoirs occurs at elevated temperatures, it was found that, at room temperature, some salts from water A remained insoluble. These were removed by centrifugation. The resulting supernatant was then used in the adsorption experiments.

The effects of all three waters on the adsorption of 4- ϕ -C₁₂ABS are shown in Fig 66.

3.7.1 Effect of Temperature on 4- ϕ -C₁₂ABS adsorption from formation water B at the Kaolin-Solution interface.

As the formation water is found at elevated temperatures an isotherm was determined at 60°C, shown in Fig 67, to investigate whether this lowered the very large loss of surfactant seen in Fig 66. In effect, this would effectively determine whether or not the suspected precipitation of DBS is soluble at higher temperatures.

3.7.2 Effect of butan-1-ol addition on 4- ϕ -C₁₂ABS adsorption from Formation water B at the Kaolin-Solution interface.

Fig 68 shows the effect of 4% v/v butan-1-ol addition on the surfactant adsorption. Again it can be seen that adsorption (or loss) of surfactant is extremely large with no plateau region occurring.

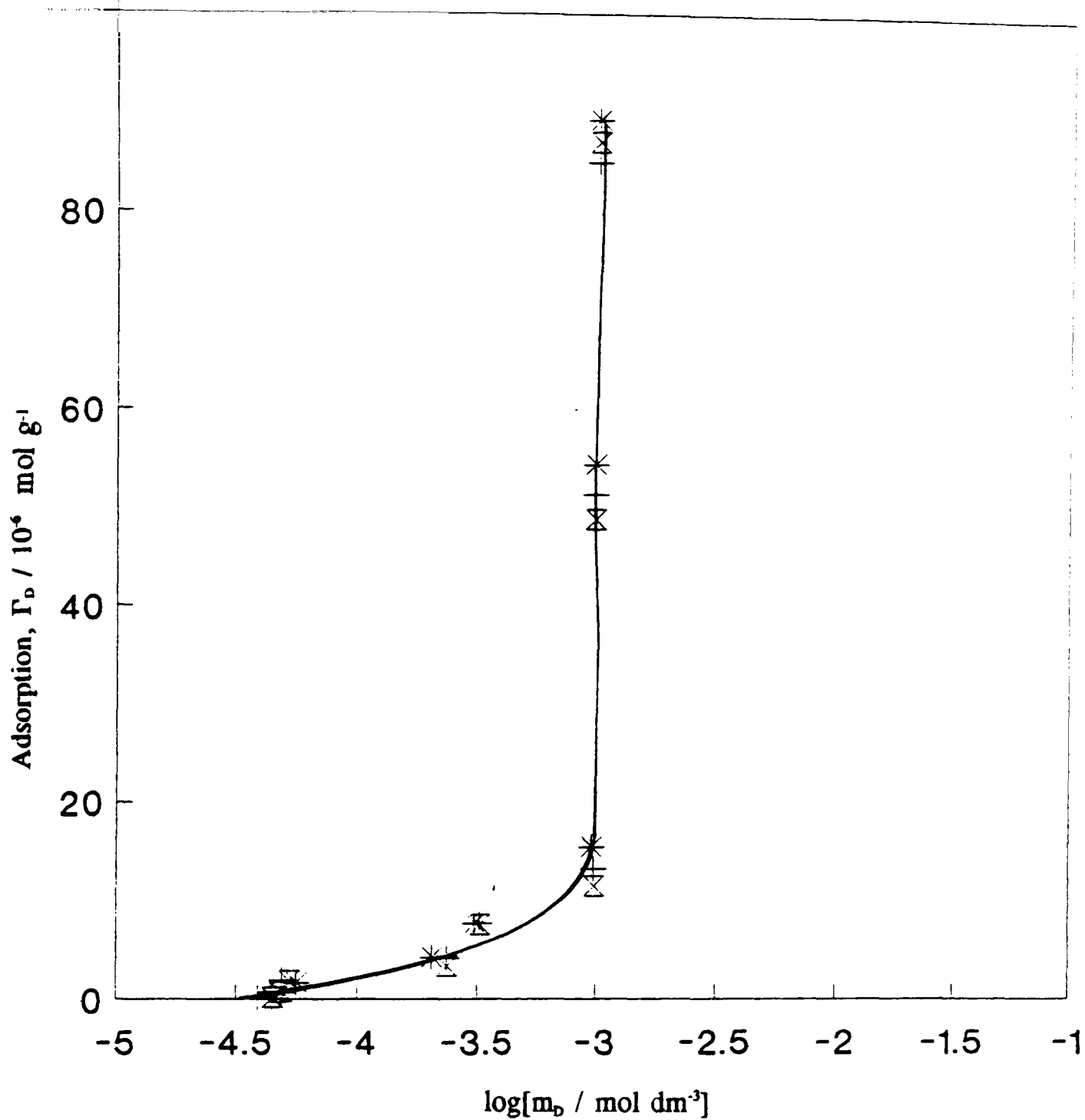


Figure 66. Adsorption of 4-φ-C₁₂ABS at the kaolin - aqueous solution interface, at 25°C, as a function of surfactant concentration in the presence of formation water. pH = 6.3, % solids = 10 and time = 24 hours. Formation water = A (⊗), B (⊕) and C (⊙).

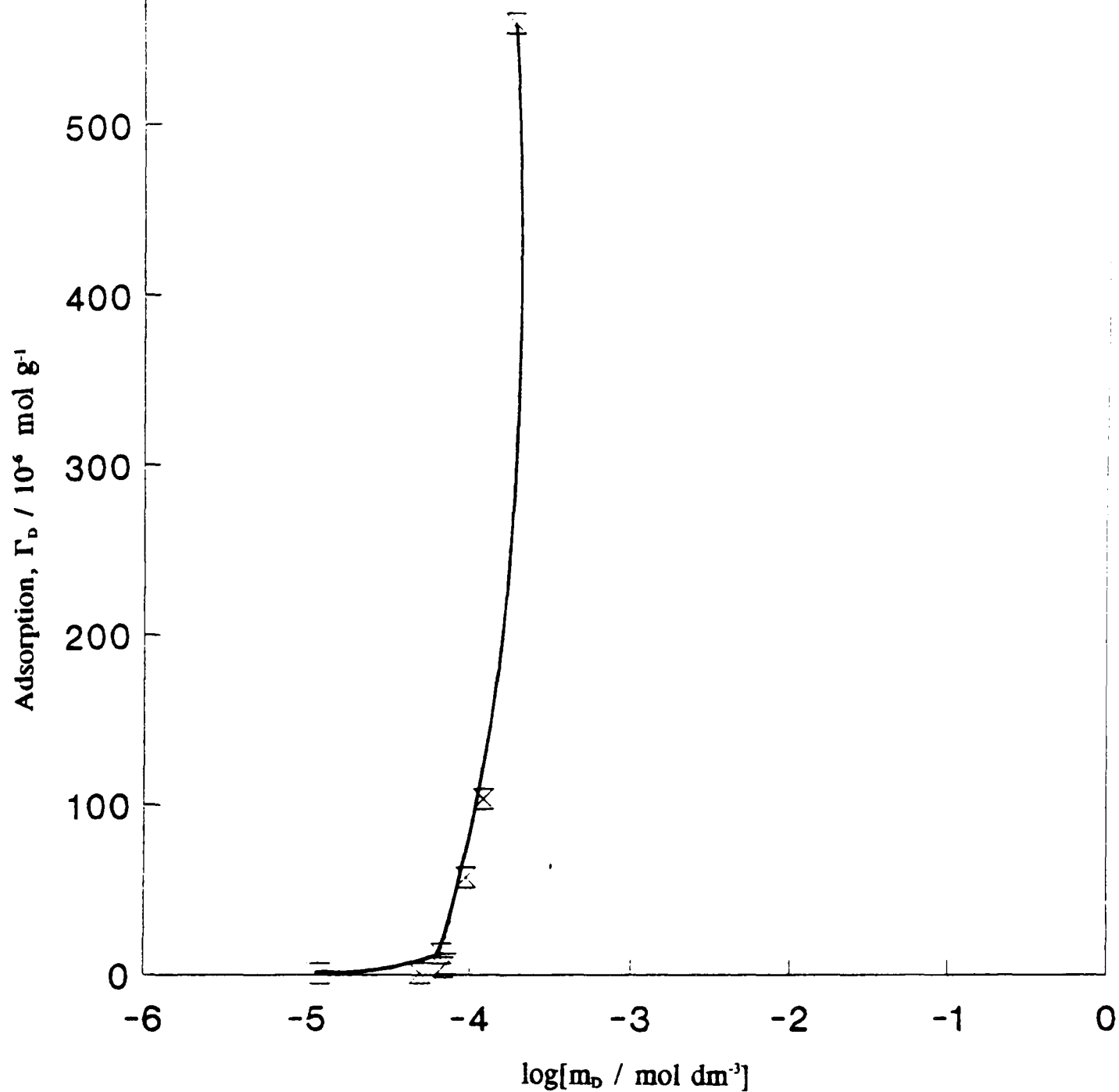


Figure 67. Effect of temperature on $4\text{-}\phi\text{-C}_{12}\text{ABS}$ adsorption from formation water, B, onto kaolin at $\text{pH} = 6.3$, % solids = 10 and time = 24 hours. Temperature = $60\text{ }^\circ\text{C}$.

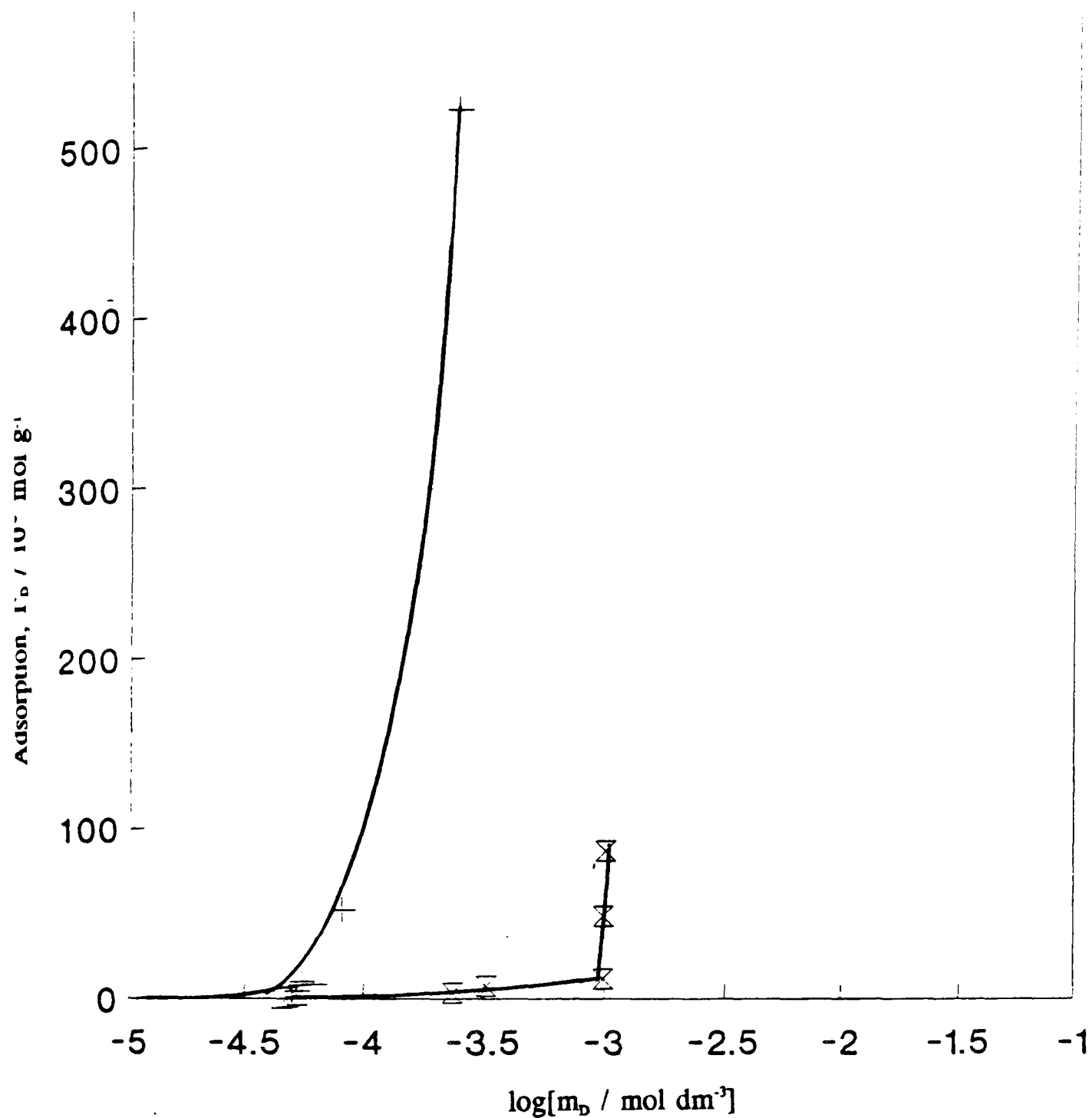


Figure 68. Effect of added butan-1-ol on 4- ϕ -C₁₂ABS adsorption from formation water, B, onto kaolin at 25°C, pH = 6.3, % solids = 10 and time = 24 hours. Butan-1-ol concentration = 0.00 (x) and 4% v/v (+).

3.7.3 Effect of Complexing agent addition on 4- ϕ -C₁₂ABS adsorption from Formation Water B at the Kaolin-Aqueous interface.

The effects of sodium citrate and sodium tripolyphosphate, under their optimum conditions, on surfactant adsorption can be seen in Fig 69. Once again, adsorption is very large with no plateau region in the isotherm.

3.7.4 Determination of ion leaching from kaolin samples by Atomic Absorption Spectroscopy.

Due to the excessive amounts of surfactant lost from solution, experiments were performed to try to determine the amount of aluminium ions and calcium ions leached from the ion washed clays. This was achieved by agitating a sample of clay in 0.1 mol dm⁻³ NaCl solutions for 24 hours at 60 agitations per minute. The solution was then centrifuged at 5000 r.p.m. for 30 minutes to remove any suspended clay, and the Al³⁺ and Ca²⁺ concentrations in the supernatant were measured by AAS (see section 2.9). The results are shown in Figs 70 and 71.

3.7.5 Effect of successive washing on ion-leaching from Kaolin.

As metal ions are leached from washed kaolins (see Figs 70 and 71), an experiment was undertaken to see if successive washing of the kaolin reduced the amount of ions leached. This could be of importance commercially as pre-removal of these ions by washing could prevent the loss of surfactant to the well. The successive washes were

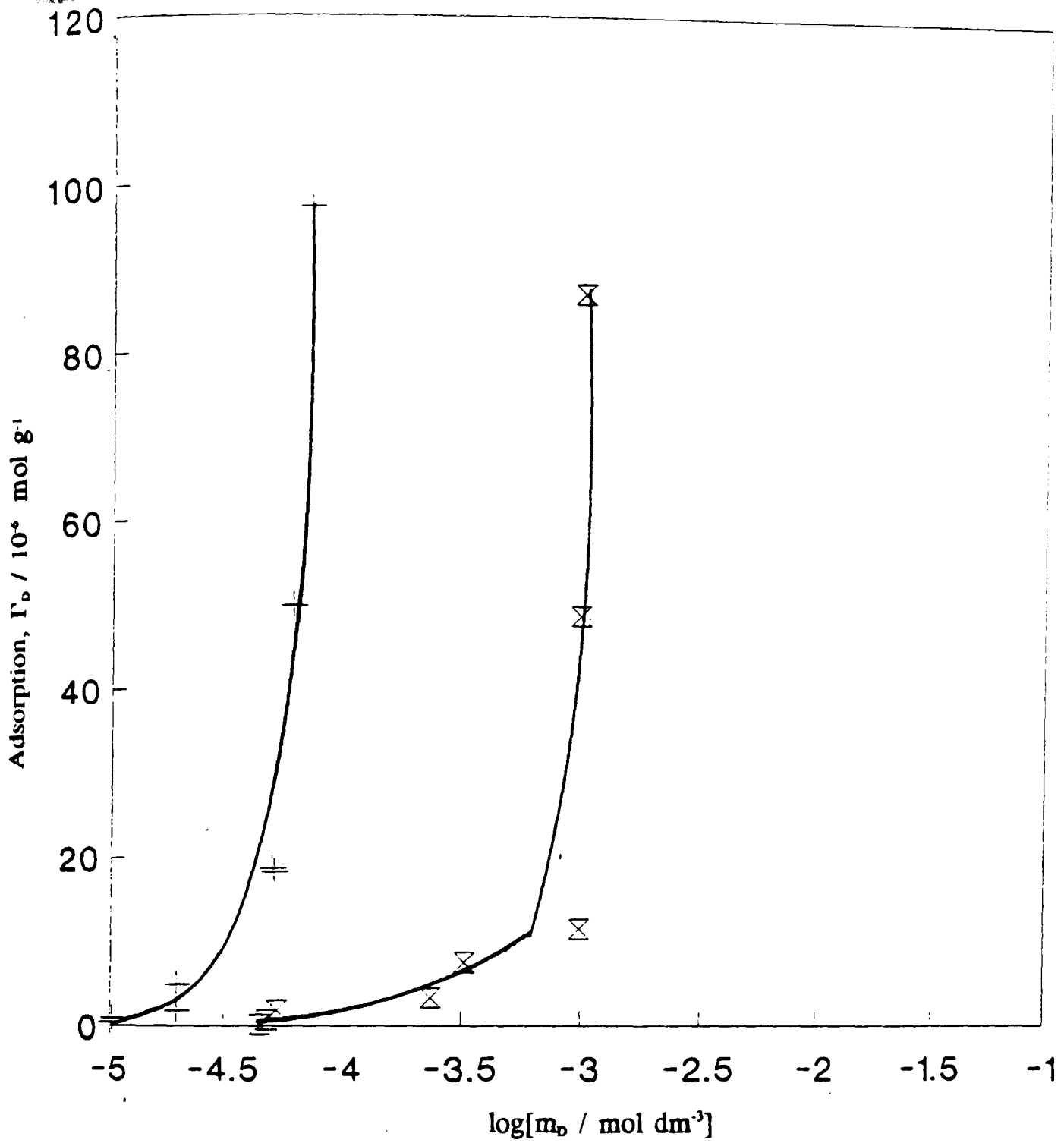


Figure 69. Effect of added sodium citrate on 4- ϕ -C₁₂ABS adsorption from formation water, B, onto kaolin at pH = 7, % solids = 10 and time = 24 hours. Sodium citrate conc = 0.00 (x) and 1 x 10⁻² (+) mol dm⁻³.

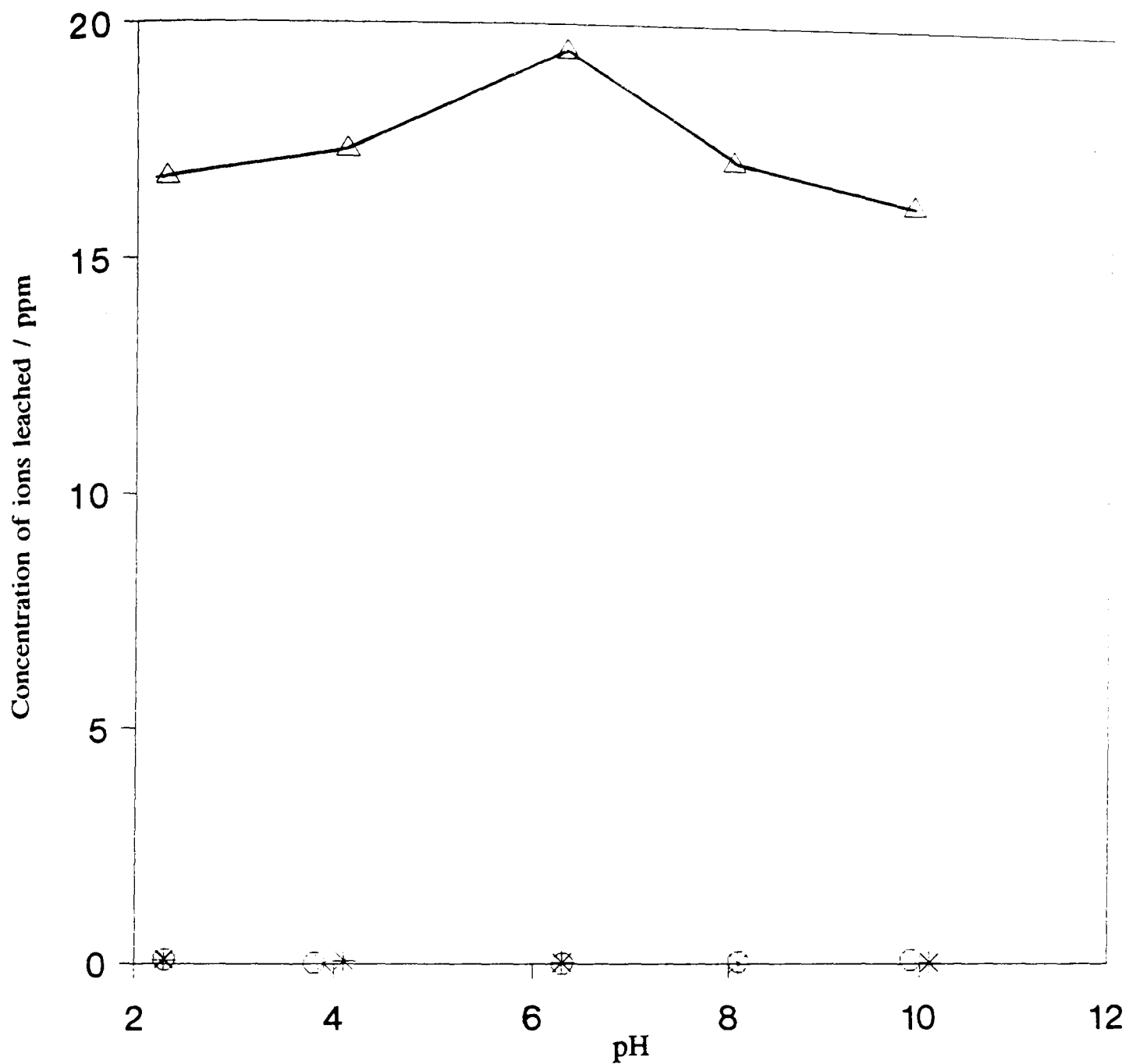


Figure 70. Leaching of aluminium from ion washed clays, determined by Atomic Absorption Spectroscopy (AAS).

Washed kaolin (○), sodium kaolin (*), calcium kaolin (⊗) and aluminium kaolin (Δ).

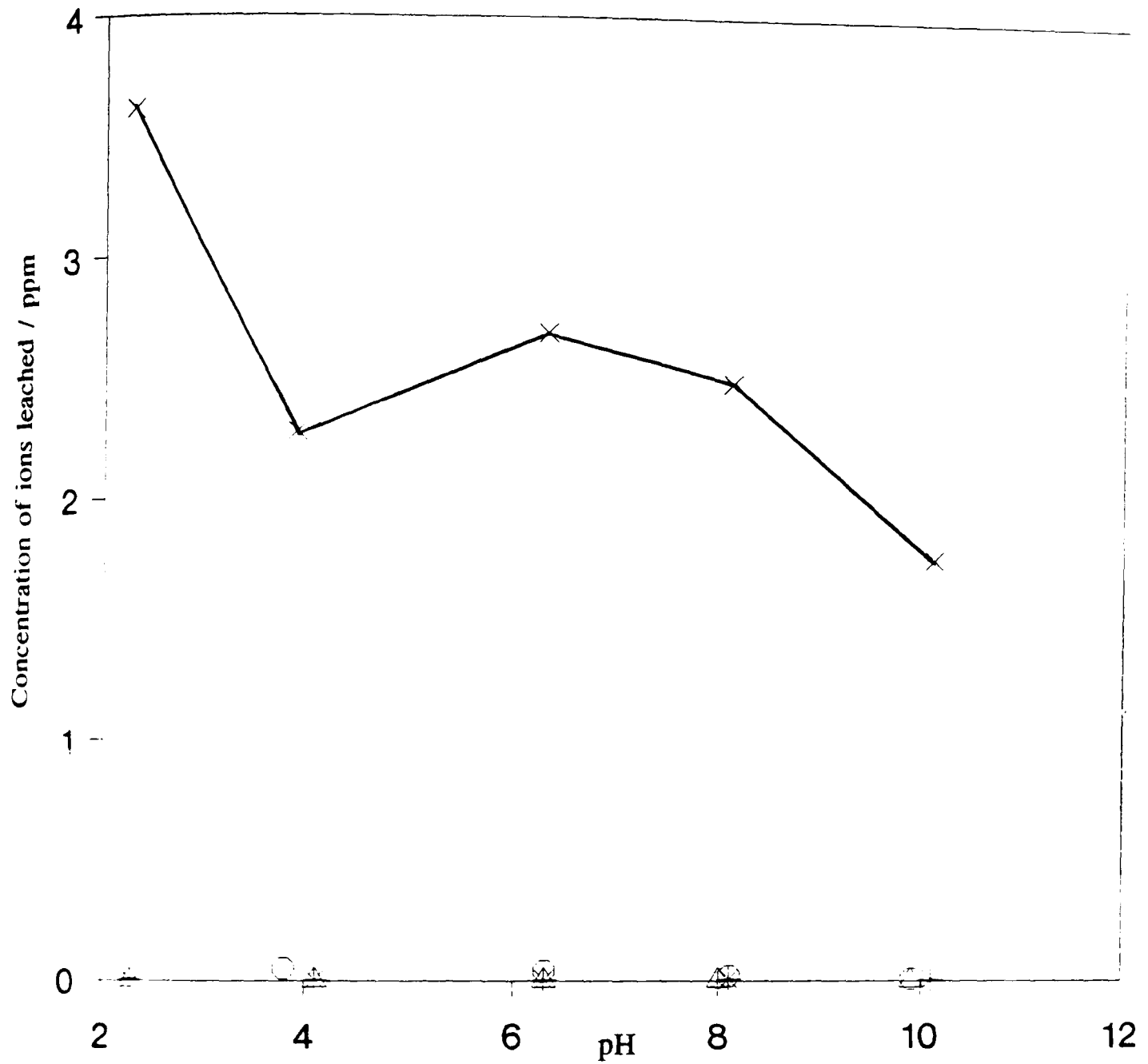


Figure 71. Leaching of calcium from ion washed clays, determined by Atomic Absorption Spectroscopy (AAS).

Washed kaolin (○), sodium kaolin (⊛), calcium kaolin (×) and aluminium kaolin (Δ).

carried out with distilled water (and not 0.1 mol dm⁻³ NaCl as before), as an increased ionic strength is known to prevent leaching (H9), to simulate the effect of preflushing. The method used was that in 3.7.4. These results are shown in Figs 72 and 73.

3.7.6 Leaching of ions from Reservoir rock samples.

The crushed core samples were weighed into a bottle and soaked in distilled water for 24 hours. The ions leached were then determined by AAS, see Table 10.

Table 10 - Leaching of ions to solution from reservoir rock samples

Sample Depth	ppm of ions leached per gram of reservoir sample					
	Fe	K	Na	Al	Ca	Mg
12395	0.03	0.44	9.90	<0.02	3.11	0.11
12417	n.d.	0.37	6.86	<0.02	1.65	0.05
12498.2	n.d.	0.36	8.13	<0.02	1.50	0.63

3.7.7 Successive Washing of Core sample 12498.2

The method used was the same as that for Kaolin (3.7.4) and the results are given in Figs 72 and 73.

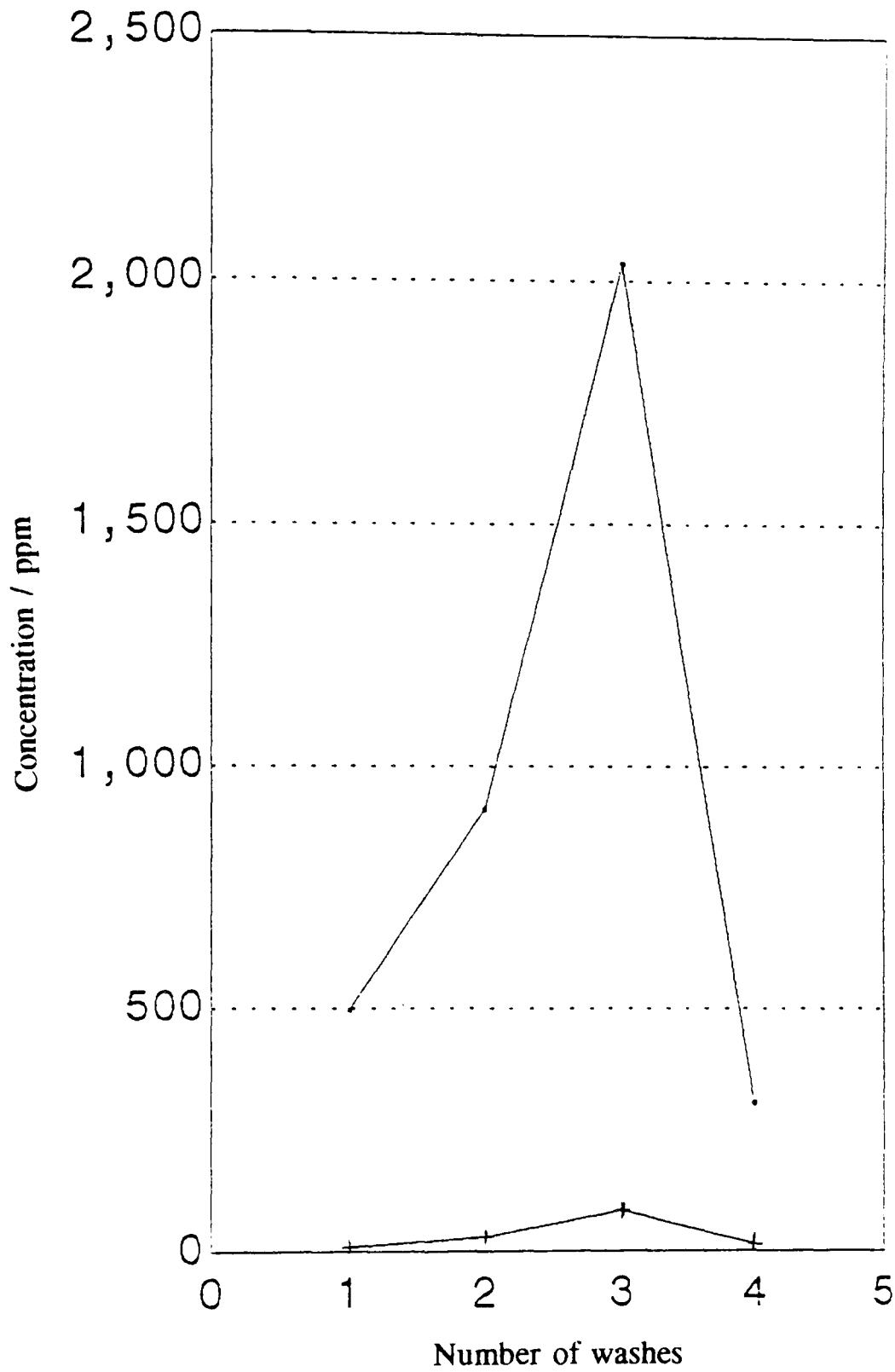


Figure 72. Determination of aluminium leached from washed kaolin and core sample 12395 by successive washings.
Kaolin (•) and Core sample 12395 (+).

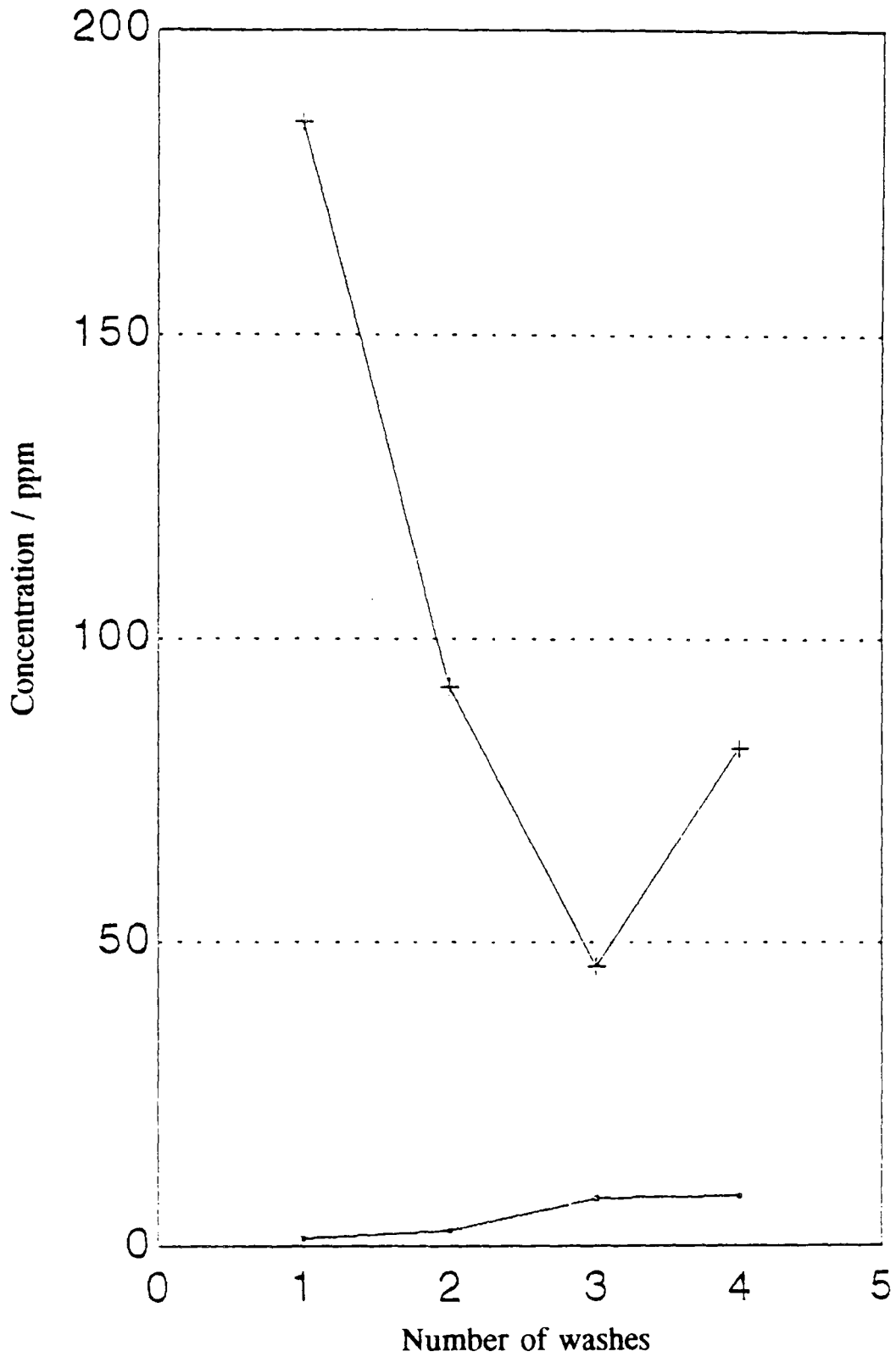


Figure 73. Determination of calcium leached from washed kaolin and core sample 12395 by successive washings.

Kaolin (•) and Core sample 12395 (+).

3.8 Adsorption of 4- ϕ -C₁₂ABS at the Kaolin-Aqueous interface in the presence of nonionic surfactant Synperonic N.

As the adsorption of 4- ϕ -C₁₂ABS was found to be extremely high in the formation water systems it was felt that the incorporation of a second surfactant of nonionic behaviour as a sacrificial agent should be evaluated. Although adsorption occurs at charged sites in the DBS/Kaolin system it is known that nonionic surfactants are adsorbed on the solid surface. A preliminary experiment was carried out from 0.1 mol dm⁻³ NaCl solution. The resulting isotherm is shown in Fig 74.

3.9 Adsorption of other anionic surfactants at the solution/air and Kaolin-Aqueous interface.

Due to the large losses of 4- ϕ -C₁₂ABS surfactant from solution it was felt that the salt tolerance of the surfactant was inadequate for the application. Therefore, other surfactants were tested to see if a lowering in adsorption could be seen.

The surfactants used were Aerosol OT, SDBS, and lignin sulphonates.

3.9.1 Aerosol OT

This surfactant was chosen as it has the ability to reduce interfacial tensions to low levels using very low concentrations of the surfactant. This is an important consideration in order to remove trapped oil from rock pores (see section 1.2.3).

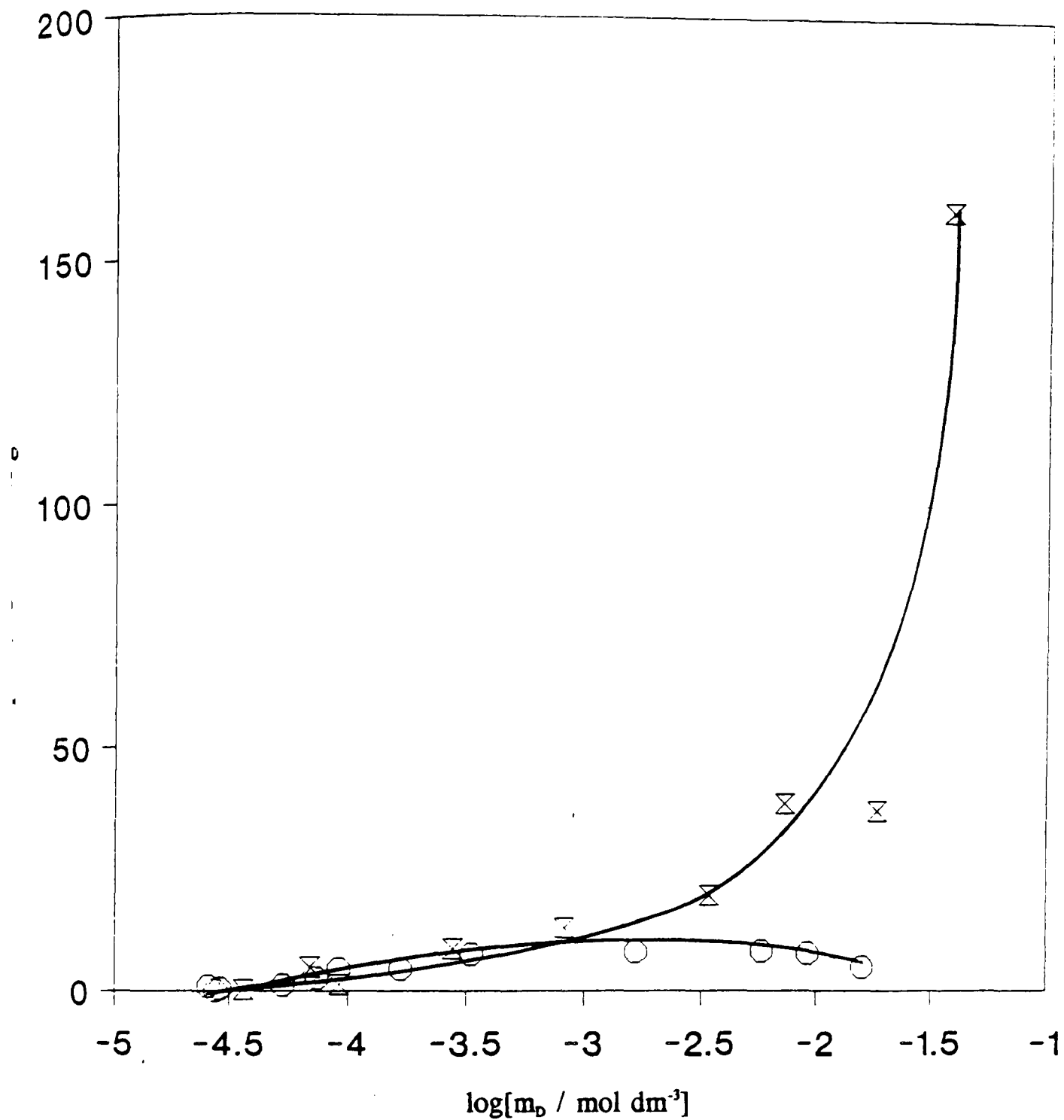


Figure 74. Adsorption of 4- ϕ -C₁₂ABS at the kaolin - aqueous solution interface, at 25°C, from 0.1 mol dm⁻³ NaCl solution in the presence of 0.54 % w/w Synperonic N. \otimes
 pH = 6.3, % solids = 10 and time = 24 hours.

Adsorption of Aerosol OT at the Solution-Air interface.

The surface tensions of aqueous solutions were determined and are shown in Fig 75. The values for CMC, area per adsorbed molecule and surface excess concentration are shown in Table 11.

Effect of 0.1 mol dm⁻³ Sodium Chloride solutions upon the adsorption of Aerosol OT at the Solution-Air interface.

Figure 75 shows the determined surface tensions of Aerosol OT solutions from 0.1 mol dm⁻³ sodium chloride solutions. Values for CMC, area per molecule adsorbed at the interface and surface excess concentration are shown in Table 11.

Adsorption of Aerosol OT at the Kaolin-Aqueous interface.

An isotherm was determined for aqueous Aerosol OT solutions using the standard techniques (see sections 2.5.5.3 and 2.7). The results are shown in Fig 76. Table 12 shows the calculated adsorption parameters.

Effect of Sodium Chloride upon the adsorption of Aerosol OT at the Kaolin-Aqueous interface.

The adsorption of Aerosol OT was determined from 0.1 mol dm⁻³ sodium chloride solutions. The results are shown in Fig 76. Adsorption parameters have been

calculated and are given in Table 12.

Table 11. Calculated adsorption parameters for Aerosol OT at the air-aqueous interface.

NaCl / mol dm ⁻³	Γ_{\max} / 10 ⁻⁶ mol g ⁻¹	A _s / nm ⁻²	CMC / 10 ⁻³ mol dm ⁻³
0.00	2.04	0.81	10.00
0.10	1.71	0.97	0.89

Table 12. Effect of NaCl on the adsorption parameters of Aerosol OT at the kaolin-solution interface.

NaCl / mol dm ⁻³	Γ_{\max} / 10 ⁻⁶ mol g ⁻¹	A _s / nm ⁻²	θ / %
0.00	258.13	0.006	-
0.10	155.67	0.011	-

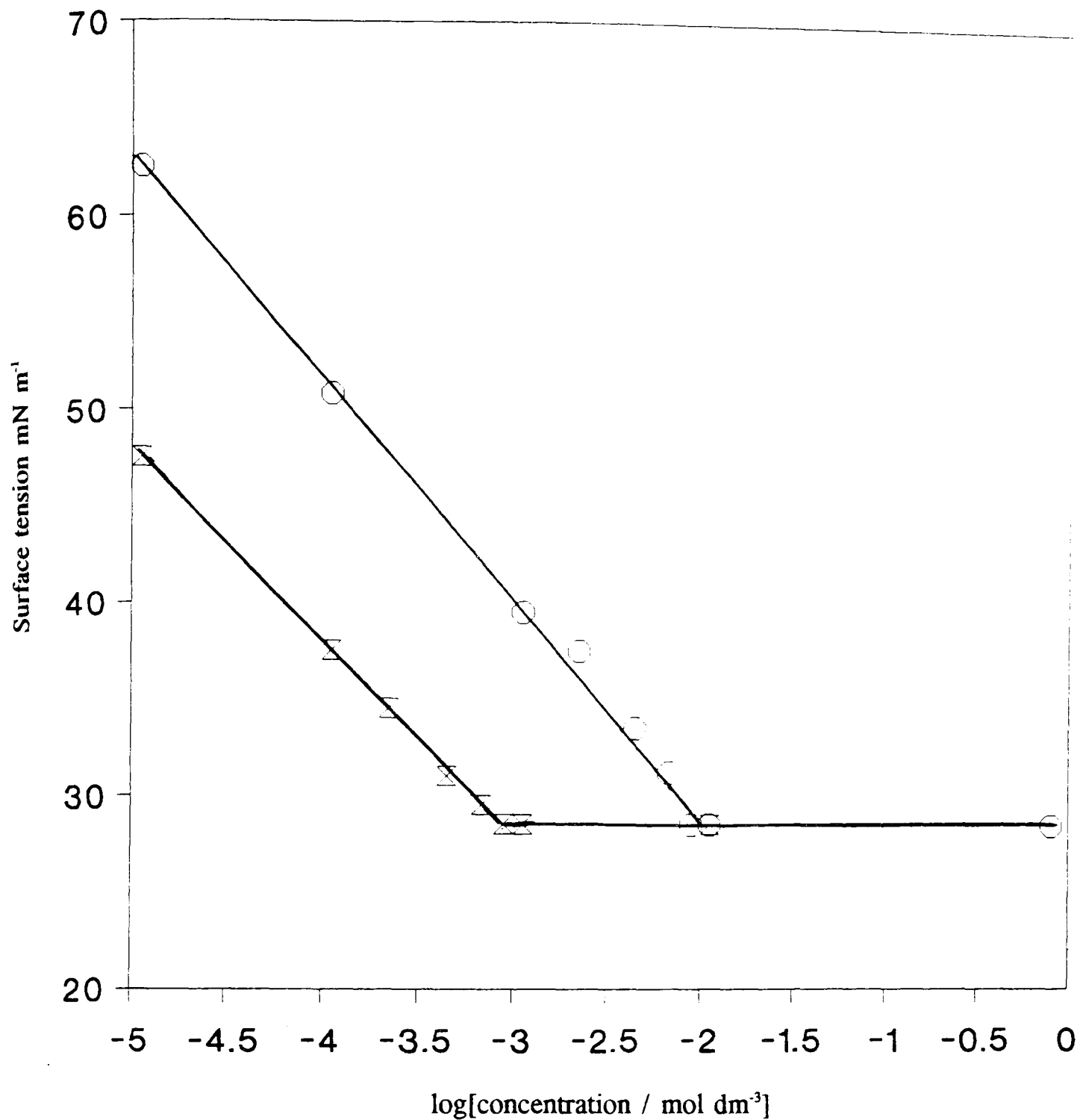


Figure 75. Surface tensions for the air-aqueous NaCl interface at 25°C as a function of Aerosol OT concentration. NaCl conc = 0.00 (○), and 0.10 (⊗) mol dm⁻³.

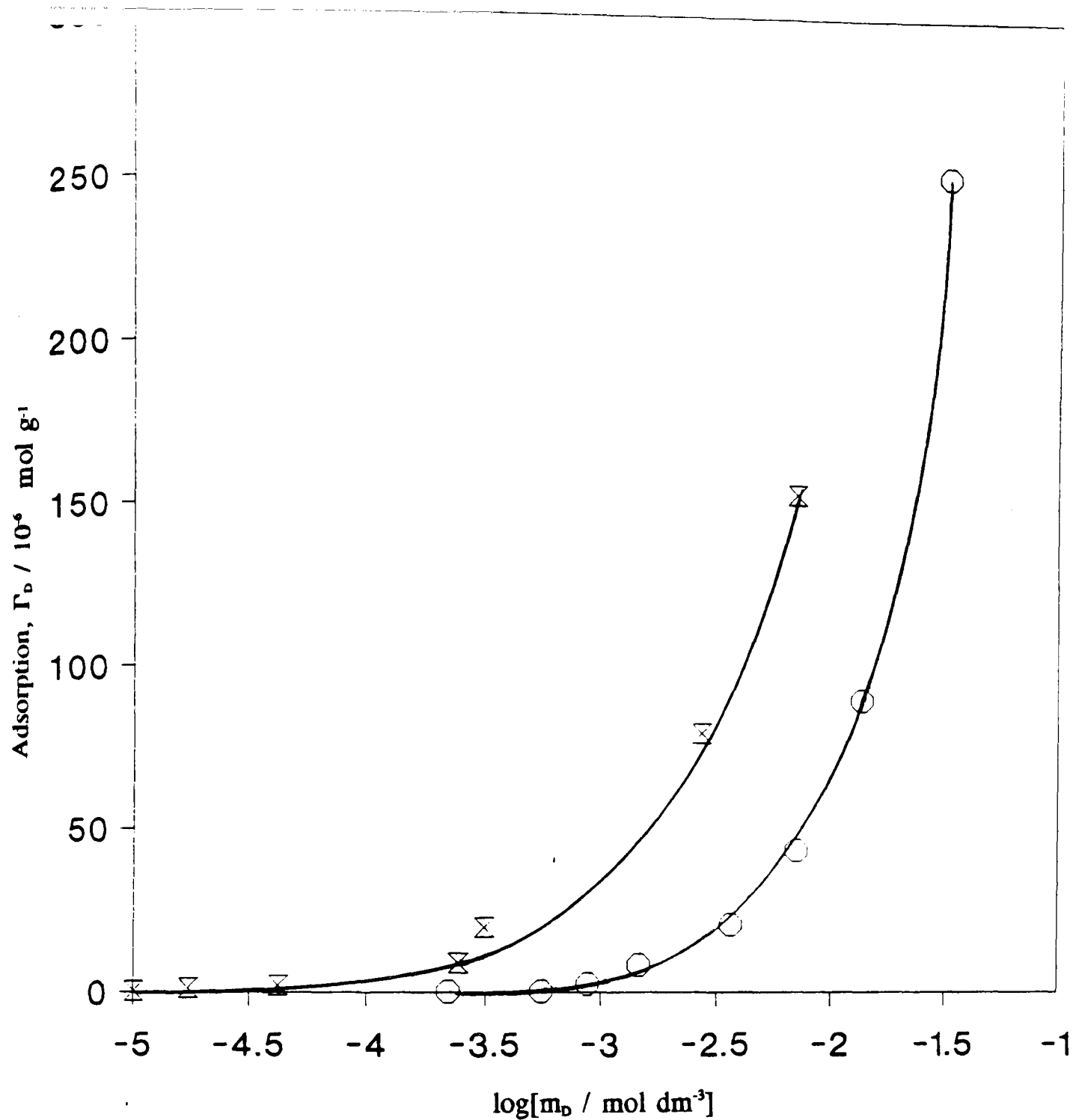


Figure 76. Adsorption of Aerosol OT at the kaolin - aqueous solution interface, at 25°C, as a function of surfactant concentration.

pH = 6.3, % solids = 10 and time = 24 hours.

NaCl conc = 0.00 (○) and 0.10 (⊗) mol dm⁻³.

Effect of butan-1-ol addition on the adsorption of Aerosol OT at the Aluminium Kaolin-Aqueous interface.

The adsorption of Aerosol OT from 0.1 mol dm⁻³ NaCl solution in the presence of 4% v/v butan-1-ol has been determined onto the aluminium washed form of kaolin.

This is shown in Figure 77. The adsorption parameters are shown in Table 13.

Table 13. Effect of butan-1-ol on the adsorption parameters of Aerosol OT at the aluminium kaolin - solution interface.

$n_{\text{BuOH}} / \% \text{ v/v}$	$\Gamma_{\text{max}} / 10^6 \text{ mol g}^{-1}$	A_s / nm^2	$\theta / \%$
0.00	217.4	0.007	-
4.00	354.8	0.004	-

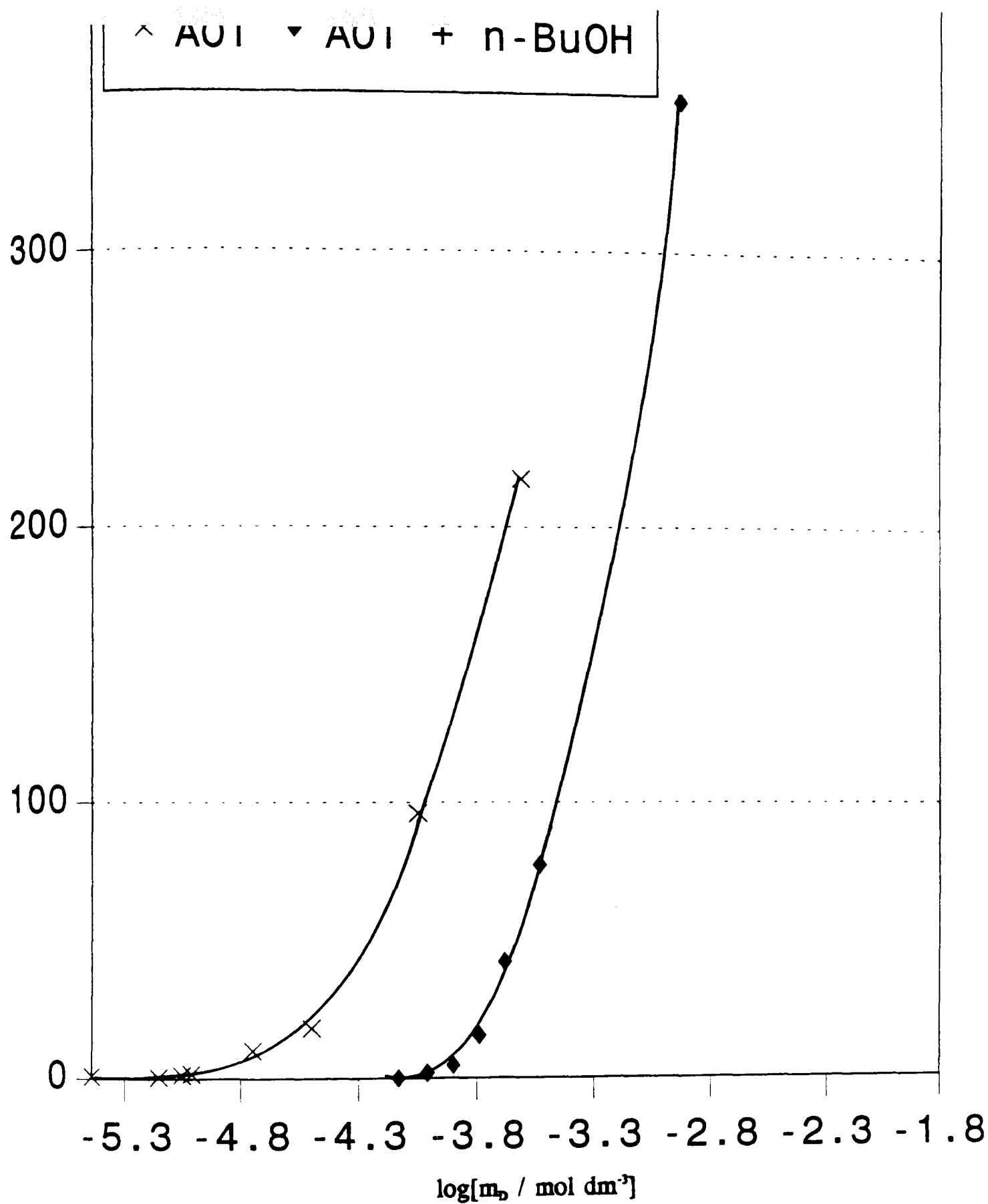


Figure 77. Effect of added butan-1-ol on Aerosol OT adsorption onto aluminium kaolin from 0.1 mol dm^{-3} NaCl solutions, at 25°C , $\text{pH} = 6.3$, % solids = 10 and time = 24 hours. Butan-1-ol conc = 0.00 () and 4% v/v ().

3.9.2 Sodium DodecylBenzeneSulphonate (SDBS)

A commercial sample of SDBS was investigated so that comparisons could be made between this and the isomerically pure form of the surfactant, 4- ϕ -C₁₂ABS. As the commercial sample can be made up of 26 different isomers then it was thought that these may influence any surfactant precipitate to remain soluble.

Adsorption of SDBS at the Kaolin-Aqueous interface.

The adsorption of commercial SDBS was determined from 0.1 mol dm⁻³ NaCl solutions onto kaolin and North Sea reservoir rock samples. The results are shown in Fig 78. The adsorption parameters are shown in Tables 14a and 14b.

Effect of complexing agents upon SDBS adsorption at the Kaolin-Aqueous interface.

The loss of SDBS from 0.1 mol dm⁻³ NaCl solution in the presence of 5 x 10⁻³ mol dm⁻³ of sodium tripolyphosphate onto kaolin has been measured. This can be seen in Fig 79. The adsorption parameters are given in Tables 14a and 14b.

Table 14a. Effect of sodium tripolyphosphate on the adsorption parameters of SDBS at the kaolin-solution interface.

Sodium tripolyphosphate / mol dm ⁻³	Γ_{\max} / 10 ⁻⁶ mol g ⁻¹	A_s / nm ⁻²	θ / %
0.00	6.89	0.24	79.15
5 x 10 ⁻³	2.32	0.72	26.65

Table 14b. Effect of sodium tripolyphosphate on the adsorption parameters of SDBS at the reservoir rock - solution interface.

Sodium tripolyphosphate / mol dm ⁻³	Γ_{\max} / 10 ⁻⁶ mol g ⁻¹	A_s / nm ⁻²	θ / %
0.00	4.02	0.41	182.8
5 x 10 ⁻³	2.41	0.69	109.6

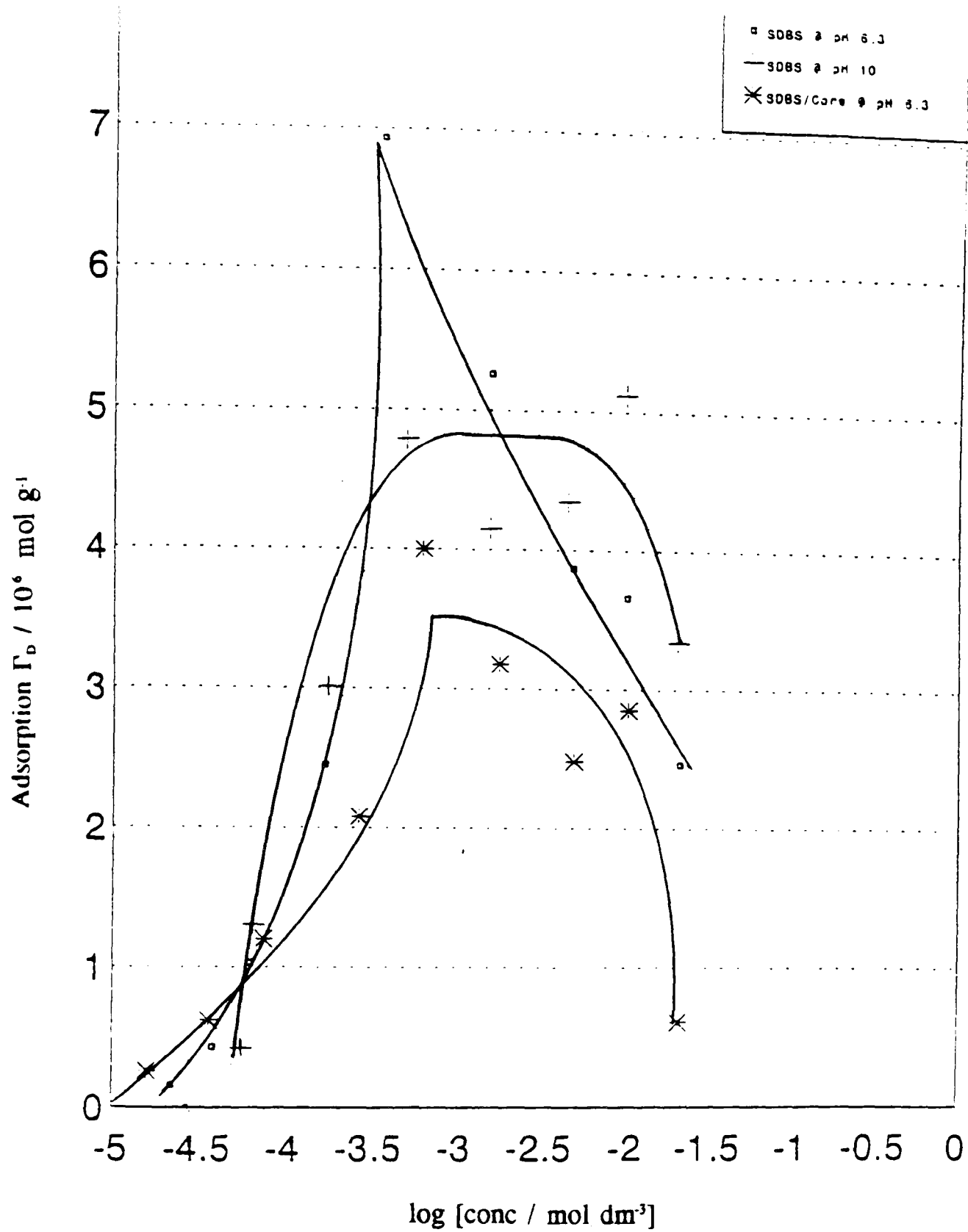


Figure 78. Adsorption of SDBS at the solid - aqueous solution interface, at 25°C, as a function of surfactant concentration from 0.1 mol dm⁻³ NaCl solutions.

% solids = 10 and time = 24 hours.

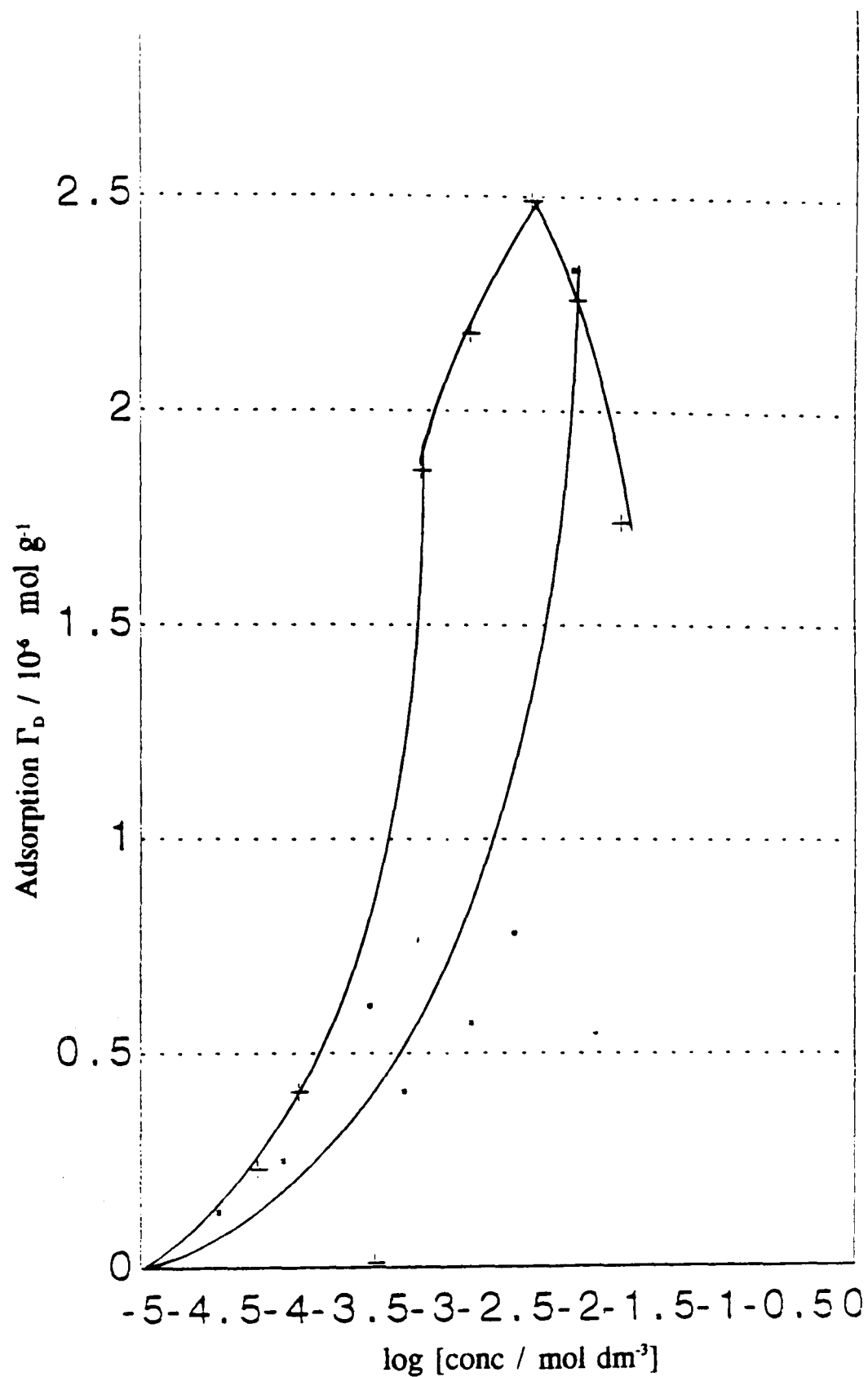


Figure 79. Effect of added sodium tripolyphosphate ($5 \times 10^{-3} \text{ mol dm}^{-3}$) on SDBS adsorption at the solid - aqueous interface, at 25°C , from 0.1 mol dm^{-3} NaCl solution. pH = 6.3, % solids = 10, and time = 24 hours. Solid = Kaolin (+) and reservoir rock (•).

3.9.3 Lignin Sulphonates

This surfactant has been used in the oil industry in drilling mud formations (A4,E2) for several years. Recently, there have been several papers (e.g. G5) regarding its use as a possible surfactant for enhanced oil recovery processes. This type of surfactant is a by-product of the paper industry and is obtained from wood pulp giving it the advantage of being both plentiful and extremely cheap. The products used here were obtained from a company based in Finland, Metsa Serla. Two grades were used; Serla Con, which is naturally acidic, and Serla Thin, which is an alkaline surfactant. The samples were commercial and hence made up of many different isomers and carbon chain lengths of the basic lignin structure which can be seen in Appendix 2. This type of surfactant has been reported to be very salt tolerant (C3) which is a necessary factor if use in the North Sea is to be considered.

Adsorption of lignin sulphonate at the liquid-air interface.

The surface tension of both Serla-Con and Serla-Thin have been measured from distilled water and the results are shown in Fig 81. Values for surface excess concentration (Γ), area per molecule adsorbed at the interface (A_s) and CMC were not calculable as over the range of concentrations determined a CMC was not reached.

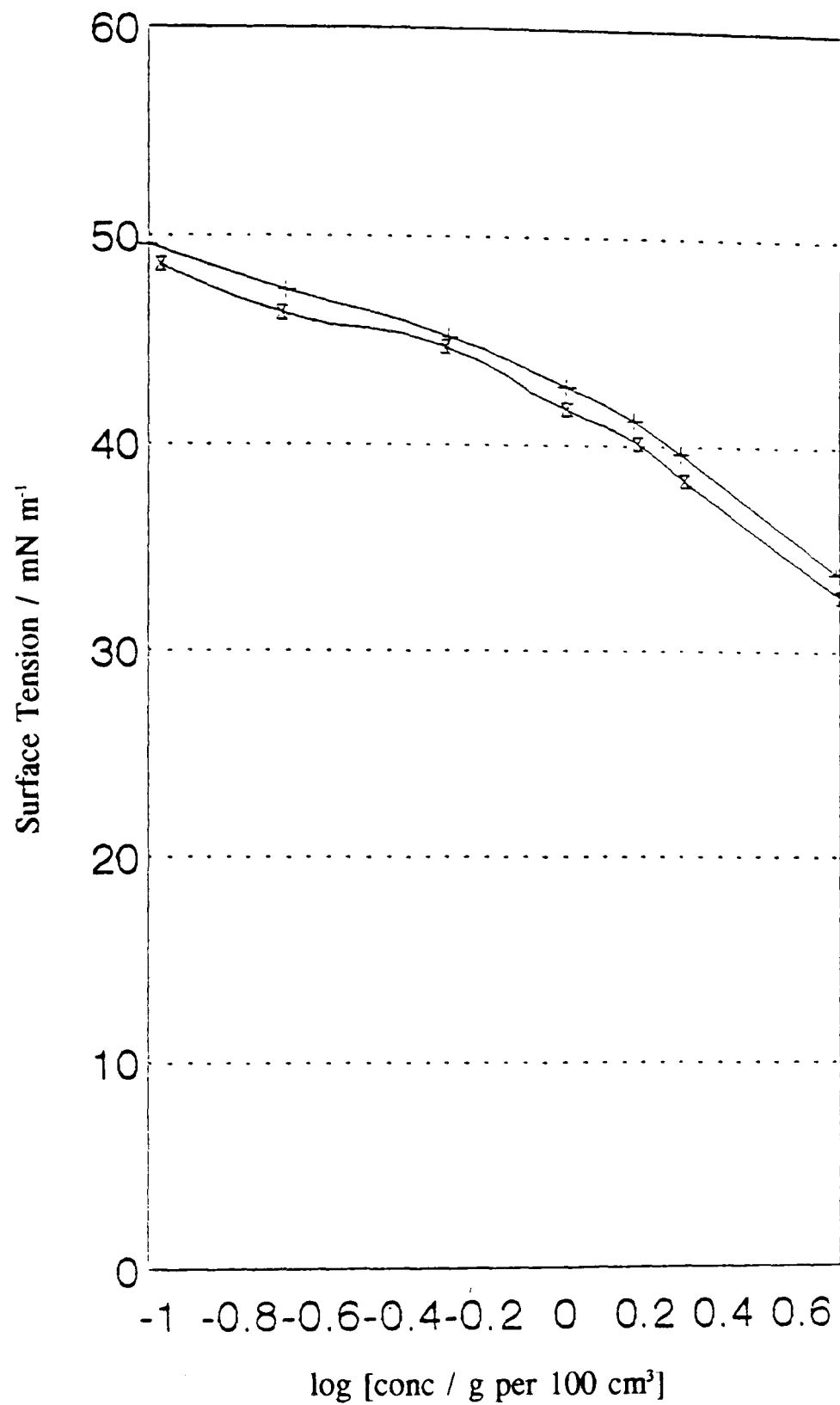


Figure 80. Surface tensions at the air - aqueous formation water (B) interface at 25°C as a function of lignin concentration. Serla-Con = (⊕) and Serla-Thin (⊗).

Effect of Formation water on the adsorption of lignin sulphonate at the liquid-air interface.

The results of surface tension measurements of both Serla-Con and Serla-Thin in the presence of Formation water B (see section 3.7) are shown in Fig 80. Again the adsorption parameters were not determined.

Adsorption of lignin sulphonates at the kaolin-Aqueous interface.

Figure 81 shows the adsorption of both lignin surfactants onto kaolin from distilled water. The adsorption parameters are given in Table 15.

Effect of formation water on the adsorption of lignin sulphonate at the Kaolin-Aqueous interface.

The adsorption of both lignin samples were determined from formation water B (see section 3.7) and the results are shown in Fig 82. The adsorption parameters have been determined and are given in Tables 16a and 16b.

Effect of butan-1-ol addition on the adsorption of lignin sulphonates at the Kaolin-Aqueous interface.

Figures 83a and 83b shows the adsorption of both lignin sulphonates from formation water B in the presence of 4% v/v butan-1-ol. The calculated adsorption parameters are given in Tables 16a and 16b.

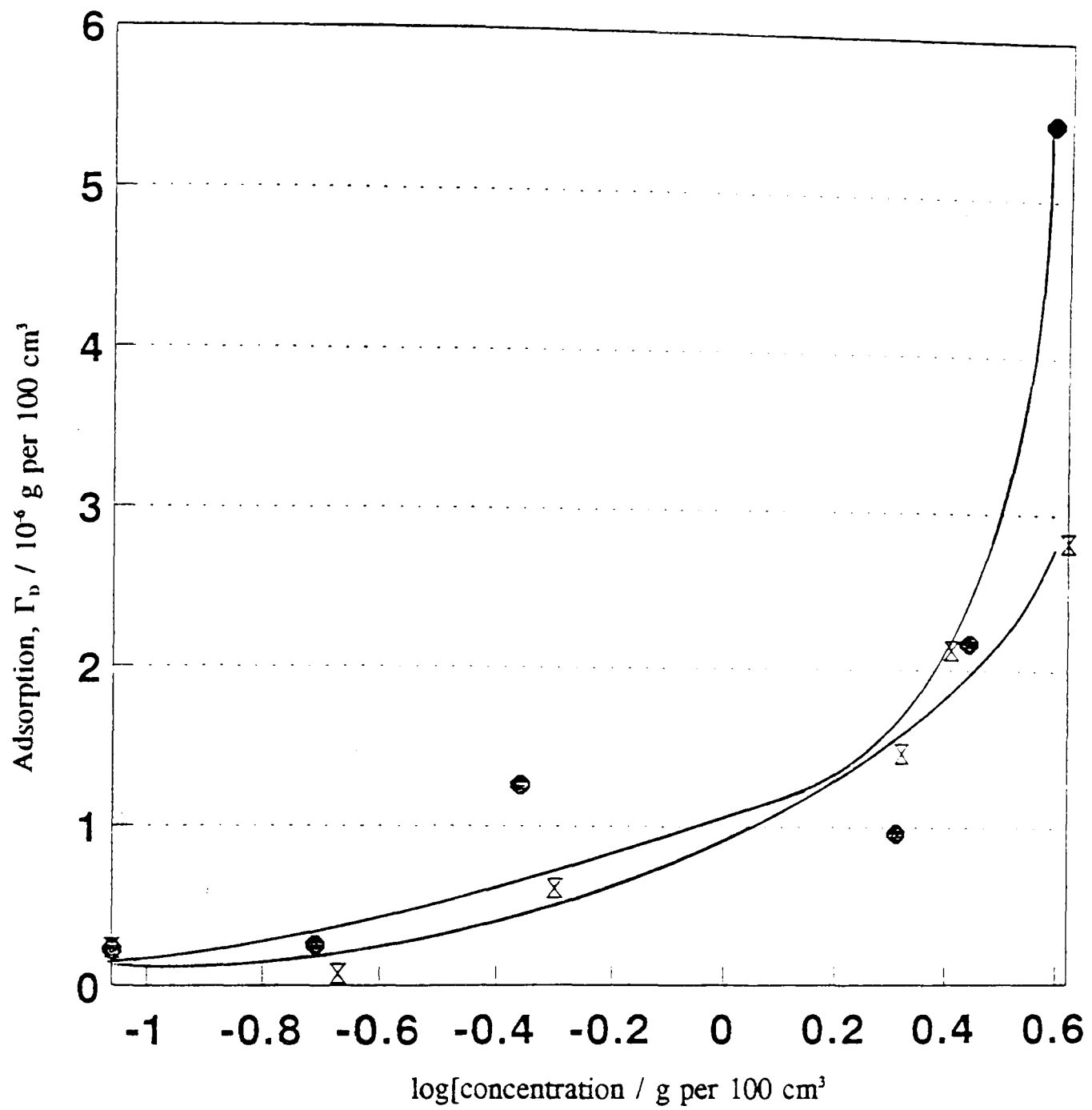


Figure 81. Adsorption of lignin sulphonates onto kaolin from distilled water at 25°C, % solids = 10 and time = 24 hours. Serla-Con @ pH = 3 (●) and Serla-Thin @ pH = 9 (⊗).

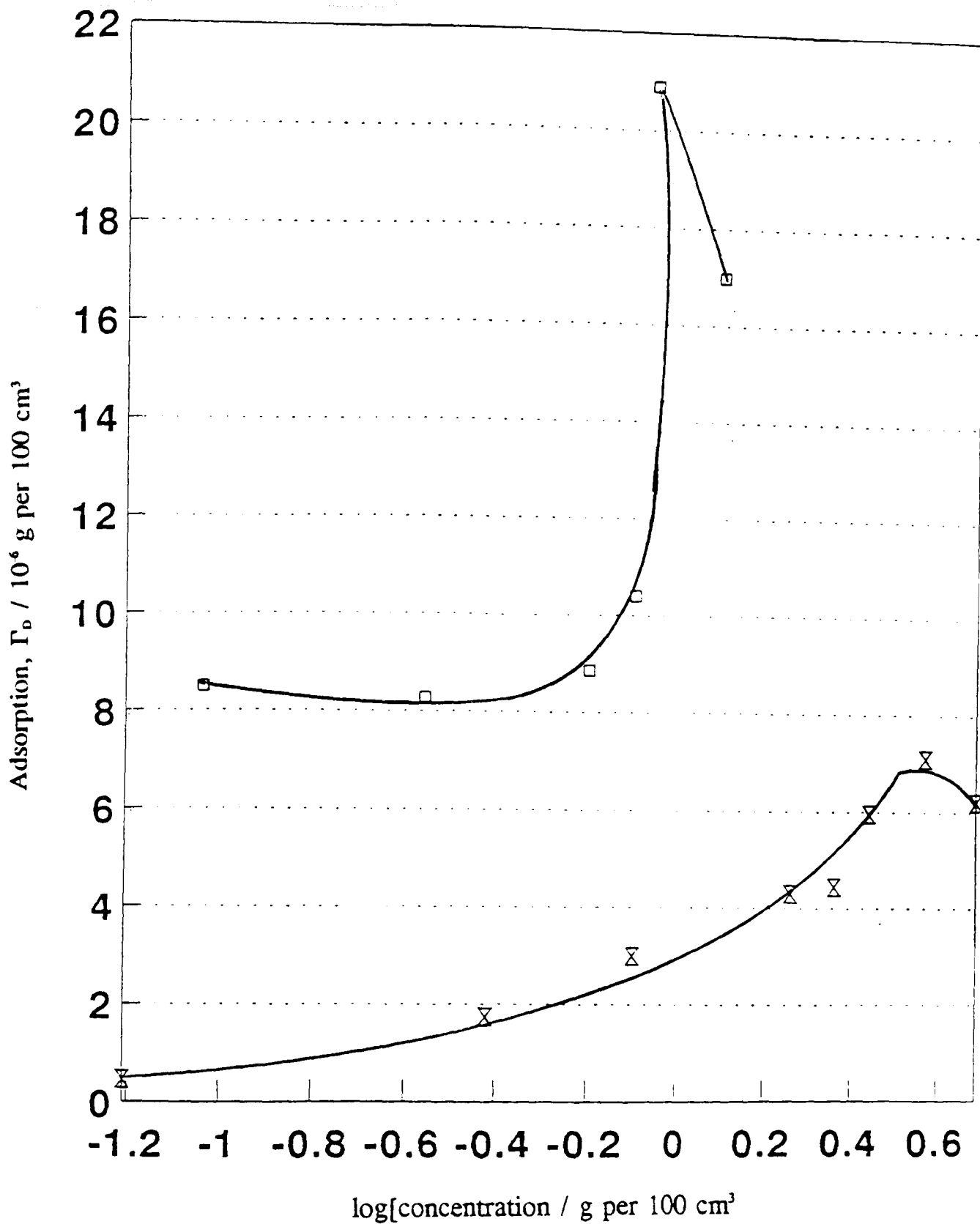


Figure 82. Adsorption of lignin sulphonates at the kaolin - formation water interface, at 25°C, as a function of surfactant concentration. % solids = 10 and time = 24 hours. Serla-Con @ pH = 7 (\square) and Serla-Thin @ pH = 7 (\otimes).

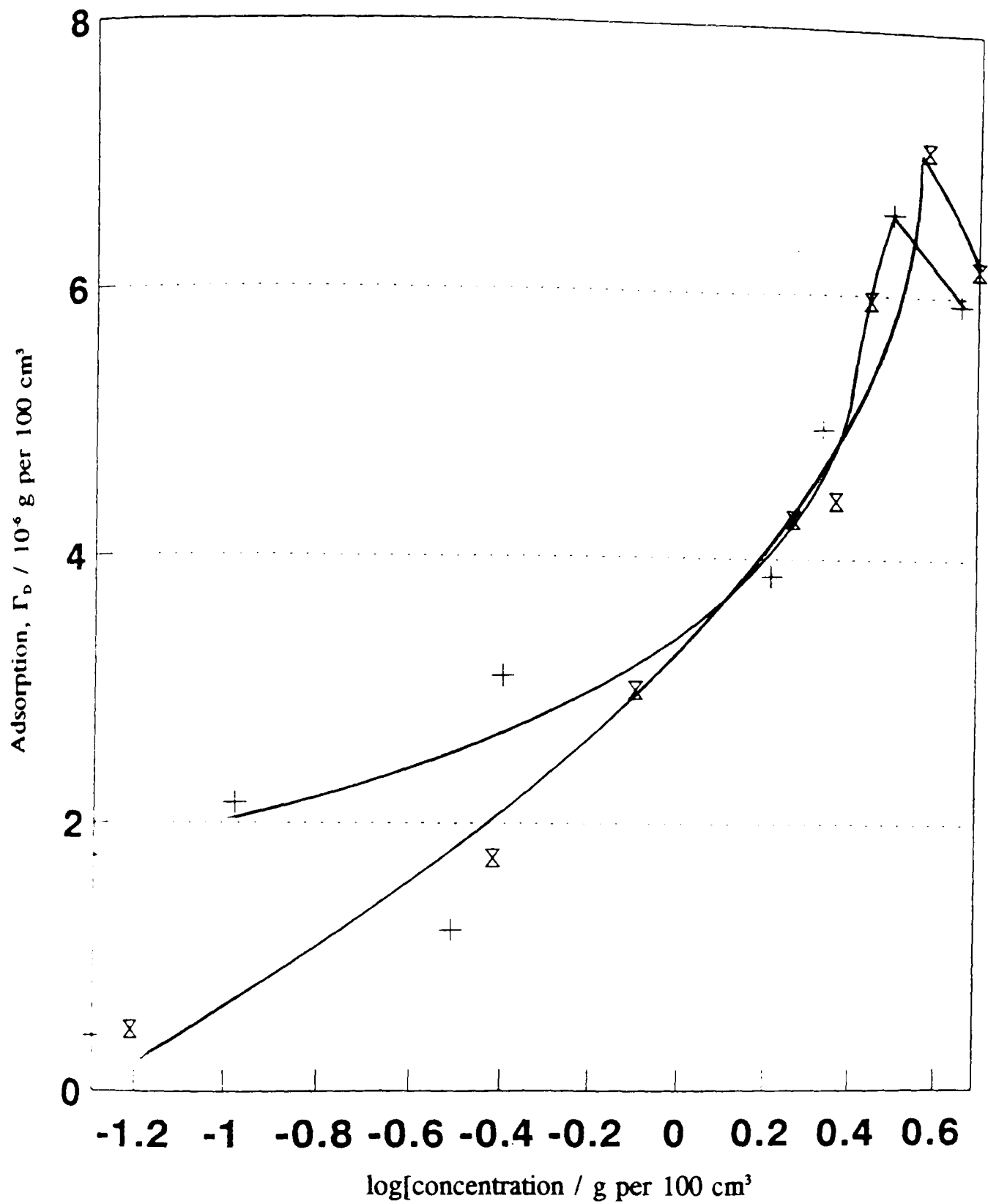


Figure 83a. Effect of added butan-1-ol on the adsorption of lignin sulphonates (Serla-Con) at the kaolin - formation water interface, at 25°C, % solids = 10 and time = 24 hours.
 Surfactant (x)
 Surfactant + butan-1-ol (+)

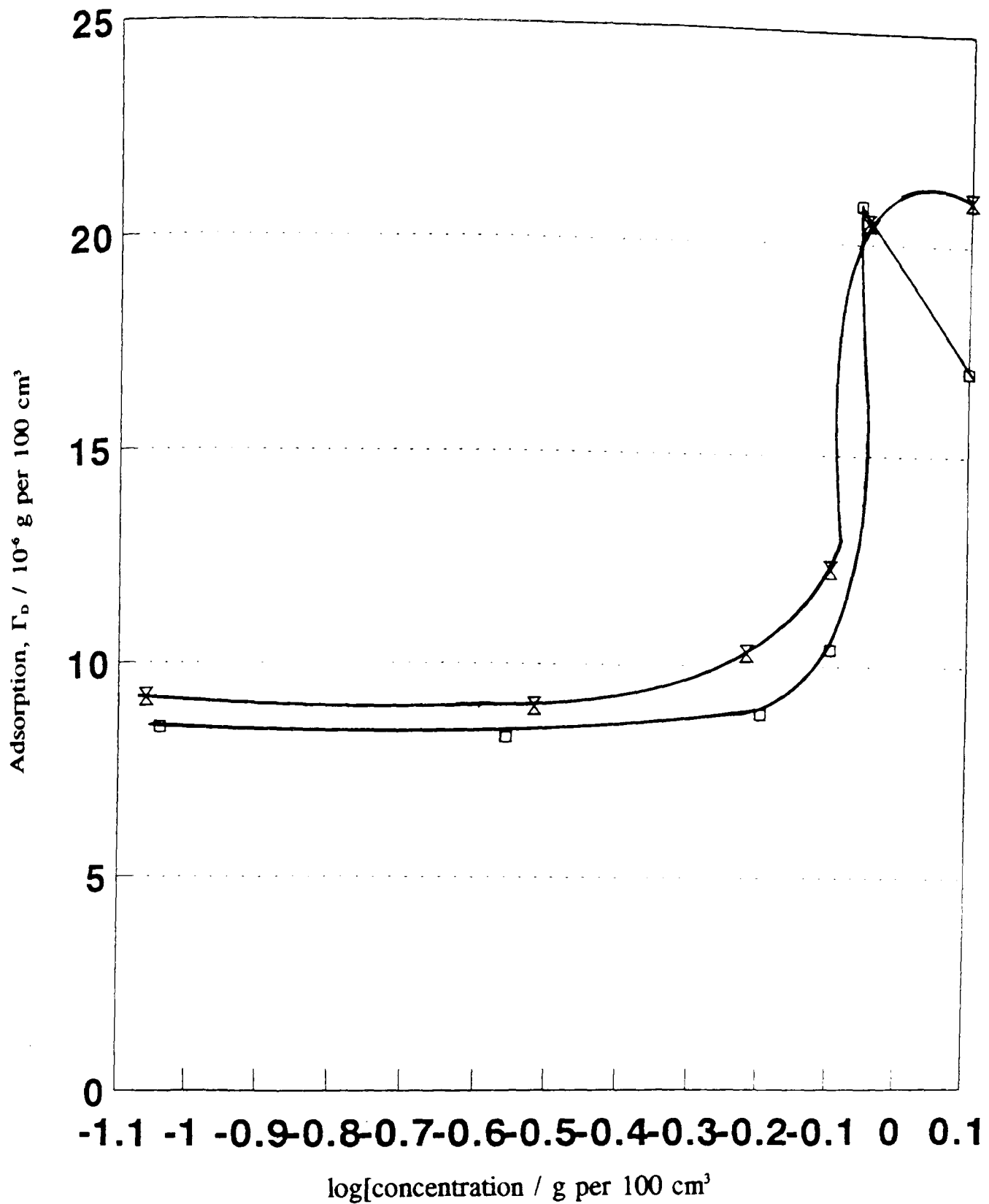


Figure 83b. Effect of added butan-1-ol on the adsorption of lignin sulphonates (Serla-Thin) at the kaolin - formation water interface, at 25°C, % solids = 10 and time = 24 hours.
 Surfactant (\square)
 Surfactant + butan-1-ol (\otimes)

Table 16a. Effect of butan-1-ol on the calculated adsorption parameters for Serla-Con at the kaolin - solution interface.

$n_{\text{BuOH}} / \% \text{ v/v}$	$\Gamma_{\text{max}} / 10^6 \text{ mol g}^{-1}$	A_s / nm^2	$\theta / \%$
-	7.11	-	-
4	8.03	-	-

Table 16b. Effect of butan-1-ol on the calculated adsorption parameters for Serla-Thin at the kaolin - solution interface.

$n_{\text{BuOH}} / \% \text{ v/v}$	$\Gamma_{\text{max}} / 10^6 \text{ mol g}^{-1}$	A_s / nm^2	$\theta / \%$
-	21.07	-	-
4	25.20	-	-

Effect of pH on the adsorption of lignin sulphonates at the Kaolin-Aqueous interface.

As both lignin surfactants alter the pH of the solution naturally, then the adsorption of these surfactants were determined from formation water at various pH values. The results are given in Fig 84 with the calculated adsorption parameters in Tables 17a and 17b.

Effect of sodium citrate addition on the adsorption of lignin sulphonates at the Kaolin-Aqueous interface.

It is known that sodium citrate reduces the adsorption of 4- ϕ -C₁₂ABS (Fig 58). Therefore, the effect of sodium citrate upon the adsorption of lignin sulphonate from formation water B was evaluated. The results are shown in Figures 85a and 85b. Tables 18a and 18b shows the determined adsorption parameters.

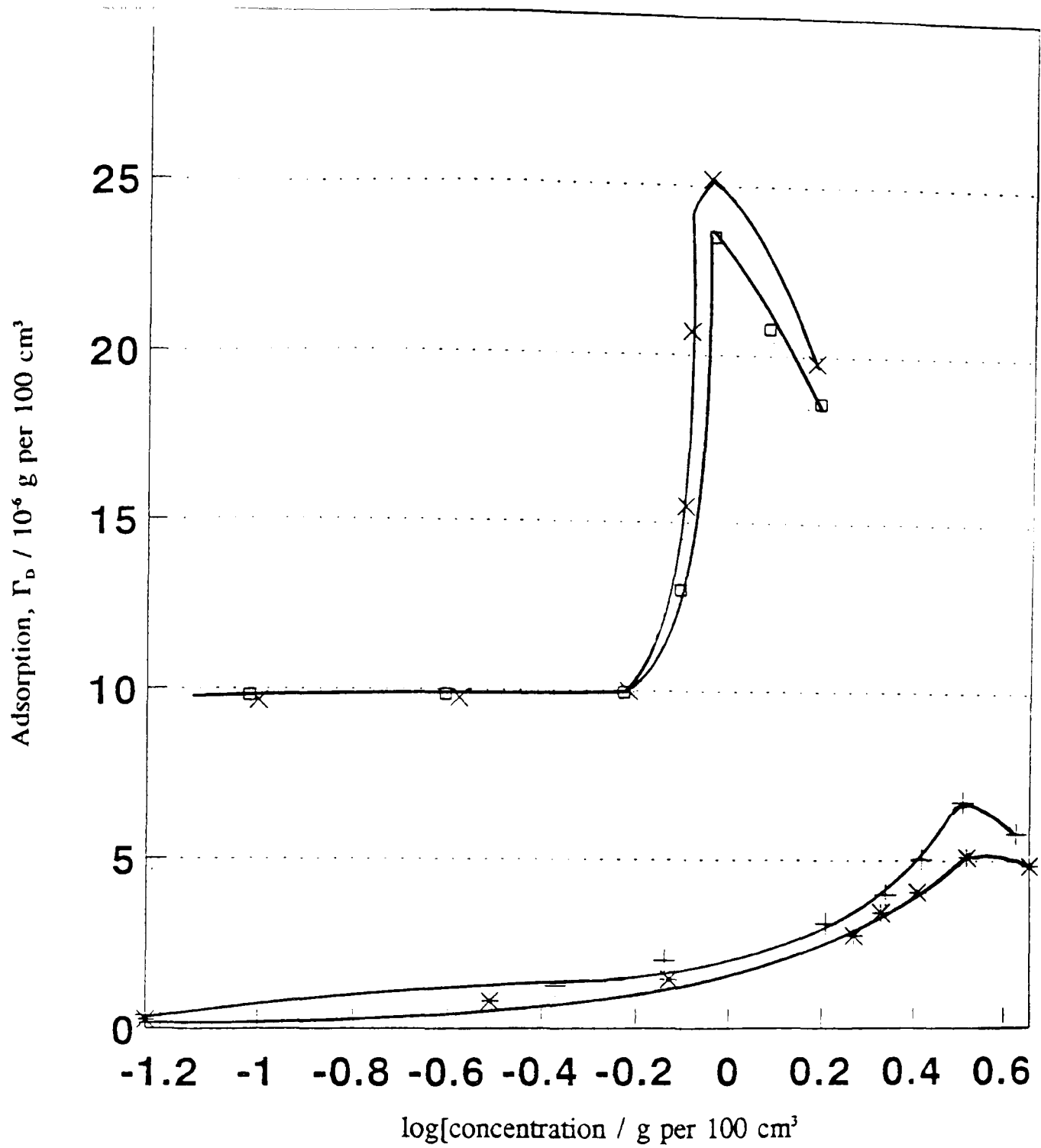


Figure 84. Effect of pH on lignin sulphonate adsorption onto kaolin from formation water at 25°C, % solids = 10 and time = 24 hours.

Serla-Con @ pH = 7 (+), and pH = 9 (x).

Serla-Thin @ pH = 4 (x), and pH = 7 (o).

Table 17a. Effect of pH on the calculated adsorption parameters for SerlaCon at the kaolin - solution interface.

pH	$\Gamma_{\max} / 10^6 \text{ mol g}^{-1}$	A_s / nm^2	$\theta / \%$
3	7.11	-	-
7	6.89	-	-
9	5.17	-	-

Table 17b. Effect of pH on the calculated adsorption parameters for Serla-Thin at the kaolin - solution interface.

pH	$\Gamma_{\max} / 10^6 \text{ mol g}^{-1}$	A_s / nm^2	$\theta / \%$
4	25.21	-	-
7	23.62	-	-
9	21.07	-	-

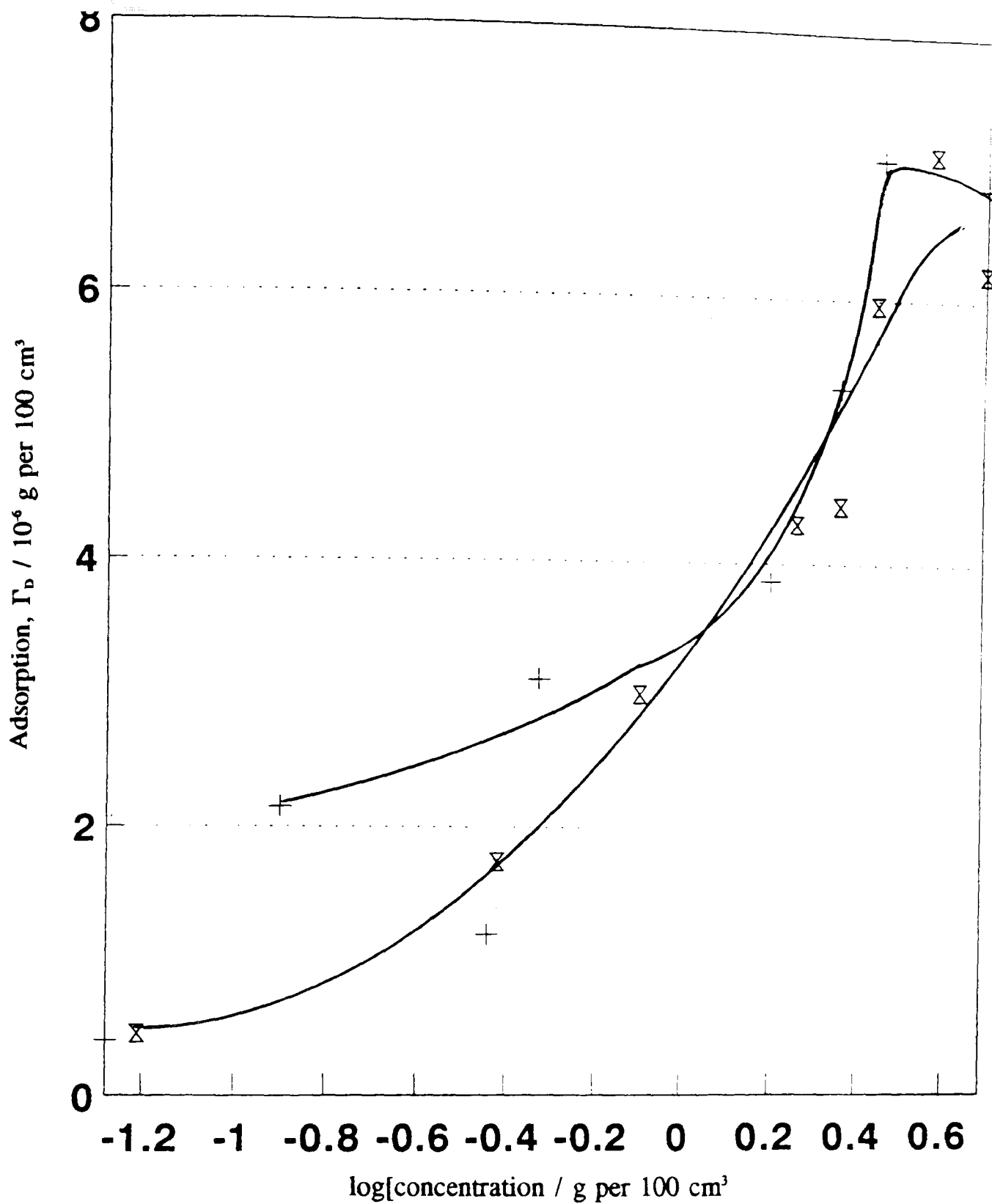


Figure 85a. Effect of added sodium citrate (1×10^{-2} mol dm^{-3}) on lignin sulphonate (Serla-Con) adsorption at the kaolin - formation water interface, at 25°C , % solids = 10 and time = 24 hours. Surfactant (x) Surfactant + citrate (+)

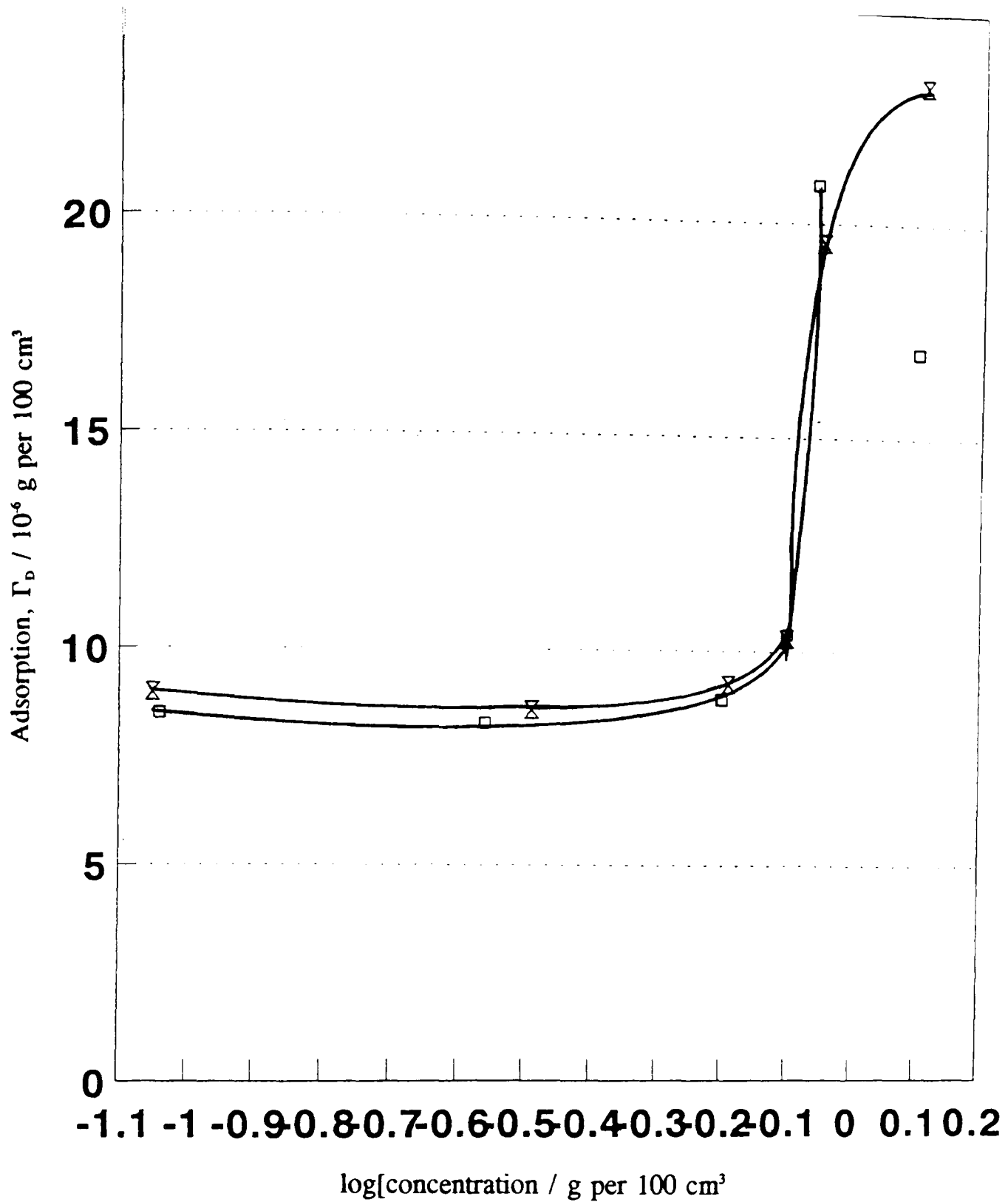


Figure 85b. Effect of added sodium citrate (1×10^{-2} mol dm^{-3}) on lignin sulphonate (Serla-Thin) adsorption at the kaolin - formation water interface, at 25°C , % solids = 10 and time = 24 hours. Surfactant (□) Surfactant + citrate (⊗)

Table 18a. Effect of Sodium citrate on the calculated adsorption parameters for Serla-Con at the kaolin - solution interface.

Sodium Citrate / mol dm ⁻³	Γ_{\max} / 10 ⁻⁶ mol g ⁻¹	A _s / nm ⁻²	θ / %
0.00	7.11	-	-
0.01	7.05	-	-

Table 18b. Effect of Sodium citrate on the calculated adsorption parameters for Serla-Thin at the kaolin - solution interface.

Sodium Citrate / mol dm ⁻³	Γ_{\max} / 10 ⁻⁶ mol g ⁻¹	A _s / nm ⁻²	θ / %
0.00	21.07	-	-
0.01	23.29	-	-

3.10 Determination of calcium ions in solution using an Ion-Selective Electrode

As the concentration of metal ions in solution appears to be very important, so that prevention of the loss of surfactant via precipitation can occur, it was decided that the determination of calcium ions in the presence of surfactant was necessary. However, it is well documented (C4,C5,L3,P6) that in the presence of surfactant the sensor compound attached to the PVC membrane in the ion-selective electrode (ISE) is attacked by the surfactant which leads to a deterioration of the electrode. The presence of sodium chloride can also interfere with the calcium determinations.

3.10.1 Effect of sodium chloride upon calcium determination by ISE

To determine the effect of sodium chloride addition upon calcium determination the change in millivolt response of the electrode with increasing calcium concentration was determined in the presence of 0.05 mol dm^{-3} NaCl. The results are given in Figure 86.

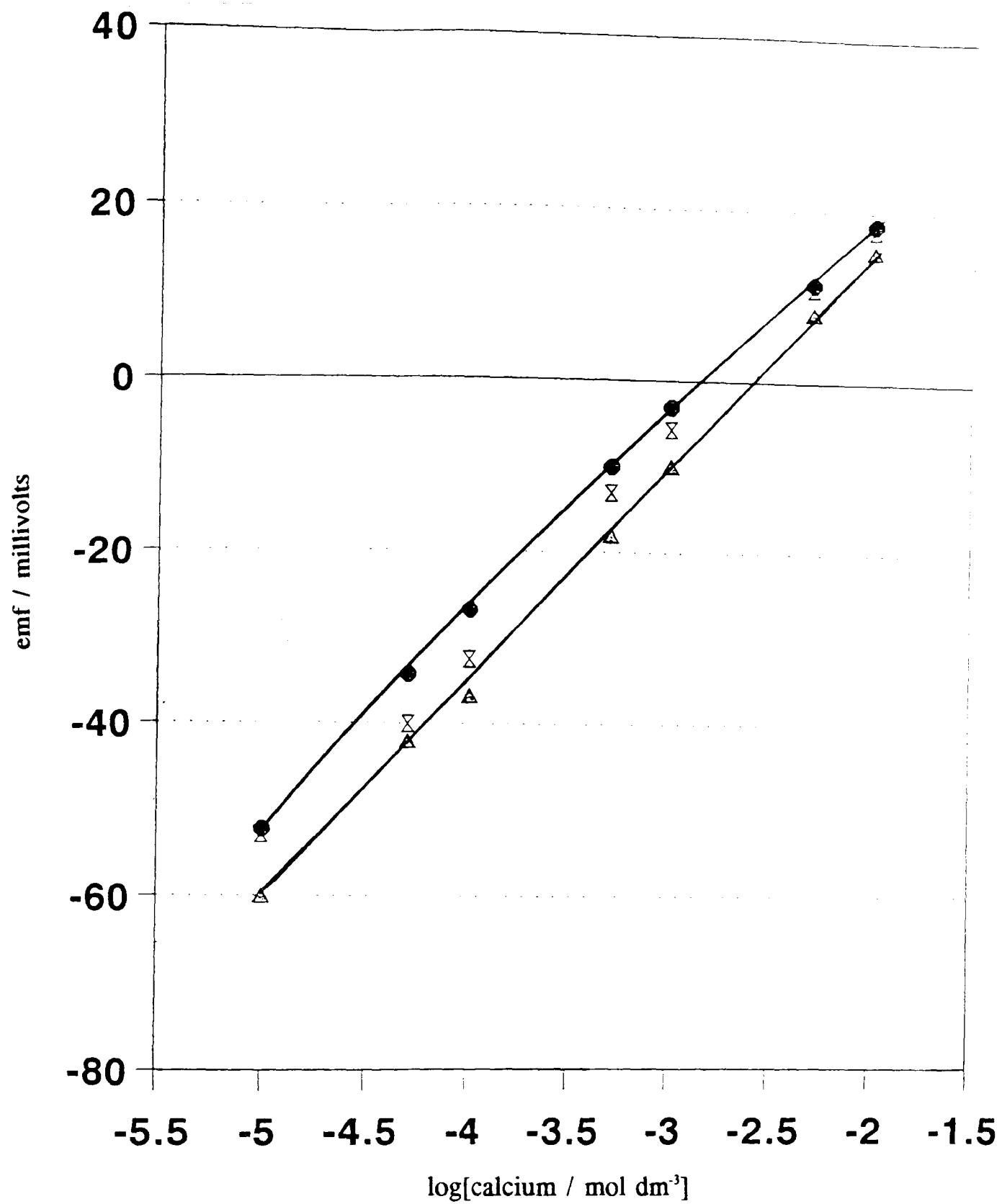
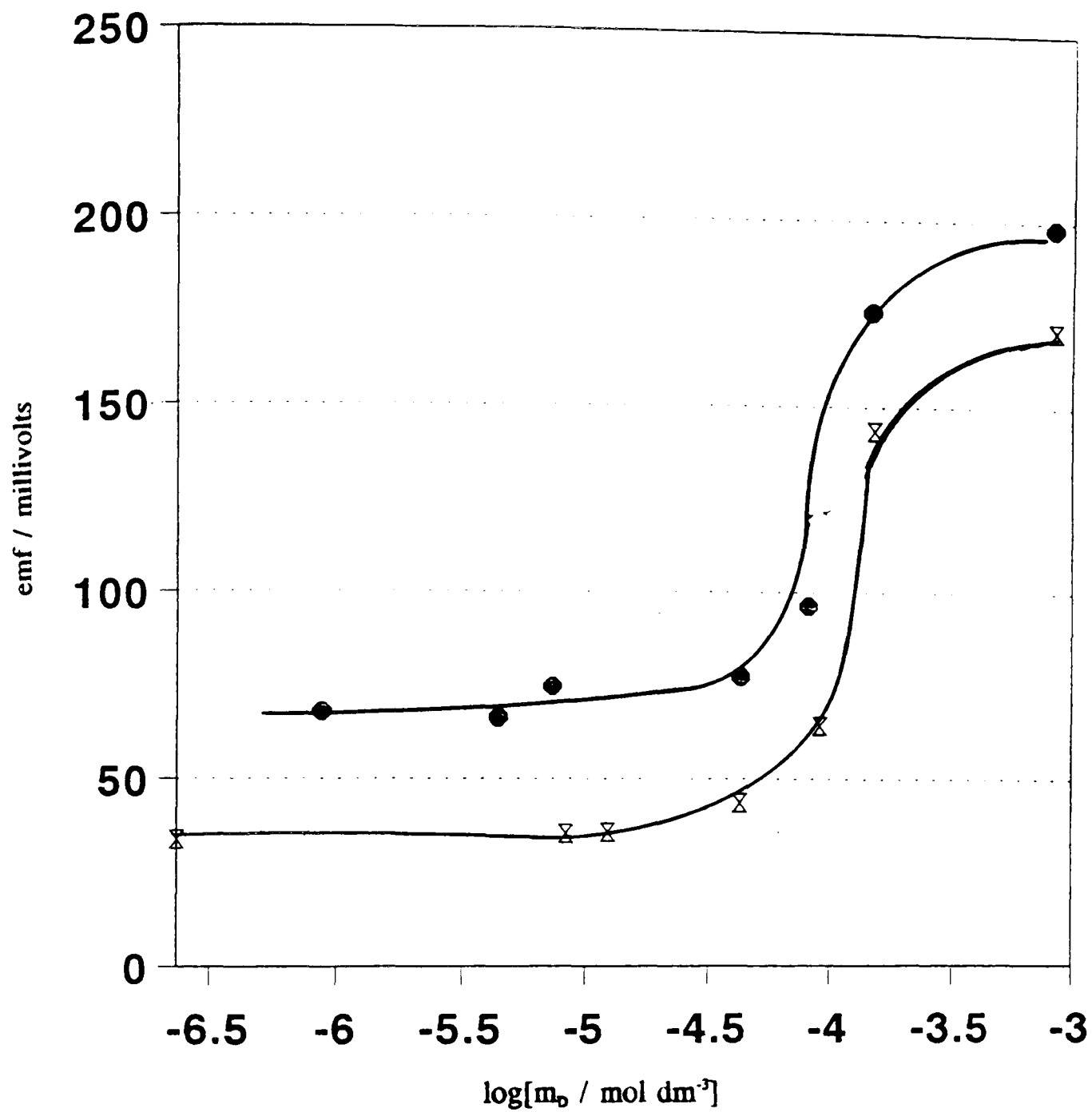


Figure 86. Effect of NaCl addition on the determination of Calcium by ISE.

NaCl conc = 0.00 (●) and 0.05 (△) mol dm⁻³.

3.10.2 Effect of 4- ϕ -C₁₂ABS on the determination of calcium by ISE

The change in millivolt response of the electrode with increasing surfactant concentration was determined for a 1×10^{-4} mol dm⁻³ calcium solution. The results are shown in Fig 87. It can be seen that the shape of the plot is not that of the ideal horizontal line. By determining the millivolt response of the surfactant alone, the difference should equate to the millivolt response solely due to the calcium alone. This will be discussed in the section 4.6.2.



Surfactant solution (●), Surfactant + calcium (x)

Figure 87. Effect of 4- ϕ -C₁₂ABS addition on the determination of calcium by ISE.

Chapter 4

Discussion

4.1 Characterisation of Kaolin and its ion-exchanged forms.

It is widely accepted (H7, B7) that the clay form of kaolin present in oil bearing rock in the North Sea is primarily that of sodium kaolin. This is regarded as occurring via a simple ion exchange of the hydrogen ion present in the hydroxyl group (see Figure 5) for the sodium from sea water, however, there are many other metallic anions in sea water which can also exchange via the same mechanism. Of these the Ca^{2+} and Al^{3+} are probably the most important. Therefore, several different forms of kaolin were prepared to investigate the effect these clays will have on surfactants in solution. The clays were prepared using the methods given in section 2.4. and were characterised using the following techniques (see section 3.1), X-ray diffraction, X-ray Fluorescence, Nitrogen Adsorption, Scanning Electron Microscopy and electrophoretic mobility determinations, to determine whether any chemical or physical changes in the clay structure had occurred.

X-ray Diffraction

XRD spectra were determined for the four forms of kaolin i.e. washed, sodium, calcium and aluminium and these can be seen in Figure 33. From this figure and the values obtained for the d-values (given in table 3) it can be seen that there is good agreement between the clays and the literature values for kaolin, however, in the three metal ion washed clays an additional peak is observed at approximately $2\theta = 9^\circ$. This peak is indicative of the ion-exchange that has occurred at the surface of the clay between the metal ions in solution and the hydrogen ions from the

hydroxyl group. It should also be noted that there is a difference in the intensity values between the metal ion washed clays and that for the water washed clays. This can be attributed to changes in the packing of the clay during the sample preparation.

X-ray Fluorescence

X-ray fluorescence, on the other hand, gives information on the surface layers of the clay and can thus be used to ascertain what had taken place on exposure of the clay to possible ion-exchanging ions. Comparing the spectra of the washed, Na^+ , Ca^{2+} and Al^{3+} clays (Figures 34-37) it can be seen that at first sight, there appears to be very little difference between them. However, by converting the signal intensity to a relative concentration, of the fluorescing species, some differences can be observed as illustrated in table 4. Using the washed kaolin as the control sample, the sodium kaolin appears to show an increase in the aluminium level by approximately 5 %. This arises as a consequence of the similar values for the aluminium k_{α} and the sodium k_{α} lines (1.48 and 1.07 KeV respectively). The high percentage of aluminium already present results in the sodium peak being unresolvable from the aluminium peak which is manifest as an apparent increase in aluminium concentration. This suggests that by washing the clay with NaCl results in the sodium exchanging at the surface but appearing as an increase in aluminium. The calcium and aluminium forms of kaolin show little difference to the control sample with only a 1 % increase observed in the calcium level for the former and a slight decrease in aluminium concentration for the latter. Coupling these slight changes

observed using XRF with the differences observed in the XRD spectra would indicate that ion-exchange is occurring to some degree.

Scanning Electron Microscopy

SEM micrographs of the washed kaolin samples are shown in Figure 38. The pseudo-hexagonal platelets can be seen quite clearly and show an edge length of approximately $1\mu\text{m}$ and of thickness approximately $0.1\mu\text{m}$. No real physical changes appear to have occurred due to the washing process although on some micrographs some aggregation of particles can be seen. This is not unexpected as the particles could easily have formed aggregates whilst drying at elevated temperatures.

Nitrogen Adsorption (surface area)

The values for the surface area of the washed, Na^+ , Ca^{2+} and Al^{3+} forms of clay are 14.95 (15.08), 8.98 (10.73), 8.48 (7.92) and 8.08 (12.74) respectively, where the figures in parentheses represent a repeat run. The surface area of kaolin has been determined by many workers (e.g. M6) and typical values lie between 8 and $15\text{ m}^2\text{ g}^{-1}$. The values obtained are within this range and suggest that the effect of ion washing is to reduce, slightly, the surface area of the clay from around $15\text{ m}^2\text{ g}^{-1}$ to approximately $9\text{-}10\text{ m}^2\text{ g}^{-1}$. Variations within the washed clays are statistically insignificant. However the exact accuracy to which these values are determined must be questioned as the equipment used recommends that any determination performed below $25\text{ m}^2\text{ g}^{-1}$ should be undertaken using krypton gas, which was not available.

Therefore, although these results are of a typical value compared to those found by other workers the exact accuracy might be questioned. The adsorption-desorption isotherm of kaolin (Figure 16) shows it to be a non-porous solid. Therefore, as with the X-ray results surface adsorption failed to indicate any significant difference between the various forms of washed kaolin.

Electrophoresis

The electrophoretic mobility of the clay particles was determined to investigate the effect of washing on the surface charge of the particle which should in turn be sensitive to the charge on the adsorbed ion (+1, +2 and +3 for sodium, calcium and aluminium respectively). From the results in Figure 39 the zeta potential of the clays show that the surface charge must have been altered and hence the surface of the clays must have been chemically changed. The values for zeta potential at pH 7 are 4.0, 6.1, 5.0 and 5.3 mV respectively for the washed, sodium, calcium and aluminium forms of kaolin. These results are similar to those of the XRF as again there appears to be little difference between the aluminium form of kaolin and the control sample, whilst both the sodium and calcium forms do show marked differences.

4.1.1 Characterisation of North Sea Reservoir Rock Samples

The reservoir rock samples were characterised using the same techniques as for the washed kaolin samples. From the results it can be seen that the reservoir rock consists of a sandstone in which clay particles are interspersed. The typical surface area of the sample being approximately $380 \text{ m}^2 \text{ g}^{-1}$ and containing approximately 2-5 % clay. The clay could not be identified as solely kaolin and was thought to contain some illite. Electrophoresis measurements could not be performed on the core samples as a fine enough dispersion could not be obtained and blocking of the capillary tube took place.

4.2 Adsorption of surfactants at the air/aqueous solution interface.

At surface saturation, the effectiveness of surfactant adsorption can be determined by calculating the surface excess concentration of the surfactant, Γ_D , as this is the maximum adsorption that can be attained (R7). From the data in tables 5 and 11 it can be seen that of the anionic surfactants used at 25°C, 4- ϕ -C₁₂ABS is the most effectively adsorbed at the air/water interface (Γ_D being 2.63 micromoles per litre for 4- ϕ -C₁₂ABS as opposed to 2.04 micromoles per litre for Aerosol OT). This can be attributed to the longer hydrophobic chain of the molecule.

The effect of solubility of the molecules is an important aspect of adsorption at the surface and an increased solubility leads to a lowering of adsorption. This can be seen by comparing the surfactants 4- ϕ -C₁₂ABS and the lignin compounds. It is known that the lignin compounds are highly soluble (up to 100 % w/w)(M9)

whereas the anionic surfactant 4- ϕ -C₁₂ABS has a maximum solubility of approximately 10 g per 100 cm³ where the viscosity of the solution increases. When comparing the adsorption at the air-water interface the surfactant 4- ϕ -C₁₂ABS has a higher adsorption than the lignins and this is primarily due to the difference in solubility.

Effect of NaCl on surfactant adsorption at the air-aqueous interface.

In the presence of NaCl then from the results in tables 5, 11 and 12 it is quite clear that the effectiveness of surfactant adsorption at the air-water interface increases (from 2.63 to 5.01 micromoles per litre for 4- ϕ -C₁₂ABS) in the presence of 0.1 mol dm⁻³ NaCl, and also the area occupied per molecule and the critical micelle concentration, decrease with increasing NaCl concentration.

The increase in surface activity, and decrease in CMC, arise from a reduction in the repulsion between ionic head groups. The Gouy-Chapman Stern model, derived for spherical colloidal particles (O4, W4) represents the electric double layer (edl) at the interface between the ionic head groups and water. The thickness of this layer, $1/\kappa$, can be related to the solution ionic strength by the following equation (A5):

$$\kappa = \left(\frac{2e^2 N_A C Z^2}{\epsilon_r kT} \right)^{1/2}$$

where, $\epsilon_r = (\epsilon/\epsilon_0) =$ the relative static permittivity of the solution.

Using this equation, the effect of adding NaCl, to the aqueous system, on $1/\kappa$ can be evaluated. Figure 88 shows the variation of $1/\kappa$ with added NaCl at 298 K. From Figure 88 it can be seen that compression of the edl occurs due to the presence of the electrolyte, thus, allowing a closer approach of the ionic head groups. As a result of this reduction in electric double layer thickness, increased surface activity and lowering of CMC's are found. In terms of bulk concentrations, the addition of NaCl to the surfactant system improves the effectiveness at which the surface tension is reduced. This can be seen by calculating the amounts of surfactant required to effect the same change in surface tension for an aqueous solution and that containing 0.1 mol dm^{-3} NaCl. Approximately 90 % less surfactant is required for the latter which could be of very beneficial effect for use in an EOR application, where effectively there is a NaCl concentration of 0.3 mol dm^{-3} present (seawater). This improvement in surface tension reduction however, has a limit which is defined by the minimum to which $1/\kappa$ can be reduced. From Figure 88, it can be seen that this minimum is reached at relatively low concentrations of monovalent electrolyte.

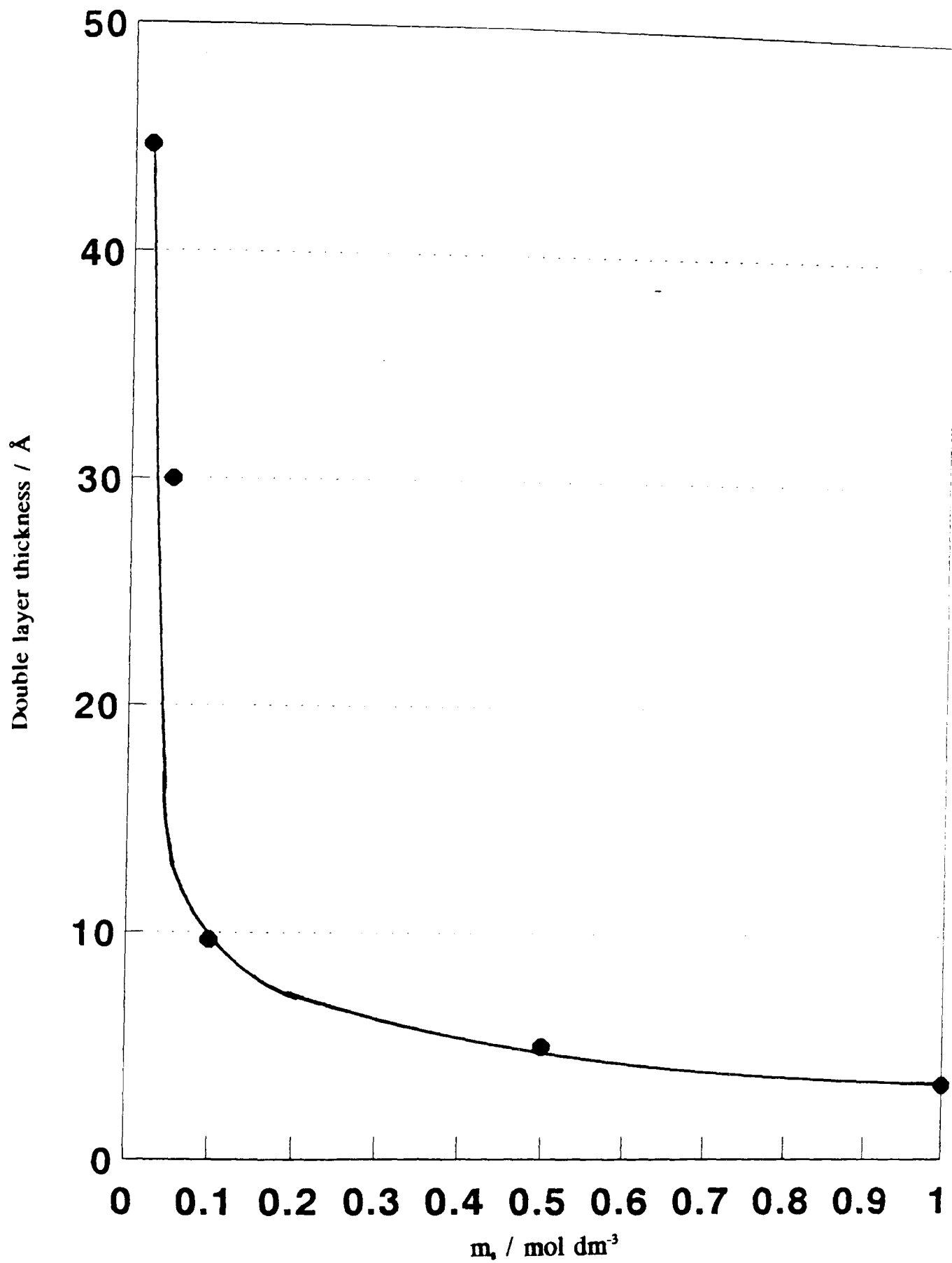


Figure 88. Variation of electric double layer thickness, $1/\kappa$, with concentration of added 1:1 electrolyte, NaCl, at 25°C.

Effect of Formation water on the surfactant adsorption at the air/aqueous interface.

In solutions made from formation water, the only surfactants that could be determined in the presence of such high ionic strength solution were the two lignin samples, Serla-thin and Serla-con, as the other surfactants were found to precipitate. For these surfactants it can be seen that the effect of formation water on the surface tension in the presence of the lignins is to increasingly lower the air/water interfacial tension with increasing bulk concentration of surfactant. However, this lowering of surface tension is not as large as would be expected due to the presence of such high concentrations of metal ions. This is probably due to the ability of these lignins to act as sequestering agents, which effectively soak up large amounts of metal ions, and thus reduce the effect the metal ions will have in reducing the edl of the lignins.

Effect of short chain aliphatic alcohols on the adsorption of surfactants at the air-aqueous interface.

Similarly, from the results in Table 5 and Figures 48 and 49 it can be seen that in the presence of the alcohols reduction in the surface tension again occurs, however, the behaviour is more complex. In the presence of 2% v/v of alcohol the change in surface tension is not as great as that for the 4% v/v solutions. It is noted that in the presence of these alcohols slight changes in critical micelle concentration values also occur. This is due to the fact that whilst alcohol adsorption at the interface is less efficient (M7) than 4- ϕ -C₁₂ABS it does influence the surfactant adsorption through

competitive adsorption. This can be seen more clearly if the values of Γ_D are examined (table 5). From this it can be seen that as alcohol concentration is increased, for any given alcohol, the value of Γ_D falls (from 2.10 to 1.22 micromoles per litre for butan-1-ol). This can be explained via a stepwise process. Consider a solution of 0.1 mol dm^{-3} NaCl, then the initial surface tension will be 72 mN m^{-1} . The addition of alcohol to the solution reduces the surface tension to less than the 72 mN m^{-1} (Figure 48). This lowering of surface tension must be due to alcohol adsorption at the air-water interface. Additions of surfactant to the system will only continue to reduce the surface tension until the CMC is reached. In the presence of alcohols the CMC for the surfactant is lowered and thus, in a similar manner to that for the effect of electrolyte on surfactant behaviour, the maximum reduction of surface tension will be achieved with a lower bulk concentration of surfactant.

A large amount of work has been carried out on the effect of short chain aliphatic alcohols (propan-1-ol to heptan-1-ol) on the properties of surfactants, above the CMC, to determine the role of these alcohols as co-surfactants in microemulsion systems (H10,H11). The alcohols are partitioned between the aqueous phase and the micellar phase and several papers investigating this distribution have been published (A6,S12,R8).

Effect of complexing agents on the adsorption of surfactants at the air-water interface.

The effects of addition of the complexing agents sodium tripolyphosphate and sodium citrate upon surfactant adsorption at the air/water interface have also been investigated and shown in Figure 50 from which it can be seen that there is little difference in the values of surface tension between the control ($0.1 \text{ mol dm}^{-3} \text{ NaCl}$) and those containing the complexing agent. Indeed there is also little or no effect on the CMC in the presence of the complexing agents. This is not unexpected, however, as essentially the complexing agents simply cause an increase in electrolyte concentration, the magnitude being relatively small in comparison to that resulting from the $0.1 \text{ mol dm}^{-3} \text{ NaCl}$ already present. Although other complexing agents were used in this investigation (see section 3.4.5) they were found not to affect surfactant adsorption at the air-kaolin interface and were therefore not investigated for their effect upon surface tension at the air-water interface.

4.3 Surfactant adsorption at the Kaolin/aqueous interface.

The influence of sodium chloride on 4- ϕ - C_{12} ABS surfactant adsorption (figure 51) can be explained by the effect of salt on the electric double layers (edl) of both the surfactant molecules and the charged sites on the kaolin surface. In solution, surfactant-surfactant interactions are enhanced with the addition of monovalent electrolyte, lowering the CMC, thus adsorption equilibria are reached at a lower bulk surfactant concentration, displacing the adsorption plateau to lower equilibria

surfactant concentrations. Similarly, the electrolyte will affect the edl of the charged sites on the solid surface, so reducing the solid-surfactant interactions. The adsorption of the surfactant is therefore controlled by a balance between these forces.

Using the isotherms, and an estimate of the size of the surfactant ion (determined from this work, section 3.3 (33 \AA_2)) the adsorption density of the monolayer can be determined. From the data and adsorption isotherms the average fractional surface coverage, Θ , has been determined. Initial calculations showed that only 10% of the surface was being covered and therefore no monolayer formation was possible. However, these calculations assumed that adsorption occurred on the whole platelet. As the surfactant can only adsorb at the edge of the kaolin platelets and these edge sites are relatively few compared to the total surface (approximately 10 %) then it is possible that monolayer coverage of the edge sites may be possible.

To determine how much of the edge surface had actually been covered the following calculation was performed.

Using the approximate measurements from the SEM data the surface area of the edge sites can be calculated as thus :

$$\begin{aligned}\text{Surface area of edge sites} &= 6 \times (1 \times 10^6) \times (0.1 \times 10^6) \\ &= 6 \times 10^{13} \text{ m}^2 \text{ per platelet.}\end{aligned}$$

The area for the face sites can be determined using simple trigonometry to give :

$$\begin{aligned}\text{Face area} &= 2 \times (2.595 \times 10^{-12}) \\ &= 5.19 \times 10^{-12} \text{ m}^2 \text{ per platelet}\end{aligned}$$

This gives a face to edge ratio of 8.65 : 1.

Therefore, as the surface area of washed kaolin is $14.95 \text{ m}^2 \text{ g}^{-1}$ only $1.55 \text{ m}^2 \text{ g}^{-1}$ is available to the surfactant.

$$\begin{aligned}\text{Therefore the number of clay particles per gram} &= 14.95 / (5.19 \times 10^{-12} + 6 \times 10^{-13}) \\ &= 2.58 \times 10^{12}\end{aligned}$$

hence in 5g of clay there are 1.29×10^{13} platelets.

As there is $6 \times 10^{-13} \text{ m}^2$ of edge surface area available from each platelet, then the total surface available to the surfactant in 5 g of clay is

$$\begin{aligned}&= (1.29 \times 10^{13}) \times (6 \times 10^{-13}) \\ &= 7.74 \text{ m}^2\end{aligned}$$

At the CMC, approximately $8 \times 10^{-6} \text{ mol}$ per gram of clay are adsorbed. Therefore, in 5 g of clay $40 \times 10^{-6} \text{ mol}$ are adsorbed.

$$\begin{aligned}\text{The number of surfactant molecules adsorbed} &= 40 \times 10^{-6} \times N_A \\ &= 2.41 \times 10^{19}\end{aligned}$$

$$\text{Area occupied by a surfactant ion} = 33.00 \text{ \AA}^2$$

$$\begin{aligned}\text{Therefore the edge site area occupied} &= (33 \times 10^{-20}) \times (2.41 \times 10^{19}) \\ &= 7.95 \text{ m}^2\end{aligned}$$

It can be seen that this figure and that for the area available to the surfactant are, within error, very close. This would indicate that monolayer coverage of the edge

sites is occurring and classic Langmuir theory is being obeyed. It has previously been proposed (M8) that hemimicelles are formed on the clay surface, however, this work does not appear to support this theory.

If we look at the adsorption regions of the isotherms (figure 51) we can see that in region I surfactant adsorption is occurring until a monolayer is reached, region II. However, the adsorption mechanisms for these two regions differ. In region I adsorption occurs due to the electrostatic interactions between the positive edge surface charge and the negative ionic head group of the 4- ϕ -C₁₂ABS surfactant molecule and hence this implies that adsorption is very dependent upon surface charge. In region II, a plateau of adsorption is reached, occurring at concentrations, at, and above the CMC. Second layer adsorption through cohesive chain interactions then becomes significant. As only monomer is adsorbed (C6) and using the phase separation model of micellisation, which states that above the CMC the monomer concentration is constant, then it is understood why little or no change in adsorption is observed over this region. In region III it can be seen that surfactant adsorption is reduced. This phenomena has been observed by other workers (S13,H7), however, only Scamehorne et al (S13) have made any attempt to interpret this effect. From this work it would appear that this decrease in adsorption is due to an increase in the concentration of micelles in solution which pull aluminium ions from the surface of the clay into solution (see section 3.4). These Al³⁺ ions will be bound to the surfactants ions that have been adsorbed at the surface. These complexes can then be solubilised by the micelles in solution resulting in an effective decrease in surfactant adsorption.

4.3.1 Effect of short chain aliphatic alcohols on the adsorption of 4- ϕ -C₁₂ABS at the kaolin/aqueous interface.

The results of section 3.4.3 (figures 52 and 53) show the effect of adding short chain aliphatic alcohols, on the adsorption to the kaolin surface, of 4- ϕ -C₁₂ABS. All the alcohols show similar isotherms as would be expected. However, butan-1-ol was found to be the most efficient in reducing surfactant adsorption. It is known that butan-1-ol adsorbs directly to the kaolin surface (J4) and the reduced surfactant adsorption may simply be due to the lower number of adsorption sites available to the surfactant. At higher concentrations of surfactant it can be seen that the reduction in surfactant adsorption observed with surfactant alone is no longer observed in the presence of alcohols. This may be attributed to interactions between the surfactant and the alcohol at the kaolin surface and in solution which prevents the solubilisation of the aluminium-surfactant complexes by the micelles.

4.3.2 Effect of complexing agents on the adsorption of 4- ϕ -C₁₂ABS at the kaolin/aqueous interface.

As adsorption or loss of surfactant occurs through interaction with the aluminium in the solid surface it was thought that by complexing these sites with specific agents a reduction in adsorption of surfactant may be seen.

Several complexing agents were used (see section 3.4.5) and of these only sodium tripolyphosphate and sodium citrate were found to reduce surfactant adsorption to

any degree.

The effectiveness of sodium tripolyphosphate only occurs at pH values that are greater than 9 and at such high pH values surfactant adsorption is known to be reduced (J4). However, by comparing the effect of sodium tripolyphosphate on the surfactant adsorption at pH 10 to the adsorption of surfactant alone at pH 10 it can be seen that a further reduction in adsorption is seen. It is known that reservoirs containing clays act as buffers and maintain a constant pH, usually between pH 4 and pH 7 (O2), hence making solutions of sodium tripolyphosphate ineffectual. Sodium citrate, on the other hand, was found to reduce surfactant adsorption at the lower value of pH 7 and as such could be used in a real reservoir situation.

The reduction in adsorption in the presence of complexing agents can partially be explained by an increase in electrolyte concentration. However, if an adsorption isotherm is performed with the same amount of NaCl (replacing the complexing agent with NaCl) the reduction is not as great and hence the complexing agents must be interacting in some way so as to reduce the adsorption. This was investigated by looking at the adsorption of complexing agents alone (see sections 3.4.7 and 3.4.8). It can be seen that both sodium tripolyphosphate and sodium citrate adsorb at the kaolin surface although not to any great extent.

Therefore, it would appear that a combination of interaction with aluminum in the solid surface and a slightly increased electrolyte concentration reduce the adsorption of 4- ϕ -C₁₂ABS in the presence of complexing agents.

4.3.3 Effect of temperature on the adsorption of 4- ϕ -C₁₂ABS onto kaolin.

Figure 54 shows the results obtained for the adsorption of 4- ϕ -C₁₂ABS in the presence of 0.1 mol dm⁻³ NaCl at different temperatures (25 and 60°C).

It can be seen that as temperature is increased a reduction in the adsorption of surfactant is observed. This can be explained by the effect of temperature on CMC. It is known that an increase in temperature reduces the CMC (S2) and thus the plateau region of the isotherm (region II, section 3.4.4) is reached earlier than that of an isotherm at lower temperature.

4.3.4 Effect of ion washed clays on 4- ϕ -C₁₂ABS adsorption at the solid/aqueous interface.

It can be seen from section 3.5 that using the ion washed systems caused massive losses of surfactant to be observed, whether in the presence or absence of either alcohol or complexing agent.

This was thought to be caused by ion exchange to the aqueous solution from the clay surface leading to a very high concentration of electrolyte ions in solution which then precipitated the surfactant. As the clay is washed to constant conductivity it is difficult to understand exactly why this should occur. One explanation for this is that the surfactant pulls the ions from the surface and is precipitated. In the water washed clay the number of metal ions sites at the surface are limited as no exchange for the -Al-O-(H) bond (where H is the exchangeable ion) has taken place. The surfactant micelles are then able to resolubilise the precipitated complex of Al(DBS)₃.

However, in a metal ion washed clay the surfactant molecules can continue to be precipitated until no more surfactant is available. Precipitation must account for the loss of surfactant to a large degree in the presence of the ion washed clays. Leaching experiments were carried out to investigate if sufficient concentrations of metal ion could be released by the clays over a 24 hour period so as to cause precipitation.

4.3.5 Leaching of metal ions from kaolin

It is known that when washed kaolin leaches aluminium ions (H9). As large quantities of surfactant have been lost to metal ion clays (figures 60 & 61) then an experiment was devised to see if sufficient quantities of metal ions are leached such that would cause precipitation. After soaking the clays for 24 hours in 0.1 mol dm^{-3} NaCl solution, the supernatant liquor was obtained by centrifugation and analysed by Atomic Absorption Spectroscopy (AAS) for Al^{3+} and Ca^{2+} . The solid was then washed again for a further 24 hours. This was repeated for four successive washes. It can be seen from figures 70-73 that for both the aluminium and calcium forms of clay metal ions are released. As expected the aluminium form of kaolin released more aluminium ions than calcium ions and vice versa for the calcium form of kaolin. These results show that although the clays were washed to constant conductivity they release large quantities of metal ions when in contact with aqueous solution for 24 hours. This would account for the large losses of surfactant observed with metal ion washed clays.

4.3.6 Effect of Formation water on the adsorption of 4- ϕ -C₁₂ABS at the kaolin/aqueous interface.

The three formation waters used in this work cover the various concentrations of formation waters found in the North Sea (R6,G5). It can be seen from table 9 that these waters are of an extremely high metal ion concentration. It was, therefore, not unexpected that the observed "adsorption" increase with these waters was of the order of 1000% higher than seen for the adsorption of kaolin from 0.1 mol dm⁻³ NaCl solution. This huge increase was, therefore, thought to be due to precipitation of the 4- ϕ -C₁₂ABS by the metal ions present. This was tested by placing a quantity of surfactant solution into the formation water. Immediately, the solution became turbid and white precipitate could be observed. As the surfactant would ultimately come into contact with such solutions within the North Sea then the use of the surfactant 4- ϕ -C₁₂ABS as a method for oil recovery must be questioned. This is not to say that 4- ϕ -C₁₂ABS cannot be used in oil recovery processes as some inland wells, especially those in the middle east, have formation waters of very low metal ion concentration which would allow the use of this surfactant.

A mechanism by which this surfactant could be used in the North Sea would be to flush the well with distilled water prior to injection of the surfactant slug to remove such waters and high metal ion concentrations. However, economically this would not be viable, and there is also some question as to the swelling of clay particles that would trap the oil by pore blocking in the reservoir rock samples (D3).

4.4 Surfactant adsorption at the core sample/aqueous interface.

Core samples obtained from Shell Expro Ltd, were used in similar experiments to the kaolin samples to determine whether a realistic comparison could be made with the adsorption experiments onto kaolin. The core samples were characterised in a similar manner to the kaolin samples (see section 3.2) and were found to consist of sandstone interspersed with varying amounts of clay (2-5%, as determined by XRD). Adsorption isotherms for three core samples were determined for the adsorption of 4- ϕ -C₁₂ABS (figure 63). It can be seen that although the adsorption is lower than that for kaolin it is not sufficiently low to be due to the 2-5% of clay alone. Therefore, the surfactant may be lost by other mechanisms i.e. precipitation due to leaching of metal ions from the core sample (see section 3.7.6) or adsorption onto the sandstone. However, it is known that sandstone adsorbs far less than kaolin (approximately 1000 times less (M4)). Alternatively, the clay within the core may not be solely kaolin. Comparing spectra of clays shows that illites have a very similar spectra to kaolinites and would be indistinguishable using the XRD technique to determine the amount of clay in the solid. This implies that the increase in adsorption from that expected could be due to the presence of illite clays which are known to adsorb more effectively than kaolin.

4.4.1 Effect of complexing agents on the adsorption of commercial SDBS at the core/aqueous interface.

For economic reasons a commercial surfactant would be used in a real reservoir. To investigate how this differs from the isomerically pure 4- ϕ -C₁₂ABS the adsorption of commercial SDBS was determined (figure 78). The effect of sodium tripolyphosphate was then determined (figure 79). It can be seen that the adsorption of commercial SDBS at pH 10 is similar to that on kaolin at pH 6.3, however, in the presence of sodium tripolyphosphate the adsorption of SDBS is seen to decrease. The reasons for this decrease will be the same as those given in section 4.3.2 for the adsorption of 4- ϕ -C₁₂ABS in the presence of complexing agents.

4.5 Mixed and other surfactant systems.

4.5.1 The effect of a mixed anionic/nonionic surfactant system on the adsorption of 4- ϕ -C₁₂ABS at the kaolin/aqueous interface.

The adsorption of 4- ϕ -C₁₂ABS in the presence of another surfactant was investigated as often a mixture of surfactants leads to micelles having properties consistent to both the surfactants. An anionic/nonionic system was used based upon 4- ϕ -C₁₂ABS and Synperonic N (a nonylphenylethoxylate). The Synperonic N was used at a concentration of 0.54% w/w as above this concentration it was found to interfere with the determination of 4- ϕ -C₁₂ABS by titration. From figure 74 it can be seen that the inclusion of a nonionic surfactant increases the loss of 4- ϕ -C₁₂ABS at high

concentrations. This could be due to a similar reason that the reduction in adsorption is not seen in the presence of alcohols (see section 4.3.1) as interactions between the anionic and nonionic surfactants prevent the solubilisation of surfactant-metal complexes.

4.5.2 Adsorption of Aerosol OT at the kaolin/aqueous interface.

This anionic surfactant was chosen as it is known to reduce interfacial tension to ultralow values (R2). This could be very useful in minimising the interfacial tension between oil and water in an EOR application. Adsorption isotherms for AOT (sodium diethylhexylsulpho-succinate) were determined (figure 76) and it can be seen that the amounts of AOT lost from solution are far higher than that for 4- ϕ -C₁₂ABS.

4.5.3 Adsorption of lignin sulphonates at the kaolin/aqueous interface.

This surfactant was chosen as it is known to be very resistant to precipitation in solutions of high electrolyte concentration (M9). This would prove particularly useful if the reservoir contains formation water of high concentrations of salts. Initially, isotherms were determined for both lignins at several pH's (figure 84). Comparing these to 4- ϕ -C₁₂ABS (figure 51) it can be seen that at their operating pH's the lignins adsorb up to 7 times as much as the 4- ϕ -C₁₂ABS. However, when the lignin surfactants were placed in formation water B (see table 9) no precipitation was observed as with 4- ϕ -C₁₂ABS (see section 4.3.6). When the isotherm of the lignins was determined in formation water only a slight increase in loss was observed

compared to that in distilled water and calculating the maximum loss this left approximately 98 % of the surfactant in solution, compared to approximately only 80% of 4- ϕ -C₁₂ABS left in 0.1 mol dm⁻³ NaCl solution. This ability to sequester substantial quantities of metal ions is probably due to the chemical composition of the Serla products which contain purified sulphonated lignins as a backbone onto which are grafted several organic monomers. The Serla-Thin compound is known to contain phenolic, carboxylic and sulphonate groups (S14).

This high electrolyte tolerance of the lignin compounds has already been used in the oil industry as a filtration control polymer to a variety of base drilling fluids (C3) and shows great potential for use as a surfactant in the recovery of oil in the North Sea. These compounds are also known to be tolerant to sustained temperatures of above 300°C (A4).

Due to the lack of micelles being present and the reduction in surface tension by the lignins not being as effective as that for the 4- ϕ -C₁₂ABS then the ability to remove oil in an enhanced oil recovery project will not be as great. However, the formation of micelles may be possible at higher concentrations.

4.6 Determination of counter-ion concentration

The determination of micellar counter-ion concentration for aluminium with commercial SDBS samples, and calcium with 4- ϕ -C₁₂ABS has been undertaken and the results are given in section 3.10. The determination with aluminium was based upon the concentrations of leached metal ions as determined by atomic absorption spectroscopy. The counter-ion concentration for calcium was determined using an

ion-selective electrode. In recent years both surfactant selective and counter-ion selective electrodes have been used extensively to study a variety of equilibria including ionic surfactants (C7,H12,P7). This work was aimed at determining the calcium counter-ion concentration so that the micellar system, that could be used in a reservoir, is understood when in contact with metal ion solutions. The calcium electrode used was a commercial electrode supplied by Orion and was used in conjunction with a double junction reference electrode. Llenado (L3) noted that in the presence of surfactant a commercial calcium ion electrode showed a sudden e.m.f. shift in the negative direction followed by a drift back to the initial e.m.f. value. This was found to be due to interactions at the electrode surface between the di(4-octylphenyl)phosphate sensor compounds within the PVC membrane matrix and the surfactant present in solution (C8). Surfactant resistant calcium electrodes have been developed (C9) and were initially tested. However it was found that no repeatable results could be obtained with the recipes used and therefore the commercial electrode was used. It was noted that the only difference in the recipes of the membranes between the surfactant resistant electrode and the commercial electrode was the incorporation of decanol.

4.6.1 Aluminium counter-ion concentration determination by AAS

The determination of aluminium counter-ions arose as part of a leaching experiment using commercial SDBS to ascertain how this affected the leaching from kaolin into solution (H9). However, by taking the results the concentration of micelles can be calculated using the following equation :

$$C_m = \frac{C - C_{CMC}}{A_n}$$

The aggregation number was taken as being that proposed by Zana (Z1) of 81 +/- 8.

The aluminium in solution was known from the leaching experiment. It can be seen that from figure 89 that before the CMC the aluminium concentration is constant. If we assume that this concentration of aluminium remains in solution at all times then only the aluminium which is leached above the CMC will be taken up as counter-ions. A graph of calculated Al³⁺ counter-ions against micelle concentration can be determined and is shown in Figure 90. From this graph it can be seen that the maximum number of aluminium counter-ions for SDBS in 0.1 mol dm⁻³ NaCl is approximately 29. This is not an unreasonable answer and within experimental error would agree with the aggregation number observed by Zana.

4.6.2 Determination of calcium counter-ions with 4- ϕ -C₁₂ABS by ISE.

It can be seen from Figure 32 that the calibration of the electrode for determination of calcium is linear over a wide concentration range. The addition of NaCl to the solutions showed a lowering in potential of the solutions especially at low concentrations of calcium. The addition of surfactant to the solutions is known to be detrimental to the life of the electrode (L3). This is due to adsorption of the

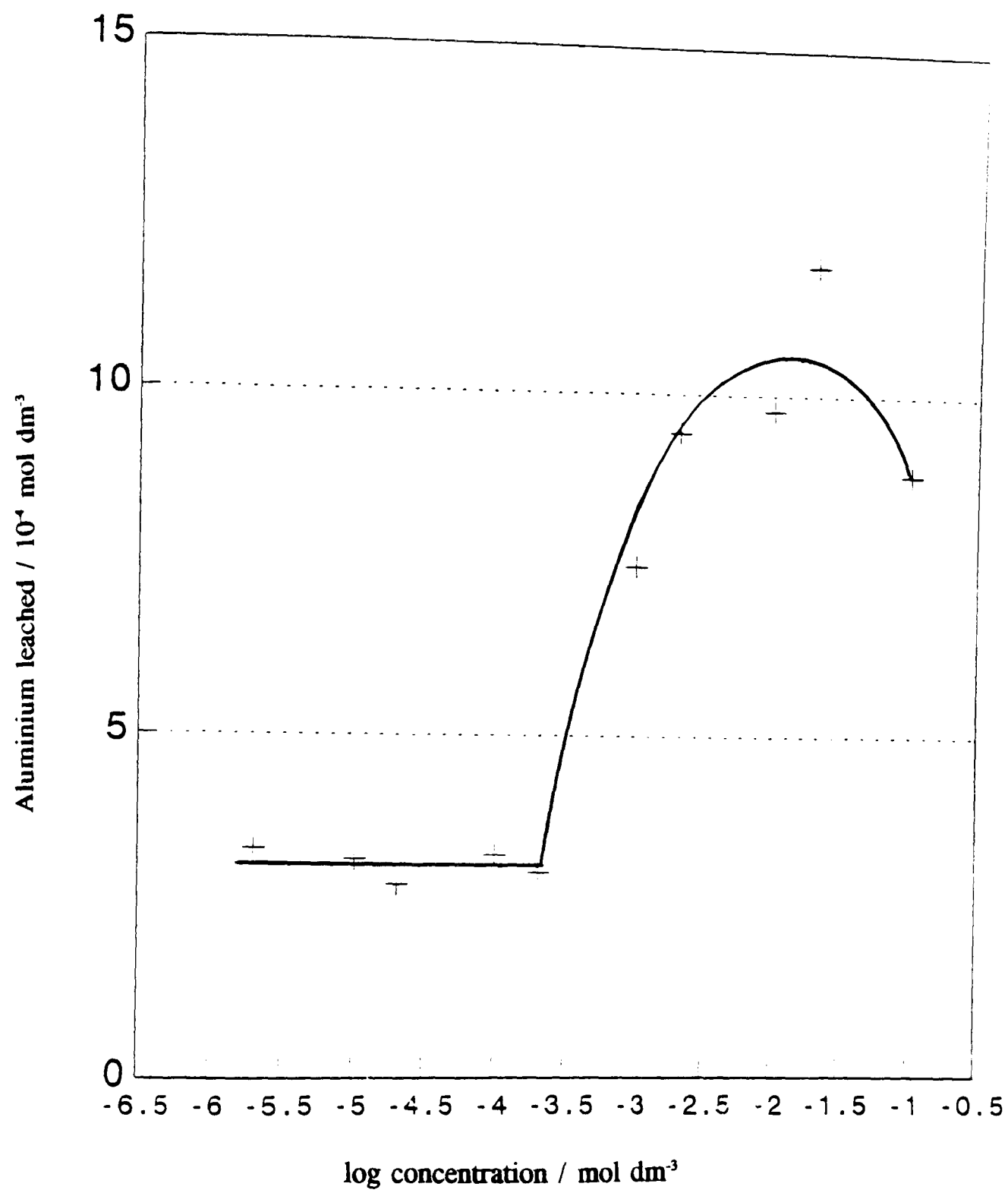


Figure 89. Leaching of aluminium ions in the presence of commercial SDBS surfactant.

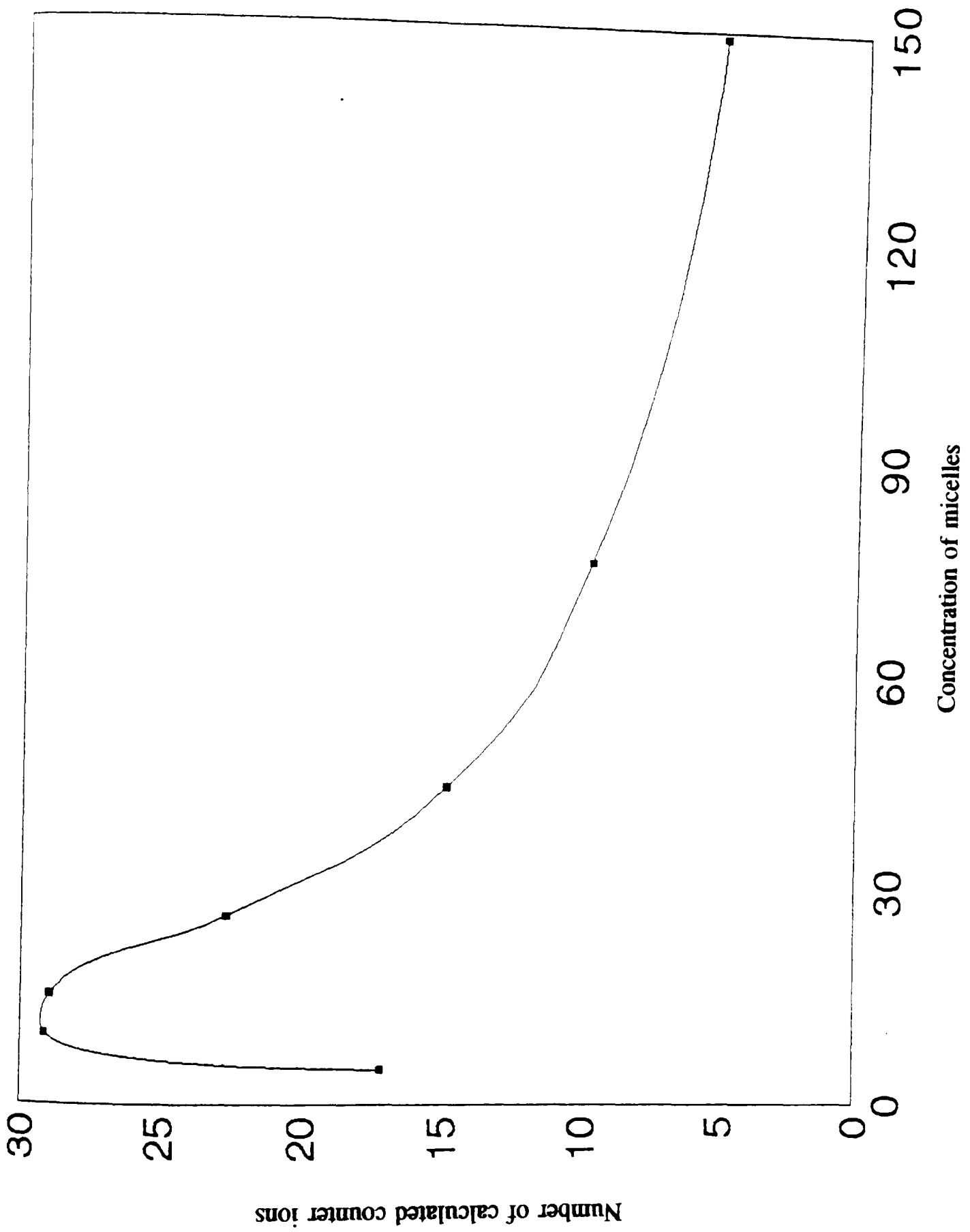


Figure 90. Calculated aluminium micelle counter ions

surfactant on to the sensor-compound sites within the PVC membrane thus reducing the number of sites and hence the accuracy. The equilibration time, therefore, was very important as prolonged exposure to the surfactant solutions would be both harmful to the electrode and the accuracy of the results obtained. It was, therefore, important that after each contact with a surfactant solution the electrode was immediately placed in a standard calcium solution of concentration $1 \times 10^{-2} \text{ mol dm}^{-3}$. This kept the equilibration times to about 90 - 120 seconds. When the equilibration times became longer and the calibration graph had a slope of less than 24 then the electrode tip was replaced and recalibrated.

From the results in Figure 87 the micellar counter-ion concentration can be determined by measuring the emf difference between the calcium surfactant solutions and the surfactant solution alone. This difference equates to the free calcium ions in solution. Knowing the concentration of micelles and the concentration of calcium ions that have been taken up by the micelles then the counter-ion concentration can be determined. The number of calcium counter-ions determined by this method is 46 which gives a micelle of aggregation number 81 a nett charge of $11+$. This value of counter-ions would appear to be a little high and this is probably due to the nature of the surfactant / di(4-octylphenyl)phosphate interactions at the electrode surface which block the sensor sites causing the electrode to detect a lower calcium concentration to be observed than is present. Therefore, the number of calcium ions taken up by the micelles appears greater than it should. However, the values of aggregation number proposed by Zana (Z1) and those for calcium ions found in this work are not too dissimilar and the use of such electrodes to determine the counter-ion concentration of micelles should be further investigated.

Conclusions

CONCLUSIONS

This project has been concerned with the application of surfactants in enhanced oil recovery and as such has investigated the conditions under which surfactant loss from the flood could be minimised whilst simultaneously reducing the surface tension at the oil-water interface to assist release of trapped oil ganglions.

The main surfactant used was isomerically pure 4- ϕ -C₁₂ABS, although other surfactants were tried in conditions under which this was inappropriate, and the adsorbent was either kaolin or ion-exchanged kaolins.

Kaolin particles are hexagonal with an edge length of 1 μm and a depth of 0.1 μm . The hexagonal face is negatively charged whilst the edge is positively charged. The adsorption isotherms for 4- ϕ -C₁₂ABS in aqueous solution on kaolin show a rapid rise region, followed by a plateau which coincides with the formation of micelles in solution, and finally a decrease in loss of surfactant from solution. The mechanism of the interaction of 4- ϕ -C₁₂ABS with kaolin appears to involve several distinct stages. At low concentrations of surfactant, $< 1 \times 10^{-4} \text{ mol dm}^{-3}$, adsorption occurs on the kaolin surface such that a monolayer is attained. At higher concentrations (i.e. above the critical micelle concentration) the adsorption reaches a plateau due to only monomer being able to adsorb to the surface. Above the cmc, the monomer concentration, given by the pseudo-phase separation model of the micellisation, is constant. Above surfactant concentrations of approximately $1 \times 10^{-2} \text{ mol dm}^{-3}$ the adsorption on the surface is seen to decrease. This is due to the resolubilisation of the

aluminium-surfactant complex formed on the kaolin surface due to the presence of excess surfactant. Supplementary light scattering studies of the reaction between Al^{3+} ions and 4- ϕ - C_{12}ABS in aqueous solution suggest that several complexes are formed depending upon the surfactant concentration. At low surfactant concentrations the complex is soluble, at intermediate concentrations it is insoluble whilst at high concentration the complex again becomes soluble. Thus the anomalous apparent reduction in the adsorption of surfactant can be attributed to the re-dissolution of precipitated aluminium-surfactant complex.

Adsorbate/adsorbent interactions appear to only involve interaction of 4- ϕ - C_{12}ABS with aluminium sites on the positively charged edge of the particle and calculations based on this hypothesis show that monolayer coverage of these sites is attained which is not the conclusion reached by other workers who considered adsorption over the whole of the particle (ie. including the negatively charged hexagonal face).

In the presence of relatively low concentrations of added electrolyte (0.1 mol dm^{-3}) the adsorption isotherm retains the same overall form, however, the adsorption maximum is (i) increased by a factor of about two with a corresponding reduction in the area occupied by the surfactant molecule again by a factor of about two, as a result of compaction of the edl due to the increased ionic-strength of the solvent and (ii) moves to lower concentration again due to the effect of ionic strength on the CMC which is reduced from about 1 to 0.1 mmol dm^{-3} . Increase in pH of the solution also results in increased adsorption.

The basic mechanism for the interaction of 4- ϕ -C₁₂ABS with kaolin is supported by the experiments involving surfactant/alcohol mixtures. In the presence of both propanol and butanol the surface tension at the air-water interface is lowered, however, this does not result in an increase in the adsorption of 4- ϕ -C₁₂ABS due to competition for adsorption sites between the alcohol and surfactant thus the plateau region is lowered. Furthermore at high surfactant concentrations the isotherm no longer shows the characteristic downturn observed in purely aqueous solution. This can be rationalized with the mechanism proposed earlier if it is assumed that the redissolution of precipitated aluminium-surfactant complex involves electrostatic interactions between the micelle and the complex since addition of short chain alcohols to surfactant solutions is known to reduce the aggregation number and hence the overall charge on the micelle. From the point of view of oil recovery, addition of small amounts (~10%) of propanol or butanol to surfactant solutions enhance their effectiveness since they simultaneously reduce both the surface tension and the loss from solution.

In any real situation the clay will be in intimate contact with formation water which contains high concentrations of Na⁺, Ca²⁺ and Al³⁺ therefore it seems reasonable to assume that ion exchange will take place between these ions and exposed ions in the surface of the clay. Attempts to prove this using physical methods, XRD, XRF, scanning electron microscopy and N₂ BET adsorption isotherms were relatively unsuccessful and showed only small differences when compared with the unmodified kaolin. Electrophoretic studies of the ion washed clays showed that the zeta potential was changed on washing the effect following the order washed clay ~ Al³⁺ < Ca²⁺

$< \text{Na}^{2+}$. This suggests that the predominant exchange is primarily with Al^{3+} in the surface of the kaolin although the fact that washing with Al^{3+} also changes the zeta potential indicates that other mechanisms of exchange are also present. In all cases contact between the clay and water resulted in leaching of metal ions from the clay surface which in turn can react with surfactant thus lowering its effectiveness as a surface tension lowering agent.

To counteract this effect low-cost sequestering agents were added to the solution. Of the three, sodium pyrophosphate, sodium tripolyphosphate and citric acid, each resulted in a significant decrease in the adsorption of $4\text{-}\phi\text{-C}_{12}\text{ABS}$, with optimum concentrations of $\text{pM}_{\text{pyrophosphate}} = \text{pM}_{\text{polyphosphate}}$ of 2.5 and $\text{pM}_{\text{citrate}}$ of 1.5. Under these conditions the reduction in loss of surfactant was by a factor of between two and three. However, in the case of the phosphate derivatives, the conditions in which it was most effective were such as to be impractical in a real situation.

Under the conditions found in North Sea oil wells (formation water) the loss of $4\text{-}\phi\text{-C}_{12}\text{ABS}$ from solution was found to be extremely high due to precipitation from solution to the extent that, without pre-flushing to reduce the ionic strength, the surfactant would be completely ineffective and alternative surfactants were investigated. Of these only lignin sulphonates were found to be stable under the extremely high ionic strength of formation water and adsorption onto kaolin was low. No evidence was found for the formation of micelles in these systems at concentrations up to 20 g per 100 cm^3 and their efficiency at reducing surface tension was less than that of $4\text{-}\phi\text{-C}_{12}\text{ABS}$.

In summary, loss of anionic surfactant from enhanced oil recovery flood solutions can be minimised by adjusting the following parameters:

- a) ionic strength
- b) alcohol addition
- c) sacrificial complexing agent addition
- d) solution pH

This statement is only applicable in such reservoirs where the formation waters are of such electrolyte concentrations that will not cause the surfactant to be precipitated. Ideally these will be inland wells such as those found in the middle east where formation waters are known to be of very low electrolyte concentration.

Surfactant loss is reduced at high surfactant concentrations due to re-dissolution of adsorbed aluminium-surfactant species.

Surfactant loss of lignin sulphonates in the presence of formation water is relatively low allowing the surfactant to reduce the interfacial tension between oil and water, although not as effectively as the alkylbenzenesulphonate type surfactants.

As lignin sulphonate is a by-product of paper manufacture, it is extremely inexpensive and as such could be used in very high concentrations.

Lignins are also an environmentally friendly product which must be an extremely important consideration in any chemical process.

References

References

- A1 Aveyard, R. and Haydon, D.A.,
"An Introduction to the Principles of Surface Chemistry",
Cambridge University Press, (1973).
- A2 Anacker, E.W.,
"Cationic Surfactants", (E. Jungerman, Ed.),
Marcel Decker Inc., New York, p.203, (1970).
- A3 Anton, A.
Anal. Chem., 32, 725, (1960).
- A4 Abdon, J.C., Jackson, B.L., and McClelland, G.S.,
"The Development of a Deflocculated Polymer Mud for HTHP Drilling"
SPE paper presented at the SPE Middle East Oil Technical Conference,
Bahrain, 11-14 March, (1989).
- A5 Adamson A.W.,
"Physical Chemistry of Surfaces", 34th Ed.,
Wiley Interscience, New York, p.115, (1976).
- A6 Abuim, E.P., and Lissi, E.A.,
J. Colloid Interface Sci., 95, 198, (1983).

- B1 Beeson, D.M., and Ortloff, G.D.,
"Laboratory Investigation of the Water Driven Carbon Dioxide
Process for Oil Recovery",
Trans. AIME, 216, 388-391, (1959).
- B2 Butler, J.A.V.,
"Chemical Thermodynamics",
Macmillan, p.553, (1960).
- B3 Balambra, R.R., Clumie, J.S., Corkill, J.M., and Goodman, J.F.,
Trans. Faraday Soc., 58, 1661-7, (1962).
- B4 Balambra, R.R., Clumie, J.S., Corkill, J.M., and Goodman, J.F.,
Trans. Faraday Soc., 60 (497), 978-85, (1964).
- B5 Bansal, V.K., and Shah, D.O.,
in "Microemulsions", (L.M. Prince, Ed.),
Academic Press, New York, London, pp.149-173, (1977).
- B6 Banwell, C.N.,
"Fundamentals of Molecular Spectroscopy", 2nd Ed.,
McGraw-Hill, (1972).

- B7 Bazin, B., and Dafives, D.,
Inst. Fr. Petr., **42**, 537, (1985).
- C1 Cross, A.,
PhD. Thesis, Liverpool Polytechnic, (1987).
- C2 Chapman, D.L.,
Philos. Mag., **25**, 475, (1913).
- C3 Clements, W.R., Jarrett, M.A., and Morton, E.K.,
"A New Class of Filtration Control Polymers Offer Exceptional
Electrolyte Tolerance."
SPE paper presented at the 62nd Annual Technical Conference of
the SPE in Dallas, Tx, September 27-30, (1987).
- C4 Craggs, A., Moody, G.J., and Thomas, J.D.R.,
Analyst, **104**, 961-972, (1979).
- C5 Craggs, A., Moody, G.J., and Thomas, J.D.R.,
Analyst, **105**, 426-431, (1980).
- C6 Cases, J.M., Goujon, G., and Smani, S.,
AIChE Symp. Ser., **71**, 100, (1975).

- C7 Carlsson, A., Lindman, B., Watanabe, T., and Shirahama, K.,
Langmuir, **5**, 1250, (1989).
- C8 Craggs, A., Moody, G.J., and Thomas, J.D.R.,
Analyst, **104**, 412-418, (1979).
- C9 Craggs, A.,
PhD. Thesis, University of Wales, p.174, (1979).
- D1 Dukhin, S.S., and Deryaguin, B.V.,
in "Surface and Colloid Science", (E. Matejevic, Ed.),
John Wiley, New York, **7**, 52, (1986).
- D2 Doe, P.H., El-Emary, M., Wade, W.H., and Schechter, R.S.,
J.Amer.Oil Chem.Soc., **54**, 570, (1977).
- D3 Delville, A.,
Langmuir, **8**, 1796-1805, (1992).
- E1 Elsworth, P.H., and Mysels, K.J.,
J. Colloid Interface Sci., **21**, 132, (1966).

- E2 Elsen, J.M., Mixon (III), A.M., and Broussard, M.D.,
"Application of a Lime-Based Drilling Fluid in a High Temperature/
High Pressure Environment".
SPE Drilling Engineering, March, (1991).
- F1 Fisher, L.R., and Oakenfull, D.G.,
"Micelles in Aqueous Solution",
Chem.Soc.Revs., **6**, 25-42, (1977).
- F2 Flegman, A.W., Goodwin, J.W. and Ottewill, R.H.,
Proc.Brit.Ceram.Soc., **13**, 31, (1969).
- G1 Gogarty, W.B.,
J.Pet.Technol., **35**, 1168, (1983).
- G2 Gregg, S.J., and Sing, K.S.W.,
"Adsorption, Surface Area and Porosity.",
Academic Press, p.22, (1983).
- G3 Gratzel, M., and Thomas, J.K.,
Mod.Fluores.Spectrosc., **2**, 169, (1976).
- G4 Gouy, G.,
J.Phys.Chem., **9**, 457, (1910).

- G5 Gilje, E., Kristensen, R., Maldal, T., and Vikane, O.,
Paper presented at the 6th European IOR Symposium in Stavanger,
Norway, May 21-23, (1991).
- G6 Guggenheim, E.A.,
Trans.Faraday Soc., 36, 407, (1940).
- H1 Hicock, C.W., Christensen, R.J., and Ramsay, H.J.,
"Progress Review of the K and S Carbonated Waterflood Project",
J.Pet.Tech., 20-24, Dec (1964).
- H2 Healy, R.N., Reed, R.L., and Carpenter, C.W.,
Soc.Pet.Eng.J., 15, 87-103, (1975).
- H3 Haydon, D.A., and Philips, J.N.,
Trans.Faraday Soc., 54, 698, (1958).
- H4 Hall, D.G., and Pethica, B.A.,
"Thermodynamics of Micelle Formation", in Non-ionic Surfactants,
(M.J. Schick, Ed.), Arnold, pp.516-577, (1967).
- H5 Haydon, D.A.,
in "Recent Progress in Surface Science", (J.F. Danielli, K.G.A. Parkhurst,
and A.C. Riddiford, Eds.), Vol.1, Academic Press, London, p.100, (1964).

- H6 Hunter, R.J.,
in "Zeta Potential in Colloid Science", (R.H. Ottewill and
R.L. Rowell, Eds.), Academic Press, London, p.75, (1981).
- H7 Hanna, M.S., and Somasundaran, P.,
J.Colloid Interface Sci., **70** (1), 181, (1979).
- H8 Healy, T.W., and White, L.R.,
Adv.Colloid Interface Sci., **9**, 303, (1978).
- H9 Hayes, S.,
Project Report, Liverpool Polytechnic, (1990).
- H10 Høiland, H., Ljosland, E., and Backlund, S.,
J.Colloid Interface Sci., **101**, 476, (1984).
- H11 Hyase, K., Hayano, S., and Tsubuta, H.,
J.Colloid Interface Sci., **101**, 336, (1984).
- H12 Hoffman, H., and Huber, G.,
Colloids Surf., **40**, 181, (1989).
- J1 Jones, E., and Barry, C.R.,
Phil.Mag., **4**, 841, (1927).

- J2 Jayson, G.G., and Cross, A.W.,
J. Colloid Interface Sci., **162**, 45-51, (1994).
- J3 Johnson, V.J.,
"A compendium of the properties of Materials at low temperatures (Phase I)"
WADD Technical Report, 56-60, October, (1960).
- J4 Jayson, G.G., McKeown, I.P., and Morris, H.,
Proc. of DoE Seminar, Imperial College, London, June, (1987).
- L1 Lefebre du Prey, E.J.,
Soc.Pet.Eng.J., **13**, 39, (1973).
- L2 Lind, Zwolenik and Fuoss,
J.Amer.Chem.Soc., **81**, 1557, (1959).
- L3 Llenado, R.A.,
Anal.Chem., **47**(13), 2243-2249, (1975).
- M1 Melrose, J.C., and Brander, C.F.,
J.Can.Pet.Tech., 54-62, Oct-Dec, (1974).
- M2 McBain, J.W., Laing, J.W., and Titley, A.F.,
J.Chem.Soc., **115**, 1279, (1919).

- M3 Micrometrics, Accusorb. Physical Adsorption Analyser Handbook (1978),
ref. P/N 210/42801/00.
- M4 McKeown, I.P., Jayson, G.G., and Morris, H.,
Proc. of DoE Seminar, Imperial College, London, June, (1986).
- M5 McKeown, I.P.,
PhD. Thesis, Liverpool Polytechnic, p.104-5, (1990).
- M6 Murray, R.S., and Quirk, J.P.,
Langmuir, 6, 122-124, (1990).
- M7 McKeown, I.P.,
PhD. Thesis, Liverpool Polytechnic, p.140, (1990).
- M8 McKeown, I.P.,
PhD. Thesis, Liverpool Polytechnic, p.265, (1990).
- M9 Metsa-Serla, Product Literature, (1993).
- O1 van Olphen, H.,
Disc.Faraday Soc., 11, 82, (1951).

- O2 van Olphen, H.,
in "An introduction to Clay Colloid Chemistry",
Wiley Interscience, New York, (1963).
- O3 Overbeek, J.Th.G., and Bisterbosch, B.H.,
in "Electrokinetic Separation Methods" (P.G. Righetti,
C.J. van Oss, and J.W. Vanderhoff, Eds.), Elsevier / North Holland
Biomedical Press, p.75, (1979).
- O4 Oshima, H., Healy, T.W., and White, L.R.,
J.Colloid Interface Sci., **90**, 17, (1982).
- P1 Parsons, R.W.,
J.Pet.Tech., **26**, 550, (1974).
- P2 Parrish, D.R., and Craig, F.F.Jr.,
"A Laboratory study of a combination of Forward Combustion and
Waterflooding - The COFCAW Process",
J.Pet.Tech., 753-761, June, (1969).
- P3 Preston, W.C.,
J.Phys.Colloid Chem., **52**, 84, (1948).

- P4 Phillips, J.N.,
Trans. Faraday., 51, 561, (1955).
- P5 Prince, L.M.,
in "Microemulsions" (L.M. Prince, Ed.),
Academic Press, New York, London, (1977).
- P6 Palepu, R., Hall, D.G., and Wyn-Jones, E.,
J.Chem.Soc. Faraday Trans., 86(9), 1535-1538, (1990).
- P7 Painter, D.M., Bloor, D.M., Takisawa, N., Hall, D.G., and Wyn-Jones, E.,
J.Chem. Faraday Trans.1, 84, 2087, (1988).
- R1 Reed, R.L., and Healy, R.N.,
"Some Physicochemical Aspects of Microemulsion Flooding: A review",
in "Improved Oil Recovery by Surfactant and Polymer Flooding",
(D.O. Shah and R.S. Schecter, Eds.),
Academic Press, pp.383-439, (1977).
- R2 Rosen, M.J.,
in "Surfactants and Interfacial Phenomena",
Wiley Interscience, New York, (1978).

- R3 Rand, B., and Melton, I.E.,
Nature, 257, 214, (1975).
- R4 Reid, V.W., Longman, G.F., and Heinerth, E.,
Tenside, 4, 292, (1967).
- R5 Rank Brothers, Operating Instructions and Manual for the Particle
Micro-Electrophoresis Apparatus Mk II., pp.3-4, (1991).
- R6 Robinson, K.,
Oil Plus Seminar Series, Aberdeen, 29th November, (1991).
- R7 Rosen. M.J., and Nakamura, Y.,
J.Phys.Chem, 81, 873, (1977).
- R8 Rao, I.V., and Ruckenstein, E.,
J.Colloid Interface Sci., 113, 375, (1986).
- S1 Stalkup, F.I.,
"Miscible Displacement", SPE Monograph, 8, (1983).
- S2 Shaw, D.J.,
in "Introduction to Colloid and Surface Chemistry",
Wiley Interscience, New York, (1978).

- S3 Shinoda, K., and Hutchinson, E.,
J.Phys.Chem., **66**, 577, (1962).
- S4 Schulman, J.H., Stoeckenius, W. and Prince, L.M.,
J.Phys.Chem, **63**, 1677, (1959).
- S5 Schofield, R.K. and Samson, H.R.,
Disc.Faraday Soc., **18**, 135, (1954).
- S6 Street, N. and Buchanan, A.S.,
Aust.J.Chem., **9**,450, (1956).
- S7 Stern, O.,
Z.Electrochem., **30**, 508, (1924).
- S8 Smith, A.L.,
in "Dispersions of Powders in Liquids", Chapter 3, (G.D. Parfitt, Ed.),
Applied Sciences Pub., Barking, (1973).
- S9 Shaw, D.J.,
"Electrophoresis", Academic Press, London, p.60, (1969).
- S10 Somasundaran, P.,
Colloids and Surfaces, **26**, 55, (1987).

- S11 Stephen, H. and Stephen, T.,
in "Solubilities of Inorganic and Organic Compounds -
Binary Systems Vol 1"., p.782, (1963).
- S12 Stilbs, D.,
J.Colloid Interface Sci., **87**, 385, (1982).
- S13 Scamehorne, J.F., Schecter, R.S., and Wade, W.H.,
J.Colloid Interface Sci., **85**, 463, (1982).
- S14 Serla-thin Product Literature, (1993).
- T1 Taber, J.J.,
Soc.Petrol.Eng.J., 3-12, March, (1969).
- T2 Taber, J.J., Kirby, J.C., and Schroeder, F.U.,
AIChE Symp. Ser. N° 127, **69**, 53, (1973).
- T3 Tranford, C.,
"The Hydrophobic Effect - The Formation of Micelles and Biological
Membranes.", Wiley, (1973).
- T4 Tschapek, M., Tcheichvelli, L., and Wasowski, C.,
Clay Minerals, **10**, 219, (1974).

- T5 Trapnell, B.M.W., and Hayward, D.O.,
"Chemisorption", 2nd, Butterworths, London, p.60, (1964).
- V1 Vogel, A.I.,
"Textbook of Qualitative Inorganic Analysis", 4th Edition,
Longmans, (1978).
- W1 Wagner, O.R., and Leach, R.O.,
Soc.Pet.Eng.J., 335-344, Dec, (1966).
- W2 Wiggins, J.L.,
"Treating Oil-Field Emulsions".,
Petrol.Eng., 29(5), 347, (1957).
- W3 Williams, D.J.A., and Williams, K.P.,
J.Colloid Interface Sci., 65(1), 79, (1978).
- W4 Weise, G.R., James, R.O., Yates, D.E., and Healy, T.W.,
"Electrochemistry" (M.T.P. Int.Rev.Sci.),
Butterworths, London, p.350, (1976).
- Z1 Zana, R., Rupert, L.A.M., van Os, M., and Binana-Limbele, W.,
J.Colloid Interface Sci., 141, 157-167, (1991).

Z2 Ziegler, W.T., and Mullins, J.C.,
Report N° 1 to the National Bureau of Standards, Project A-663,
Georgia Institute of Technology, Atlanta, April (1963).

Appendices

Appendix 1

Program to calculate various BET parameters.

In order to calculate the figures required to plot the BET line a calculation sheet was used. This was very time consuming and prone to errors by mis-calculation. A program, listed below, was written to overcome these problems.

```
10  REM CALCULATION OF BET PARAMETERS
20  PRINT "THIS IS A PROGRAM TO CALCULATE THE VARIOUS"
30  PRINT "FIGURES IN THE BET CALCULATION SHEET"
40  PRINT "*****"
50  PRINT "PLEASE INPUT SAMPLE ID, SAMPLE WEIGHT, H1 AND H2"
60  INPUT N$, W, H1, H2
70  PRINT "NOW INPUT TS AND PS"
80  INPUT TS, PS
90  REM THIS IS THE END OF MAIN DATA INPUT
100 PRINT "*****"
110 LET VD = 28.47
120 LET Q = 130.6
130 LET Z = 6.6E-5
140 LET S = 16.2
150 LET T1 = (307.2 + TS) / 2
160 LET K = 0
170 LET VS = TS * ((VD * (H1-H2/307.2) - (3.65 * H2)/T1/H2))
```

```

180 LET A1 = (0.001169 * (VD + Q) /W)
190 LET A2 = (0.001169 * VD)/W
200 PRINT VS
210 LET B = (0.3593 * VS)/(TS *W) + 1.311 / (T1 * W)
220 LET C = (0.3593 * VS * Z) / (W * TS)
230 PR#1
240 PRINT "*****"
250 PRINT "T1 VALUE = ";T1 "K"
260 PRINT "VS VALUE = ";VS "mls"
270 PRINT "A1 VALUE = ";A1
280 PRINT "A2 VALUE = ";A2
290 PRINT "B VALUE = ";B
300 PRINT "C VALUE = ";C
310 PR#0
320 REM THIS IS THE END OF THE PARAMETER DETERMINATION
330 PRINT "PLEASE INPUT NUMBER OF DATA POINTS"
340 INPUT N
350 FOR I = 1 TO N
360 PRINT "PLEASE INPUT EXTRA VOLUME CODE, 1 IF USED"
370 PRINT " 0, IF NOT."
380 INPUT J
390 IF J = 1 GOTO 410
400 IF J = 0 GOTO 430
410 LET O = A1

```

```

420 GOTO 440
430 LET O = A2
440 PRINT "PLEASE INPUT P1 (;I"),P2(;I"),PE(;I)"
460 LET D = P1 - P2
470 LET E = P2 -PE
480 LET F = P2^2 - PE^2
490 LET G = O * D
500 LET H = B * E
510 LET J = C * F
520 LET VA = G - H - J
530 GOTO 2000
540 LET V = VA + U
550 LET K = VA
560 LET X = P2 / PS
570 LET Y = X (V * (1 - X))
580 PR#3
590 PR#1
600 PRINT "*****"
610 REM THIS IS THE END OF THE CALCULATION SECTION
620 PRINT "P1 (;I) =" , P1
630 PRINT "P2 (;I) =" , P2
640 PRINT "PE (;I) =" , PE
650 PRINT "D (;I) =" , D
660 PRINT "E (;I) =" , E

```

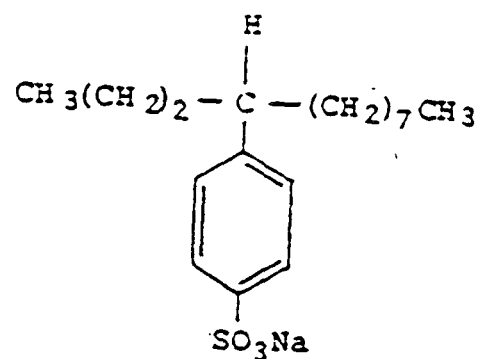
```

670 PRINT "F (;I) =" , F
680 PRINT "G (;I) =" , G
690 PRINT "H (;I) =" , H
700 PRINT "J (;I) =" , J
710 PRINT "VA/WS (;I) =" , VA
720 PRINT "V (;I) =" , V
730 PRINT "X (;I) =" , X
740 PRINT "Y (;I) =" , Y
750 REM END OF PRESENTATION SCREEN
760 PRINT "*****"
770 PR#0
780 IF I = N GOTO 2020
790 NEXT I
2000 LET U = K
2010 GOTO 540
2020 PRINT " CALCULATION COMPLETE."
2025 PRINT "DO YOU WANT ANOTHER RUN?"
2030 PRINT "IF YES TYPE 1, IF NO TYPE 0"
2040 INPUT R
2050 IF R = 1 GOTO 20
2060 END

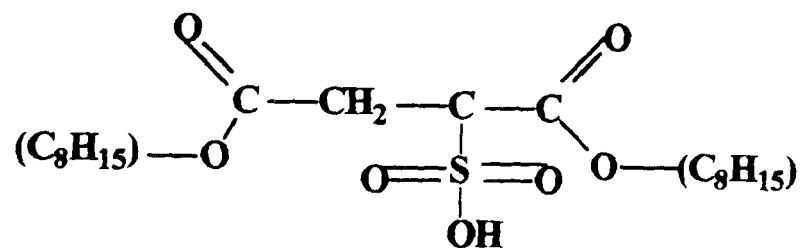
```

Appendix II
Chemical structure of the compounds used

i) 4-φ-C₁₂ABS

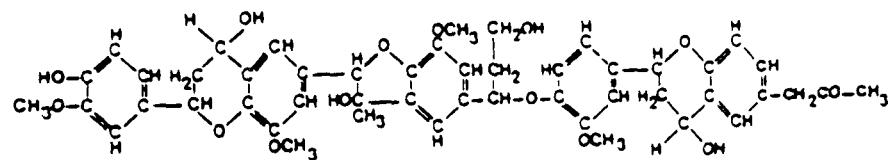


ii) Aerosol OT



iii) Lignin sulphonate

The exact structure of lignin sulphonate is not known with any precision and only a suggested structure can be given for the lignin monomer.



Appendix III

Derivation of the Gibbs, Langmuir, Freundlich and Tempkin Equations

A.1.1 The Gibbs Equation (1878)

The Gibbs equation quantitatively relates the amount of surfactant adsorbed at an interface to the reduction in interfacial tension produced. Gibbs considered the surface as a mathematical plane dividing the phases. This is illustrated in Figure A1, where the composition of the two phases, α and β , are homogeneous up to the planes AA' and BB' respectively. The dividing plane is taken at some arbitrarily chosen location.

The general form of the Gibbs equation, which describes changes in surface tension between the limits AA' and BB' can be written (A1):

$$(d\gamma)_T = -\sum_i \Gamma_i \cdot d\mu_i \quad (1)$$

where, γ = the surface tension of the surfactant solution, mN m^{-2}

μ_i = the chemical potential of the i^{th} component

and Γ_i = the surface excess concentration of the i^{th} component
per unit area of the interface, mol m^{-2} .

Thus for a two-component liquid mixture, equation (1) becomes :

$$- d\gamma = \Gamma_1 d\mu_1 + \Gamma_2 d\mu_2 \quad (2)$$

where subscripts 1 and 2 refer to the solvent and solute respectively. Whilst equation (2) describes the surface excess for any given position of the dividing plane, SS' is usually set such that the surface excess concentration of the solvent is zero ($\Gamma_1 = 0$).

Equation (2) may now be written:

$$- d\gamma - \Gamma_2 d\mu_2 \quad (3)$$

(where Γ_2 is more accurately defined as the "relative" surface excess concentration).

Noting that

$$\mu_2 = \mu_2^\phi + RT \ln a_2 \quad (4)$$

and

$$d\mu_2 = RT d \ln a_2 \quad (5)$$

where a_2 = the activity of component 2 in the bulk solution.

Substitution of this equation into equation (3) gives :

$$- d\gamma = RT \Gamma_2 d \ln a_2 \quad (6)$$

which on rearrangement gives:

$$\Gamma_2 = \frac{1}{RT} \cdot \frac{d\gamma}{d \ln a_2} \quad (7)$$

Using equation (7), surface excess concentrations can be determined from changes in the surface tension of aqueous surfactant solutions with increasing bulk activity.

The main criticism of the Gibbs dividing plane approach is that the interface will have a finite thickness (possibly up to several hundred angstroms), and may thus be better considered as a separate phase (σ in Figure A2) of not less than one molecular layer in depth (A1).

The surface phase approach (e.g. Guggenheim (G6)), illustrated in Figure A2, again considers the bulk phases, α and β , to be homogeneous up to the planes AA' and BB' respectively, but that the change from one phase to the other occurs over the distance AB (the surface phase σ). Thus rewriting equation (1), and considering the interface as a separate phase, we have:

$$- d\gamma = \Gamma_1^\sigma \cdot d\mu_1 + \Gamma_2^\sigma \cdot d\mu_2 \quad (8)$$

where Γ_1^σ and Γ_2^σ are the total concentrations of components 1 and 2 in the surface phase.

Since the Gibbs-Duhem relationship for a two-component liquid mixture (at constant temperature and pressure) is given as :

$$N_1 \cdot d\mu_1 = -N_2 \cdot d\mu_2 \quad (9)$$

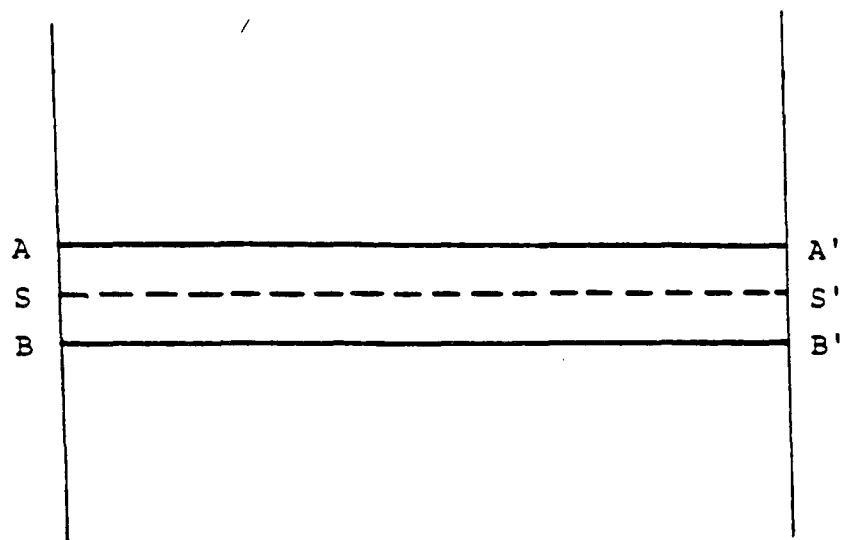


Figure A1 The Gibbs dividing plane model

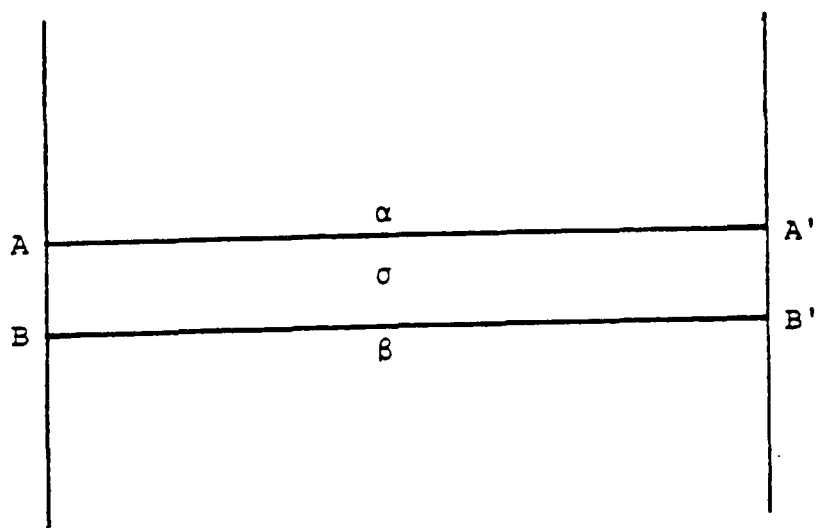


Figure A2 The surface phase model

where, N_1 and N_2 denote the bulk mole fraction of components 1 and 2 respectively, then equation (8) may be expressed as:

$$-d\gamma = \Gamma_2^\sigma - \frac{N_2}{N_1} \cdot \Gamma_1^\sigma \cdot d\mu_2 \quad (10)$$

Substitution of equation (10) into (3) gives:

$$\Gamma_2 = \Gamma_2^\sigma - \frac{N_2}{N_1} \cdot \Gamma_1^\sigma \quad (11)$$

The quantity Γ_2 is thus defined as the total surface concentration of component 2, less that which is present in the bulk region which contains an equivalent number of moles of component 1 (A1). Clearly, at dilute solutions of a strongly adsorbing surfactant, the last term of equation 10 is small compared to the first and the equation reduces to that of the dividing plane model (equation (3)).

A.1.2 The Langmuir Equation

The Langmuir equation is based on the characteristic assumptions that :

- (i) only monolayer adsorption takes place
- (ii) adsorption is localised, and
- (ii) the heat of adsorption (ΔH) is independent of surface coverage (θ).

As a result of the first assumption, the rate of adsorption is proportional to the fraction of surface which is bare, $(1-\theta)$, as well as the number of molecules striking the surface (Z). Gas kinetic theory predicts that the collision rate of molecules with a surface per cm^2 per second is given by :

$$Z = PN \left(\frac{1}{2\pi MRT} \right)^{1/2} \quad (12)$$

where P = pressure in N m^{-2}

N = the number of molecules considered

M = the relative molecular mass.

Thus, the rate of adsorption per unit area is :

$$R_a = k_1 X (1 - \theta) \quad (13)$$

The rate of desorption of molecules from the surface is proportional to the surface coverage and inversely proportional to a desorption energy term ($\exp \Delta H/RT$). The rate of desorption per unit area is therefore:

$$R_d = k_2 \theta \exp \frac{\Delta H}{RT} \quad (14)$$

At equilibrium, $R_a = R_d$, giving:

$$k_1 Z (1 - \theta) = k_2 \theta e^{\frac{\Delta H}{RT}} \quad (15)$$

Rearranging equation (15):

$$\theta = \frac{bP}{1 + bP} \quad (16)$$

in which,

$$b = \frac{k_1}{k_2} \cdot \frac{N}{(2\pi MRT)^{1/2}} \cdot e^{\frac{\Delta H}{RT}}$$

Alternatively, θ can be replaced by V / V_m , where V denotes the volume of gas adsorbed and V_m represents the monolayer volume, thus :

$$V = \frac{V_m b P}{1 + b P} \quad (17)$$

and rearranging equation (17) gives :

$$\frac{P}{V} = \frac{1}{V_m b} + \frac{P}{V_m} \quad (18)$$

so that the plot of P/V versus P gives a straight line with a slope of $1/V_m$.

For adsorption from solution, the equation (18) may be expressed by :

$$\frac{M_D}{\Gamma_D} = \frac{1}{\Gamma_m \cdot b} + \frac{M_D}{\Gamma_m} \quad (19)$$

where, M_D = the equilibrium bulk concentration of solute, in mol dm^{-3}

Γ_D = the amount of solute adsorbed per unit area of adsorbent, in mol m^{-2}

Γ_m = the monolayer capacity, in mol m^{-2}

b = a constant, given above, in $\text{dm}^3 \text{mol}^{-1}$.

A.1.3 The Freundlich Equation

The Freundlich equation can be derived theoretically from the Langmuir equation if certain assumptions are made concerning the nature of the surface and the mechanism of adsorption (S2).

Expressing the Langmuir equation as

$$\theta = \frac{bP}{1+bP}$$

This equation is true if the quantity "b" is independent of θ . If this is not the so, the total surface coverage can be obtained by a process of summation. Thus, dividing the surface into a number of groups of identical sites, designated as "i", each of

which has a particular value of "b", the above equation can be expressed as:

$$\theta_i = \frac{b_i P}{1 + b_i P} \quad (20)$$

and the total coverage is given by :

$$\theta = \sum \theta_i n_i \quad (21)$$

where n_i = the fraction of sites of type "i".

If the "b" values are sufficiently close in value to form a continuous distribution then equation (21) can be reduced to :

$$\theta = \int n_i \theta_i d_i \quad (22)$$

where $n_i d_i$ is the frequency of occurrence of θ_i between i and $i + d_i$. In general this integration cannot be carried out because the distribution function n_i is unknown.

However, if the variation of b_i is simply due to the variation of ΔH , i.e. the heat of adsorption, then equations (20) and (22) may be expressed as :

$$\theta_H = \frac{b_{\Delta H} P}{1 + b_{\Delta H} P} \quad (23)$$

and

$$\theta = \int n_{\Delta H} \cdot \theta_{\Delta H} \cdot d\Delta H \quad (24)$$

If $n_{\Delta H}$ is exponentially dependent on ΔH then :

$$n_{\Delta H} = n_o e^{\frac{-\Delta H}{\Delta H_m}} \quad (25)$$

where, n_o and ΔH_m = constants representing the total number of adsorption sites, and the minimum heat of adsorption respectively.

Substitution of equations (23) and (25) into equation (24) gives an expression that can be solved :

$$\theta = \int_0^{\infty} n_o e^{\frac{-\Delta H}{\Delta H_m}} \cdot \frac{b_{\Delta H} P}{(1 + b_{\Delta H} P)} \cdot d\Delta H \quad (26)$$

Now, expressing $b_{\Delta H} = b_o e^{(\Delta H/RT)}$, equation (26) becomes, after rearranging :

$$\theta = \int_0^{\infty} \frac{n_o e^{\frac{-\Delta H}{\Delta H_m}}}{1 + e^{\frac{-\Delta H}{RT} + \frac{\Delta H}{\Delta H_m}}} \cdot d\Delta H \quad (27)$$

which upon integration gives :

$$\theta = b_o P^{\frac{RT}{\Delta H_m}} \cdot n_o \Delta H_m \quad (28)$$

or

$$\theta = k P^{\frac{1}{n}} \quad (29)$$

where, $k = b_o n_o \Delta H_m$, and

$$\frac{1}{n} = \frac{RT}{\Delta H_m}$$

This is the Freundlich equation. Therefore the Freundlich equation represents the summation of a distribution of Langmuir equations, however, the amount of adsorbate adsorbed (i.e. the surface coverage) is not depicted as approaching a limiting value as in a single Langmuir equation.

A.1.4 The Temkin Equation

The Temkin equation may be derived by inserting in the Langmuir equation, the condition that the heat of adsorption decreases directly with surface coverage (B6). Such a reduction can arise either on a uniform surface from lateral (repulsive) interactions, or from surface heterogeneity.

(a) Derivation for a uniform surface

Expressing the Langmuir equation in the form :

$$\theta = \frac{bP}{1 + bP}$$

and substitution for b gives, upon rearrangement, the expression:

$$\frac{\theta}{(1 - \theta)} = P \cdot B_0 e^{\frac{\Delta H}{RT}} \quad (30)$$

Since all sites are identical it is sufficient to insert into equation (30) the condition that ΔH varies with θ according to the equation :

$$\Delta H = \Delta H_o(1 - \beta\theta) \quad (31)$$

in which, ΔH_o = the heat of adsorption at $\theta = 0$ in J mol⁻¹ and

β = a constant, in J mol⁻¹.

Thus,

$$\frac{\theta}{1 - \theta} = P \cdot b_o e^{\frac{\Delta H_o(1 - \beta\theta)}{RT}} \quad (32)$$

Taking logarithms and rearranging:

$$\ln P = \frac{\ln \theta}{(1 - \theta)} - \ln b_o e^{\frac{\Delta H_o}{RT}} + \frac{\Delta H_o \beta \theta}{RT} \quad (33)$$

For $0.2 < \theta < 0.8$, variations in $\ln \theta / (1 - \theta)$ may be neglected and thus equated to zero (its value at $\theta = 0.5$).

Thus, equation 33 simplifies to :

$$\theta = \frac{RT}{\Delta H_o \beta} \ln P \cdot b_o e^{\frac{\Delta H_o}{RT}} \quad (34)$$

the Tempkin Equation.

(b) Derivation for a non-uniform surface

Here, it is necessary to divide the surface into a number of uniform elements, ds , on each of which the heat of adsorption is constant, and the Langmuir equation is expressed as :

$$\theta = \frac{bP}{1 + bP}$$

therefore,

$$\theta_s = \frac{b_0 e^{\frac{\Delta H}{RT}} \cdot P}{1 + b_0 e^{\frac{\Delta H}{RT}} \cdot P} \quad (35)$$

and the value of θ over the whole surface is obtained by integration :

$$\theta = \int \theta_s \cdot ds \quad (36)$$

Since ΔH falls linearly with s :

$$\Delta H = \Delta H_0 (1 - \beta s) \quad (37)$$

Inserting equations (35) and (37) into (36) and assuming the total surface area is unity :

$$\theta = \int_0^1 \frac{b_0 e^{\frac{\Delta H_0(1 - \beta s)}{RT}} \cdot P \cdot ds}{1 + b_0 e^{\frac{\Delta H_0(1 - \beta s)}{RT}} \cdot P} \quad (38)$$

which gives :

$$\theta = \frac{RT}{\Delta H_o \beta} \ln \frac{1 + b_o e^{\frac{\Delta H_o}{RT}} \cdot P}{1 + b_o e^{\frac{\Delta H_o}{RT}} \cdot P \cdot e^{\frac{-\Delta H_o \beta}{RT}}} \quad (39)$$

Now, assuming that for $0.2 < \theta < 0.8$, P is sufficiently large for $[b_o e^{(\Delta H_o / RT)} \cdot P]$ to be much greater than unity but still low enough for $[b_o e^{(\Delta H_o / RT)} \cdot P \cdot e^{(\Delta H_o \beta / RT)}]$ to be less than unity, equation (39) simplifies to :

$$\theta = \frac{RT}{\Delta H_o \beta} \ln P \cdot b_o e^{\frac{\Delta H_o}{RT}} \quad (34)$$

i.e. the Tempkin equation, which may then be written as :

$$\theta = A \ln B + A \ln P \quad (40)$$

in which $A = RT / (\Delta H_o \beta)$

and $B = b_o \exp (\Delta H_o / RT)$.

The Tempkin equation is thus valid for $0.2 < \theta < 0.8$ (T5).

GLOSSARY

a	activity of a species / mol dm ⁻³
A	Cross-sectional area / m ²
A_n	Aggregation number of monomers in a micelle
A_s	Area occupied per surfactant molecule at the interface / m ²
c_x	concentration of component x / mol dm ⁻³
C	Electric double layer capacitance / F m ⁻²
C_i, C_f	Initial and final surfactant concentrations respectively / mol dm ⁻³
C_m	Concentration of micelles / mol dm ⁻³
CMC	Critical micelle concentration / mol dm ⁻³
d	internal diameter / m
e	Electronic charge / C
F	Faradays constant
IEP	Iso-electric point
K	A constant related to the free energy of adsorption / mol dm ⁻³
l_c	Cell length / m
L	Molarity of SDS solution / mol dm ⁻³
m_D	Equilibrium surfactant concentration / mol dm ⁻³
m_s	Concentration of salt in solution / mol dm ⁻³
n_{BuOH}	
n_{PrOH}	Equilibrium concentration of alcohol / % v/v
n_{PrOH}	
n_o	Bulk concentration of ions / mols m ⁻³

N_A	Avogadro's constant
N_c	Capillary number
PZC	Point of zero charge / V
r	pore radius / cm
R	Universal gas constant / $J K^{-1} mol^{-1}$
T	Absolute temperature / K
V	Electrophoretic mobility / $m s^{-1}$
V_m	Volume of Hyamine used to reach the end point / cm^3
W_s	Weight of sample / g
x	Distance from a particle surface / m
Z	Valency of the ions present
γ	Surface (or interfacial) tension / $N m^{-1}$
Γ	Surface excess concentration of surfactant / $mol m^{-2}$
ΔG_m	Free energy of micellisation / $J mol^{-1}$
ΔP	Pressure gradient / $dynes cm^{-2}$
ϵ	Static permittivity of the medium / $F m^{-1}$
ζ	Zeta potential / V
Θ	Percentage surface coverage of edge sites
$1/\kappa$	Electric double layer thickness / m
μ	Chemical potential / $J mol^{-1}$
π	Surface pressure / $N m^{-2}$
σ	Surface charge density / $C m^{-2}$
ψ	Electrical potential / V